Influence of Sorption and Nitrification Processes on Pharmaceutical Attenuation During Biological Wastewater Treatment

A dissertation

submitted by:

Sandeep Sathyamoorthy

In partial fulfillment of the requirements

for the degree of

Doctor of Philosophy

in

Civil and Environmental Engineering

TUFTS UNIVERSITY

August, 2013

Advisor: Dr. C. Andrew Ramsburg

Front Matter

Abstract

Reports of the deleterious impacts of microconstituents in the environment have raised concerns in the scientific and lay communities in recent years. Pharmaceuticals (PhACs) are a group of microconstituents of particular concern considering the importance of these chemicals in improving quality of life and the consistent increase in their use. The vast majority of PhACs are synthetic chemicals, making them particularly recalcitrant in the environment. Wastewater treatment plants (WWTPs) provide a direct route for PhACs to enter the environment. While WWTPs are not currently designed to treat PhACs, recent studies have documented attenuation and degradation of these compounds within the treatment process. This research is motived by those studies which suggest that operation of biological treatment processes at solids retention times typically used for nitrification are recommended to achieve effective PhAC removal. The overall objective of this research was to evaluate the role of sorption and nitrification processes in PhAC biodegradation during biological wastewater treatment.

The central hypothesis of this research, in relation to the synergy between nitrification and PhAC biodegradation, is that PhAC biodegradation, when it occurs concurrent with nitrification, is a result of cometabolism by ammonia oxidizing bacteria. This hypothesis was evaluated by integrating laboratory-scale experiments with mathematical modeling. Results from batch experiments evaluating the biodegradation of the beta-blockers atenolol (ATN), metoprolol (MET) and sotalol (SOT) suggest that, of

this group of structurally similar PhACs, only ATN was biodegraded during nitrification. The biodegradation of ATN was linked to the activity of ammonia oxidizing bacteria (AOB) and heterotrophs, but not nitrite oxidizing bacteria (NOB). To describe the biodegradation of ATN a cometabolic process-based (CPB) model was developed. The CPB model links ATN cometabolism to ammonia oxidizing bacteria (AOB) within the ASM framework. Transformation coefficients fitted to the ATN biodegradation data describe rates of cometabolism under AOB growth and non-growth conditions. Furthermore, ATN was observed to inhibit AOB growth; which was described using a competitive inhibition coefficient. Results from batch experiments with naproxen (NAP) suggest that the CPB model holds more general utility to describe cometabolic biodegradation of PhACs by AOB.

The influence of AOB and NOB biokinetic parameters on the ATN biodegradation and competitive inhibition coefficients was evaluated using novel application of elasticities integrated with application of the generalized likelihood uncertainty estimation (GLUE) technique. Results suggest that the growth-related coefficient for cometabolic biodegradation of ATN is relatively insensitive to variation in ammonia and nitrite oxidizing biokinetic parameters. In contrast, the non-growth related coefficient describing ATN biodegradation by AOB appears to be sensitive to the maximum specific growth rate of ammonia oxidizing bacteria. Application of elasticities suggests that seasonal temperature variations may be an important factor in pharmaceutical biodegradation during biological wastewater treatment.

PhAC sorption is explored in this research through mathematical modeling. The central hypothesis is that predictive models describing PhAC sorption based upon octanol-water partitioning, as is conventionally done for environmental pollutants, are

incapable of describing PhAC sorption during biological wastewater treatment. Rather poly-parameter modeling capturing the disparate interactions between the biosolids surface and PhACs are needed. Results suggest that log K_{OW} alone is unable to effectively describe the sorption of PhACs. Polyparameter models are significantly more effective, with the charge of the dominant species at the reactor conditions being the most important single predictor of PhAC sorption.

Future research directed towards understanding the relationship between PhAC properties and biodegradation is recommended. Such research may provide an opportunity to begin the process of developing predictive models to assess the PhAC fate in WWTPs as part of the PhAC development process based on its chemometric properties. Additional research aimed at understanding the mechanism of PhAC biodegradation by heterotrophs in mixed populations in WWTPs is also recommended.

Dedication

For my wife YooRee.

Front Matter

Acknowledgements

First, I would like to thank my wife, YooRee. She has been a constant source of love, support, encouragement and motivation, and also *provider of a swift kick in the hind parts* when needed. Without her, none of this would have been possible. I am very thankful to my Mom and Dad. Ever since I can remember, they have encouraged us to be curious, explorative and follow our dreams. I can unequivocally say that I would not be here without their love, support and encouragement over the years.

I would like thank my advisor, Dr. C. Andrew Ramsburg, whose guidance has proved immeasurable. I am grateful that he gave me an opportunity to be a part of his research group at Tufts. More importantly, I am thankful to him for giving me opportunities outside of my research at Tufts; teaching, participating in engineering-education related research and generally allowing me to fuel my broader interests. Perhaps most importantly, I am grateful for his understanding in giving me time to adjust when our son was born. I hope that in some small way, I have been able to contribute to his research group.

I would like to thank all my committee members, Dr. Natalie Cápiro, Dr. Steven Chapra, Dr. Mark J. Laquidara and Dr. H. David Stensel. I am grateful for their time, guidance and support. I am grateful to Dr. Cápiro for early discussions related to application of qPCR in my research. I would like to thank Dr. Chapra for inspiring me learn more about numerical methods and in particular, his suggestions related to application of Monte Carlo analysis in my research. I am grateful to Dr. Stensel, for his insightful questions early in this research related to potential for nitration in batch experiments, which led me to refine my experimental protocol. Thanks are also due to Dr. Stensel for probing the issue of PhAC inhibition. Results of that investigation led to

description of ammonia oxidizing bacteria inhibition by atenolol in this research. I have much to thank Mark for – he has been extremely supportive of me, both at AECOM and as through my graduate work. I have long admired his ability to rapidly hone in on the "so what" questions and find ways to link research to application in the *real-world* with ease. On a personal note, I must acknowledge he's a pretty good brewmaster. I owe a special debt of gratitude to Dr. Richard M. Vogel at Tufts. I consider him a mentor and have sought counsel from him on multiple occasions. He has had a significant impact on my learning and development.

I am grateful to Dr. Kartik Chandran of Columbia University and members of his research group for helping me to learn qPCR techniques and for the use of their facilities. I am grateful to Dr. Philip M. Gschwend of MIT for helpful discussions related to the development of QSAR models for pharmaceutical sorption. At AECOM, I am very grateful to Ms. Beverly Stinson who has been very supportive of my research endeavors.

I would like thank everyone I have worked with in the IMPES lab at Tufts. In particular I would like to thank Ms. Katie Muller, Ms. Kelly Smith, Ms. Catherine Hoar, Mr. Oren Sharabi, Ms. Justina Chen and Mr. Yuki Tanimoto for their help with SBR operations. I am also grateful to my dear friend Dr. Ali Boroumand for his help in improving my MATLAB proficiency.

Finally, I would like very much to thank the different funding sources which made this research possible. Partial support was provided by the Massachusetts Water Resources Research Center under project number 2011MA291B. Seed support to establish my sequencing batch reactor at Tufts was provided by AECOM. I am also grateful to have been a recipient of the Jonathan Curtis fellowship, a graduate student research award and a travel grant at Tufts University.

Front Matter

Table of Contents

List of Figures

List of Tables

List of Parameters and Symbols

Symbol	*Description*	*Dimension*
pH	*pH value*	*[--]*
θ	*Temperature*	*[θ]*
t	*Time*	*[T]*
X	*Biomass concentration*	*[$M_{BIOMASS}/L^3$]*
HRT	*Hydraulic Retention Time*	*[T]*
SRT	*Solids Retention Time*	*[T]*
X_{HET}	*Heterotrophic (HET) biomass concentration*	*[$M_{BIOMASS}/L^3$]*
X_{NIT}	*Nitrifying biomass concentration*	*[$M_{BIOMASS}/L^3$]*
q_{NIT}	*Maximum specific respiration rate of nitrifying bacteria*	*[$M_{O2}/M_{Biomass}T$]*
$\mu_{MAX,NIT}$	*Maximum specific growth rate of nitrifying bacteria*	*[T^{-1}]*
μ_{NIT}	*Specific growth rate of nitrifying bacteria*	*[T^{-1}]*
$r_{NIT\text{-}GROWTH}$	*Growth rate of nitrifying bacteria*	*[$M_{BIOMASS}/L^3T$]*
$K_{O,NIT}$	*Half saturation DO concentration for nitrifying bacteria*	*[M_{O2}/L^3]*
$r_{NIT\text{-}DECAY}$	*Decay rate of nitrifying bacteria*	*[$M_{BIOMASS}/L^3T$]*
b_{NIT}	*Specific decay rate of nitrifying bacteria*	*[T^{-1}]*
$K_{O,NIT\text{-}DECAY}$	*Half saturation DO concentration for decay of nitrifying bacteria*	*[M_{O2}/L^3]*
$\eta_{NIT\text{-}AX}$	*Anoxic decay rate modification factor for nitrifying bacteria*	*[--]*
X_{AOB}	*Ammonia oxidizing bacteria (AOB) concentration*	*[$M_{BIOMASS}/L^3$]*
q_{AOB}	*Maximum specific respiration rate of AOB*	*[$M_{O2}/M_{Biomass}T$]*
$\mu_{MAX,AOB}$	*Maximum specific growth rate of AOB*	*[T^{-1}]*
μ_{AOB}	*Specific growth rate of AOB*	*[T^{-1}]*
$r_{AOB\text{-}GROWTH}$	*Growth rate of AOB*	*[$M_{BIOMASS}/L^3T$]*
$K_{O,AOB}$	*Half saturation DO concentration for AOB growth*	*[M_{O2}/L^3]*
b_{AOB}	*Specific decay rate of AOB*	*[T^{-1}]*
$b_{AOB,AE}$	*Specific decay rate of AOB under aerobic conditions*	*[T^{-1}]*
$b_{AOB,AX}$	*Specific decay rate of AOB under anoxic conditions*	*[T^{-1}]*
$r_{AOB\text{-}DECAY,AE}$	*Decay rate of AOB under aerobic conditions*	*[$M_{BIOMASS}/L^3T$]*
$r_{AOB\text{-}DECAY,AX}$	*Decay rate of AOB under anoxic conditions*	*[$M_{BIOMASS}/L^3T$]*
$K_{O,AOB\text{-}DECAY}$	*Half saturation DO concentration for AOB decay*	*[M_{O2}/L^3]*
X_{NOB}	*Nitrite oxidizing bacteria (NOB) concentration*	*[$M_{BIOMASS}/L^3$]*
q_{NOB}	*Maximum specific respiration rate of NOB*	*[$M_{O2}/M_{Biomass}T$]*

Symbol	Description	Dimension
$\mu_{MAX,NOB}$	Maximum specific growth rate of NOB	$[T^{-1}]$
μ_{NOB}	Specific growth rate of NOB	$[T^{-1}]$
$r_{NOB\text{-}GROWTH}$	Growth rate of NOB	$[M_{BIOMASS}/L^3T]$
$K_{O,NOB}$	Half saturation DO concentration for NOB	$[M_{O2}/L^3]$
b_{NOB}	Specific decay rate of NOB	$[T^{-1}]$
$b_{NOB,AE}$	Specific decay rate of NOB under aerobic conditions	$[T^{-1}]$
$b_{NOB,AX}$	Specific decay rate of NOB under anoxic conditions	$[T^{-1}]$
$r_{NOB\text{-}DECAY,AE}$	Decay rate of NOB under aerobic conditions	$[M_{BIOMASS}/L^3T]$
$r_{NOB\text{-}DECAY,AX}$	Decay rate of NOB under anoxic conditions	$[M_{BIOMASS}/L^3T]$
$K_{O,NOB\text{-}DECAY}$	Half saturation DO concentration for NOB decay	$[M_{O2}/L^3]$
S_{NH}	Ammonia nitrogen concentration	$[M_N/L^3]$
K_{NH}	Half saturation ammonia nitrogen concentration for AOB	$[M_N/L^3]$
K_{NHi}	Half saturation ammonia nitrogen concentration for inhibition of NOB growth	$[M_N/L^3]$
S_{FA}	Free ammonia nitrogen concentration	$[M_N/L^3]$
$K_{I,FA}$	Half saturation free-ammonia nitrogen concentration for inhibition of NOB growth	$[M_N/L^3]$
S_{NO2}	Nitrite nitrogen concentration	$[M_N/L^3]$
K_{NO2}	Half saturation nitrite nitrogen concentration for NOB	$[M_N/L^3]$
S_{FNA}	Nitrous acid concentration	$[M_N/L^3]$
K_{FNA}	Half saturation nitrous acid-nitrogen concentration for NOB	$[M_N/L^3]$
$K_{I,FNA}$	Inhibition constant for nitrous acid-nitrogen concentration on NOB	$[M_N/L^3]$
S_{NO3}	Nitrate nitrogen concentration	$[M_N/L^3]$
S_O	Dissoved oxygen (DO) concentration	$[M_{O2}/L^3]$
K_O	Half saturation DO concentration	$[M_{O2}/L^3]$
$K_{O,NIT}$	Half saturation DO concentration for Nitrifiers	$[M_{O2}/L^3]$
$K_{O,AOB}$	Half saturation DO concentration for AOB	$[M_{O2}/L^3]$
$K_{O,NOB}$	Half saturation DO concentration for NOB	$[M_{O2}/L^3]$
F_A	Fraction of biomass active for cometabolism	[--]
$k_{C,MAX}$	Maximum specific rate of utilization of non-growth (cometabolic) substrate, C	$[M_C/M_BT]$
k_C	Specific rate of utilization of cometabolic substrate, C	$[M_C/M_BT]$
S_C	Concentration of cometabolic substrate, C	$[M_C/L^3]$
KC	Half saturation concentration of cometabolic substrate, C	[MC/L3]
S_G	Concentration of growth substrate, G	$[M_G/L^3]$

Symbol	Description	Dimension
K_G	Half saturation concentration of growth substrate	$[M_G/L^3]$
T_C	Cometabolic substrate transformation capacity for non-growth substrate, C	$[M_C/M_G]$
k_{BIO}	Pseudo first order biodegradation rate	$[L^3/M_{BIOMASS}T]$
$T_{PhAC\text{-}AOB}$	Growth related tranformation coefficient for cometabolic pharmaceutical biodegradation by AOB	$[L^3/M_{BIOMASS}]$
$k_{PhAC\text{-}AOB}$	Non-growth tranformation coefficient for cometabolic pharmaceutical biodegradation by AOB	$[L^3/M_{BIOMASS}T]$
$T_{PhAC\text{-}HET}$	Growth related tranformation coefficient for cometabolic pharmaceutical biodegradation by HET	$[L^3/M_{BIOMASS}]$
$k_{PhAC\text{-}HET}$	Non-growth tranformation coefficient for cometabolic pharmaceutical biodegradation by HET	$[L^3/M_{BIOMASS}T]$
$\alpha_{PhAC\text{-}HET}$	Biomass normalized rate coefficient for pharmaceutical biodegradation by HET	$[L^3/M_{BIOMASS}T]$
S_{PhAC}	Soluble PhAC concentration	$[M_{PhAC}/L^3]$
W_{PhAC}	Sorbed PhAC concentration	$[M_{PhAC}/M]$
$M_{PhAC,T}$	Total PhAC mass	$[M_{PhAC}]$
V_{AQ}	Volume of water in a reactor	$[L^3]$
V_{TOT}	Total reactor volume	$[L^3]$
K_D	Partioning (sorption) coefficient	$[L^3/M]$
$f_{PhAC,X}$	Sorbed fraction of PhAC	$[M_{PhAC\text{-}sorbed}/M_{PhAC\text{-}Total}]$
$f_{PhAC,WAS}$	Fraction of PhAC wasted from biological process through the waste activated sludge	$[M_{PhAC\text{-}wasted}/M_{PhAC\text{-}Total}]$

List of Acronyms

Acronym	Description	Acronym	Description
A2/0	*Anaerobic-anoxic/oxic process*	*NOB*	*Nitrite oxidizing bacteria*
AIC	*Akaike information criterion*	*nRB*	*Number of rotatable bonds*
AIC_C	*Small-sample Akaike information criterion*	*NXR*	*Nitrite oxidoreductase*
AOB	*Ammonia oxidizing bacteria*	*NSE*	*Nash-Sutcliffe efficiency*
AMO	*Ammonia monooxygenase*	*ORP*	*Oxidation-reduction potential*
ASM	*Activated Sludge Models*	*PCP*	*Personal Care Products*
ATU	*Allylthiourea*	*PCR*	*Polymerase chain reaction*
BOD_5	*5-day biochemical oxygen demand*	*PFO*	*Pseudo first order*
CAS	*Conventional activated sludge*	*PA*	*Phosphoric acid*
COD	*Chemical oxygen demand*	*PiEnergy*	*Pi Energy*
CPB	*Cometabolic process based*	*PhAC*[1]	*Pharmaceutical or Pharmaceutically Active Compound*
DAD	*Diode array detector*	*PS-DRPFO*	*Population specific dual rate pseudo first order*
DCA	*1,1-dichloroethane*	*PSA*	*Polar surface area*
DNA	*Deoxyribonucleic acid*	*PTFE*	*Poly tetrafluorethylene*
DO	*Dissolved oxygen*	*qPCR*	*Quantitative real time polymerase chain reaction*
DRPFO	*Dual-rate pseudo first order*	*QSAR*	*Quantitative structural activity relationship*
FA	*Free ammonia*	*QSPR*	*Quantitative structural property relationship*
FLD	*Fluoresencedetection*	*RPM*	*Revolutions per minute*
FNA	*Free nitrous acid*	*rRNA*	*Ribosomal ribonucleic acid*
HAO	*Hydroxylamine oxidoreductase*	*SBR*	*Sequencing batch reactor*
HET	*Heterotrophic bacteria*	*SEF*	*Size exclusion fltration*
HPLC	*High performance liquid chromatography*	*SG*	*Suspended growth*
HRT	*Hydraulic retention time*	*SNR*	*Specific nitrification rate*
IC	*Ion chromatograph*	*SRT*	*Solids retention time*
IWA	*International Water Association*	*SSE*	*Sum of square error*

[1] A separate list of pharmaceutical acronyms is provided

Acronym	Description	Acronym	Description
LC50	*Lethal concentration 50*	*TCA*	*1,1,1-trichloroethane*
LFER	*Linear free energy relationship*	*TCE*	*Trichloroethylene*
LOD	*Limit of detection*	*TKN*	*Total kjedahl nitrogen*
MBR	*Membrane bioreactor*	*TN*	*Total nitogen*
MF	*Microfiltration*	*TOC*	*Total organic carbon*
ML	*Mixed liquor*	*TP*	*Total phosphorus*
MLE	*Modified Lutzak Ettinger*	*TPSA*	*Topoplogical polar surface area*
MLSS	*Mixed liquor suspended solids*	*TSS*	*Total suspended solids*
MLVSS	*Mixed liquor volatile suspended solids*	*UF*	*Ultrafiltration*
MMO	*Methane monooxygenase*	*UV*	*Ultraviolet*
MV	*Molecular volume*	*vdWSA*	*Van der waals surface area*
MW	*Molecular weight*	*VSS*	*Volatile suspended solids*
nHBA	*Number of hydrogen bond acceptors*	*WWTP*	*Wastewater Treatment Plant*
nHBD	*Number of hydrogen bond donors*	*WWTF*	*Wastewater Treatment Facility*

List of Pharmaceutical Acronyms

	Name		Name		Name		Name
ACM	Acetaminophen	DLR	Desloratadine	IRB	Irbesartan	TEL	Telmisartan
AFL	Afluzosin	DPZ	Donepezil	KET	Ketoprofen	TMP	Trimethoprin
ALP	Alprazolam	DXP	Doxepine	LOP	Loperamide	TRA	Tramadol
AMT	Amitryptiline	DXT	Duloxetine	LOR	Loratidine	VEN	Venlafaxine
ATN	Atenolol	DZP	Diazepam	MAP	Maprotiline	VRP	Verampil
ATV	Atorvastatin	EPR	Eprosartan	MET	Metoprolol		
AZL	Azelastine	ERY	Erythromycin	MFA	Mefanamic Acid		
BIP	Biperiden	EZE	Ezetimibe	MIA	Mianserin		
BIS	Bisoprolol	FEX	Fexofenadine	NAP	Naproxen		
BUP	Bupropion	FLU	Flutamide	NEF	Nefadozone		
BZF	Bezafibrate	FLX	Fluoxetine	ORP	Orphenadrine		
CBZ	Carbamazapine	FPN	Fenoprofen	OZP	Oxazepam		
CHD	Cyproheptadine	GLC	Glibenclamide	PAR	Paroxetine		
CLA	Clofibric Acid	GLM	Glimepiride	PIZ	Pizotifen		
CMP	Clomipramine	GMF	Gemfibrozil	PRO	Propanolol		
CPL	Celiprolol	HAL	Haloperidol	REP	Repaglinide		
CPT	Chloprothixene	HCT	Hydrochlorothiazide	RIS	Risperidone		
CTZ	Clotrimazol	HYZ	Hydroxyzine	SER	Sertaline		
DCF	Diclofenac	IBP	Ibuprofen	SMX	Sulfamethaxazole		
DCV	Dicycloverin	IDM	Indomethacin	SOT	Sotalol		

[This page intentionally left blank]

Chapter I. Introduction

I.1. Pharmaceuticals in the Environment

In recent years, the environmental impact of microconstituents[1] has received significant attention across the engineering, science, and lay communities (Daughton and Ternes, 2000; Kolpin et al., 2002; Associated-Press, 2008). In a landmark national reconnaissance study, the United States Geological Survey measured the prevalence of 95 microconstituents in 139 surface water bodies across the United States (Kolpin et al., 2002). There has since been a rapidly increasing number of studies of microconstituents in surface and ground waters, including drinking water sources around the world (Metcalfe et al., 2003b; Tixier et al., 2003; Drillia et al., 2005; Zimmerman, 2005; Ternes, 2007; Siemens et al., 2008; Li et al., 2012). It is important to note here that research documenting the occurrence of chemicals now included in the growing list of microconstituents in natural environments is not new in the scientific community; they have been an environmental engineering challenge for over three decades (Keith, 1976; Hignite and Azarnoff, 1977; Bouwer et al., 1984; Richardson and Bowron, 1985; Knackmuss, 1996; Halling-Sørensen et al., 1998). However, it is only in recent years that managing the potential ecotoxicoloical risks posed by the more than 3,000 microconstituents has come to the forefront of environmental science and engineering (Daughton and Ternes, 1999; Kolpin et al., 2002).

[1] The term microconstituents here is intended to be consistent with the definition proposed by the Water Environment Federation (WEF): *Natural and manmade substances, including elements and inorganic and organic chemicals, detected within water and the environment, for which a prudent course of action is suggested for the continued assessment of the potential effect on human health and the environment* WEF (2007). Microconstituents Glossary. Alexandria, VA, Water Environment Federation.

Introduction

To date no data have been published on any adverse effects of microconstituents on humans through environmental exposure. Assessments of the human health risks due to microconstituents through drinking water and fish consumption suggest margins of safety of greater than 100 (Cunningham et al., 2009; Bruce et al., 2010; Kumar et al., 2010). There is, however, an increasing body of evidence that suggests chronic exposure, even at extremely low concentrations could have adverse effects on ecosystems, such as impaired embryo development, modified feeding behavior, suppression of algae growth and reduction in algal respiration rates (Cleuvers, 2004; Kostich and Lazorchak, 2008; Quinn et al., 2009; Rossi-Marshall et al., 2013). While some of these effects are reversible, other anatomical, physiological, and genetic alterations are permanent (Larsen, 2009). Thus, the challenge of assessing, understanding, and mitigating the deleterious influence of microconstituents on the environment is one of the great challenges facing the environmental engineering and science community (Schwarzenbach et al., 2006).

The environmental effects of pharmaceuticals (PhACs) as microconstituents are particularly concerning. PhACs are typically designed to target biologically active organisms (Danish-Environmental-Protection-Agency, 2002; Boxall, 2004; Boxall et al., 2012), warranting concerns related to environmental exposure to PhACs. Although the reported environmental concentrations of PhACs are low (nanogram per liter to microgram per liter levels), studies suggest these compounds can be highly recalcitrant and persist in the environment for months to years (Andreozzi et al., 2003; Monteiro and Boxall, 2009 and 2010). That notwithstanding, PhACs are essential to modern society – to eradicate and control disease and improve the quality of life.

Introduction

There is an extensive body of knowledge evaluating the benefits and risks of PhAC to humans. However, until recently, there has been relatively little research directed towards understanding the ecotoxicological impacts of PhACs. Studies evaluating chronic exposure to PhACs at microgram per liter levels report decreased embryo hatching, reduced growth rate in fish and impacts on endocrine system activity in aquatic species (Massarsky et al., 2011; Ings et al., 2012). Management of PhAC discharges into the environment through regulation and enhancement of treatment processes could alleviate such deleterious effects on aquatic organisms.

Wastewater treatment plants (WWTP) effluents are a significant point source of PhACs into the environment. In fact, PhACs have been found at high frequencies in WWTP effluents and receiving waters downstream of WWTP effluent discharge points (Kolpin et al., 2002; Metcalfe et al., 2003a; Castiglioni et al., 2006; Ternes et al., 2007; Sui et al., 2011). Current WWTP effluent quality requirements (e.g., BOD_5, TSS, TN, and TP) are largely focused on mitigating the impact of nutrient discharges on the environment and may be insufficient to address PhAC reductions. An exclusive focus on nutrient removal without addressing the potential environmental risks posed by PhACs and the other over 3,000 microconstituents is not an environmentally sustainable proposition.

Interestingly however, incomplete removal PhACs in WWTPs has been reported in numerous WWTPs. Furthermore, some studies have linked removal of PhACs to operation at solids retention times (SRTs) typically associated with biological nutrient removal (Clara et al., 2005; Oppenheimer et al., 2007). Consequently, effluent quality targets for low nitrogen and phosphorus levels may provide an opportunity to address some of the emerging concerns related to the environmental impact of PhACs, and

microconstituents more generally. Few studies, however, have attempted to elucidate the biochemical processes responsible for PhAC degradation. Therefore, there is a critical need for mechanistic research that elucidates processes that degrade or remove PhACs during biological nutrient removal. This need is particularly urgent given the explosion in development and use of PhACs not only in the developed, but also in developing countries, over the last thirty years (Robinson et al., 2007).

The goal of this research is to evaluate the potential synergy between biological nutrient removal processes and PhAC attenuation. Experiments and modeling in this research are focused on assessing the role of nitrification processes, specifically ammonia oxidation, in PhAC biodegradation. The application of a cometabolic model to describe PhAC biodegradation during ammonia oxidation is explored. It is anticipated that experimental and modeling results will help fill knowledge gaps related to predicting PhAC biodegradation during biological nutrient removal. Also included in this body of research is a critical evaluation of PhAC attenuation in biological wastewater treatment processes. Peer reviewed studies from the literature are utilized to assess the role of sorption and biodegradation in PhAC attenuation across multiple WWTPs, processes and unit operations. Results from this assessment may have relevance for the wastewater treatment design and operations community of practice.

I.2. Dissertation Organization

This dissertation is organized into ten chapters including this introduction. A review of the literature related to nitrification and cometabolic biodegradation processes is provided in Chapter II. A critical review of studies evaluating the removal, biodegradation and sorption of PhACs during biological wastewater treatment is presented in Chapter III. The specific objectives and hypotheses evaluated in this research and presented in Chapter IV. Details related to experimental and mathematical modeling methods employed in this research are provided in Chapter V. The development and assessment of predictive models to describe PhAC sorption during biological wastewater treatment is explored in Chapter VI. The development and implementation of a cometabolic process based model to describe PhAC biodegradation by ammonia oxidizing bacteria, using a set of beta-blockers as a test case, is presented in Chapter VII. An evaluation of the Generalized Likelihood Uncertainty Assessment (GLUE) methodology to develop confidence and prediction intervals when modeling nitrification coupled with pharmaceutical biodegradation is explored in Chapter VIII. Subsequent testing and evaluation of the cometabolic process based model developed in this research is discussed in Chapter IX using naproxen as a model PhAC. Finally a synthesis of conclusions and recommendations for further research are presented in Chapter X.

Chapter II. Literature Review of Nitrification and Cometabolic Biodegradation

II.1. Nitrification in Wastewater Treatment

II.1.1. Nitrogen Management and Wastewater Treatment

Management of the nitrogen cycle and more specifically reduction of nitrogenous discharges into the environment are significant challenges faced by the environmental engineering/science community (National Academy of Engineering, 2010). Consequently, nitrogen management features prominently in the design and operation of modern wastewater treatment plants (WWTPs) (Gujer, 2010). Influents to WWTPs largely consist of nitrogen in the form of organic nitrogen and ammonia (collectively Total Kjedahl Nitrogen, TKN). WWTPs convert TKN into inorganic nitrogen species (nitrite and nitrate) and nitrogen gas through a combination of aerobic and anaerobic biological processes. The conventional processes utilized to achieve this are ammonification (conversion of organic nitrogen to ammonia), nitrification (conversion of ammonia nitrogen to inorganic nitrogen) and denitrification (Degrémont S.A., 1991; Grady et al., 1999; Metcalf & Eddy et al., 2003; Chapra, 2008). Conventional biological nitrification in WWTPs typically occurs in two steps with the involvement of two bacterial consortia – ammonia oxidizing bacteria (AOB) and nitrite oxidizing bacteria (NOB) – in an aerobic environment. In recent years research has been conducted to evaluate the mechanisms of nitrous oxide (N_2O) production during nitrification given the role of N_2O as a greenhouse gas (USEPA, 2009; Ahn et al., 2010). Increased attention is also being been paid to alternate nitrification processes which result in significant

energy savings such as aerobic ammonium oxidation (Anammox) (Mulder et al., 1995; van Loosdrecht, 2008; van der Star et al., 2011). The focus in this research is on conventional biological nitrification.

II.1.2. Ammonia Oxidation & AOB

Oxidation of ammonia to nitrite by AOB proceeds through a multistep process involving the oxidation of ammonia to hydroxylamine catalyzed by ammonia monooxygenase (AMO) followed by oxidation of hydroxylamine to nitrite catalyzed by hydroxylamine oxidoreductase (HAO) as illustrated in Figure II-1 (Arp and Stein, 2003). AOB are autotrophic in aerobic environments, deriving energy from ammonia oxidation and carbon from inorganic sources (Prosser, 1989). In the first step, ammonia (NH_3), rather than ammonium (NH_4^+), is oxidized to hydroxylamine by membrane bound AMO enzyme (Suzuki et al., 1974) with molecular oxygen providing the reducing power (see Equation II-1). In the second step, hydroxylamine is oxidized to nitrite by HAO, using oxygen derived from water for reducing power as shown in Equation II-2 (Prosser, 1989; Hooper et al., 1995).

$$NH_3 + O_2 + 2H^+ + 2e^- \xrightarrow{AMO} NH_2OH + H_2O \qquad \Delta G = -120 \text{ kJ/mol} \quad \text{(II-1)}$$

$$NH_2OH + H_2O \xrightarrow{HAO} HNO_2 + 4H^+ + 4e^- \qquad \Delta G = -114 \text{ kJ/mol} \quad \text{(II-2)}$$

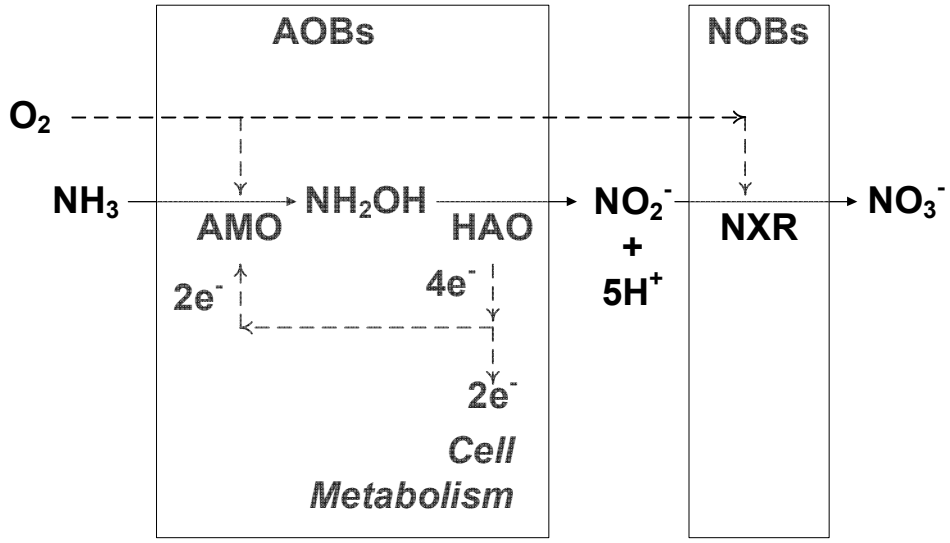

Figure II-1: Enzyme systems involved in ammonia oxidation by AOB and nitrite oxidation by AOB Processes in Aerobic Environments [Adapted from (Arp et al., 2002)]

II.1.2.1. Ammonia Monooxygenase (AMO)

AMO, both membrane bound and in soluble form, is capable of oxidizing ammonia to hydroxylamine (Gilch et al., 2009). However, it is not known whether the oxidation of ammonia occurs on the periplasmic or cytoplasmic side of the membrane. Researchers have hypothesized that it would be advantageous for the bacteria if the oxidation occurs in the periplasm thereby ensuring no hydroxylamine (which is toxic to the bacteria) exists in the cytoplasm (Arp and Stein, 2003).

Known substrates and inhibitors of AMO are non-polar compounds suggesting that the active site of AMO is hydrophobic (Hooper et al., 1997). AMO demonstrates a broad substrate specificity with an ability to oxidize a wide range of organic compounds (Keener and Arp, 1994; Arp et al., 2001; Batt et al., 2006; Khunjar et al., 2011; Taher and Chandran, 2013), suggesting it may be relevant in the oxidation of some PhACs. Inhibition of AMO by copper chelators (Hooper and Terry, 1973) and activation of AMO by copper (II) (Ensign et al., 1993) suggest that copper plays an integral role in the enzymatic mechanism of AMO. Electron paramagnetic resonance (EPR) spectroscopy

and inactivation studies with nitrapyrin suggest that iron (II) is present in the enzymatic pocket (Zahn et al., 1996). AMO in pure cultures of *N.Europaea spp.* shows irreversible product toxicity with increasing nitrite concentrations. For example, the reduction in NH_4^+ oxidizing activity is approximately 15% and 55% at 0.5 mM and 20 mM NO_2, respectively (Stein and Arp, 1998).

II.1.2.2. Hydroxylamine Oxidoreductase (HAO)

HAO is an abundant periplasmic protein. Crystallographic studies suggest that HAO is trimer shaped, like a head of garlic (Igarashi et al., 1997). Sequencing of the genome of Nitrosomonas Europaea (*N.Europaea spp.*), the most widely studied model AOB, indicates there are multiple copies of the genes encoding for both AMO and HAO (Chain et al., 2003). Interestingly, the multiple copies of these two gene clusters are within proximity of each other. HAO is critical for electron and proton transport as part of the energy metabolism (i.e., nitrification process) in AOB. Two of the four electrons produced from oxidation of HAO mediated hydroxylamine oxidation are required for AMO function, while two others are used for ATP synthesis within the cell (Hooper et al., 1997).

II.1.3. Nitrite Oxidation & NOB

Nitrite oxidation is catalyzed by nitrite oxidoreductase (NXR) (Spieck et al., 1996). NOB are facultative chemolithoautotrophs responsible for the oxidation of nitrite to nitrate (Equation II-3).

$$NO_2^- + 0.5O_2 \xrightarrow{NXR} NO_3^- \qquad \Delta G = -54\ kJ/mol \quad (II\text{-}3)$$

To date, four genera of NOB have been identified: *Nitrospira*, *Nitrobacter*, *Nitrosococcus* and *Nitrospina* (Teske et al., 1994). Molecular analyses of bacterial cultures have shown that *Nitrospira* like bacteria are the dominant NOB species in WWTPs (Juretschko et al.,

1998; Okabe et al., 1999; Daims et al., 2001). This has been attributed to two primary factors: (i) the typically low nitrite concentrations in biological treatment processes in WWTPs and (ii) that *Nitrospira* are K-strategists whereas *Nitrobacter* are r-strategists (Schramm et al., 1999; Schramm et al., 2000). K-strategists have high substrate affinities and typically lower maximum specific growth rates than r-strategists (Andrews and Harris, 1986; Schramm et al., 1999). The enzyme responsible for nitrite oxidation is nitrite oxidoreductase (NXR).

II.1.3.1. Nitrite Oxidoreductase (NXR)

NXR is both a membrane bound enzyme responsible for the oxidation of nitrite to nitrate. Crystallographic studies and genome sequence of the nitrite oxidizing bacteria Nitrobacter Winogradsky (*N.Winogradsky spp.*) indicate that NXR consists of two subunits alpha (large) and beta (small) encoded by nxrA and nxrB, respectively (Spieck et al., 1996; Starkenburg et al., 2006). The NXR enzyme encoding complex also consists of one additional upstream gene (Starkenburg et al., 2006) which is predicted to encode c-type cytochromes previously found in enzyme purification and evaluation studies (Tanaka et al., 1983; Sundermeyer-klinger et al., 1984). In the downstream section of the NXR cluster are genes which provide denitrification (i.e., nitrate reduction) capabilities to nitrite oxidizing bacteria and a nitrite/nitrate transporter. The alpha-subunit of the enzyme, consisting of the nitrite-substrate binding site, contains zinc, molybdenum, iron and copper. The beta subunit, consisting of multiple iron-sulfur centers, is responsible of electron transport between NXR and the electron transport chain.

II.1.4. Modeling Nitrification in Wastewater Treatment

Modeling of nitrification in wastewater treatment is carried out at the process-scale rather than the enzyme-scale. The solutes accounted for in nitrification models are ammonia-nitrogen (S_{NH}), nitrite- nitrogen (S_{NO2}) and nitrate- nitrogen (S_{NO3}). AOB are modeled as a single biomass unit, rather than modeling the AMO and HAO enzyme systems and similarly, NOB are modeled rather than NXR.

The Activated Sludge Models (ASM) framework established by the International Water Association (IWA) (Henze et al., 2000), is extensively used to model biological processes in WWTPs. Since the publication of the IWA task group's work on developing a unified modeling framework for wastewater professionals, numerous authors have adapted and extended the ASM models to include a wide array of processes. A detailed review of all upgrades to the ASM modeling framework is outside the scope of this research. For the purposes of this research, extensions related to implementation of a two-step nitrification process model (rate equations and parameters) and critical aspects in their development are described in this section.

II.1.4.1. Modeling AOB Growth

The growth of AOB is modeled using Monod kinetics with ammonia nitrogen as the primary substrate. The effect of reactor dissolved oxygen (DO) on AOB growth is also incorporated through the use of a Monod saturation function as a switching function as shown in Equations II-4 and II-5 (Henze et al., 2000). While other formulations for AOB growth have previously been proposed by researchers (e.g., first order model proposed by Balakrishnan and Eckenfelder (1969)), the saturation kinetics model for AOB growth is well established in environmental engineering (Orhon and Artan, 1994; Grady et al., 1999; Metcalf & Eddy et al., 2003).

$$\mu_{AOB} = \mu_{MAX,AOB}\left(\frac{S_{NH}}{K_{NH}+S_{NH}}\right)\left(\frac{S_O}{K_{O,AOB}+S_O}\right) \quad \text{(II-4)}$$

$$r_{AOB} = \left[\mu_{MAX,AOB}\left(\frac{S_{NH}}{K_{NH}+S_{NH}}\right)\left(\frac{S_O}{K_{O,AOB}+S_O}\right)\right]X_{AOB} \quad \text{(II-5)}$$

Reported values for AOB growth biokinetic parameters are shown in Table II-1. Measured values for $\mu_{MAX,AOB}$ vary from 0.24±0.12 d^{-1} (Chandran et al., 2005) to 1.6 d^{-1} (Munz et al., 2011a) (see Table II-1) with lower values typically associated with longer SRT (Munz et al., 2011a). Values of K_{NH} and K_O range from 0.14 to 1.0 mg-NL^{-1} and 0.34 – 0.8 mgL^{-1}, respectively. Careful attention must be paid to reactor operating conditions when utilizing these AOB biokinetic parameters.

Table II-1: Reported literature values for nitrifier and AOB growth related biokinetic parameters

Reference	$\mu_{MAX,NITRIFIERS}$ (d^{-1})	$\mu_{MAX,AOB}$ (d^{-1})	K_{NH} (mg N/L)	$K_{O,AOB}$ (mg O_2/L)	Expt. Temp. (^oC)	Comments
Henze et al. (1987)	0.80		1.0	0.40	20	ASM1 model (IWA task group)
	0.3		1.0	0.40	10	ASM1 model (IWA task group)
Henze et al. (1995) Henze et al. (1999)	1.00		1.0	0.50	20	ASM2 & ASM2d models (IWA task group)
	0.35		1.0	0.50	10	ASM2 & ASM2d models (IWA task group)
Henze et al. (2000)	1.0		1.0	0.50	20	ASM3 model (IWA task group)
	0.35		1.0	0.50	10	ASM3 model (IWA task group)
Koch et al. (2000)	1.3±0.4		1.0	0.50	20	
Chandran et al. (2005)		0.24±0.12 0.48±0.07 1.2±0.02	0.58±0.29 0.58±0.15 0.44±0.095	N.R	25	
Vadivelu et al. (2006)		1.03±0.17	N.R	N.R	30	Enriched Nitrosomonas culture
Ahn et al. (2008)		1.08±1.03 0.73±0.70		0.74	22-25	Experiments at room temperature K_O values from Guisasola et al. (2005) Under DO limitation conditions
Jubany et al. (2008); Jubany et al. (2009)		1.21		0.74	25	Andrews model for dependence on free ammonia (FA); Inhibition of growth by free nitrous acid (FNA).

Table II-1: Reported literature values for nitrifier and AOB growth related biokinetic parameters

Reference	$\mu_{MAX,NITRIFIERS}$ (d^{-1})	$\mu_{MAX,AOB}$ (d^{-1})	K_{NH} (mg N/L)	$K_{O,AOB}$ (mg O_2/L)	Expt. Temp. (^oC)	Comments
Kaelin et al. (2009)		0.8 - 1.1	0.14±0.07	0.79±0.08	20	Experiments at 14 & 20 ^oC, but values reported at 20^oC
Munz et al. (2010)		0.49±0.08 0.35±0.07	N.R	N.R	20	MBR process, SRT = 20 d
		0.45±0.04	N.R	N.R	20	Suspended growth process, SRT = 20 d
		0.72±0.2	N.R	N.R	20	Suspended growth process, SRT = 8 d
Munz et al. (2011a)		0.80 - 1.2	N.R	0.34	20	AE SBR, SRT = 2-5 d
		0.8 - 1.6	N.R	0.40	20	AE/AX alternating SBR, SRT = 2-5 d

Notes:
1. N.R. – Not Reported

II.1.4.2. Modeling AOB Decay

Aerobic decay of AOB is modeled as first order relative to the AOB concentration. A saturation function is used to lower the effective decay rate at low DO concentration in a fashion similar to modification of the AOB growth rate (Manser et al., 2006; Munz et al., 2011b). In the original ASM model – ASM1 – the decay rate of AOB was considered to be independent of DO and first order as a function of biomass concentration. The IWA task group did note however that this modeling approach for decay was selected for its simplicity and utility but did not necessarily capture the mechanistic processes involved in biomass decay. The task group further acknowledged that additional research was needed to evaluate the impact of environmental conditions on the biomass decay rate (Henze et al., 1987).

The decay rate of AOB (b_{AOB}) and nitrifiers (b_{NIT}) is lower under anoxic conditions than aerobic conditions (Siegrist et al., 1999; Manser et al., 2006; Munz et al., 2011b). Siegrist et al. (1999) proposed two critical modifications to the nitrifier decay process rate equation in the ASM1 model. A rate modification parameter ($\eta_{NIT\text{-}AX}$) was incorporated to lower the base nitrifier decay rate under anoxic conditions ($b_{NIT\text{-}AX}$) and two switching functions were included to reduce the aerobic decay rate ($b_{NIT\text{-}AE}$) as the DO is lowered and increase the anoxic decay rate ($b_{NIT\text{-}AX}$) as the DO is lowered (Equation II-6). Siegrist et al. (1999) proposed a value of 0.333 for ($\eta_{AOB\text{-}AX}$) and 0.50 for $K_{O,AOB}$. Slower nitrifier decay rate under anoxic conditions was confirmed by Lee and Oleszkiewicz (2003) who found that $b_{NIT\text{-}AX}/b_{NIT\text{-}AE} = 0.36$.

Rate equations for nitrifier decay rates proposed by Siegrist et al. (1999)

$$r_{NIT-DECAY} = b_{NIT}\left[\left(\frac{S_O}{K_{O,NIT-DECAY}+S_O}\right)+\eta_{NIT-AX}\left(\frac{K_{O,NIT-DECAY}}{K_{O,NIT-DECAY}+S_O}\right)\right]X_{NIT} \quad \text{(II-6)}$$

This formulation for nitrifier decay proposed by Siegrist et al. (1999) does not differentiate between the decay rates of AOB and NOB. This shortcoming was addressed by Manser et al. (2006), who extended the ASM3 model to include separate process equations for growth and decay of AOB and NOB. Two separate processes were proposed for AOB decay under aerobic and anoxic conditions. Under aerobic conditions, the AOB decay rate ($r_{AOB\text{-}DECAY,AE}$) was considered proportional to the biomass concentration and a saturation function was used to reduce the decay rate at lower DO conditions (Equation II-7). Under anoxic conditions (Equation II-8), an inverse saturation function was used to model the impact of DO on the anoxic decay rate ($r_{AOB\text{-}DECAY,AX}$). In addition, nitrate was considered inhibitory to endogenous respiration of AOB and its effect is captured using an additional saturation function to reduce the base anoxic decay rate. This use of separate process rate equations for aerobic and anoxic decay allows for dissolved oxygen to be seamlessly modeled as being used during aerobic decay but not during anoxic decay.

Rate equations for AOB decay rates under aerobic and anoxic conditions proposed by Manser et al. (2006):

$$r_{AOB-DECAY,AE} = b_{AOB,AE}\left(\frac{S_O}{K_{O,AOB-DECAY}+S_O}\right)X_{AOB} \quad \text{(II-7)}$$

$$r_{AOB-DECAY,AX} = b_{AOB,AX}\left[\left(\frac{K_{O,AOB-DECAY}}{K_{O,AOB-DECAY}+S_O}\right)\left(\frac{S_{NO3}}{K_{NO3}+S_{NO3}}\right)\right]X_{AOB} \quad \text{(II-8)}$$

Iacopozzi et al. (2007) proposed a comprehensive update to the ASM3 model to include a two-step nitrification and denitrification of both nitrate and nitrite. Aerobic AOB decay was described using a process identical to Manser et al. (2006) (Equation II-9). Anoxic decay, however, was modeled as being inhibited by nitrite (Equation II-10), rather than nitrate as previously proposed by Manser et al. (2006). The experimental evidence used to develop this equation are not described by the authors, rather it is attributed to previous work from the same research group (Marsili-Libelli et al., 2001). These details are also not provided in the previous paper. The half saturation value of oxygen with respect to AOB decay proposed by Henze et al. (2000) from the initial ASM3 formulation was used by the authors. The base aerobic and anoxic specific decay rates for AOB – set equal in this work - are attributed to the previously noted work of Marsili-Libeli et. al, 2001.

Rate equations for AOB decay rates under aerobic and anoxic conditions proposed by Iacopozzi et al. (2007):

$$r_{AOB-DECAY,AE} = b_{AOB,AE}\left(\frac{S_O}{K_{O,AOB-DECAY}+S_O}\right)X_{AOB} \qquad \text{(II-9)}$$

$$r_{AOB-DECAY,AX} = b_{AOB,AX}\left[\left(\frac{K_{O,AOB}}{K_{O,AOB-DECAY}+S_O}\right)\left(\frac{S_{NO2}}{K_{NO2}+S_{NO2}}\right)\right]X_{AOB} \qquad \text{(II-10)}$$

Ahn et al. (2008) and Jubany et al. (2009) applied the aerobic formulation proposed by Manser et al. (2006) to model AOB decay in aerobic reactors under DO limited conditions. This approach is acceptable if the system under consideration is operated at aerobic oxidative conditions and the DO is higher than $K_{O,AOB}$. At DO levels at or lower than $K_{O,AOB}$, use of these models results is large changes in $b_{AOB,AE}$ with small changes in DO.

Hiatt and Grady (2008) elected to update ASM1, rather than ASM3, as previously done by Iacopozzi et al. (2007). AOB decay in the updated model proposed by Hiatt and Grady (2008) was assumed to be independent of DO concentration and first-order with respect to the AOB concentration. Kaelin et al. (2009) used the complete formulation proposed by Manser et al. (2006) to modify the ASM3 model framework proposed by the IWA Task Group. In the proposed revision to ASM3, the ratio of the anoxic specific decay rate to the aerobic specific decay rate ($\eta_{AOB\text{-}AX} = b_{AOB,AX}/b_{AOB,AE}$) was set to 0.10.

Munz et al. (2011b) evaluated the decay rate of AOB in a lab scale SBR and proposed a model where the specific decay rate approaches a minimum value ($b_{AOB,AN}$) when the DO equals zero mg/L (Equation II-11). The value of $K_{O,AOB}$ reported by the authors (1.6 mg-O_2/L) is higher than that proposed by previous researchers. And, because of the additive formulation, the specific decay rate at high DO levels is higher than that proposed by previous authors (see Figure II-2).

Rate equations for AOB decay rates under aerobic and anoxic conditions proposed by Munz et al. (2011b):

$$r_{AOB-DECAY,AE} = \left[b_{AOB,AE}\left(\frac{S_O}{K_{O,AOB} + S_O} \right) + b_{AOB,AN} \right] X_{AOB} \qquad \text{(II-11)}$$

Review of the proposed models and parameters for AOB decay in a two-step nitrification model indicates a wide variation in AOB decay rates, particularly under aerobic conditions (Figure II-2).

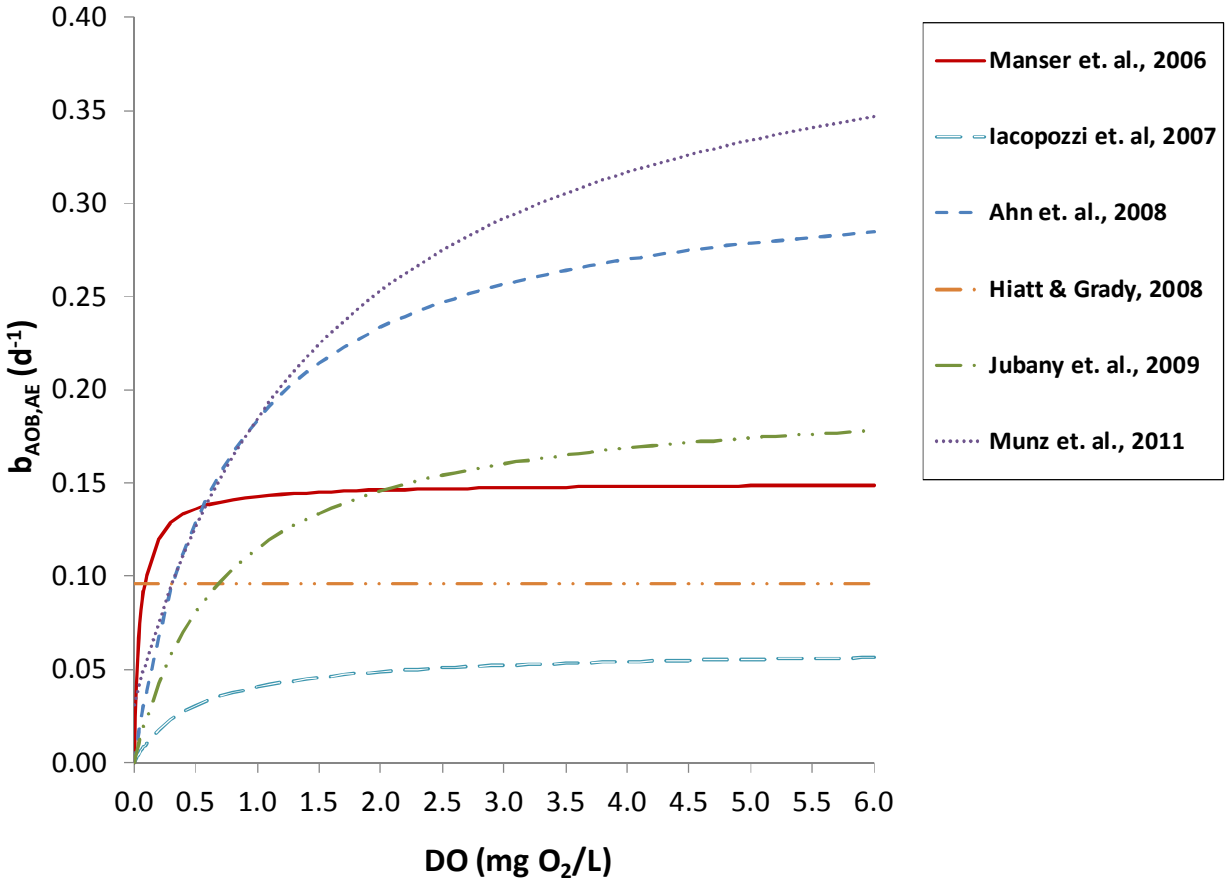

Figure II-2: AOB decay rates as a function of dissolved oxygen levels

Table II-2: Nitrifier and AOB Decay Rates

Condition	Reference	$b_{NITRIFIERS}$ (d^{-1})	b_{AOB} (d^{-1})	$K_{O,AOB\text{-}DECAY}$ (mg O_2/L)	Expt. Temp. (^oC)	Comments
Aerobic	Henze et al. (2000)	0.15				ASM models (IWA task group)
	Siegrist et. al., 1999	0.19 ± 0.05		0.5	12	
		0.21 ± 0.05			20	
	Lee and Olesewicz, 2003	0.153 ± 0.022			20	Non inhibited SBR
		0.152 ± 0.042			20	Inhibited SBR
	Manser et. al., 2006		0.15 ± 0.02	0.5	20	Batch experiments with biomass from suspended growth CAS system. K_O from Koch et. al., 2000
			0.14 ± 0.02	0.5	20	Batch experiments with biomass from MBR. K_O from Koch et. al., 2000
	Iacopozzi et. al., 2007		0.061	0.5		b_{AOB} from Marsili-Libeli et. al, 2001. K_O from Henze et. al., 2000
	Ahn et. al., 2008		0.32 ± 0.34	0.74	room temp	Suspended growth CAS system K_O from Guisasola et. al., 2005
	Hiatt & Grady, 2008		0.096	N/A	20	Only model where decay rate is independent of DO.
	Kaeilin et. al., 2009		0.15	0.80	20	b_{AOB} from Manser et. al., 2006
	Jubany et. al., 2009		0.20	0.74	25	Suspended growth CAS system K_O from Guisasola et. al., 2005
	Munz et. al., 2011a		0.40	1.6	35	Lab scale SBR nb: $b_{AOB,AN}$ = 0.031 ± 0.006 d^{-1}

Table II-2: Nitrifier and AOB Decay Rates

Condition	Reference	$b_{NITRIFIERS}$ (d^{-1})	b_{AOB} (d^{-1})	$K_{O,AOB\text{-}DECAY}$ (mg O_2/L)	Expt. Temp. (^oC)	Comments
Anoxic (AX)	Siegrist et. al., 1999	0.10 ± 0.05			12	
		0.10 ± 0.05			20	
	Manser et. al., 2006		0.015 ± 0.004		20	Batch experiments with biomass from suspended growth CAS system. K_O from Koch et. al., 2000
			0.01 ± 0.003		20	Batch experiments with biomass from MBR. K_O from Koch et. al., 2000
	Iacopozzi et. al., 2007		0.061	0.5		b_{AOB} from Marsili-Libeli et. al, 2001 KO from Henze et. al., 2000
	Ahn et. al., 2008		0.20 ± 0.22	0.74	room temp	Suspended growth CAS system. K_O from Guisasola et. al., 2005
	Kaeilin et. al., 2009		0.015	0.80	20	$b_{AOB,AX}$ calculated using $h_{AOB,AX}$ (0.10)

II.1.4.3. Modeling NOB Growth

As previously noted, nitrification was originally modeled as a single step process in the ASM model framework (Henze et al., 1987) even though the biochemistry of nitrification was well known at the time. Chandran and Smets (2000) compared the original 1-step nitrification with a new 2-step nitrification model for batch experiments. NOB growth was modeled using Monod kinetics with nitrite as the substrate (Equation II-12). It is interesting to note that DO – which is included in growth models for NOB by other researchers - is not included in the formulation proposed by Chandran and Smets (2000) because batch experiments carried out by the authors is at DO concentrations significantly higher than the half saturation value.

Rate equations for NOB growth rate developed by Chandran and Smets (2000):

$$r_{NOB\text{-}GROWTH} = \mu_{MAX,NOB}\left[\left(\frac{S_{NO2}}{K_{NO2}+S_{NO2}}\right)\right]X_{NOB} \qquad \text{(II-12)}$$

Marsili-Libelli et al. (2001) modified the ASM2d model to include two steps for nitrification in order to model an SBR. NOB growth was modeled using saturation functions for nitrite and oxygen. An inhibition function was used to model the effect of ammonia on NOB growth (Equation II-13) based on experimental evidence presented by Andreottola et al. (1997).

Rate equations for NOB growth rate evaluated by (Marsili-Libelli et al., 2001):

$$r_{NOB-GROWTH} = \mu_{MAX,NOB}\left[\left(\frac{S_{NO2}}{K_{NO2,NOB}+S_{NO2}}\right)\left(\frac{S_O}{K_{O,NOB}+S_O}\right)\left(\frac{K_{NHi}}{K_{NHi}+S_{NH}}\right)\right]X_{NOB} \qquad \text{(II-13)}$$

Hiatt and Grady (2008) modeled NOB growth occurring autotrophically using nitrite as well as mixotrophically using readily biodegradable COD. It is important to note that Hiatt and Grady (2008) use free nitrous acid (FNA) as the substrate for autotrophic

growth rather than nitrite as typically used by other researchers. The primary motivation for this modification by the researchers was that the intended use of this model is for systems with high nitrogen levels. FNA is considered inhibitory to NOB and the authors use the Andrews equation (Andrews, 1968) to model this inhibition (Equation II-14). FNA is calculated as a function of the nitrite concentration, temperature and pH as shown in Equation II-15. Ammonia inhibition to NOB growth is also incorporated into this model; however, free ammonia (FA) is considered inhibitory rather than total ammonia-nitrogen. FA is calculated as a function of the total ammonia-nitrogen concentration and the system pH (Equation II-16).

Rate equations for NOB growth rate proposed by Hiatt and Grady (2008)

$$r_{NOB-GROWTH} = \mu_{MAX,NOB}\left[\left(\frac{S_{FNA}}{K_{FNA}+S_{FNA}+\frac{S_{FNA}^2}{K_{I,FNA}}}\right)\left(\frac{S_O}{K_{O,NOB}+S_O}\right)\left(\frac{K_{I,FA}}{K_{I,FA}+S_{FA}}\right)\right]X_{NOB} \quad \text{(II-14)}$$

$$S_{FNA} = S_{NO2}\left[\frac{1}{\left(e^{-[2{,}300(273+\theta)]}\right)+10^{pH}}\right] \quad \text{(II-15)}$$

$$S_{FA} = S_{NH}\left[\frac{10^{pH}}{\left(e^{\left[6{,}344/(273+\theta)\right]}\right)+10^{pH}}\right] \quad \text{(II-16)}$$

II.1.4.4. Modeling NOB Decay

Decay of NOB is modeled as first order relative to the NOB concentration. A saturation function is used to lower the effective decay rate at low DO concentration in a fashion similar to modification of AOB decay rate. Nowak et al. (1995) proposed a dual equation

formulation, with separate decay equations for aerobic and anoxic/anaerobic conditions (Equations II-17 and II-18). Iacopozzi et al. (2007) proposed a similar formulation, however, anoxic decay of NOB was linked to nitrate concentration (S_{NO3}) in addition to the dissolved oxygen concentration (Equations II-19 and II-20). Note that this is analogous to the AOB decay equations developed by the researchers. One drawback of such dual equation formulations is the decision of what is considered anoxic condition versus aerobic condition. For example, when the dissolved oxygen is 0.5 mg/L – use of the aerobic equation proposed by Nowak et al. (1995) results in a specific decay rate (b_{NOB}) of 0.11 d^{-1}, whereas use of the anoxic equation under the same conditions results in b_{NOB} = of 0.27 d^{-1}.

Rate equations for NOB decay rates under aerobic and anoxic conditions proposed by Nowak et al. (1995):

$$r_{NOB-DECAY,AE} = b_{NOB,AE}\left(\frac{S_O}{K_{O,NOB-DECAY}+S_O}\right)X_{NOB} \quad \text{(II-17)}$$

$$r_{NOB-DECAY,AX} = b_{NOB,AX}\left[\left(\frac{K_{O,NOB-DECAY}}{K_{O,NOB-DECAY}+S_O}\right)\right]X_{NOB} \quad \text{(II-18)}$$

Rate equations for NOB decay rates under aerobic and anoxic conditions proposed by Iacopozzi et al. (2007):

$$r_{NOB-DECAY,AE} = b_{NOB,AE}\left(\frac{S_O}{K_{O,NOB-DECAY}+S_O}\right)X_{NOB} \quad \text{(II-19)}$$

$$r_{NOB-DECAY,AX} = b_{NOB,AX}\left[\left(\frac{K_{O,NOB-DECAY}}{K_{O,NOB-DECAY}+S_O}\right)\left(\frac{S_{NO3}}{K_{NO3}+S_{NO3}}\right)\right]X_{NOB} \quad \text{(II-20)}$$

Ahn et al. (2008) and Jubany et al. (2009) have proposed models where the decay rate of NOB is zero when the dissolved oxygen equals zero (Equation II-21). Interestingly, the value of $b_{NOB,AE}$ proposed by the separate references are significantly different – 0.75 ± 0.8 d^{-1} and 0.17 d^{-1} for Ahn et al. (2008) and Jubany et al. (2009), respectively. However both use a half saturation oxygen concentration ($K_{O,NOB\text{-}DECAY}$) of 1.75 mg-N/L, based on Guisasola et al. (2005).

Rate equations for NOB decay rates under aerobic and anoxic conditions proposed by Ahn et al. (2008) and Jubany et al. (2009):

$$r_{NOB\text{-}DECAY,AE} = b_{NOB,AE}\left(\frac{S_O}{K_{O,NOB\text{-}DECAY}+S_O}\right)X_{NOB} \qquad \text{(II-21)}$$

The model proposed by Munz et al. (2011b) for NOB decay, Equation II-22, incorporates the effect of DO proposed by previous researchers, but uses a baseline decay rate under anaerobic conditions ($b_{NOB,AN}$) when the DO equals 0 mg/L. This framework assumes that the decay of NOB is not influenced by the nitrate concentration (S_{NO3}).

Rate equations for NOB decay rates under aerobic and anoxic conditions proposed by Munz et al. (2011b):

$$r_{NOB-DECAY,AE} = \left[b_{NOB,AE}\left(\frac{S_O}{K_{O,AOB}+S_O}\right)+b_{AOB,AN}\right]X_{NOB} \qquad \text{(II-22)}$$

II.1.4.5. Modeling Ammonia, Nitrite and Nitrate

Ammonia is oxidized to nitrite by AOB and consumed as a nutrient by both AOB and NOB. Nitrite is produced as a result of AOB growth and consumed through NOB growth. Nitrate is produced through NOB growth.

II.2. Cometabolic Biodegradation of Environmental Pollutants

II.2.1. Introduction to Cometabolic Biodegradation

Bacteria possess enzymes which are able to degrade certain compounds without using them as either a source of energy or as a growth substrate. Fortuitous transformation of a compound through this mechanism is considered cometabolic biodegradation (Criddle, 1993). Extensive research has been conducted evaluating cometabolic transformations of organic compounds over the last 40 years. Horvath (1972) identified twenty different bacterial species and a similar number of organic compounds which are cometabolically degraded. Since then, a number of authors have identified cometabolic degradation of environmentally relevant pollutants ranging from chlorinated and aromatic organic compounds (Alvarez-Cohen and McCarty, 1991; Criddle, 1993; Keener and Arp, 1994; Kocamemi and Cecen, 2005 and 2007 and 2009 and 2010b and a) to endocrine disrupting compounds (Skotnicka-Pitak et al., 2009). The majority of research related to environmental applications and implications of cometabolic biological processes is related to the fate of chlorinated solvents in the environment. Alvarez-Cohen and Speitel (2001) reviewed the range of kinetic models developed and used in environmental engineering. Cometabolic biodegradation during nitrification is typically attributed to AOB, which have been shown to catalyze oxidation of a wide array of aliphatic, aromatic and chlorinated organic substrates (Keener and Arp, 1994; Hooper et al., 1995; Kocamemi and Cecen, 2005 and 2009 and 2010b and a) and endocrine disrupting compounds (Gaulke et al., 2009; Skotnicka-Pitak et al., 2009). This ability to cometabolically biodegrade a wide range of organic compounds has been attributed to the lack of substrate specificity of AMO.

II.2.2. Cometabolic Biodegradation During Biomass Growth

Consumption of the primary growth or energy substrate is typically modeled using Monod kinetics to describe the growth of the biomass and consumption of the substrate. A critical assumption of this modeling approach is that biomass growth depends on the concentration of the substrate. In the case of cometabolic biodegradation, where the degradation of the compound under consideration occurs fortuitously and does not contribute to growth, this assumption is invalid.

An alternate formulation for biomass growth independent of substrate concentration can be developed using a logistic model for biomass growth and saturation kinetics to describe degradation of the cometabolically degraded compound (Schmidt et al., 1985). The primary advantage of using the logistic function to describe biomass growth, rather than a Monod function, is the ability to obtain a closed form analytical solution to the growth equation. A limitation of this approach for wastewater treatment plant modeling is the need to define a maximum carrying capacity for biomass in the reactor (X_{MAX}), particularly considering the dynamic nature of the wastewater treatment plant. Using the base-model shown in Equation II-23 (in Table II-3), Schmidt et al. (1985) derived limiting cases based on the biomass concentration and cometabolic substrate concentration.

Researching the cometabolic degradation of chlorinated solvents (TCE) by methanotrophs, Strand et al. (1990) hypothesized that the chlorinated solvent competed with the primary substrate (methane) for catalytic sites on methane monooxygenase (MMO). To model the process, the authors assumed Monod kinetics for degradation of both the growth substrate (methane) and the chloroethene (TCE). However, the half saturation value for TCE was modified assuming competitive

inhibition (Bailey and Ollis, 1986) by the growth substrate (methane) (see Equation II-24 in Table II-3). The impact of starvation conditions was also evaluated by the authors. Early in the starvation process – the degradation rate was first order but the rate dropped sharply after approximately 65 hours of starvation. No model was proposed by the authors for the cometabolic degradation of TCE during endogenous respiration/biomass decay.

A model for cometabolism coupled with competitive inhibition was also evaluated by Semprini and McCarty (1991 and 1992) for subsurface biodegradation of chlorinated aliphatics by methanotrophs. A salient modification of the classical competitive inhibition model was the inclusion of a decay function to capture the attenuation in cometabolic transformations of chlorinated aliphatics by methanotrophs (Equation II-25 in Table II-3). The model proposed Semprini and McCarty (1992) also explicitly incorporated the need for aerobic conditions for the cometabolic process. This model is an early adopter of the biomass decay (and resulting reduction in enzyme activity) within the context of cometabolism. The fraction of biomass *active for cometabolism* (F_A) is considered 1.0 when biomass is growing and decays exponentially once growth is complete (Equation II-26 in Table II-3).

The degradation of the cometabolic substrate can also be linked to the consumption of the growth substrate using the ***transformation capacity approach*** described by Criddle (1993), where the transformation capacity (T_C) is defined as the mass of non-growth compound transformed per unit mass of growth (or energy) substrate consumed during growth. In addition, Criddle (1993) noted that it is conceivable that the bacteria have the capability to degrade the non-growth compound in the absence of the growth substrate (i.e., during endogenous respiration/decay)

which is discussed in more detail in the next section. These two concepts are coupled in the model proposed by Criddle (1993) for the cometabolic degradation of a compound during bacterial growth (Equation II-27 in Table II-3). The model as presented, is only relevant in systems where the nongrowth compound is not inhibitory – with competitive inhibition between the growth substrate and the cometabolic substrate the half saturation for the cometabolic substrate to be modified (Chang and Criddle, 1997).

A noncompetitive model was used by Keenan et al. (1994) to model the degradation of TCE in the presence of a mixed consortium of growing propane oxidizers (Equation II-28 in Table II-3). The presence of propane does not impact the half saturation value of TCE, but the maximum specific rate of cometabolic substrate degradation is impacted by the growth substrate.

The research described thus far was developed through studies using suspended mixed or axenic cultures. It is thought that the same treatment may not be appropriate for biofilms considering the potential mass transfer limitations of the film, the changing redox conditions within the film and the presence of extracellular polymeric substances containing active enzymes on the outside of the film (Wilderer and Characklis, 1989). Arcangeli and Arvin (1997) researched cometabolic biodegradation of TCE in fixed film systems with toluene oxidizing mixed cultures and evaluated a degradation model hypothesizing that (i) toluene and TCE are cross-competitive and (ii) a minimum concentration of toluene (and consequently biomass growth) is required for cometabolic degradation of TCE (Arcangeli et al., 1995; Arcangeli and Arvin, 1997). While the model proposed by the authors (Equation II-29 in Table II-3) is framed in terms of the need for the growth substrate to provide reducing equivalents for the cometabolic process to continue, it is effectively equivalent to noting that cometabolic

degradation only occurs when biomass is growing. For biofilm systems however, monitoring the growth rate of biomass is significantly more challenging than for suspended growth system – it may therefore be advantageous to link degradation of the cometabolic substrate to the growth substrate.

Table II-3: Models for cometabolic degradation during biomass growth

Reference	Model
Schmidt et al. (1985)	$-\frac{dS_C}{dt} = k_C \frac{S_C}{K_C + S_C} \frac{X_{MAX}}{\left\{1 + \left[\left(\frac{X_{MAX} - X_0}{X_0}\right)\right] e^{-rt}\right\}}$ (II-23)
Strand et al. (1990)	$-\frac{dS_C}{dt} = k_C \frac{S_C}{\left[K_C\left(1 + \frac{S_G}{K_G}\right)\right] + S_C} X$ (II-24)
Semprini and McCarty (1992)	$-\frac{dS_C}{dt} = k_C \left(\frac{S_C}{\left(K_C\left(1 + \frac{S_G}{K_G}\right)\right) + S_C}\right)\left[\frac{S_O}{K_O + S_C}\right](F_A X)$ (II-25) $-\frac{dF_A}{dt} = -b_d F_A$ (II-26)
Criddle (1993) **Chang and Criddle (1997)**	$-\frac{dS_C}{dt} = \left(T_C q_G + k_C\right)\left(\frac{S_C}{K_C + S_C}\right)$ (II-27)
Keenan et al. (1994)	$-\frac{dS_C}{dt} = k_C \left(\frac{S_C}{\left(K_C + S_C\right)\left(1 + \frac{S_G}{K_{IG}}\right)}\right) X$ (II-28)
Arcangeli and Arvin (1997)	$-\frac{dS_C}{dt} = k_C \left(\frac{S_C}{\left(K_C\left(1 + \frac{S_G}{K_G}\right)\right) + S_C}\right)\left(\frac{S_C}{K_C + S_C}\right) X$ (II-29)

II.2.3. Cometabolic Biodegradation during Endogenous Respiration/Decay

Enzymes with low substrate specificity responsible for catabolism of the primary substrate and degradation of the cometabolic substrate may retain activity after the primary substrate is depleted, with the reductant(s) required to catalyze reactions obtained from internal storage polymers (e.g., poly hydroxybutyrate, PHB) (Alvarez-Cohen and Speitel, 2001). Consequently, cometabolic biodegradation may continue after bacterial growth is complete and the bacterial maintenance or endogenous respiration has commenced. The use of typical saturation kinetics to model this cometabolic process results in errors in parameter estimates since these models do not account for a loss in the ability of the biomass to degrade the cometabolic substrate (Criddle, 1993).

Early models accounting for this effect of reduced biomass/enzyme activity were developed through studies of cometabolic biodegradation of chlorinated organic compounds. The coupled Monod-logistic model developed by Schmidt et. al, 1985 (see Equation II-23 in Table II-3) can be easily extended to conditions where no biomass growth occurs (i.e., the biomass concentration is at the carrying capacity) and $X \approx X_{MAX}$ (Schmidt et al., 1985). Results from experiments with methylotrophic bacteria noted that both the rate and extent of 1,1-dichloroethane (DCA) production from degradation of 1,1,1-trichloroethane (TCA) was linked to the concentration of TCA at the end of the biomass exponential growth phase (Gälli and McCarty, 1989). The work of Gälli and McCarty (1989) was the first to suggest that the decrease in cometabolic transformation over time - in the absence of growth substrate - resulted from a decrease in the transformation capacity (equivalent to a reduction in enzyme activity or biomass decay).

The model proposed by Gälli and McCarty (Equation II-30 in Table II-4) was the first to incorporate a reduction in the cometabolic degradation rate resulting from biomass decay.

A critical assumption in the models proposed by phase (Gälli and McCarty, 1989) and Schmidt et al. (1985) is that the cometabolic substrate does not impact biomass decay. With certain compounds however, the cometabolic substrate is toxic to the biomass and as a result, the activity of the decaying cells appears to decrease over time in proportion to the mass of the cometabolic substrate biodegraded (Alvarez-Cohen and McCarty, 1991). The novel aspect in this formulation (Equation II-31 in Table II-4) presented by Alvarez-Cohen and McCarty (1991) is the definition of a Transformation Capacity (T_C) due to the toxic effect of the cometabolic substrate which limits the amount of the cometabolic substrate which can be biodegraded/transformed by a given quantity of biomass. While this model does incorporate potential toxic effects of the cometabolic substrate on the biomass it is not suitable for systems where the cometabolic substrate might itself be toxic to the biomass. Implicit in the model is the assumption that the cometabolic substrate is biodegraded (T_C), but that the cometabolic substrate diminishes the ability of the biomass to degrade it due to competitive inhibition of the biomass growth (Alvarez-Cohen and McCarty, 1991).

A similar approach based on a transformation capacity was implemented by Saez and Rittmann (1991) to model biodegradation of 4-chlorophenol by *P.Putida spp*. A salient difference between the models proposed by Saez and Rittmann (1991) (Equation II-32 in Table II-4) and Alvarez-Cohen and McCarty (1991) is the interaction between the cometabolic substrate and biomass. The model proposed by Saez and Rittmann (1991) is predicated on the concept that biodegradation of the cometabolic

substrate requires electrons which are supplied by the autooxidation of biomass (i.e., endogenous respiration) but the decay of biomass is not impacted by the cometabolic substrate as proposed by Alvarez-Cohen and McCarty (1991). Thus, for cometabolic substrate which are not inhibitory to the biomass the model proposed proposed by Saez and Rittmann (1991) may be particularly useful.

Chang and Alvarez-Cohen (1995) developed a mechanistic model to describe the cometabolic degradation process which integrates biomass growth, decay, potential inhibition and/or toxicity of the cometabolic substrate and NAD(P)H (i.e., reducing power) limitations for the enzyme (Equation II-33 in Table II-4). During biomass growth, the reductant required for enzyme operation is typically obtained from degradation of the primary growth substrate. During endogenous respiration, reductant may be supplied endogenously by autoxidation or from an exogenous reductant source. The models incorporate competitive inhibition of degradation of the cometabolic substrate by the presence of the primary growth substrate. In the absence of the growth substrate ($S_G = 0$) or when the concentration of the growth substrate is substantially lower than the half saturation concentration ($S_G << K_G$), the competitive inhibition is alleviated. In this case, the degradation of the cometabolic substrate assumes a Monod kinetics dependence on the cometabolic substrate and reductant concentration.

Table II-4: Models for cometabolic degradation in the absence of biomass growth

Reference	Model	
Gälli and McCarty (1989)	$-\frac{dS_C}{dt} = k_{SC}\left(\frac{S_C}{K_C + S_C}\right) X_{END-GR} e^{-bt}$	(II-30)
Alvarez-Cohen and McCarty (1991):	$-\frac{dS_C}{dt} = k_C\left(\frac{S_C}{K_C + S_C}\right)\left[X_{END-GR} - \left(\frac{1}{T_C}\left(S_{C,END-GR} - S_C\right)\right)\right]$	(II-31)
Saez and Rittmann (1991)	$-\frac{dS_C}{dt} = T_C\left(X_{END-GR} e^{-bt}\right)$	(II-32)
Chang and Alvarez-Cohen (1995)	$-\frac{dS_C}{dt} = k_C\left[\frac{R}{K_R + R}\right]\left[\frac{S_C}{K_C\left(1 + \frac{S_G}{K_G}\right) + S_C}\right] X$	(II-33)

II.2.4. Integrating Cometabolic Processes in Wastewater Treatment Process Models

The ASM framework) (Henze et al., 2000) is almost universally used to model wastewater treatment processes. Growth and decay processes for biomass consortia are treated separately as described previously for AOB and NOB. Integration of cometabolic biodegradation of a particular substrate within this framework may be effectively achieved using models described in Sections 2.2 – 2.3, where biodegradation of the cometabolic substrate during biomass growth and endogenous respiration/decay.

Chapter III. Pharmaceutical Removal, Sorption and Biodegradation during Wastewater Treatment

III.1. Introduction

Wastewater treatment plants (WWTPs) provide a direct route for PhACs to enter the environment (see Figure III-1). While WWTPs are not currently designed to treat PhACs, recent studies have documented attenuation and degradation of these compounds within the treatment processes (Andreozzi et al., 2003; Bendz et al., 2005; Chefetz et al., 2008; Onesios et al., 2009; Jelic et al., 2012; Siegrist and Joss, 2012). Attenuation mechanisms for PhACs in WWTPs include sorption, biodegradation (partial or complete mineralization), chemical (i.e., abiotic) oxidation, photodegradation, volatilization, and physical filtration (i.e., size exclusion) (Ternes et al., 2004b). Each of these mechanisms is not relevant throughout a WWTP; size exclusion filtration, for example, is irrelevant in the preliminary or primary treatment processes of a WWTP. A summary of the potential relevant processes in each stage of wastewater treatment is provided in Table III-1. In conventional WWTPs, the majority of PhAC removal occurs in the biological treatment process. Primary treatment offers minimal removal of these compounds. In advanced WWTPs, where reverse osmosis, ozonation or advanced oxidation processes may be utilized, these tertiary treatment processes provide an extremely high degree of PhAC attenuation (Snyder et al., 2006).

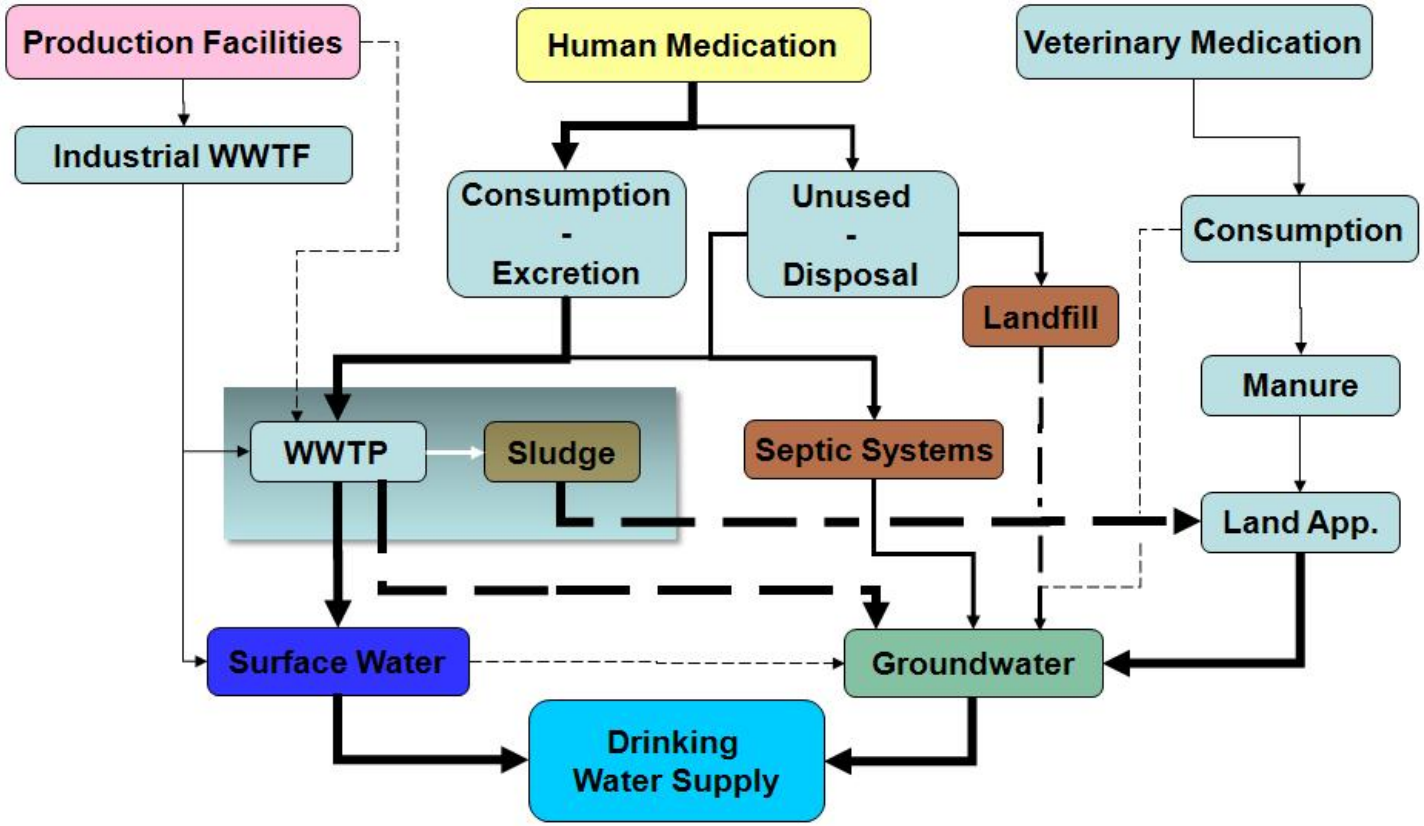

Figure III-1: Tracing the fate of PhACs from production to the environment. WWTPs are a critical point of entry of PhACs into the environment affecting surface and groundwater sources, in addition to farming through land applied biosolids (figure adapted from Halling-Sørensen et al. (1998); Heberer (2002). Note that this figure illustrates the fate and transport pathways for PhACs and not concentration or mass loadings. Dilution of WWTP effluent flows play an important role in determining the environmental concentration of PhACs.

Table III-1: Relevant Removal Mechanisms for PhACs in WWTP Processes

Removal Mechanism	Primary Treatment	Biological Treatment	Tertiary Treatment	Disinfection
sorption	++	+	+	-
biodegradation	-	++	-	-
abiotic oxidation	-	-	-	+
photodegradation	+	-	-	+
volatilization	-	+	-	-
size exclusion filtration	-	-	++[3]	-

[1] Relative importance of mechanisms shown using - (not important), + (potentially important), ++ (important).

[2] Assumes primary treatment operated with a low sludge blanket and negligible biological treatment in primary treatment process.

[3] Size exclusion filtration (SEF) is only relevant in WWTPs where reverse osmosis is included as part of tertiary treatment (e.g., WWTPs designed for high quality reuse applications). SEF is not relevant in WWTPs employing membranes having pore sizes larger than those found in reverse osmosis membranes (e.g., ultrafiltration and microfiltration).

III.2. PhAC Removal in Primary Wastewater Treatment Processes

Primary treatment processes are designed for the removal of large particles in the influent that are able to settle through zone settling (Metcalf & Eddy et al., 2003). Conventional primary treatment processes rely on gravity settling of such particles. Enhanced primary treatment (or Chemically Enhanced Primary Treatment) additionally incorporates chemicals, specifically a coagulant (e.g., aluminum sulfate) with or without a polymer (e.g., high molecular weight polyacrylamides) to enhance the solids removal efficiency and in certain applications, remove specific wastewater pollutants such as phosphorus and metals (WEF, 2005).

A limited number of studies have evaluated the removal of PhACs and personal care products (PCPs) in primary treatment wastewater processes. More studies have focused on the fate of PhACs and PCPs in primary treatment systems in water treatment plants (e.g., Adams et al., 2002; Westerhoff et al., 2005; Stackelberg et al., 2007). The removal of PhACs in both conventional and enhanced primary treatment is extremely variable, ranging from less than 1% total removal to greater than 90% (Carballa et al., 2005; Suarez et al., 2009; Zorita et al., 2009). Sorption is thought to be the dominant mechanism for PhAC attenuation in primary treatment (Carballa et al., 2005; Stackelberg et al., 2007) with lipophilic compounds removed to a greater extent. The addition of a coagulant in bench tests improves the removal of PhACs and PCPs (Carballa et al., 2005).

III.3. PhAC Removal during Biological Treatment

PhAC removal during biological wastewater treatment has been studied at a range of scales from lab-scale systems to full-scale WWTPs in recent years (Jelic et al., 2011; Kraigher and Mandic-Mulec, 2011; Majewsky et al., 2011; Prasse et al., 2011; Camacho-Munoz et al., 2012; Helbling et al., 2012; Suarez et al., 2012; Fernandez-Fontaina et al., 2013). Consequently, there is a growing database of information regarding PhAC removal using different treatment process conditions (e.g., aerobic and anoxic reactors), operating conditions (e.g., SRT, MLSS, HRT) and unit operations (e.g., activated sludge, MBRs). In recent years, there have been reviews of PhAC removal through wastewater treatment processes as part of a broader survey of a wider set of microconstituents (Kagle et al., 2009; Onesios et al., 2009; Oulton et al., 2010). In addition, the United States EPA has compiled a comprehensive database of microconstituent removal for a wide range of treatment process and full-scale systems in both water and wastewater treatment plants and experimental systems (United States Environmental Protection Agency, 2010).

A consistent theme across individual studies and broader reviews is the significant variability observed in PhAC removal during biological treatment. The reported PhAC removals from 293 data for 51 PhACs (Figure III-2, see Appendix A for study details) demonstrate the significant variability in PhAC removal from 0% (e.g., with carbamazepine) to almost complete removal e.g., for naproxen (NAP), acetaminophen (ACM) and ibuprofen (IBP). It is important to note that one PhAC may be represented multiple times in Figure III-2. Median removal for this set of 51 PhACs is 47%.

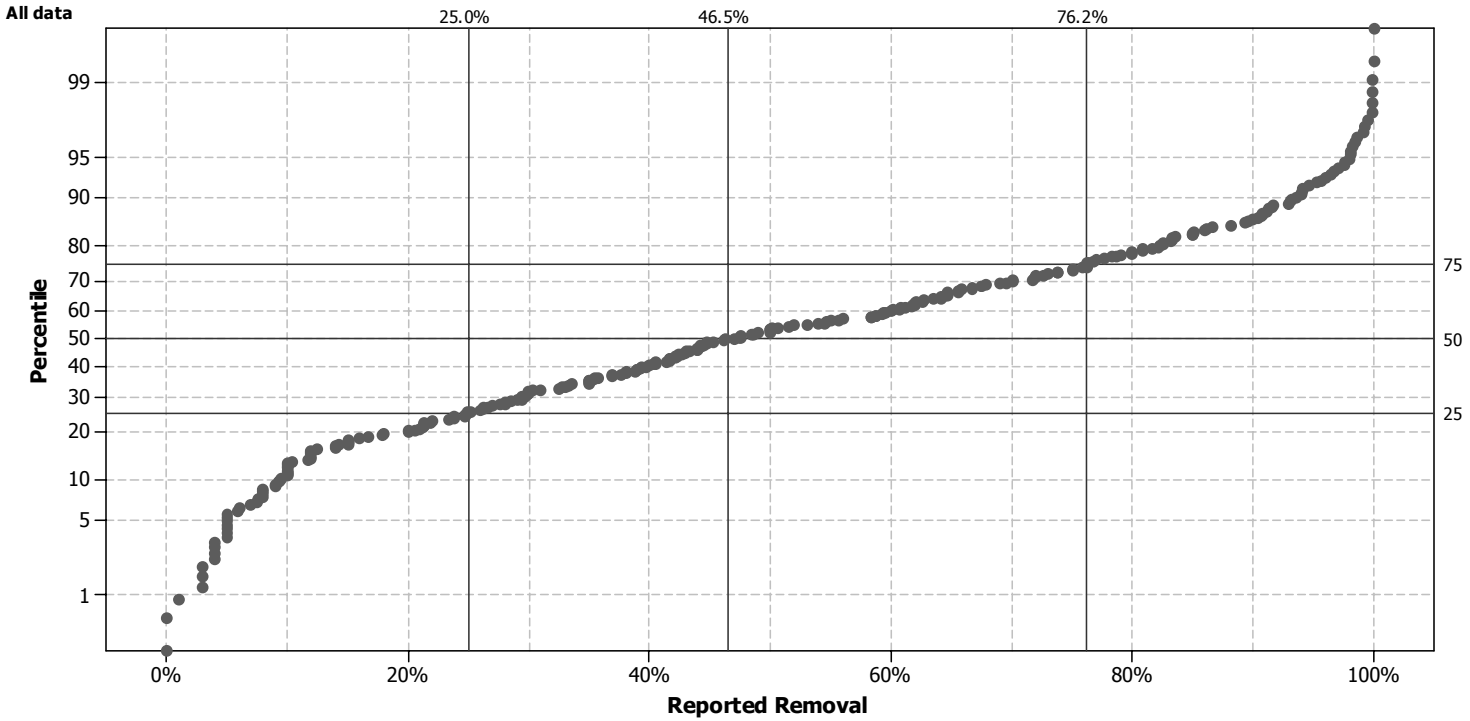

Figure III-2: Aggregate distribution of reported PhAC removal in full scale and bench scale studies. Full scale studies include suspended growth and membrane bioreactor processes. Data is comprised of 293 data points for 51 PhACs. Note that one PhAC may be represented multiple times in this aggregate data set. Shown for reference are 25th, 50th (median) and 75th percentile removals.

The extent of PhAC removal in biological treatment systems is reported to depend on a number of factors, including unit operation type (e.g., suspended growth vs. fixed film) and configuration, mixed liquor concentration, solids retention time (SRT), hydraulic retention time (HRT) and PhAC properties (Ternes et al., 2004b; Joss et al., 2006; Stephenson and Oppenheimer, 2007; Oulton et al., 2010). The influence of these variables on PhAC removal is explored here.

III.3.1. PhAC Removal and SRT

The importance of SRT as a design/operational variable influencing the removal of PhACs, and microconstituents more widely, has received significant attention in recent years. Early work by researchers as part of the European Union's Poseidon project indicated improved PhAC removal in WWTPs operated at long SRTs (≥ 8-10 days) (Kreuzinger et al., 2004; Ternes et al., 2004b; Clara et al., 2005a; Joss et al., 2006). Numerous research studies have since suggested and/or observed a link between PhAC removal and SRT in WWTPs. Suarez et al. (2012), for example, suggested that the removal of SMX increased from 38% to 63 - 70% when the SRT of a suspended growth MLE pilot process was increased from <20 to >40 d. Importantly however, the authors reported that increasing SRT had no impact of removals of CBZ, DZP, DCF, FLX, NAP, CIT, TMP and ERY. Schroder et al. (2012), studying PhAC removal in two parallel MBRs operating at SRTs of 15 and 30 d, reported improved removal rates for ROX, SMX and TMP with no improvements for ACM, NAP and KET. Increased PhAC removal at longer SRTs has been attributed by Gobel et al. (2007) to wider bacterial biodiversity in the activated sludge system. Reif et al. (2008) suggested that enhanced PhAC removal is a result of the presence of slow growing bacteria at longer SRTs which are critical to the

PhAC degradation/removal. Strenn and coworkers have suggested that lower removal rates of DCF with increasing SRT of the biological treatment process is related to the sorption of DCF to biomass rather than biodegradation due to its hydrophobicity (log K_{OW} = 4.51) (Clara et al., 2003; Kreuzinger et al., 2004; Strenn et al., 2004).

Despite the attention given to the possible link between SRT and PhAC removal, the correlation is not accepted by all researchers. Majewsky et al. (2011) argued that long SRTs would reduce the removal efficiency of SMX and DCF as attenuation results primarily due to heterorophic bacteria (HET) and an increase in SRT would decrease the active HET. Furthermore, several studies have reported that certain PhACs, such as carbamazepine (CBZ) and diclofenac (DCF) are poorly removed even at very long SRTs in both suspended growth and MBR systems (Clara et al., 2005a; Nakada et al., 2006; Radjenovic et al., 2007; Xue et al., 2010; Majewsky et al., 2011).

Clara et al. (2005a) and Stephenson and Oppenheimer (2007) suggested the utility of a *critical SRT*, defined as minimum SRT which provides a predetermined removal of the PhAC, to classify the removal of PhACs. While there may be debate related to what such a predetermined level should be such an approach provides a uniform basis to evaluate PhAC attenuation. In addition, the use of SRT as a *master control-variable* for PhAC removal is attractive to the WWTP design and operations community as it provides a specific and achievable target. One drawback of this approach from an environmental impact standpoint is that it fails to account for the potential impact of biodegradation metabolites produced in the treatment processes. This may prove particularly important considering studies which have shown increasing ecotoxicity along degradation pathways (Isidori et al., 2005). Further, while this approach provides a measure for the extent of attenuation of the parent PhAC and

minimum SRT required to achieve the removal benchmark, it provides limited process design relevant information (e.g., process configuration, redox conditions, degradation rate).

The observed impact of SRT on removal of PhACs in suspended growth systems (included in the studies in Appendix A) is shown in Figure III-3. The data include a diverse set of WWTPs including MLE, A2O and high rate systems. Reported operating SRTs were classified into one of seven SRT categories (<5 days, 5-10 days, 10-15 days, 15-20 days, 20-25 days, 25-30 days and >30 days). There are a total of 14 PhACs for which a comparison of removal between suspended growth systems operated at <5 days and 5-10d is possible. To compare removals for PhAC in WWTPs operated at 10-15d, 15-20d and 20-25d with <5d there are a total of 19, 14 and 5PhACs available, respectively. No data were available in this data set for longer SRTs. Analyses of these data shows that there are a set of PhACs which are effectively removed even in WWTPs operated at SRTs < 5d (NAP, IBP, ACM). There are a set of PhACs whose removal is greatly increased with increasing SRT. Interestingly, there are a set of PhACs for which increasing the SRT appears to have little to no impact, and in certain cases even a detrimental impact, on removal (e.g., DCF, RAN).

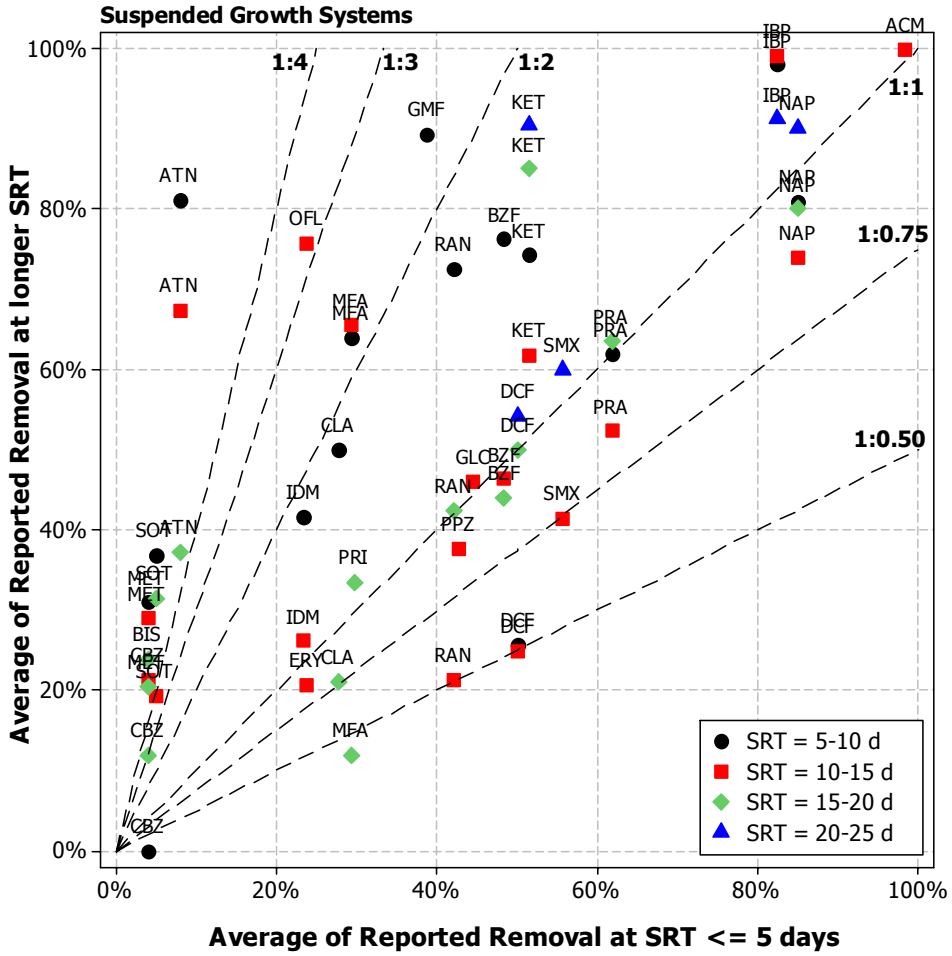

Figure III-3: PhAC removal of PhACs in suspended growth systems operated at an SRT of less than 5 days compared with removal in suspended growth systems operated at longer SRTs. Data shown are average* of reported removals for PhACs. Also shown for reference are lines at 1:0.50, 1:0.75, 1:1, 1:2, 1:3 and 1:4.

***For removals at <5d SRT (i.e., x-axis data): n=1 for all PhACs except MET (n=2). For removals at 5-10d SRT: n=1 for 8 PhACs, n=2 for 6 PhACs (ATN, DCF, KET, MFA, NAP, SOT). For removals at 10-15d SRT: n = 1 for 6 PhACs (GLC, IBP, IDM, MFA, OFL, PPZ), n = 2 for 7 PhACs (ACM, BZF, CBZ, ERY, KET, PRA, RAN), n = 3 for 5 PhACs (DCF, MET, NAP, SMX, SOT) and n = 4 for 1 PhAC (ATN). For removals at 15-20d SRT: n = 1 for 4 PhACs (BZF, MET, PRA, RAN), n = 2 for 8 PhACs (BIS, CBZ, CLA, DCF, KET, NAP, PRI, SOT) and n = 3 for 1 PhAC (ATN). For removal at 20-25d: n = 1 for 1 PhAC (SMX), n = 2 for 3 PhACs (IBP, KET, NAP), n = 3 for 1 PhAC (DCF).**

III.3.2. Comparison of PhAC Removal in MBR and Suspended Growth Processes

Membrane bioreactors (MBRs) have gained popularity in recent decades as an attractive treatment process for biological treatment processes given the ability to produce high quality effluents with small footprints. A number of recent publications have evaluated PhAC removal in MBRs (Kimura et al., 2005; Radjenovic et al., 2007; Reif et al., 2008; Tambosi et al., 2010; Xue et al., 2010; Tadkaew et al., 2011; Schroder et al., 2012) or experimentally compared PhAC removal between suspended growth (SG) systems and MBRs (e.g., Clara et al., 2004; Clara et al., 2005b; Bernhard et al., 2006; De Wever et al., 2007; Radjenovic et al., 2009; Sipma et al., 2010; Sui et al., 2011; Fernandez-Fontaina et al., 2013). Results to date provide a diverse range of opinions regarding the benefits of MBRs versus SG systems for PhAC removal. Kimura et al. (2005) , Radjenovic et al. (2009), Sui et al. (2011) and Schroder et al. (2012) among others have reported high removal rates (>80%) for PhACs such as NAP, ACM and TMP and suggest that MBRs in general tend to outperform SG processes. (Cirja et al., 2008) compared the removal of 23 PhACs and EDCs in SG and MBR processes and concluded that there was no significant difference in performance. A similar conclusion was reached by Sipma et al. (2010) who compared the average removals of 30 different PhACs in SG and MBR processes from thirteen different studies.

Evaluation of aggregate data set - removals for 51 PhACs from a range from WWTPs – suggests that PhAC removals are highly variable for both suspended growth and MBR systems (see Figure III-4). The median removal for this set of PhACs in suspended growth and MBR processes is 42% and 65%, respectively). This comparison, however, does not provide an evaluation of the specific benefits of MBRs for PhAC

removal considering the differences in operating conditions (e.g., SRT and MLSS) which influence PhAC removal. Comprehensive operating data are not often reported in full-scale studies making it extremely difficult to find identical operating conditions for suspended growth and MBR processes. Or, when the data are provided, MBRs are often operated at significantly higher MLSS and longer SRT than the suspended growth system making side-by-side comparisons complex (e.g., Bernhard et al., 2006). Therefore, to facilitate this analysis SRT was used as a surrogate measure for operating conditions. Reported operating SRTs were classified into one of 7 SRT categories (<5 days, 5-10 days, 10-15 days, 15-20 days, 20-25 days, 25-30 days and >30 days). Shown in Figure III-5 are comparisons of PhAC removals in suspended growth and MBR processes. Data were only available for 3 different SRT categories: 10-15 d (6 data points: ACM, ATN, CBZ, DCF, NAP, SMX), 15-20 d (5 data points: CLA, DCF, KET, MFA, NAP) and 20-25 d (1 data point: DCF). Analysis of the 10-15 d and 15-20 d data indicates that the process type does not have a statistically significant impact on PhAC removals when these processes are operated at a similar SRT. Evaluation of these data indicates that PhACs which are removed to a great extent in suspended growth systems are also effectively removed in MBRs. MBRs, therefore, offer no significant advantage for PhAC removal.

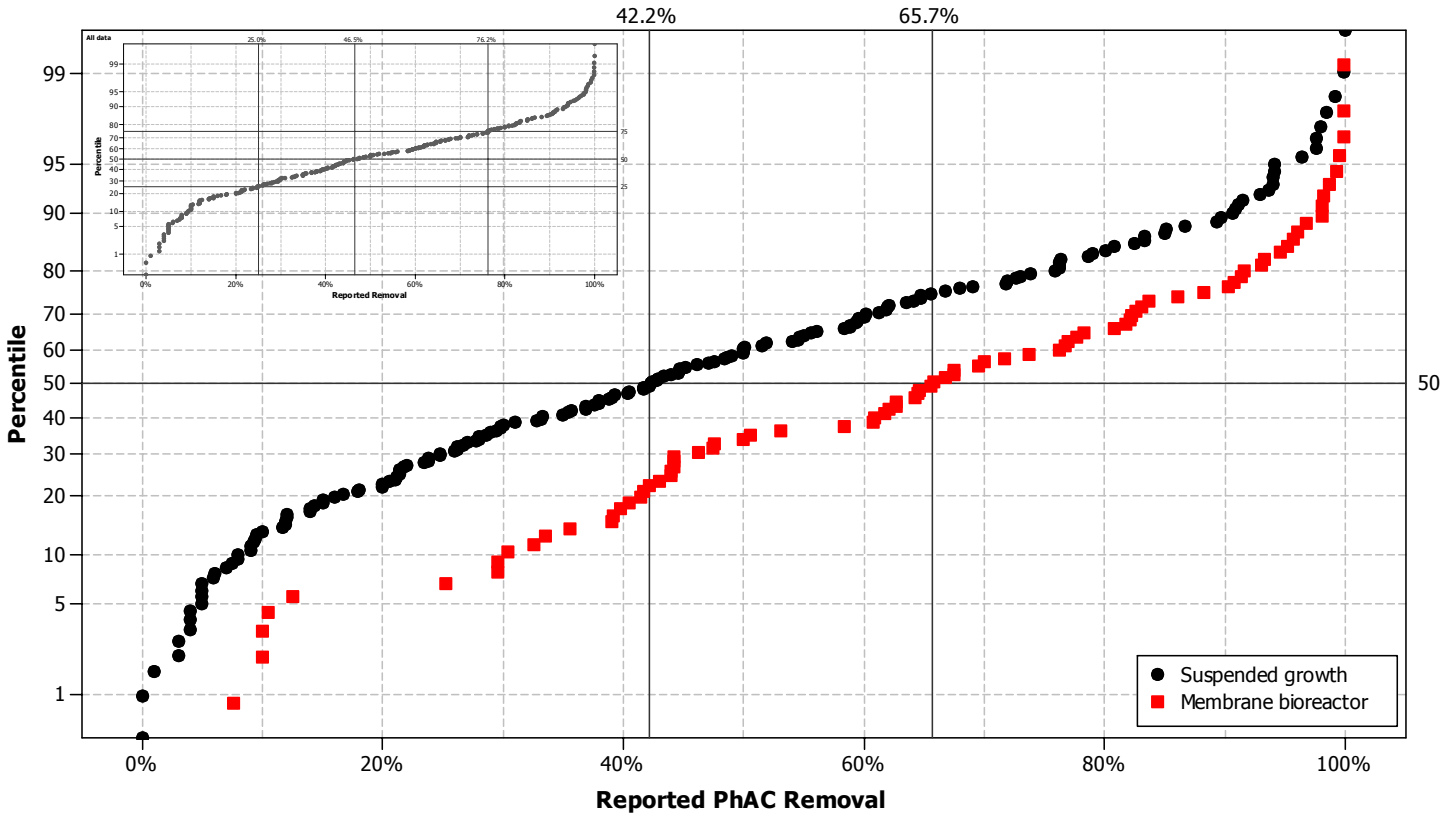

Figure III-4: Distribution of PhAC removal in suspended growth and membrane bioreactor processes in full scale WWTPs. There are a total of 259 data points (suspended growth – 175, membrane bioreactor – 84). Median values for each data set are indicated. Also shown in the distribution of removal for all data from full scale WWTPs and bench scale studies as a single data set (inset) - there are a total of 293 data points here.

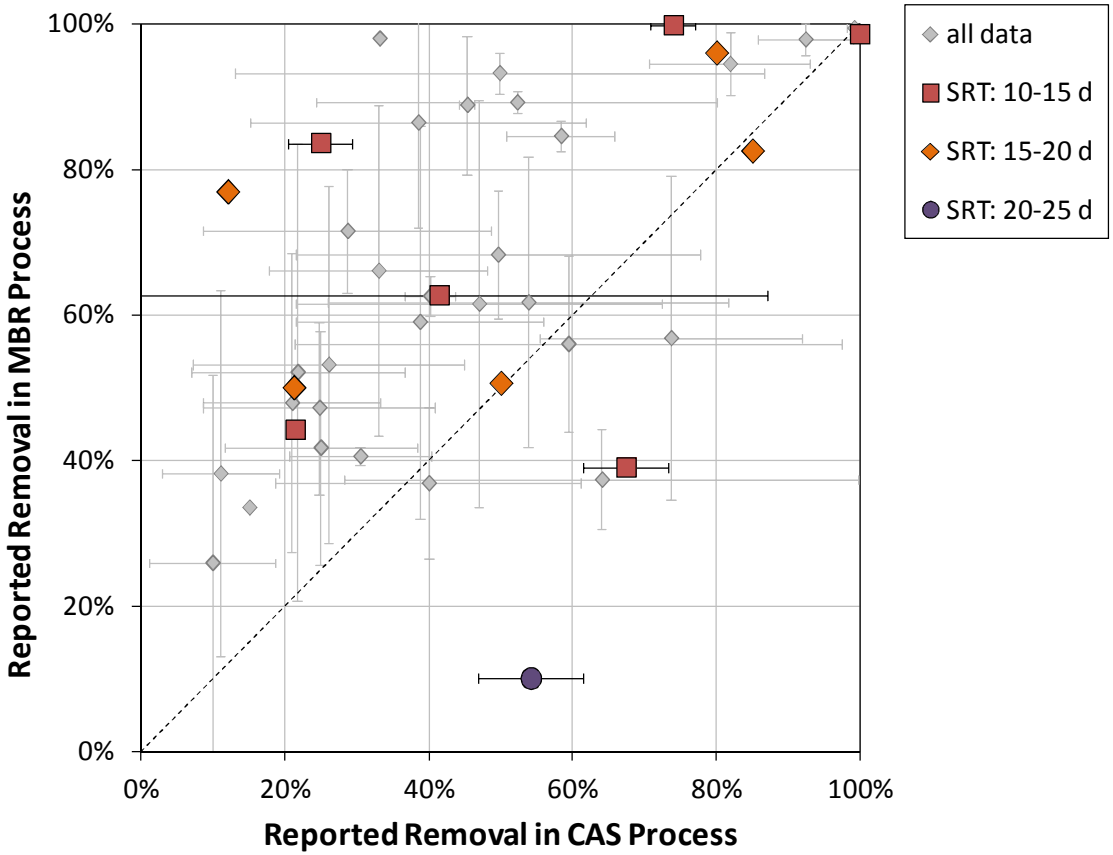

Figure III-5: Comparison of PhAC removals in suspended growth (CAS) and MBR systems. Data shown are average of reported removals for PhACs where data are available. Where available, data are also shown as a function of SRT. Also shown (background) are averages of all data (independent of reported SRT).

III.4. Sorption of PhACs during Biological Treatment

III.4.1. Review of Data for PhAC Sorption during Biological Treatment

Conventional wisdom suggests sorption of PhACs to biomass during treatment may be described using a linear, equilibrium isotherm. Use of this approach suggests that the distribution of a given solute between the aqueous phase and suspended solids can be described by a single distribution coefficient (K_D). A number of studies employ this approach for PhACs (see Appendix B for details related to the sorption studies). A survey of PhAC sorption studies produced 388 measured sorption coefficients (K_D) for 66 PhACs, so it is important to note that that there are multiple data points for most PhACs considered in this review. For many PhACs, data for the sorption to suspended solids do not exist or are sparse. Only 66 of over 2,000 FDA approved PhACs have been studied. While many of these over 2,000 PhACs are used sparingly or in controlled settings, the pharmaceutical industry regularly ranks (by prescriptions) the top 200 PhACs in two classes - branded and generic PhACs (e.g., Drug-Topics, 2011a). A comparison of the PhAC use with sorption studies indicates that sorption data are available for less than 10% of the 231 unique PhACs appearing on the top 200 lists for generic PhACs in 2009 and 2010 (Drug-Topics, 2010 and 2011b).

Sorption data for the 66 PhACs that have been studied are often restricted to a limited range of experimental conditions. For example, 45 of the 66 PhACs for which sorption data are available have fewer than five reported K_D values. Data from only 13 of the remaining 21 PhACs include multiple measurement techniques (batch versus continuous) conducted under many experimental conditions (TOC, pH, suspended solids concentration, etc.). These 13 PhACs are: atenolol (ATN), carbamazepine (CBZ), clofibric

acid (CLA), diclofenac (DCF), gemfibrozil (GMF), glibenclamide (GLC), ibuprofen (IBP), ketopofen (KET), metoprolol (MET), naproxen (NAP), propranolol (PRO) sulfamethaxazole (SMX) and trimethoprim (TMP) (see Table SD-2). While the reason for an emphasis on these PhACs are unclear, it likely relates to patterns in the production and use of these PhACs coupled with the development of experimental and analytical methods.

The majority of PhAC sorption studies employ batch experiments to quantify the equilibrium distribution of PhACs between the aqueous phase and suspended solids (Ternes et al., 2004a; Urase and Kikuta, 2005; Maurer et al., 2007; Wick et al., 2009; Xue et al., 2010; Horsing et al., 2011; Stevens-Garmon et al., 2011). Fewer studies assess sorption using continuously operating reactors (e.g., Abegglen et al., 2009; Radjenovic et al., 2009). To assess whether or not the type of experiment - batch vs. continuous - influences measurement of K_D we conducted a meta-analysis of reported sorption coefficients. Our analysis focuses on those PhACs for which there are at least three K_D values reported for both the batch and continous methods. Shown in Figure III-6 are the nine PhACs for which there are sufficient data. Data for the other 57 pharmaceuticals (for which there are K_D measurements) are insufficent for comparison between experimental methods. Results of the analysis indicate that the type of experiment for these nine PhACs has no statistically-significant influence on the reported sorption coefficient (i.e., Mann Whitney test at 95% confidence level). Though, it should be noted that several PhACs have >1 order-of-magnitude variation in the reported K_D values, which mask any differences resulting from measurement technique.

In the majority of batch studies, biomass is inactivated using either chemical (mercuric chloride, silver nitrate or sodium azide) or physical means (lyophilization). Chemical inactivation methods may interact with the PhAC or modify surface characteristics of the biomass, thereby influencing measured values of K_D (Stevens-Garmon et al., 2011). Maurer et al. (2007) report that addition of silver nitrate to a filtered (0.45 μm filter) WWTP effluent containting MET and ATN decreased aqueous concentrations by 60% and 75%, respectively. Mercuric chloride was found to decrease aqueous concentration of ATN and sotalol (SOT) by 20% and 10%, respectively, and increase aqueous concentrations of MET and PRO by 35% and 15%, respectively. The influence of chemical inactivation has been specifically explored by Dickenson et al. (2010) who compared the efficacy of sodium azide (5 g/L), silver nitrate (0.0125g/g-SS) and azide based cocktail (sodium azide 10 g/L, barium chloride 5mM, and nickel chloride 5mM) in sorption studies using biomass from a nitrification tank at the Colorado School of Mines – Mines Park WWTP (MLSS = 1,650 mg/L). Sodium azide used alone was the most effective in inhibiting biomass. Moreover, no reactions between azide and the selected PhACs (NAP, IBP, CBZ and indolebutyric acid (IBA)) were observed in the absence of biomass. Silver nitrate was found to be less ineffective for IBP and IBA as neither PhAC was detected in the system afer 50 hours. In addition, the authors report observing fine white particulates upon addition of silver nitrate to abiotic control systems comprising synthetic wastewater. To explore the role of inactivation method further, we looked across studies to find only three PhACs (ATN, CBZ , and diazepam (DZP)) for which measured K_D can be compared with respect to the method of inactivation (no inactivation, chemical inactivation and physical inactivation). Data for the other 63 PhACs were insufficent for comparison between experimental inactivation

methods. ATN is the only PhAC for which sufficient data are available to statistically evaluate all three inactivation methods. Results for ATN indicated that there are no statistical differences between the methods of inactivation (pair wise Mann Whitney Tests: $p>0.05$) (Figure III-7). Results for DZP confirm the observation made with ATN that there are no statistical differences between reported K_D data measured using physical inactivation and no inactivation (Figure III-7).

Results for CBZ are illustrative of the difficulties in attempting this sort of comparison. Results of the pair-wise Mann Whitney test suggest that there is a statistically significant difference when K_D values are measured using physical inactivation methods versus when no inactivation is used. However, it is important to note two critical elements of such comparisons through meta analyses. First, there are far fewer data collected for each type of inactivation than those collected from studies not employing inactivation. This is because where inactivation is necessary or desired; the experimental protocol employed rarely utilizes multiple types of inactivation. Second, reported K_D values in the absence of inactivation can be highly variable (spanning nearly four orders of magnitude in the case of CBZ). Variability may result from differences in the surface characteristics or activity of the biomass employed in each experiment.

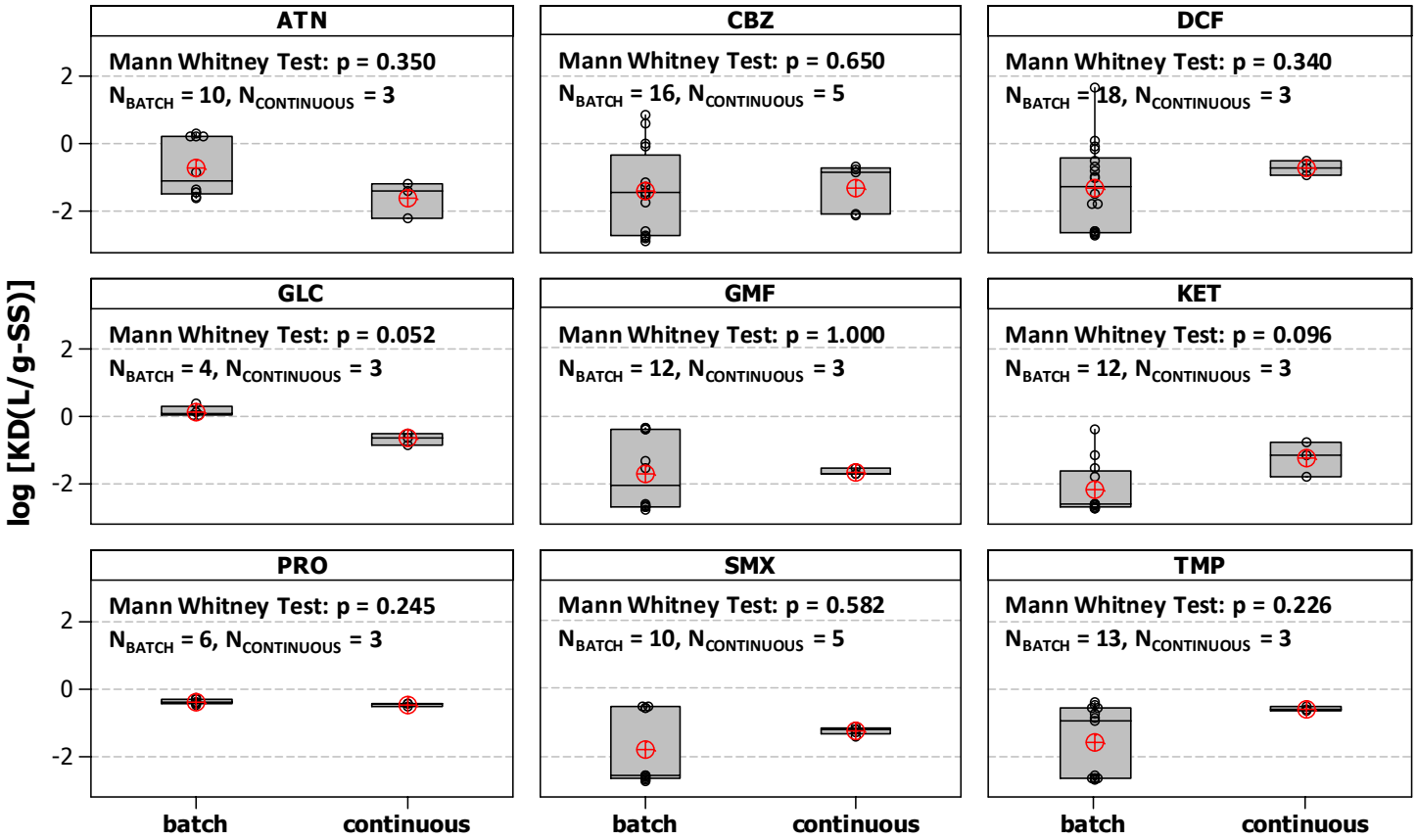

Figure III-6: Comparison of measured sorption coefficients for atenolol (ATN), carbamazepine (CBZ), diclofenac (DCF), glibenclamide (GLC), gemfibrozil (GMF), ketoprofen (KET), propranolol (PRO), sulfamethaxazole (SMX) and trimethoprim (TMP) from batch and continuous experiments. Individual data points shown using small black circles; horizontal line indicates median; mean indicated by large red circle with cross-hairs. Box extents indicate 25th (Q1) and 75th (Q3) percentile with whiskers extending to upper limit [Q3 + 1.5(Q3-Q1)] and lower limit [Q1 - 1.5(Q3-Q1)]. Also shown are p-value of one-tailed Mann Whitney test and number of data points from batch [n (batch)] and continuous [n (continuous)] experiments.

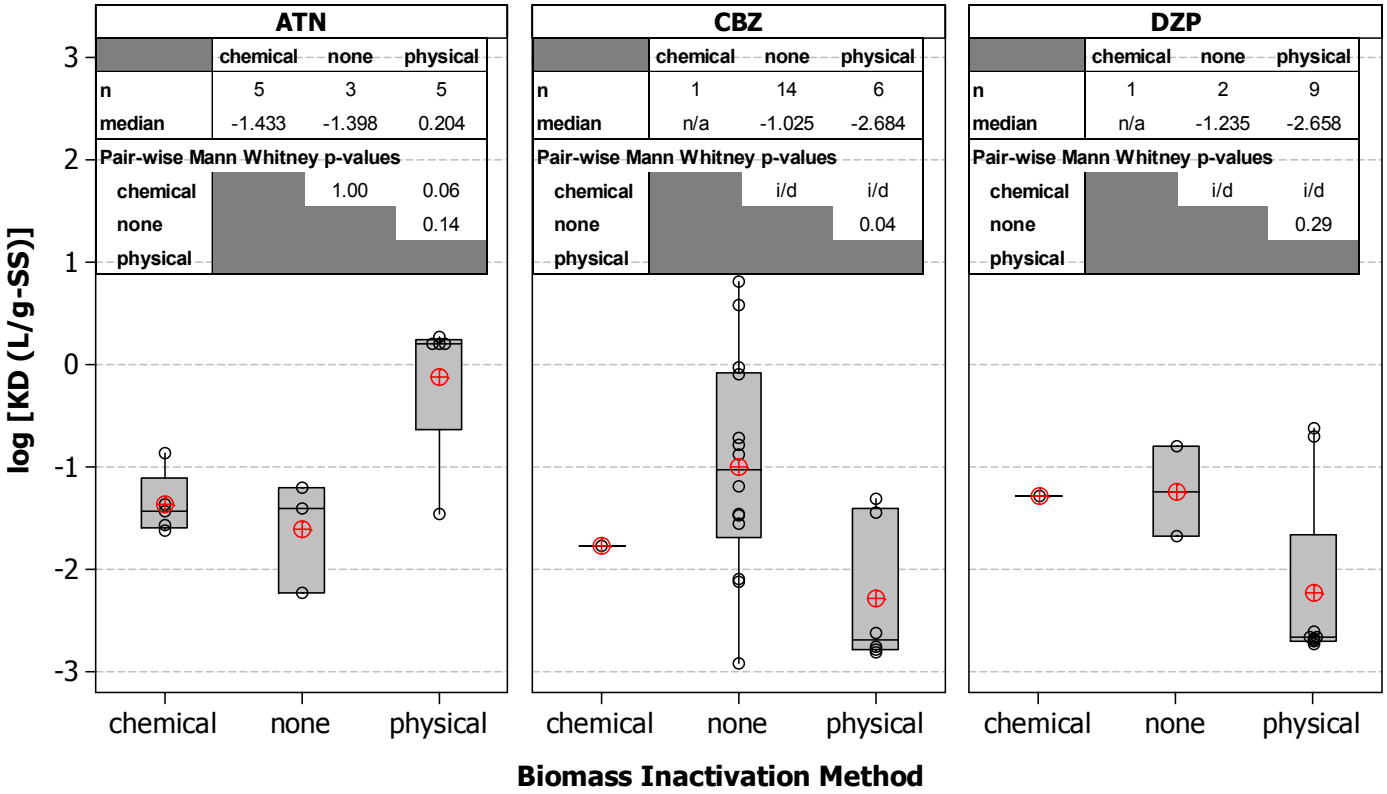

Figure III-7: Measured sorption coefficients for atenolol (far left), carbamazepine (middle) and diazepam (right) from batch and continuous experiments using chemical inactivation (e.g., NaN_3) no biomass inactivation, and physical inactivation (e.g., lyophylization). Individual data points shown using small black circles; horizontal line indicates median; mean indicated by large red circle with cross-hairs. Box extents indicate 25th (Q1) and 75th (Q3) percentile with whiskers extending to upper limit [Q3 + 1.5(Q3-Q1)] and lower limit [Q1 - 1.5(Q3-Q1)]. Also shown are number of data points (n), median log[K_D(L/g-SS)] and p-value of one-tailed Mann Whitney test evaluating differences between inactivation methods (note: n/a = not applicable, i/d = insufficient data available for statistical evaluation).

III.4.2. Importance of PhAC Sorption in WWTPs

The importance of PhAC sorption as an attenuation mechanism during biological treatment processes depends not only the PhAC properties, but also on WWTP operating parameters (e.g., MLSS and SRT) and the influence of operating parameters on the sorbent characteristics as previously discussed. In this section we aim to evaluate the engineering significance of sorption as a pathway for PhAC attenuation. In view of the relatively weak capabilities of models to predict K_D using PhAC molecular descriptors and SRT we have elected to assess the implications of sorption based on a priori knowledge of K_D. That is to say, the inputs to our assessment are K_D and operational parameters. Thus the approach can be used with measured or estimated values for K_D. The sorbed fraction under a particular operating condition can be related to K_D and MLSS using a mass balance by assuming local equilibrium (Schwarzenbach et al., 2003). This relationship is described in Equations III-1 and III-2.

$$M_{PhAC,T} = (V_{AQ}\, S_{PhAC}) + (V_{TOT}\, XW_{PhAC}) \quad \text{(III-1)}$$

$$f_{PhAC,X} = \frac{X \cdot K_D}{\left(X \cdot K_D + \left(1 - \frac{X}{\rho_X}\right)\right)} \quad \text{(III-2)}$$

where, variables are:

$M_{PhAC,T}$ =	total PhAC mass	$[M_{PhAC}]$
V_{AQ} =	volume of water in reactor	$[L^3_{AQ}]$
V_{TOT} =	total reactor volume	$[L^3_{ML}]$
X =	mixed liquor (ML) concentration	$[M_{ML}/L^3_{AQ}]$
S_{PhAC} =	soluble PhAC concentration	$[M_{PhAC}/L^3_{AQ}]$
W_{PhAC} =	sorbed PhAC concentration	$[M_{PhAC}/M_{ML}]$
$f_{PhAC,X}$ =	sorbed fraction of PhAC	$[M_{PhAC\text{-}SORBED}/M_{PhAC\text{-}TOT}]$
ρ_X =	mixed liquor density (assumed ≈ ρ_{AQ})	$[M_{ML}/L^3_{ML}]$
K_D =	PhAC sorption coefficient	$[L^3/M_{ML}]$

Shown in Figure III-8 are the fractions of PhAC mass associated with the suspended solids as a function of PhAC K_D and MLSS. The shaded bands represent the three types of systems: membrane bioreactor (MBR), conventional activated sludge (CAS) and laboratory batch reactors (lab) (respectively, from left to right in Figure III-8. As one may expect, the influence of sorption becomes stronger at higher concentrations of suspended solids. It is, informative to consider the point at which the PhAC mass is evenly distributed between the aqueous and solid phases for both CAS and MBR systems - that is the K_D for which the aqueous and solid phases are equally relevant in terms of PhAC mass. Take for example, a CAS system operating at 4,000 mg/L MLSS. PhAC mass is evenly distributed between the aqueous and solid phases for a $K_D = 0.25\ L/g_{MLSS}$. For an MBR operating at 10,000 mg/L MLSS the same point occurs at $K_D = 0.099\ L/g_{MLSS}$. This suggests that unlike more traditional, hydrophobic, organic contaminants for which sorption is a major attenuation mechanism within a plant, PhAC fate through the treatment process requires careful consideration as the role of sorption in attenuation may be minor. Given that rates of biodegradation are also likely to be proportional to the biomass concentration, processes operated at a high MLSS may have substantial potential for treating PhACs in wastewater. Sorption of PhACs to activated sludge could conversely make it unavailable for biodegradation. Therefore, there is a need for research which elucidates the coupled roles of sorption and biodegradation in PhAC attenuation.

The fraction of PhAC mass associated with the solid phase can be informative, but PhAC mass removal from the biological treatment process depends on the rate of sludge wasting. Thus, we consider the fraction of PhAC removed via sludge wasting by

relating it to typical WWTP design and operating parameters – specifically SRT, MLSS and HRT as shown in Equation III-3.

$$f_{PhAC-WAS} = \frac{\left(X \cdot \frac{HRT}{SRT}\right) \cdot K_D}{\left(1 + \left(X \cdot \frac{HRT}{SRT}\right) \cdot K_D\right)} \quad \text{(III-3)}$$

where variables are:

$f_{PhAC-WAS}$ =	fraction of PhAC removed in waste actived sludge (WAS)	$[M_{PhAC-WASTED}/M_{PhAC-TOT}]$
X =	mixed liquor (ML) concentration	$[M_{ML}/L^3_{AQ}]$
K_D =	PhAC sorption coefficient	$[L^3/M_{ML}]$
HRT=	hydraulic retention time	[T]
SRT =	solids retention time	[T]

Shown in Figure III-9 is the fraction of PhAC removed from biological reactors through the waste activated sludge (WAS) (i.e., $f_{PhAC-WAS}$). As can be seen in the figure, sludge wasting is most relevant for PhACs having K_D greater than 1.00 L/g-SS. Note that a K_D=1.00 L/g-SS corresponds to the 70th percentile value for the data analyzed as part of this review. Consider that sludge wasting in a conventional activated sludge processes having a 12 h HRT and operated at a 2 day SRT with 2 g/L MLSS (i.e., X*HRT/SRT = 0.5 g_{MLSS}/L) accounts for no greater than 25% of the mass of most PhACs entering the treatment unit. Removal of PhACs via WAS in this system is greater than 50% only if K_D > 2.00 L/g_{MLSS} - a K_D value which corresponds to the 77th percentile for the data analyzed as part of this review. Although the high mixed liquor concentration of MBRs may be advantageous for sorption of PhACs having relatively higher K_D, MBRs are often used in process configurations with a long SRT (e.g., Ng and Hermanowicz, 2005). Thus, the benefit of sorption as potential pathway for PhAC removal is often times offset by

limited sludge wasting. For example, in an MBR operating under typical nitrifying conditions (SRT = 15 d, HRT = 8 h, MLSS = 10 g/L - i.e., X*HRT/SRT = 0.22 g_{MLSS}/L), less than 10% of the mass of most PhACs is removed through sorption to WAS. Results from these calculations suggest that PhAC attenuation via sorption and wasting has only limited relevance in most biological treatment systems.

The analyses presented here offer a tool to aid assessment of PhAC removal under specific operating conditions. It should be noted, however, that these analyses are highly simplified and do directly consider factors that can influence sorption of specific PhACs in real systems. When using Figure 11 and 12 it is tempting to associate one PhAC with a single value of K_D irrespective of the operating conditions. Doing so, however, assumes that biomass characteristics are the same for all types of operation. For example the simplified approach assumes that the floc morphology and characteristics are similar for MBRs and CAS processes, which is rarely seen to be the case. At short SRTs, MBRs and CAS reactors tend to have similar floc size (mean floc diameter, d_{50} ca. 80 – 240 μm). As the SRT is increased, MBRs have smaller, more compact floc compared to CAS processes (Holbrook et al., 2005; Masse et al., 2006). This may in turn influence the sorption characteristics for PhACs. More importantly, with extracellular polymeric substances (EPS) playing a critical role in sorption of PhACs and other microconstituents (Yi and Harper, 2007; Khunjar and Love, 2011), the differences in bound EPS content between CAS and MBR sludge may also influence the sorption behavior. Additional research is necessary to link the changes floc morphology and characteristics of MBRs to sorption of PhACs in these systems.

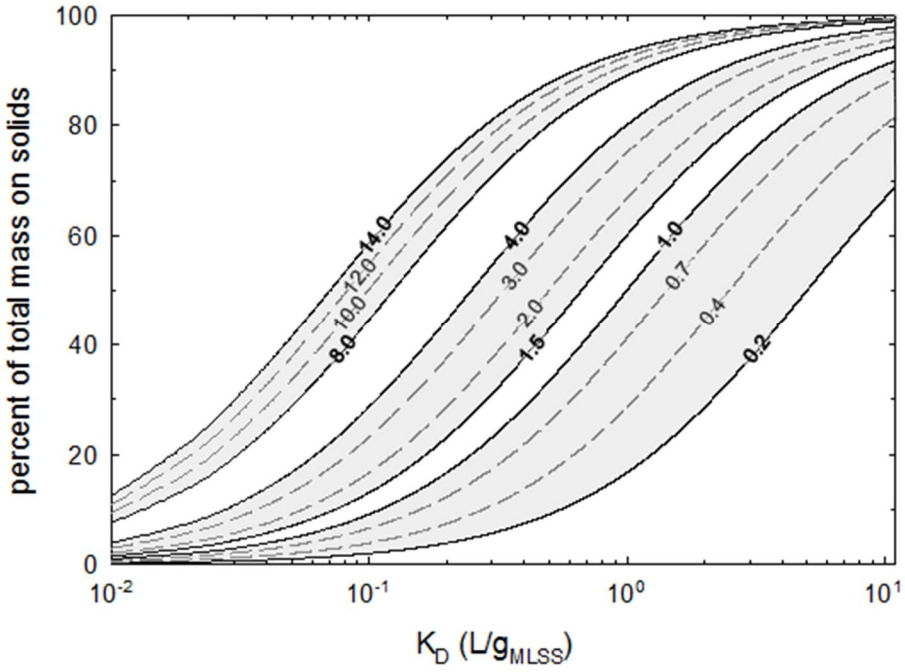

Figure III-8: Fraction of PhAC sorbed to mixed liquor solids for PhACs with K_D values ranging from 0.01 to 10 L/g-SS. Lines are shown for different reactor mixed liquor concentrations (indicated on the plot in g/L). Three data bands are shown for (from left to right): membrane bioreactors (MLSS = 8.0 – 14.0 g/L), suspended growth/conventional activated sludge systems (MLSS = 1.5 – 4.0 g/L) and lab scale systems (MLSS = 0.2 – 1.0 g/L).

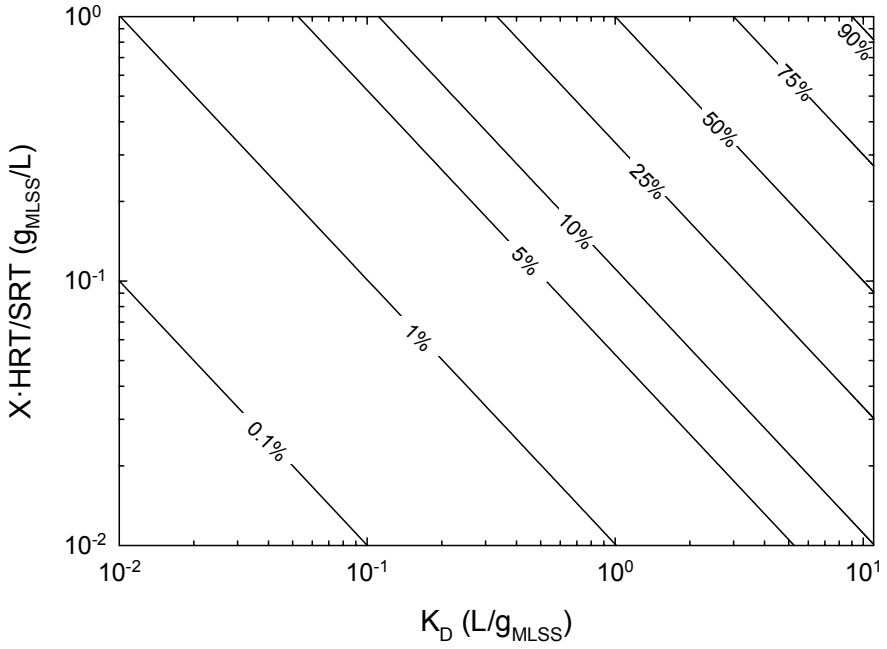

Figure III-9: Contour plot showing fraction of PhAC removed from a biological reactor in waste activated sludge (WAS) based on PhAC K_D (x-axis) and operating conditions – MLSS(X), HRT and SRT (y-axis).

III.5. Biodegradation of PhACs

III.5.1. Review of Studies Reporting Biodegradation of PhACs

PhAC biodegradation is typically modeled assuming first-order biodegradation kinetics with a pseudo first order biodegradation coefficient (k_{BIO} [$L^3/M_{BIOMASS}/T$]) related to the biomass concentration in the reactor (typically using either MLSS or MLVSS) as shown in Equation III-4 (Urase and Kikuta, 2005; Joss et al., 2006; Maurer et al., 2007; Fernandez-Fontaina et al., 2012; Helbling et al., 2012; Fernandez-Fontaina et al., 2013; Pomies et al., 2013).

$$\frac{dS_{PhAC}}{dt} = -(k_{BIO}X\ )S_{PhAC} \qquad \text{(III-4)}$$

A review of recent studies of PhAC biodegradation (see Appendix A for study details) produced a total of 176 data for k_{BIO} for 38 PhACs. Five studies - Clara et al. (2005b); Urase and Kikuta (2005); Joss et al. (2006); Abegglen et al. (2009); Wick et al. (2009) – account for 80% of the data. The range of these k_{BIO} data is 0.007 to 173 Lg-$SS^{-1}d^{-1}$, with 25th percentile, median and 75th percentile values of 0.18, 0.64 and 3.68 Lg-$SS^{-1}d^{-1}$, respectively (Figure III-10). Out of the 176 data, 70 result from experiments or WWTPs using MBRs while the remaining 106 are from SG systems and SRT information is provided for only 86 (47 SG and 39 MBR).

The aggregate data are best described using a 2-parameter log normal distribution, and although k_{BIO} for this data set spans over 4 orders of magnitude, 90% of the data are between 0.1 and 10 Lg-$SS^{-1}d^{-1}$. Researchers have suggested categorizing PhACs based on the measured biodegradation rate coefficients. Joss et al. (2006) for example, classified the 25 PhACs studied in three categories: no removal (k_{bio} < 0.1 Lg-$SS^{-1}d^{-1}$); partial removal (0.1 < k_{bio} < 10 Lg-$SS^{-1}d^{-1}$) and transformed by more than 90%

(k_{BIO} > 10 Lg-$SS^{-1}d^{-1}$). This approach is useful when considering specific biological systems, but may lack utility as a general design approach (see Figure III-11 for PhACs where five or more k_{BIO} data are available). With BZF for example, there is a 3-order of magnitude range in the measured k_{BIO} values. Therefore, analyses of the biodegradation rate coefficients would be required for each biological system unless QSAR/QSBR techniques can be used to link the biodegradation rate coefficients to biological system design and/or operating conditions and PhAC properties.

The pseudo-first order approach to modeling PhAC fate during biological wastewater treatment does not provide a means to link specific biochemical reactions to PhAC degradation and mineralization in WWTPs. To achieve this consortium-level approach a model such as the activated sludge models (ASM) framework (Henze et al., 2000) is required. The ASM model framework is flexible; specific processes can be added or modified as more knowledge becomes available. Because the ASM models are based on microbial consortia and their related growth and decay processes, the process kinetics and conceptual models may be extended beyond engineered WWTPs to the natural environment (for example, see (Reichert et al., 2001)). Limitations of using the ASM-framework approach to model PhAC biodegradation include the number of variables required to completely model the fate of PhACs during wastewater treatment and the complexity of experiments required to obtain the requisite model parameters.

This approach has been evaluated to a limited extent to describe the fate of certain PhACs (Plósz et al., 2010) or proposed within the context of potential upgrades to the ASM modeling framework to model other micropollutants (Peev et al., 2004; Hiatt and Grady, 2008; Schoenerklee et al., 2009). Peev et al. (2004) used Monod kinetics to model micropollutant degradation by a fraction of heterotrophs (*specialized*

heterotrophs). Plósz et al. (2010) used the ASM modeling framework to evaluate the fate of three anitibiotics (sulfamethaxazole, tetracylcine and ciprofloxacin) in batch experiments using sludge collected from the aerobic reactor of an MLE-process. The authors considered sorption and biodegradation of the parent PhAC in addition to formation of the parent PhAC from conjugated or glucorinated species within the bioreactor. Biodegradation of the PhACs due to heterotrophic versus autotrophic biomass in the MLE process is not separately incorporated into the model. While this is a convenient means to evaluate the attenuation of the PhACs, changes in the operating conditions (e.g., SRT) will inevitably change the biomass composition and potentially the values of the kinetic coefficients developed using this approach. In effect, while the authors use the analytical approach proposed in the ASM modeling framework, they do not take full advantage of the process modeling capabilities it offers.

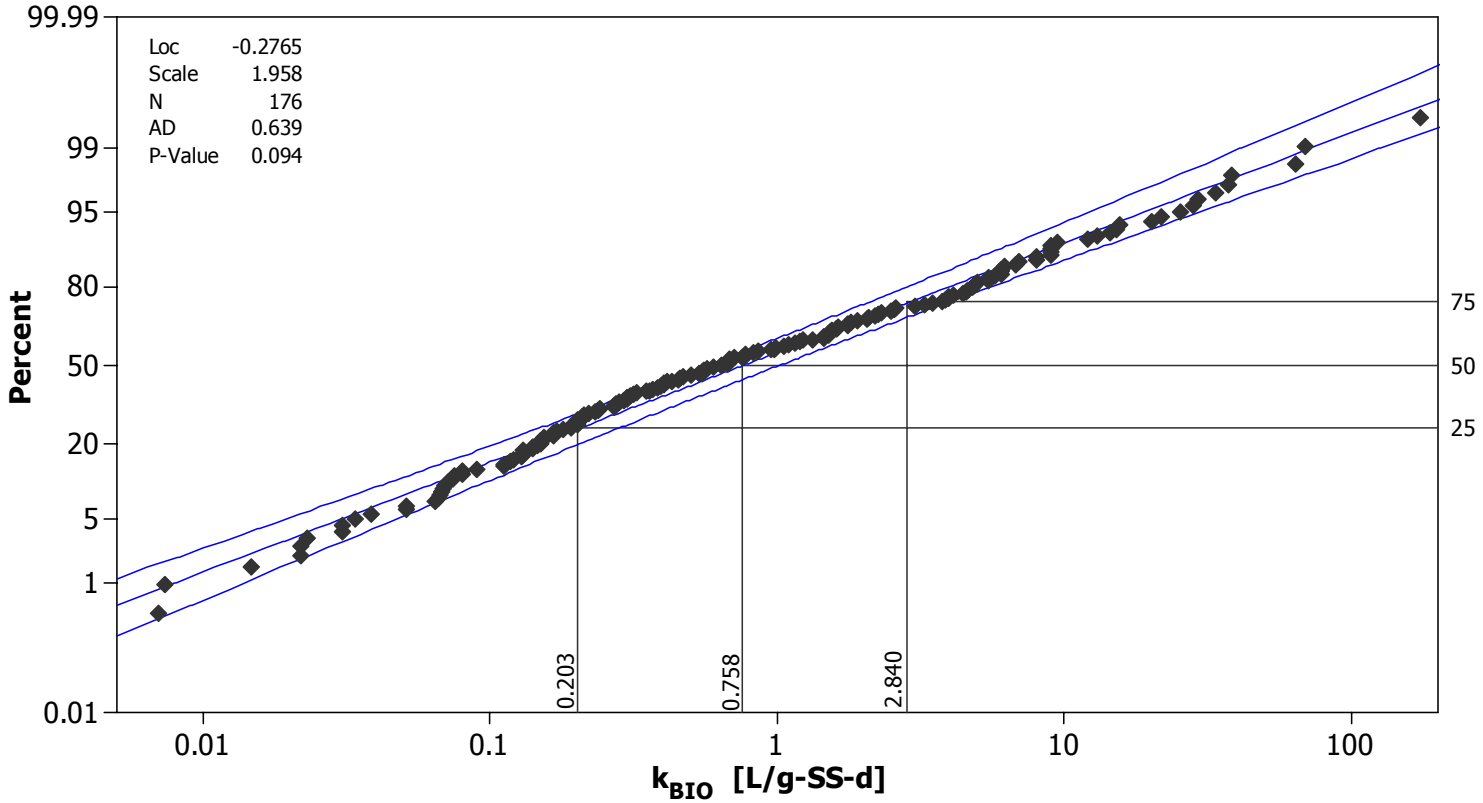

distribution fit: lognormal with 95% CI

Figure III-10: Distribution of reported pseudo first order degradation rate constants for PhACs (k_{BIO}). Data are fit with a 2-parameter log normal distribution. Distribution parameters (location and scale) are provided in the legend along with number of data (N) , Anderson darling statistic and p-value. Also provided are 25th, 50th and 75th percentile values for LN-2 distribution fit to these data. Note that a single PhAC may be represented by multiple data points.

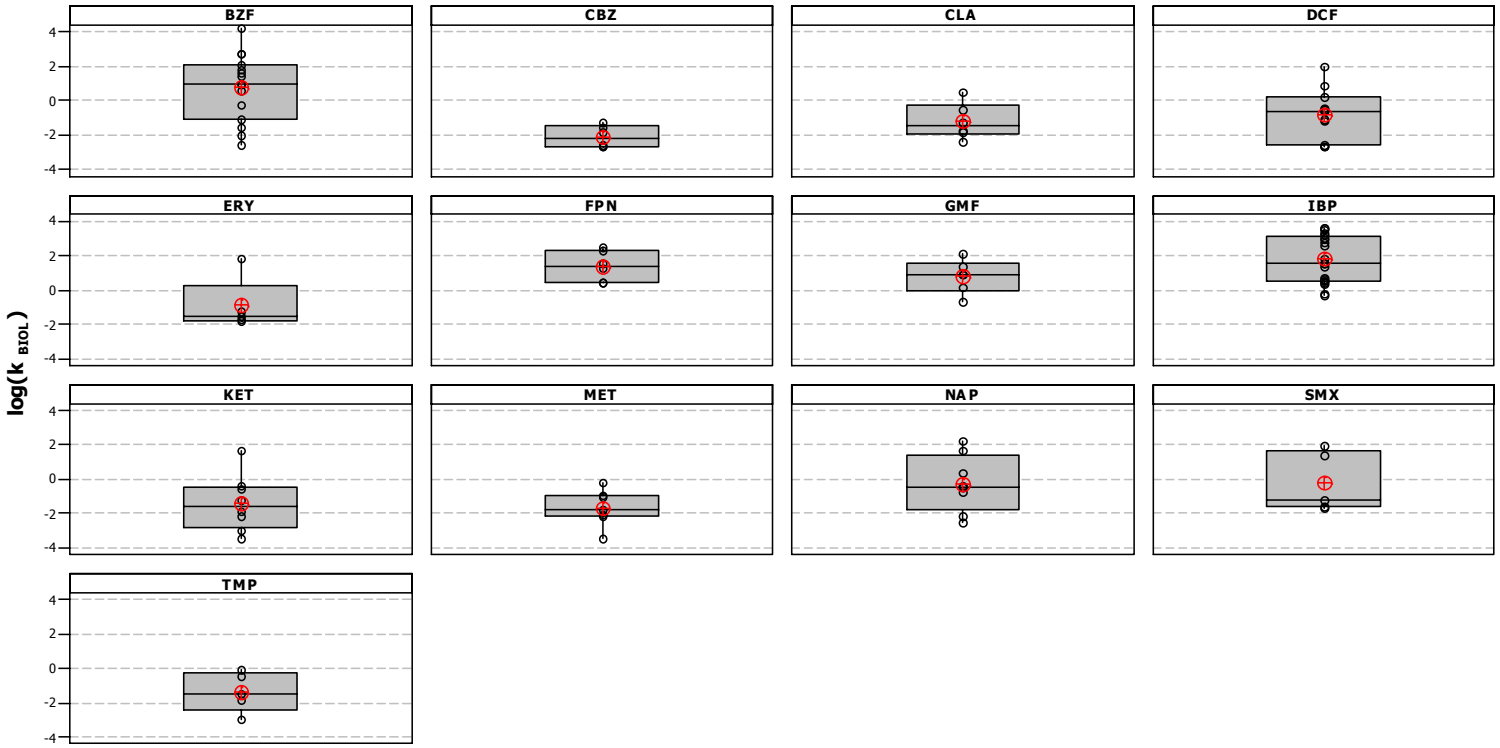

Figure III-11: Measured biodegradation rate coefficients for 13 PhACs for which 5 or more data are available. Individual data points shown using small black circles; horizontal line indicates median; mean indicated by large red circle with cross-hairs. Box extents indicate 25th (Q1) and 75th (Q3) percentile with whiskers extending to upper limit [Q3 + 1.5(Q3-Q1)] and lower limit [Q1 - 1.5(Q3-Q1)].

III.5.2. Assessing Factors which Influence PhAC Biodegradation Rate Coefficients

III.5.2.1. Influence of Process Design and Operating Conditions

When considered independently, no single operations variable (specifically MLSS/VSS, SRT, redox conditions) is correlated with k_{BIO} (in all cases $R^2 < 0.15$). For example, shown in Figure III-12 are data for the four PhACs for which there are five or more corresponding values of k_{BIO} and SRT – BZF, DCF, IBP and MET. Analysis of these limited data suggest no general relationship between SRT and PhAC k_{BIO}. Increases in SRT result in diversification of the microbial community within a WWTP (Valentin-Vargas et al., 2012) which could result in enhanced biodegradation options for PhACs. However, an increase in SRT also results in a decrease in the active biomass fraction in the mixed liquor which perhaps may counterbalance the increased diversity. Changes in SRT therefore cannot be used directly to predict k_{BIO}. These observations are consistent with the conflicting data in the literature related to the influence of SRT on biodegradation and k_{BIO} (Stasinakis et al., 2010; Majewsky et al., 2011). In fact, given the lack of a correlation between SRT and PhAC removal (see Section 3.1) or k_{BIO}, there is no basis for a generalizable recommendation regarding design SRT as a metric to achieve PhAC attenuation or degradation during wastewater treatment. This is in contrast to the widespread use of SRT as an effective guide for WWTP design and operation to achieve COD or nutrient removal targets.

Comparison of the k_{BIO} data for SG and MBR systems suggests that SG processes tend to be more effective for PhAC biodegradation (Figure III-13). The median values of k_{BIO} for suspended growth and MBR are 1.38 and 1.15 Lg-$SS^{-1}d^{-1}$, respectively. This is in contrast to the impact that unit operation selection has on PhAC removal as discussed in

Section 3.2. Considering that SRT has negligible influence on k_{BIO}, biosolids characteristics, resulting from operation in suspended growth systems relative to MBRs, could play a role in explaining the observed differences in k_{BIO} data. Sperandio et al. (2005), for example, have shown that MBRs and activated sludge processes operated at similar SRTs have distinctly different floc size distributions and EPS concentrations. Although k_{BIO} values appear to be higher for suspended growth processes based on these data, it is important to note that MBRs are typically operated at significantly higher biomass concentrations. A comparison of the effective biodegradation rate coefficient (i.e., $k_{BIO}X$, using the data shown in Figure III-13) for suspended growth and MBR processes operating with MLSS concentrations of $1.5-4$ and $8-10$ gL^{-1}, respectively, indicates that the MBRs are between 3 to 5 times more effective for PhAC biodegradation than suspended growth processes.

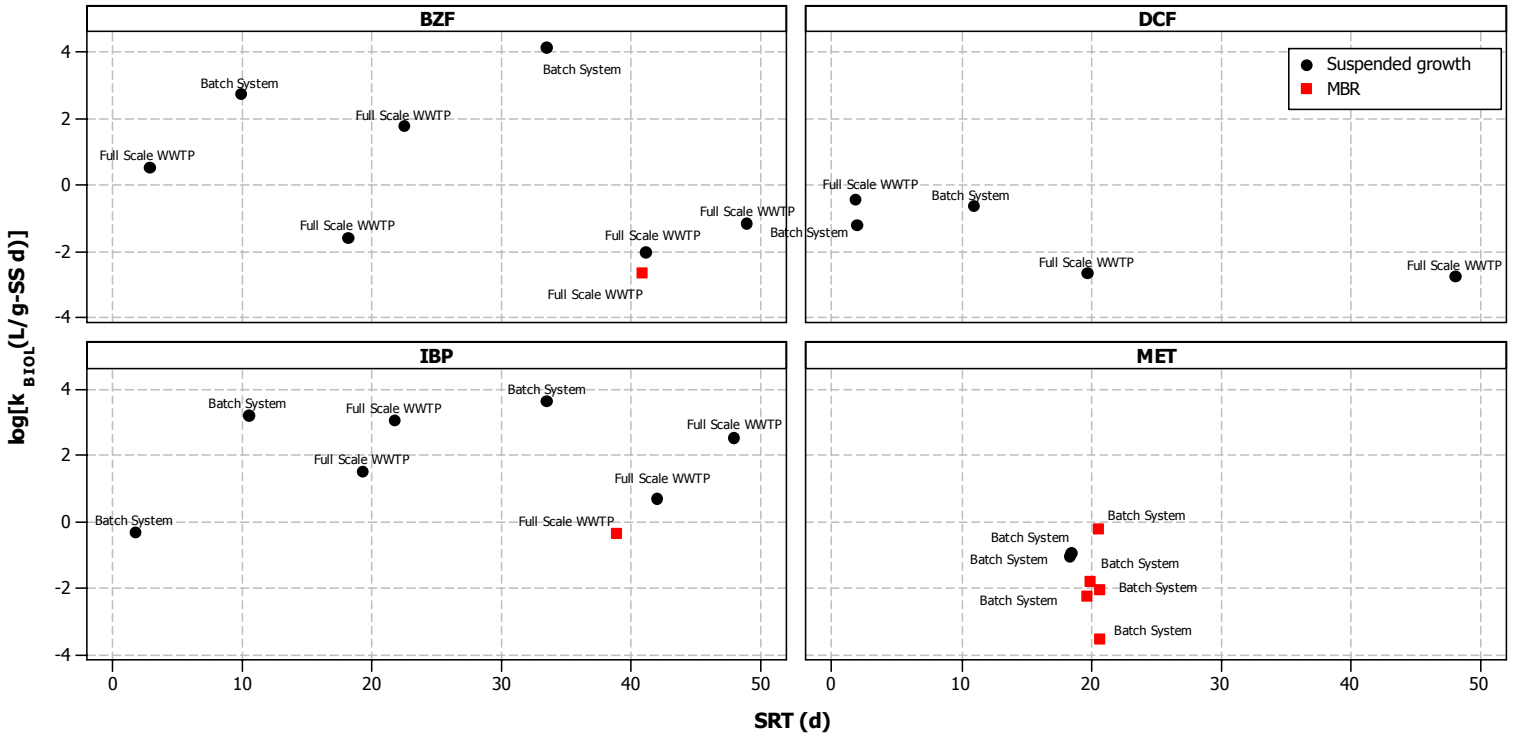

Figure III-12: Evaluating the relationship between SRT and k_{BIO} for BZF, DCF, IBP and MET (PhACs for which there are 5 or more data with both k_{BIO} and SRT). Data are classified by experimental system where measurements were made (data label: Batch System or Full Scale WWTP) and type of Biological system (legend: suspended growth or MBR).

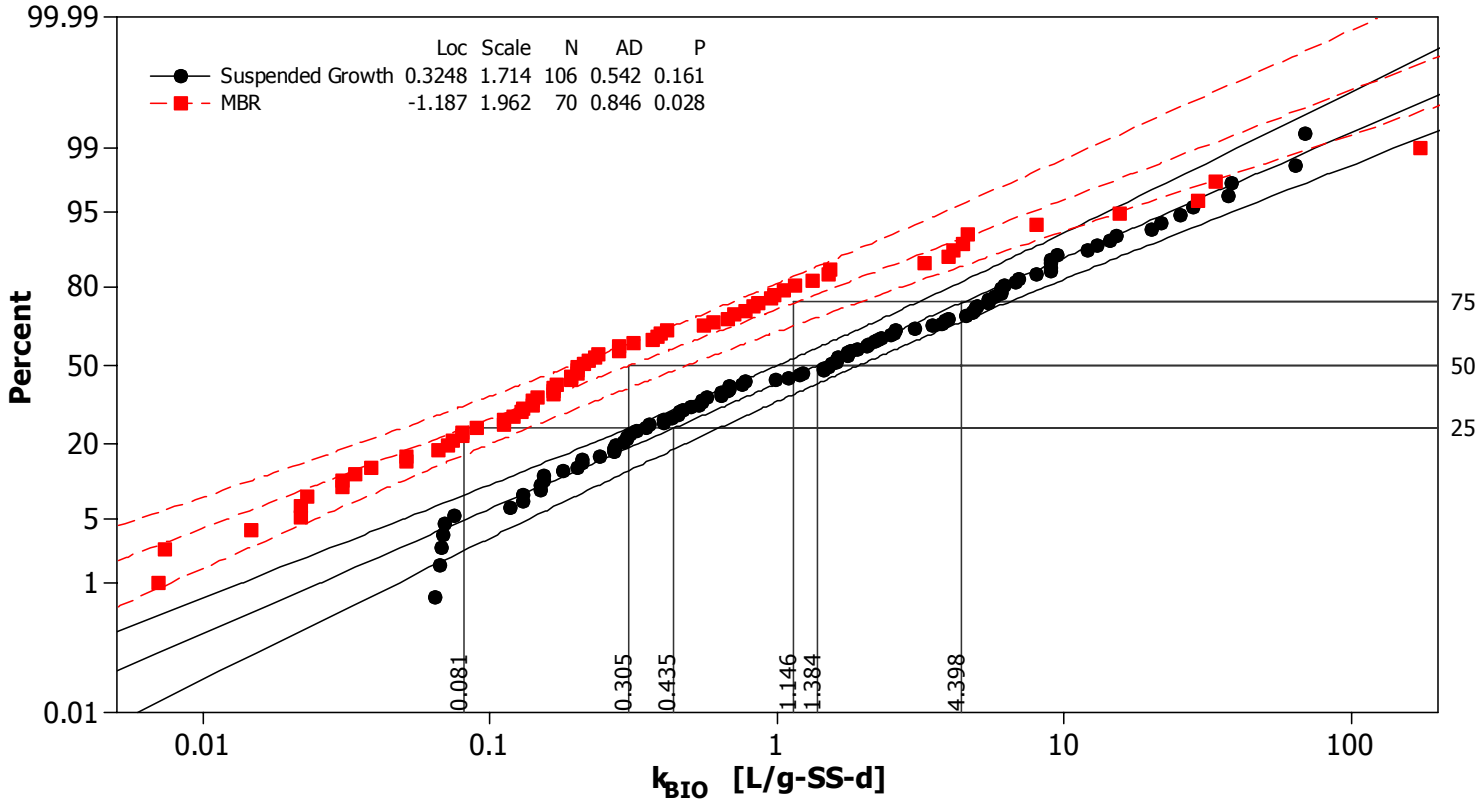

Figure III-13: Distribution of reported pseudo first order degradation rate coefficients for PhACs (k_{BIO}) for available data from studies utilizing suspended growth (black circles) or MBR (red squares). Both data sets are fit with a 2-parameter log normal distribution. Distribution parameters (location and scale) are provided in the legend along with number of data (N) , Anderson darling statistic (AD) and p-value. Also shown are 25th, 50th and 75th percentile values for LN-2 distribution fit to these data. Note that a single PhAC may be represented by multiple data points.

III.5.2.2. PhAC Properties and Biodegradation

Review of the available data for k_{BIO} indicates that acidic PhACs tend to have higher k_{BIO} values than those for basic PhACs (Figure III-14). The median values for acidic and basic PhACs are 1.37 and 0.49 Lg-SS^{-1}·d^{-1}, respectively. While the reasons for these differences have not been explored in the literature, one hypothesis is that differences in the charge of the dominant species in result in differences in the transport mechanism for PhACs into bacteria. The acid dissociation coefficient (pK_A) values for the acidic PhACs included in this evaluation ranged from 3 to 6 and between 8 and 14 for the basic PhACs. Consequently, the dominant species for acidic PhACs (>85%) in typical biological treatment processes where the pH is ~7-8 are typically negatively charged, whereas the dominant species for the majority of basic PhACs are uncharged. Note that the dominant species also plays a significant role in determining the extent of PhAC sorption during biological wastewater treatment (Sathyamoorthy and Ramsburg, 2013). Evaluation of the influence of chemometric properties typically used in PhAC design and development (see Sathyamoorthy and Ramsburg (2013) for details of PhAC properties) indicates that k_{BIO} for acidic and basic PhACs are weakly correlated with the fraction of aromatic carbon atoms and molecular volume, respectively (see Table III-2).

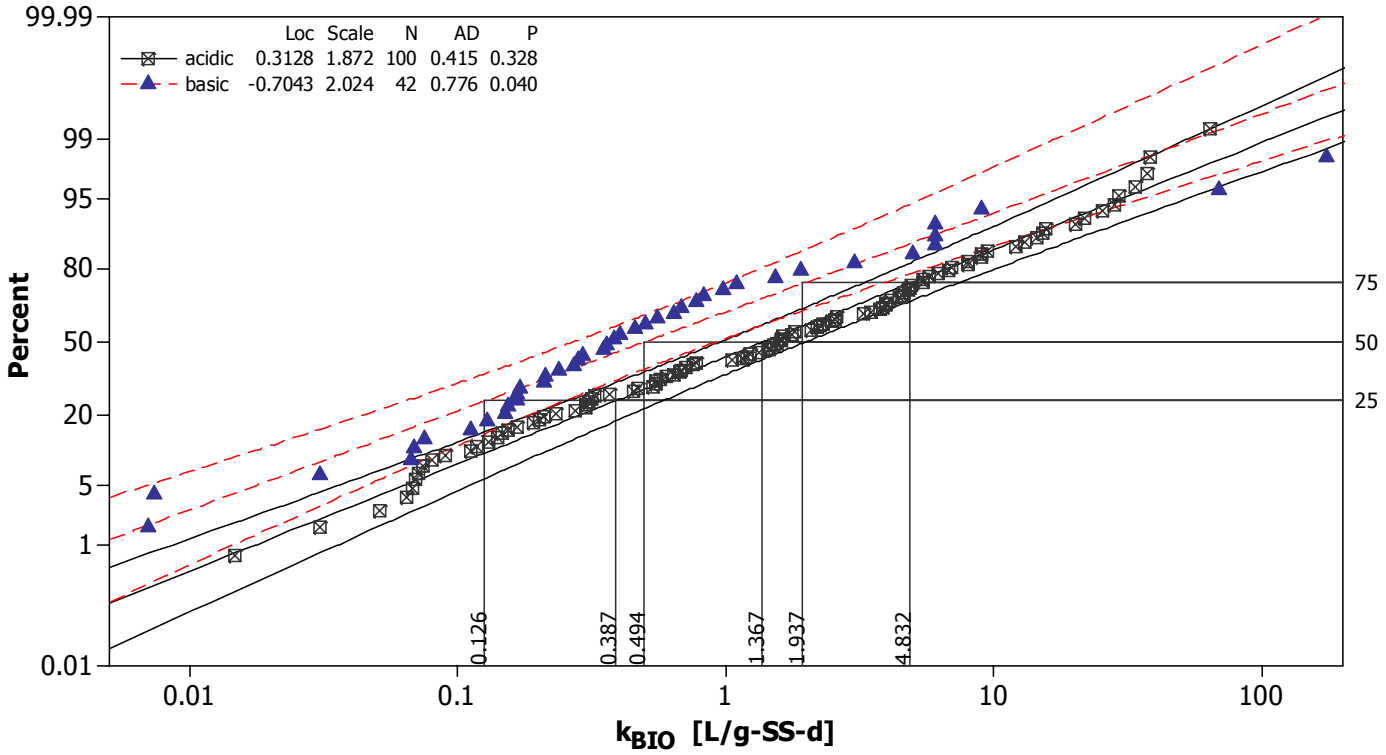

distribution: lognormal with 95% CI

Figure III-14: Distribution of reported pseudo first order degradation rate coefficients for PhACs (k_{BIO}) for available data for acidic (square with x) and basic pharmaceuticals (blue triangles). Both data sets are fit with a 2-parameter log normal distribution. Distribution parameters (location and scale) are provided in the legend along with number of data (N) , Anderson darling statistic (AD) and p-value. Also shown are 25th, 50th and 75th percentile values for LN-2 distribution fit to these data. Note that a single PhAC may be represented by multiple data points.

Table III-2: Statistically significant Pearson Correlation Coefficients (R) (i.e., p-value < 0.05) between k_{BIO} and PhAC molecular, structural and partitioning properties

Property			Pearson R	
			Acidic	Basic
Molecular Volume	MV	$Å^3$	*N/S*	**-0.386**
Van der Waals Surface Area	vdWSA	$Å^2$	*N/S*	*N/S*
Polar Surface Area	TPSA	$Å^2$	*N/S*	*N/S*
Fraction of Organic Carbon Atoms	f_{OC}	--	**-0.334**	*N/S*
Pi Energy	PiEnergy		*N/S*	*N/S*
Hydrogen Bond Donors	nHBD	#	*N/S*	*N/S*
Hydrogen Bond Acceptors	nHBA	#	*N/S*	*N/S*
Number of Rotatable Bonds	nRB	#	*N/S*	*N/S*
Octanol-Water Partitioning Coefficient	log K_{OW}	--	*N/S*	*N/S*

Note: N/S – Pearson R is not reported because it is not statistically significant (i.e., p > 0.05).

III.6. Nitrification and PhAC Removal

Researchers have begun to study the links between nitrification and PhAC degradation motivated by observations that PhAC attenuation is enhanced in BNR processes. While several studies have evaluated PhAC attenuation using biomass from WWTPs operated at long SRT where nitrification occurred, only few have specifically addressed the role of nitrification in PhAC removal or biodegradation. Both Batt et al. (2006) and Tran et al. (2009) compared PhAC removal in the presence and absence of nitrification using batch systems with nitrification inhibited using allylthiourea (ATU), a specific inhibitor of ammonia oxidizing bacteria (AOB) (Ginestet et al., 1998). Their results suggest that the occurrence of nitrification in these experimental systems did enhance PhAC removals although all the PhACs evaluated were degraded to some extent even when nitrification was inhibited (Figure III-15). The benefits of nitrification for PhAC degradation have also been demonstrated in flow-through systems operated under conditions that promote nitrification by Suarez et al. (2010). Their data are, however, inadequate to conclude that the observed increases in PhAC attenuation at longer SRTs is a direct result of the activity of nitrifying bacteria. Fernandez-Fontaina et al. (2012) suggest that PhAC biodegradation rates and extents depends on the specific nitrification rate (SNR, [mg-N/g-VSS·d]). For a set of six PhACs studied by Fernandez-Fontaina *et al.* (IBP, NAP, TMP, ERY, ROX, FLX), the specific conversion rate of PhACs (μg-PhAC/g-VSS·d) increased with increasing SNR. It is should be noted that the pseudo first order biodegradation rate coefficient (k_{BIO} [Lg-$VSS^{-1}d^{-1}$]), increased for only four of the six PhACs. For ERY and ROX, the k_{BIO} data are highly scattered and a negative correlation with SNR is suggested by the authors (R^2=0.028 and 0.118 for ERY and ROX, respectively).

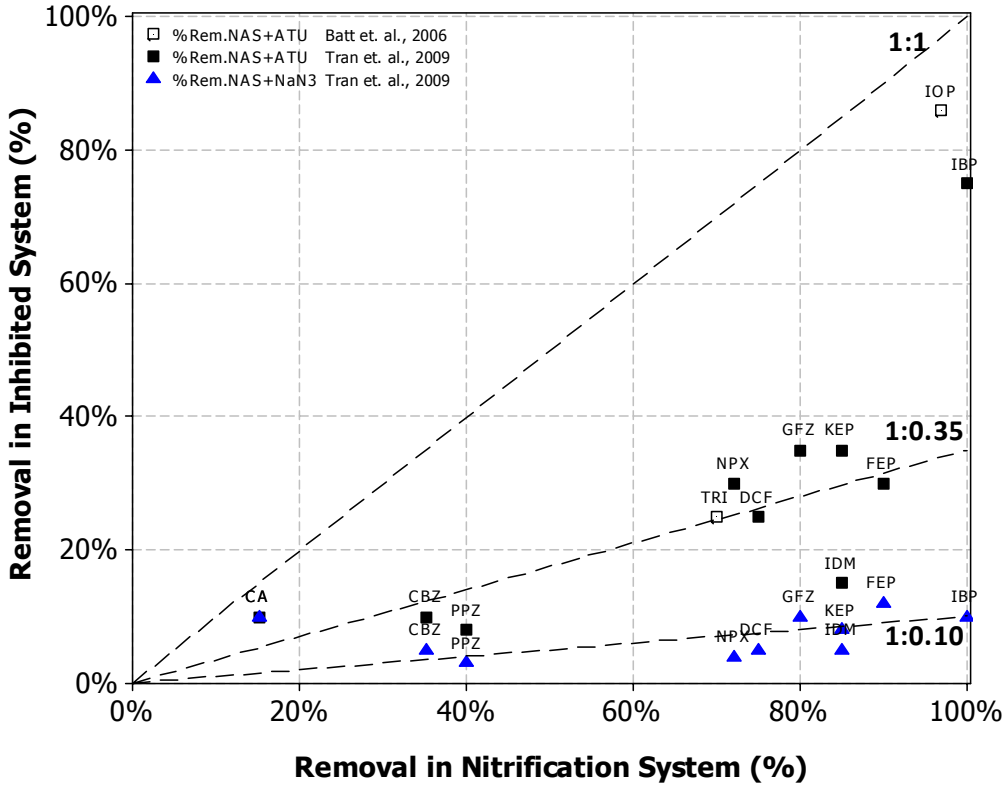

Figure III-15: Comparison of PhAC removal with nitrification with PhAC removal when nitrification is inhibited (using ATU) and biomass is inactivated (using NaN_3) from Tran et. al., 2009. Also shown for comparative purposes are reference lines at 10%, 35% and 100%

Measured biodegradation rate coefficients (k_{BIO}) from three studies specifically evaluating PhAC removal under nitrifying conditions is summarized in Figure III-16. There is a large range for the degradation rate constants with ibuprofen being rapidly degraded in one study (Suarez et al. (2010): $k_{BIO,IBP}$ = 20 L/g-VSS·d) but much more slowly in another (Tran et al. (2009): $k_{BIO,IBP}$ = 3.63 L/g-VSS·d). While these data are useful in providing order of magnitude estimates of the attenuation rates of these PhACs, care should be exercised to ensure biomass conditions reflect those used in these studies when using these rate coefficients to predict PhAC biodegradation.

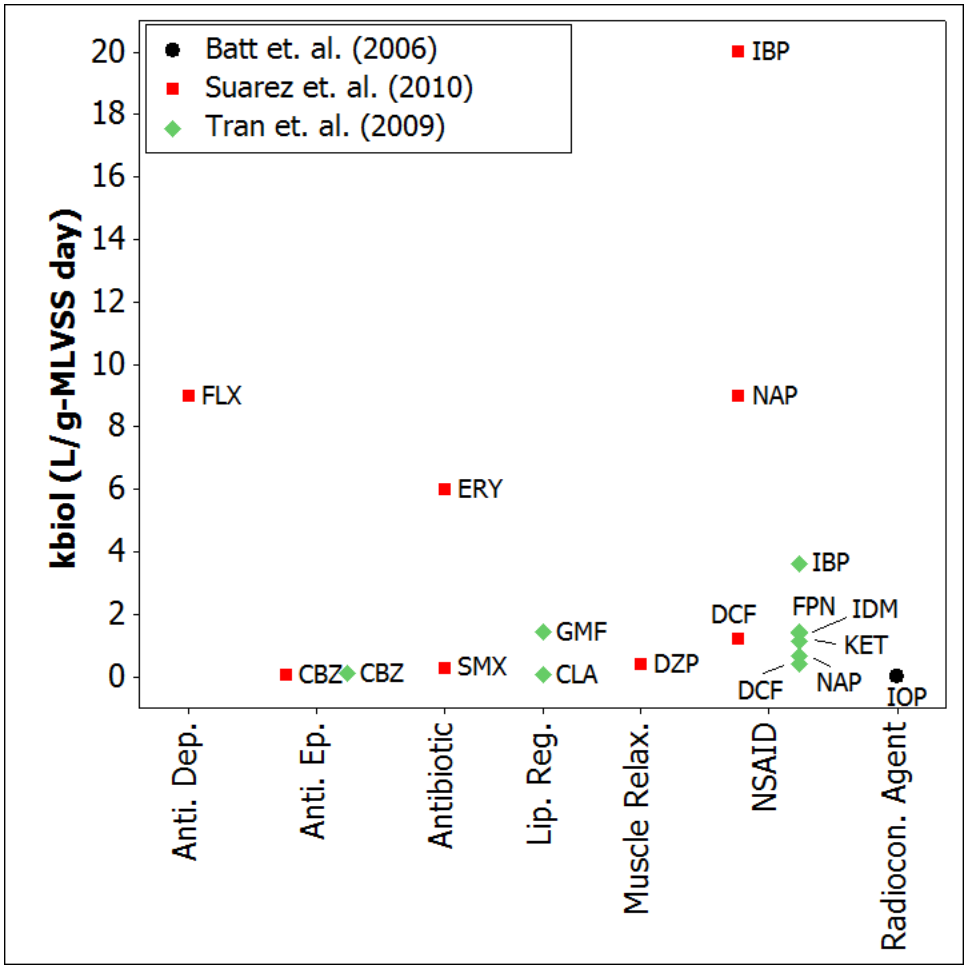

Figure III-16: Biodegradation Rate Constants for PhACs in Nitrifying Systems [Data from (Batt et al., 2006; Tran et al., 2009; Suarez et al., 2010)**]**

Recently, it has been suggested that heterotrophic bacteria may have a significant role in the degradation of microconstituents even at long SRTs while nitrifying bacteria may play only a minor role (Gaulke et al., 2009; De Gusseme et al., 2011). Researchers have also suggested that the observed degradation of PhACs and other micoconstituents may result from abiotic nitration rather than biodegradation during nitrification (Gaulke et al., 2008; Chiron et al., 2010). Abiotic nitration of pharmaceuticals could result due to attack by nitronium ion (NO_2^+) or by reactive nitrogen species (RNS) such as such as nitrogen dioxide radicals ($NO_2\bullet$) or peroxynitrate ($ONOO^-$)in solution. Nitrification, particularly at low dissolved oxygen levels, results in

the formation of precursors to both NO_2^+ and RNS (Arp and Stein, 2003). Chiron et al. (2010) evaluated the biodegradation of ACM at a relatively high concentration of 100 μg/L in activated sludge using batch experiments designed for nitrification (initial ammonia nitrogen concentration 10 mg-N/L). The seed sludge was collected from the second stage of a two-stage WWTP (1st stage: BOD removal, 2nd stage: nitrification) where the second stage was operated at a 16-day SRT, 15-h HRT. The seed sludge was preconditioned to minimize biodegradable COD. ACM was attenuated in batch experiments where nitrification occurred and control experiments where nitrification was inhibited. The biodegradation rate was lower when nitrification was inhibited however with ACM half lives of 1.77 ± 0.14 and 2.43 ± 0.19 days in the nitrification experiments and nitrification inhibition control, respectively. The results suggest that heterotrophs in the control reactor degraded the ACM. A similar observation has been noted by other researchers for ACM and other PhACs (Tran et al., 2009; De Gusseme et al., 2011). Interestingly, while 3-hydroxy acetaminophen was formed as an intermediate metabolite in both systems, 3-nitro acetaminophen was only produced in the nitrification experiment system. Hydroxylation is often reported as a mechanism of aromatic compound attack in natural and engineered biological systems (Perez and Barcelo, 2008; Topp et al., 2008), this is however, the first evidence of nitration of PhACs in activated sludge. Nitration yield of ACM was demonstrated to increase at lower pH conditions.

Experiments which specifically evaluate the role of nitrification in PhAC removal and biodegradation suggest that nitrification processes have a role in PhAC biodegradation. However, the specific pathways of PhAC degradation, whether cometabolic or nitration, remain unclear and additional research aimed at

understanding the role of nitrifying bacteria and specific enzyme systems in PhAC biodegradation is required. While the percentage of nitrifiers (AOB and NOB), even in second stage separate-sludge nitrification systems may be small, the results to date suggest that the metabolites produced through the nitrification process are persistent and may be discharged into the environment in WWTP effluents.

III.7. Evaluating the Impact of Pharmaceuticals on the Treatment Process

The focus of this chapter thus far has been on evaluating the treatability of PhACs in wastewater treatment processes, however, an equally important aspect is the impact of PhACs on the bacterial consortia within the wastewater treatment plant. LC50 levels for carbamazepine (CBZ), diclofenac (DCF) and clofibric acid (CLF) of >81 mg/L, 91.8 mg/L and 11.5 mg/L, respectively have been found using the *microtox®* toxicity assay (Ferrari et al., 2003). These levels are significantly higher than typically reported WWTP influent or effluent levels, suggesting that these PhACs present minimal, if any, lethal risks to biota in a WWTP. A similar conclusion was reached by Dokianakis et al. (2004), who evaluated the impact of six PhACs (ofloxacin, propranolol, clofibrate, carbamazepine, diclofenac and sulfamethoxazole) and the antibacterial agent triclosan on NOB.

Wang et al. (2008) illustrated that NAP, KET and CBZ have a significant negative impact on microbial growth at a concentration of 10 μM (approximately 2,000 – 2,500 μg/L for this set of PhACs). CLF at 10 μM did not impact microbial growth. This concentration range is significantly higher than the typical concentration noted in WWTP effluents. In their experiments, ethanol was the carbon source (ethanol

concentration 0.2% v/v, theoretical COD approx. 2,890 mg/L) and ammonium sulfate was used for the nitrogen source (43 mg-N/L).An increase in the ethanol concentration to 2% v/v (theoretical COD approx. 28,900 mg/L) was observed to completely mitigate the impacts of all PhACs on microbial growth. The authors suggested that this is related to the growth of specific heterotrophic strains at the high COD which might conceal inhibition of growth of other strains (Wang et al., 2008); however this hypothesis is yet to be tested. In separate experiments, this research team evaluated the impact of NAP, KET, CBZ and gemfibrozil (GMF) on a single sludge COD removal/nitrification SBR (Wang and Gunsch, 2011a). When introduced to the activated sludge individually, none of these PhACs negatively impacted COD removal or nitrification, even at concentrations as high as 10 μM. However, the PhACs were observed to negatively impact nitrification when introduced as mixtures at total PhAC concentrations of 1 μM. A reduction in AOB diversity was also observed. Collectively, these data suggest that mixture effects are particularly important when evaluating the ecotoxicological impact of PhACs. The mechanistic nature of the interaction of the PhACs and the AMO enzyme system or transport of these compounds into the bacterial cells is not well enough understood to conclusively state the reason for these differences between two separate mixed cultures or the mixed culture and pure culture system. It is possible that the diversity of AOB in the mixed culture provides a set of AOB which are more resistant to PhACs than *N.Europaea*. Wang and Gunsch (2011b) showed that exposure to the PhACs at 1 and 10 μM, reduced the percentage of live *N.Europaea* cells in the pure culture studies.

Acclimation of the biota to PhACs has an impact on extent of nitrification inhibition. Rantindine (a anti-ulcer diamine, Zantac®) inhibited nitrification by 5.6% at a concentration of 5 mg/L in a lab-scale SBR operating at a 14 day SRT which has been

acclimated with the PhAC. Activated sludge from a WWTP which was not exposed to any RAN exhibited no nitrification inhibition up to concentrations of 10 mg/L (Carucci et al., 2006). In the same study, atenolol had no impact on nitrification at high nitrification rates (5.83 and 7.59 mg-NH_4-N/g-VSS·h). At a lower ammonia loading rate however (nitrification rate = 2.91 mg-NH_4-N/g-VSS·h), a 10% inhibition was noted at 10 mg/L ATN. The inhibition increased to 28.8% at 40 mg/L.

III.8. Conclusions and Research Needs

Concerns related to the environmental impact of PhACs and other microconstituents has resulted in a dramatic increase in research related to their fate and ecotoxicology in engineered and natural environmental systems. Studies of PhAC fate during biological wastewater treatment indicate that existing infrastructure and processes are capable of PhAC attenuation through sorption and biodegradation.

Peer reviewed studies assessing PhAC removals have been reviewed in this chapter. Reported PhAC removals vary over a wide range, even for a single PhAC. Moreover, removals of a given PhAC or set of PhACs observed at a single WWTP are not generalizable. A critical review of the observed removals in both SG and MBR processes suggests that no design or operating parameters (e.g., SRT or MLVSS) are adequate to explain the variation in PhAC removal data. In fact, SRT, a commonly used parameter for WWTP design and operations is a poor indicator of PhAC removal performance across WWTPs. And, targeting a specific SRT to achieve PhAC removal is not a useful design or operations strategy. While the knowledge related to PhAC fate during biological wastewater treatment has increased significantly in recent years, there are still key knowledge gaps which merit further research.

The sorbed fraction of a PhAC could account of up to 80% of the total PhAC mass in MBRs. Sorption therefore plays a critical role in determining the fate of several PhACs. There is however a wide variation in PhAC K_D values, even for a single PhAC, making it difficult to predict the extent of PhAC sorption *a priori*. The variation is unrelated to the experimental protocol or biomass inactivation method in sorption experiments. Therefore, research exploring whether differences in PhAC properties or biosolids surface characteristics can be utilized to explain the variation in PhAC sorption would be beneficial to develop a predictive capability for PhAC sorption during biological wastewater treatment.

The pseudo-first-order approach (Equation III-4) is frequently used to model PhAC degradation despite its lack of mechanistic or process significance. While this approach is convenient, it is of limited value when comparing PhAC degradation across unit operations and processes. The main limitation being that it does not link PhAC degradation with specific biochemical processes. This can be effectively accomplished by integrating PhAC biodegradation to processes such as biomass growth, decay, COD removal and nitrification. The ASM framework (Henze et al., 2000) offers a well-established, flexible modeling framework to accomplish this. Research elucidating the specific biological processes responsible for PhAC biodegradation and an effective predictive model to describe the process would be invaluable to the environmental engineering and science community.

Chapter IV. Objectives and Hypotheses

IV.1. Motivation for Research

Modern wastewater treatment plants (WWTPs) are increasingly designed to meet low nutrient (i.e., nitrogen and phosphorus) discharges to limit eutrophication in receiving streams. Significant progress has been made; with WWTPs achieving total nitrogen levels as low as 3 mg-NL^{-1} and phosphorus levels below 0.05 mgL^{-1} (Barnard, 2006; Gujer, 2010). Reducing the influx of anthropogenic microconstituents into the environment could be an important additional regulatory challenge for environmental professionals in the future (Schwarzenbach et al., 2006; Daughton, 2010; Gujer, 2010). In recent years, the ecological effects of microconstituents has been of interest to both the scientific and lay communities (e.g., Daughton and Ternes, 2000; Kolpin et al., 2002; Associated-Press, 2008). A few regulatory agencies have even begun the process of monitoring for selected microconstituents, specifically pharmaceuticals (PhACs) and personal care products (California Department of Public Health, 2007). However, there are currently no regulatory requirements to meet effluent standards pertaining to PhACs.

WWTPs are an important point source of PhACs in the environment. Incomplete PhAC removal has been reported during biological treatment (Ternes et al., 2004; Onesios et al., 2009), though such observations are serendipitous as treatment plant designed is based upon bulk water quality. This research is motivated by an observed correlation between SRT and PhAC removal - specifically that WWTPs operated at SRTs to achieve biological nutrient removal demonstrate improved pharmaceutical (PhAC) attenuation (Clara et al., 2005; Batt et al., 2006; Oppenheimer et

al., 2007; Tran et al., 2009; Chiron et al., 2010; Suarez et al., 2010; Khunjar et al., 2011; Fernandez-Fontaina et al., 2012). The goal of this research is to explore the possible synergy between biological nutrient removal, specifically nitrification, and PhAC biodegradation.

IV.2. Research Objectives

The overall objective of this research is to evaluate the biodegradation and sorption of selected PhACs during nitrification. As such, this research aims to separately evaluate the two mechanisms of PhAC attenuation during biological treatment and examine the role of ammonia and nitrite oxidizing bacteria within the microbial consortia routinely used for treatment. Research herein integrates laboratory-scale experiments with mathematical modeling to meet the specific objectives described below.

Objective 1: Evaluate whether or not PhAC attenuation and biodegradation during biological wastewater treatment can be linked to WWTP specific unit operations, design or operating conditions.

In recent years, PhAC attenuation has been studied at the pilot- and full-scale in numerous WWTPs and lab-scale systems (Jelic et al., 2011; Kraigher and Mandic-Mulec, 2011; Majewsky et al., 2011; Prasse et al., 2011; Camacho-Munoz et al., 2012; Helbling et al., 2012; Suarez et al., 2012; Fernandez-Fontaina et al., 2013). While there have been reviews of PhAC removal as one set of many microconstituents, there are few studies evaluating the role of biological treatment processes to include process conditions, unit operations and operating condition coupled with PhAC properties.

Furthermore, a review of individual studies suggests conflicting conclusions related to the role of operating conditions based on observations at specific WWTPs. *It is hypothesized that a meta-analysis of PhAC removals reported at individual WWTPs will enable the distillation and formation of generalizable conclusions and recommendations.* This hypothesis will be tested using PhAC removal and biodegradation data from the peer-reviewed scientific literature. It is anticipated that this research will provide a practical basis upon which to build a decision framework for the wastewater treatment community (e.g., WWTP designers and operators). Note that results from this research related to this objective have been presented in the form of a literature review in Chapter III.

Objective 2: Examine the factors which influence PhAC sorption to biosolids during biological wastewater treatment.

A number of bench- and full-scale studies of sorption of PhAC during biological treatment have concluded that equilibrium sorption may be related to hydrophobicity and PhACs with high octanol-water partitioning coefficient (K_{OW}) will sorb to a greater extent to biosolids (Urase and Kikuta, 2005; Stevens-Garmon et al., 2011; Hyland et al., 2012). Such conclusions suggest that non-specific hydrophobic interactions are the dominant mechanism of PhAC sorption to biosolids. Given the complex nature of PhACs however, *it is hypothesized that K_{OW} alone is insufficient to predict equilibrium sorption of PhACs during biological treatment. It is further hypothesized that a multivariate framework incorporating multiple interactions (e.g., hydrogen bonding and pi-pi interactions) will enhance the predictive capability for PhAC sorption to biosolids*. These

hypotheses will be tested through an evaluation of the PhAC sorption data available in peer-reviewed literature sources.

Objective 3: Assess the biodegradation of selected pharmaceuticals during nitrification.

The interplay between PhAC biodegradation and nitrification processes is evaluated to elucidate which nitrification step(s) (i.e., ammonia oxidation or nitrite oxidation) are involved for PhAC biodegradation. *The hypothesis evaluated here is that PhAC biodegradation, when occurring during nitrification, can be linked to ammonia oxidation activity.* This hypothesis is based on evidence that ammonia monooxygenase (AMO), the enzyme responsible for ammonia oxidation by AOB during nitrification, is known to catalyze oxidation of a wide array of aliphatic, aromatic and chlorinated organic substrates (Keener and Arp, 1994; Hooper et al., 1995) and endocrine disrupting compounds (Gaulke et al., 2009; Skotnicka-Pitak et al., 2009). The ability of AOB to catalyze non-specific oxidation of several compounds stems from the broad substrate range of ammonia monooxygenase (AMO) enzyme (Hooper et al., 1997). It is important to note here that this approach does not assume that all PhACs are biodegraded by nitrifying organisms. The hypothesis will be tested using a set of structurally and functionally similar PhACs.

Objective 4: Develop a predictive framework to model PhAC biodegradation during nitrification.

The ability to predict PhAC biodegradation utilizing process based models will provide a powerful tool to evaluate PhAC fate and transport in engineered and natural

systems. To date, the majority of biodegradation models for PhACs in environmental systems have utilized pseudo-first order kinetics on an aggregate biomass basis in spite of its lack of mechanistic significance, particularly in complex mixed community biological reactors (e.g., Urase and Kikuta, 2005; Joss et al., 2006). Here, the objective is to develop a biomass specific, process-based module for PhAC biodegradation during nitrification. *The hypothesis tested here is that PhAC biodegradation during ammonia oxidation is a result of cometabolic biodegradation by AMO.* This hypothesis is based on the broad substrate specific of AMO described above and the autotrophic nature of AOB under aerobic conditions. Existing approaches to model cometabolic biodegradation (Criddle, 1993; Alvarez-Cohen and Speitel, 2001) will be adapted to model PhAC biodegradation.

While AOB rely on AMO for ammonia oxidation as part of its energy metabolism (Arp and Stein, 2003), the cometabolic oxidation of organic compounds by AMO does not result in energy generation. In fact organic compounds undergoing cometabolic oxidation may negatively impact ammonia oxidation by competitively binding to the same catalytic site (Arp et al., 2007) or an allosteric alternate site (Taher and Chandran, 2013) on AMO. Therefore, *it is further hypothesized that PhACs which are cometabolically biodegraded by AMO exert an inhibitory effect on AMO and consequently reduce the rate of AOB growth.* Modifications to the Monod equation, typically used to describe AOB growth, incorporating inhibition by PhACs, will be tested (Bailey and Ollis, 1986; Grady et al., 1999). These hypotheses will tested using those PhACs evaluated under Objective 3.

Objective 5: Integrate PhAC biodegradation processes into the Activated Sludge Modeling framework.

The activated sludge model (ASM) framework (Henze et al., 2000) is now a widely accepted as the standard for modeling and simulating biological treatment processes in WWTPs. In fact, since the publication of the IWA report on developing a unified modeling framework for wastewater professionals (Henze et al., 1987; Henze et al., 2000), the ASM model has been extensively adapted and extended to include a wide array of processes and even applied to natural systems (Reichert et al., 2001; Iacopozzi et al., 2007; Hiatt and Grady, 2008; Janus and Ulanicki, 2010; Plosz et al., 2012). The objective here is to integrate PhAC attenuation resulting from cometabolic biodegradation by AOB (see Objective 4) into process models for WWTPs and surface water pollutant fate models (Henze et al., 2000; Deksissa et al., 2004; Pauer and Auer, 2009). *It is hypothesized this can be achieved through a set of cometabolic biodegradation coefficients linked to AOB growth.* This hypothesis will be tested using those PhACs evaluated under Objective 3 which are observed to be biodegraded by AOB. The cometabolic biodegradation coefficients developed in this research cannot be employed more generally without consideration of their uncertainty and sensitivity to model inputs. Therefore, sensitivity analyses are conducted to assess the effect of changes in AOB biokinetic parameters on the cometabolic biodegradation coefficients.

Chapter V. Materials and Methods

V.1. Materials

Chemicals used for anion standards were purchased from suppliers as noted in Table V-1 as used as received. Pharmaceuticals (PhACs) for this research were purchased from suppliers as noted in Table V-2 and used as received. Chemicals used for HPLC analyses are listed in Table V-3. Chemicals utilized for the synthetic feed for the lab-scale nitrification enrichment SBR (see details in Section V.2.2) are listed in Table V-4. Ultrapure water (referred to in the remainder of this chapter as MilliQ water) (resistivity ≥ 18.2 MΩ-cm, TOC ≤ 8 ppm) for this research utilized to make chemical standards and the requisite solutions for analyses was obtained from a MilliQ Gradient A-10 system (Millipore, Inc.).

Table V-1: Chemicals used in multi-anion and individual anion standards

Name	Molecular Formula	CAS Number	Manufacturer	Item Number
Potassium Chloride	KCl	7447-40-7	Fisher Chemicals, Fairlawn, NJ	P217-500
Potassium Nitrite	KNO_2	7758-09-0	Acros Organics, Geel, Belgium	423065000
Potassium Nitrate	KNO_3	7757-79-1	Acros Organics, Geel, Belgium	424155000
Potassium Phosphate (monobasic)	KH_2PO_4	7778-77-0	Acros Organics, Geel, Belgium	205920025
Sodium Phosphate	Na_2SO_4	7757-82-6	Fisher Chemicals, Fairlawn, NJ	S415-1

Table V-2: Pharmaceuticals purchase for research study

Name	Molecular Formula	Supplier	CAS Number	Manufacturer	Item Number	Purity
Atenolol (ATN)	$C_{14}H_{22}N_2O_3$	Fisher Scientific	29122-68-7	MP Biomedicals	190017	≥ 99%
Metoprolol Acid (MAC)[1]	$C_{14}H_{21}NO_4$	Santa Cruz Biotechnology	S6392-14	Santa Cruz Biotechnology	SC-211903	≥ 98%
Metoprolol tartarate (MET)	$(C_{15}H_{25}NO_3)_2{\cdot}C_4H_6O_6$	Sigma Aldrich	56392-17-7	LKT laboratories	M1879	≥ 99%
Naproxen (NAP)	$C_{14}H_{14}O_3$	Fisher Scientific	22204-53-1	ACROS Organics	ICN19024750	≥ 99%
Sotalol Hydrochloride (SOT)	$C_{12}H_{20}N_{20}O_3S.HCl$	Sigma Aldrich	959-24-0	Sigma life sciences	S0278-100MG	≥ 99%

1. Metoprolol acid is a metabolite resulting from atenolol and metoprolol hydroxylation

Table V-3: Chemicals used for HPLC mobile phase

Name	Molecular Formula	Supplier	CAS Number	Manufacturer	Item Number	Purity
Acetonitrile (MeCN)	CH_3CN	Fisher Scientific	75-05-8	Fisher Chemical	A998-4	HPLC grade (≥ 99.9%)
Phosphoric acid, 85% w/w (PA)	H_3PO_4	Fisher Scientific	7664-38-2	Fisher Chemical	A242-1	Certified ACS grade

Table V-4: Chemicals used in Nit-SBR Synthetic Feed

Function	Name	Molecular Formula	CAS Number	Manufacturer	Item Number	SBR Concentration (at max. volume) (g/L)
Nitrogen Source	Ammonium Sulfate Ammonia-N	$(NH_4)_2SO_4$	7738-20-2	Fisher Chemicals, Fairlawn, NJ	A702-10	2,629 557
Phosphorus Source	Potassium Phosphate	KH_2PO_4	7778-77-0	Acros Organics, Geel, Belgium	205920025	102.5
Alkalinity	Sodium Bicarbonate	$NaHCO_3$	144-55-8	Fisher Chemicals, Fairlawn, NJ	S233-500	45
Micronutrients	Magnesium Sulfate	$MgSO_4.7H_2O$	7487-88-9	Acros Organics Geel, Belgium	124900010	54
	Copper (II) Sulfate	$CuSO_4.5H_2O$	7758-98-7		423615000	0.6
	Calcium Chloride	$CaCl_2.2H_2O$	10043-52-4		207780010	54
	Cobalt Nitrate	$Co(NO_3)_2.6H_2O$	10141-05-6		423585000	0.6
	Zinc Sulfate	$ZnSO_4.7H_2O$	7733-02-0	Fisher Chemicals, Fairlawn, NJ	Z68-500	0.6
	Iron (II) Sulfate	$FeSO_4.7H_2O$	7782-63-0		I146-500	0.6
	Sodium Molybdate	$Na(MoO_2).2H_2O$	7631-95-0		S336-500	0.6
	Manganese (II) Sulfate	$MnSO_4.H_2O$				0.6

1. All chemicals were ACS grade

V.2. Experimental Methods

V.2.1. Analytical Methods

V.2.1.1. Ammonia-N

Ammonia nitrogen (NH_3) concentrations were measured using a colorimetric assay: HACH method 10031 (HACH Company, 2008) with UV absorbance measured at 655 nm using a Perkin Elmer lambda 25 UV/VIS spectrophotometer. HACH assays were purchased in boxes of 50-assays per box. One seven point calibration curve was developed for each box. The method quantification limit for ammonia nitrogen was 0.10 mg N/L.

V.2.1.2. Nitrite and Nitrate

Nitrite (NO_2^-) and nitrate (NO_3^-) concentrations were measured using Dionex ICS 2000 Ion Chromatograph (IC) system equipped with a Dionex AS-50 autosampler. Isocratic separation was achieved using 32 M KOH mobile phase on a Dionex Ionpac AS-18 (4 x 250 mm) column equipped with a Dionex AG-18 guard column (4 x 250 mm). Quantification was achieved using a conductivity detector. Samples were introduced into the IC following centrifugation (11,000 RPM, 10 min) or filtration (0.20 um filter), as appropriate. A summary of the IC system and analytical protocol is provided in Table V-5. IC data were analyzed using Chromelean® software (version 6.60 SP3, Dionex ThermoFisher, Sunnyvale, CA).

An eight point calibration curve using multi-ion standards was developed prior to each experiment and five of these standards (randomly selected) were measured every twelve to fifteen experimental samples. Standards of individual solutes were also

measured prior to each experimental sample set and every twelve to fifteen samples to verify peak identification. Chemicals used to make anion standards for IC analyses are listed in Table V-1. All standards were made using MilliQ® water. Method detection limits for nitrite (NO_2^-) and nitrate (NO_3^-) were 0.10 mg-NL^{-1}.

Table V-5: Ion Chromatography Method for Detection of Nitrite and Nitrate

Method Overview:	Separation	Isocratic
	Flow rate	1 ml/min
	Run Time	14 min
	Injected Sample Volume	25 uL
Eluent (isocratic):	Concentration	32 mM KOH
Autosampler:	Manufacturer/Model	Dionex/ AS-50
Guard Column:	Manufacturer/Model	Dionex/ Ionpac AG-18
	Length/Diameter	50 mm/ 4 mm
	Particle Size	13 um
	functional group	alkanol quaternary ammonium
	Temperature	30°C
Analytical Column:	Manufacturer/Model	Dionex/ Ionpac AS-18
	Length/Diameter	250 mm/ 4 mm
	Particle Size	7.5 um
	functional group	alkanol quaternary ammonium
	Temperature	30°C
Suppressor:	Manufacturer/Model	Dionex/ ASRS Ultra II 4mm
	Currrent	75 mA
	Detector:	
Detector:	Type	Conductivity
	Manufacturer/Model	Dionex/057985
	Serial No.	04030305
	Cell Constant	132.99

V.2.1.3. Pharmaceutical Analyses

Pharmaceutical concentrations were measured using high performance liquid chromatography (HPLC) with fluorescence (FLD) or UV detection using an Agilent Series 1100 system equipped with a C-18 column (Phenomenex: Kinetix, 2.1 mm x 150 mm, 100 Å). A summary of the HPLC-UV and HPLC-FLD methods developed for this research is provided in Table V-6. Where FLD was utilized for quantification, optimal FLD parameters, specifically excitation (λ_{EX}) and emission (λ_{EM}) wavelengths and photomultiplier (PMT) gain were determined using fluorescence scans of three separate PhAC calibration standards (concentration range 10 – 1,000 μg-PhAC/L). Standards were prepared as follows. PhAC Neat Stock was made in methanol, typically at a concentration of 200 – 250 mg-PhAC/L. A subsequent concentrated standard (~50,000 – 100,000 μg-PhAC/L) was made using the Neat Stock and MilliQ water ensuring that the concentrated standard was no greater than 0.50% by mass Neat Stock. Subsequent diluted standards and feed solutions for sorption and biodegradation experiments were made using the concentrated standard and MilliQ water. When analyzing experimental samples, the instrument was calibrated each day of use or every 20 samples (whichever was more frequent) using an eight-point calibration curve.

Table V-6: HPLC-FLD Methods developed in this research to detect PhACs in Water/Wastewater

	ATN	MAC	MET	NAP	SOT
General					
Separation	Isocratic	Isocratic	Isocratic	Isocratic	Isocratic
Flow rate (ml/min)	0.40	0.40	0.40	0.40	0.40
Run time (min)	8	8	8	8	8
Mobile Phase					
ACN (%vol.)	5%	5%	12%	45%	5%
0.10% w/v PA (%vol.)	95%	95%	88%	55%	95%
Sample					
Injection volume (uL)	50	50	50	50	50
Column					
Temperature (^{o}C)	30	30	30	30	30
Peak Retention Time (min)	3.95 ± 0.04	1.27 ± 0.02	4.31 ± 0.05	3.92 ± 0.01	2.67 ± 0.05
FLD Parameters					
λ_{ex} (nm)	235	233	228	230	235
λ_{em} (nm)	314	315	324	356	319
Method Performance - Limits of Detection (mass on column)					
in MilliQ (pg)	50	100	100	5	100
In Mixed Liquor (pg)	100	150	150	10	150

V.2.1.4. Volatile and Suspended Solids

Total suspended solids (TSS) and volatile suspended solids (VSS) were measured using methods 2540 D and 2540 E of Standards Methods, respectively (APHA et al., 1999).

V.2.1.5. Microbial Analyses

Biomass DNA was extracted using MOBio Powersoil isolation kits (MOBIO, Carlsbard, CA) following to the manufacturer's protocol. Extracted DNA was stored at -80^{o}C for convenience until further analyses. Quantitative real time polymerase chain reaction (qPCR) was used to measure the abundance of total bacteria (EUB), AOB and NOB. AOB abundance was measured using the ammonia monooxygenase subunit A (amoA) (Rotthauwe et al., 1997; Park et al., 2010). Since there is no single primer/probe set for all NOB – abundance of both Nitrospira (NOB-Ns) and Nitrobacter (NOB-Nb) were measured by targeting the 16s rRNA (NOB-Ns Kindaichi et al. (2006); NOB-Nb: Graham et al. (2007)). EUB abundance was measured using 16s rRNA targeted primers (Ferris et al., 1996; Park et al., 2010).

The qPCR analyses were conducted using an iQ5 real-time PCR thermal cycler (BioRad, Hercules, CA) using a SYBR® green chemistry at the *Columbia University Biomolecular Environmental Sciences Laboratory (access and equipment usage courtesy of Prof. Kartik Chandran)*. The qPCR reactions were performed in a 25 uL reaction mixture with the specific components of the reaction mixture as follows. Mastermix 12.5 μL (iQ SYBR® Green Supermix), forward primer 1.0 μL, reverse primer 1.0 μL, nuclease free water 9.5μL. Primer sequences used in this research (see Table V-7 for primer sequence details) were purchased from Invitrogen (Carldbad,CA). Primer stock solutions used in the qPCR reactions were made at a concentration of 5 μM. The qPCR

reactions were performed in triplicate for each sample with a set of standards and no-template controls included in each plate. The standards used in each assay were generated through serial dilutions of a stock standard of plasmid DNA. The gene copies concentration of the stock standard (and subsequent serial dilutions) was calculated as shown in Equation V-1.

$$C_{GENE-COPIES-DNA.STD}\left(\frac{copies}{\mu L}\right)=\left[C_{DNA}\left(\frac{ng}{uL}\right)*1x10^{-9}\left(\frac{g}{ng}\right)\right]\left[\frac{1}{660}\left(\frac{mol-bp}{g-DNA}\right)\right]\left[6.022x10^{23}\left(\frac{bp}{mol-bp}\right)\right]\left[\frac{1}{(L_{AMPLICON}+L_{VECTOR})}\left(\frac{copies}{bp}\right)\right] \quad \text{(V-1)}$$

Target gene-copies in each sample were calculated using a standard curve generated using standards based on the threshold cycle obtained in each PCR as shown in Equation V-2.

$$C_{SAMPLE-GENE-COPIES}\left(\frac{copies}{L}\right)=\frac{\left[N_{GC}(copies)\,V_{DNA-EXTRACTED}(\mu L)\right]}{\left[V_{DNA-PCR.RXN}(\mu L)\,V_{SAMPLE}(L)\right]} \quad \text{(V-2)}$$

The biomass cell concentration in each sample was calculated from the gene-copies concentration as shown in Equation V-3 using the numbers of gene copies per cell indicated in Table V-7.

$$C_{CELLS-SAMPLE}\left(\frac{cells}{L}\right)=\frac{\left[C_{SAMPLE-GENE-COPIES}\left(\frac{copies}{L}\right)\right]}{\left[C_{CELL-GENE-COPIES}\left(\frac{copies}{cell}\right)\right]} \quad \text{(V-3)}$$

The biomass concentration was calculated from the cell concentration in each sample as shown in Equation V-4 using a value of 1.42 for the COD:VSS ratio (f_{CV}) and the cell mass as indicated in Table V-7.

$$X_{BIOMASS}\left(\frac{g-COD}{L}\right)=\left[C_{CELLS-SAMPLE}\left(\frac{cells}{L}\right)M_{BACTERIAL-CELL}\left(\frac{g-VSS}{cell}\right)\right]\left[1.42\left(\frac{g-COD}{g-VSS}\right)\right] \quad \text{(V-4)}$$

Table V-7: 16s rRNA primers for qPCR reactions

Target	Primer Information				Cell Gene Copies Information		Cell Mass Information	
	Primer ID	Sequence (5'-3')	Pos.	Primer Sequence Reference	$C_{CELL-GENE-COPIES}$ (copies/cell)	Reference	$M_{BACTERIAL-CELL}$ (g-VSS/cell)	Reference
UB	1055f	ATGGCTGTCGTCAGCT	1055-1070	(Ferris et al., 1996)	4.2	(Klappenbach et al., 2001; Graham et al., 2007)	$2.8x10^{-13}$	(Ahn et al., 2008)
	1392r	ACGGGCGGTGTGTAC	1392-1406					
OB moA	amoA-1F	GGGGTTTCTACTGGTGGT	332-339	(Rotthauwe et al., 1997)	2.5	(Norton et al., 2002)	$1.6x10^{-13}$	(Farges et al., 2012)
	amoA-2R	CCCCTCKGSAAAGCCTTCTTC	802-822					
OB-Ns	NTSPAf	CGCAACCCCTGCTTTCAGT	1081–1099	(Kindaichi et al., 2006)	1	(Graham et al., 2007)	$1.4x10^{-13}$	(Farges et al., 2012)
	NTSPAr	CGTTATCCTGGGCAGTCCTT	1128–1147					
OB-Nb	1198f	ACCCCTAGCAAATCTCAAAAAACCG	1198-1223	(Graham et al., 2007)	1	(Starkenburg et al., 2006)	$1.4x10^{-13}$	(Farges et al., 2012)
	1423r	CTTCACCCCAGTCGCTGACC	1423-1443					

Table V-8: AOB PCR reactions – primer concentrations and thermocycler program

Step	**N_{CYCLES}, Duration, Temperature (^{o}C)**			
	amoA	**NOB-Nb**	**NOB-Ns**	**EUB**
PCR: Hotstart	1 cycle of: 2 min, 95 ^{o}C	1 cycle of: 5 min, 94 ^{o}C	1 cycle of: 2 min, 95 ^{o}C	1 cycle of: 3 min, 94 ^{o}C
Denature	40 cycles of: 30 s, 94 ^{o}C	40 cycles of: 20 s, 94 ^{o}C	40 cycles of: 15 s, 95 ^{o}C	45 cycles of: 30 s, 94 ^{o}C
Anneal	40 s, 57 ^{o}C	60 s, 58 ^{o}C	60 s, 60 ^{o}C	45 s, 53 ^{o}C
Extension	30 s, 72 ^{o}C	40 s, 72 ^{o}C	40 s, 72 ^{o}C	45 s, 72 ^{o}C
Melt Curve Analysis:	81 cycles of: 55 – 95 ^{o}C	81 cycles of: 55 – 95 ^{o}C	81 cycles of: 55 – 95 ^{o}C	81 cycles of: 55 – 95 ^{o}C
	hold, 4 ^{o}C	hold, 4 ^{o}C	hold, 4 ^{o}C	hold, 4 ^{o}C

V.2.2. Setup and Operation of Lab Scale Nitrification Enrichment SBR

V.2.2.1. SBR Seeding and Enrichment

The biodegradation and sorption of PhACs in this research was conducted using seed biomass from a lab-scale nitrification enrichment sequencing batch reactor operated in the IMPES lab at Tufts University. A simplified process and instrumentation diagram for the nit-SBR is shown in Figure V-1. The nit-SBRs was seeded on three separate occasions as detailed in Table V-9.

Taunton WWTP (NPDES Permit MA-0100897) is operated as a single sludge facility at an SRT of 8 – 11 days, achieving full nitrification. Marlborough Easterly Wastewater Treatment Facility (WWTF) (NPDES Permit MA-0100498) where the biological treatment process consists of two separate sludge systems: a secondary process (short SRT) for BOD removal and a nitrification process (long SRT) to achieve nitrification. Operations personnel at Marlborough not typically operate the WWTF to achieve a target SRT, rather to achieve a biomass inventory (targeting a MLSS in the range of 3,500 – 4,500 mg/L year round).

The enrichment process was begun by concentrating the biomass from the source treatment plant settling, then decanting the supernatant. A portion of the supernatant was retained to start up the SBR and the synthetic SBR feed (see Section V.2.2.2, below) and DI-water were supplemented to fill the SBR. SBR performance was regularly monitored based on the specific nitrification rate. Biomass was not used for batch experiments until the nit-SBR specific nitrification rate was at least three times greater than that measured at seeding.

Table V-9: Summary of SBR Seeding in this Research

Date	Seed Source	Reason for (Re)Seeding
June 2009	Taunton WWTP	Starting operation
December 2010	Marlborough Easterly WWTF	Previous SBR failed due to electrical fault resulting pH ~ 12-13 for extended period of time
July 2012	Marlborough Easterly WWTF	Previous SBR failed due to operational error resulting in pH ~ 12-13 for extended period of time

V.2.2.2. SBR Feed

To enrich the nit-SBR with a nitrifying population, the nit-SBR was fed with a synthetic influent consisting of ammonium sulfate, potassium dihydrogen phosphate, sodium bicarbonate and micronutrients (Table V-4) to promote the growth of AOB and NOB (Hockenbury and Grady, 1977; Sato et al., 1985; Chandran and Smets, 2000). No exogenous organic carbon was added to the SBR. Feed stock was stored in a 150 liter high density polyethylene container (Nalgene) at room temperature. A new batch of feed stock was made approximately every two - three weeks.

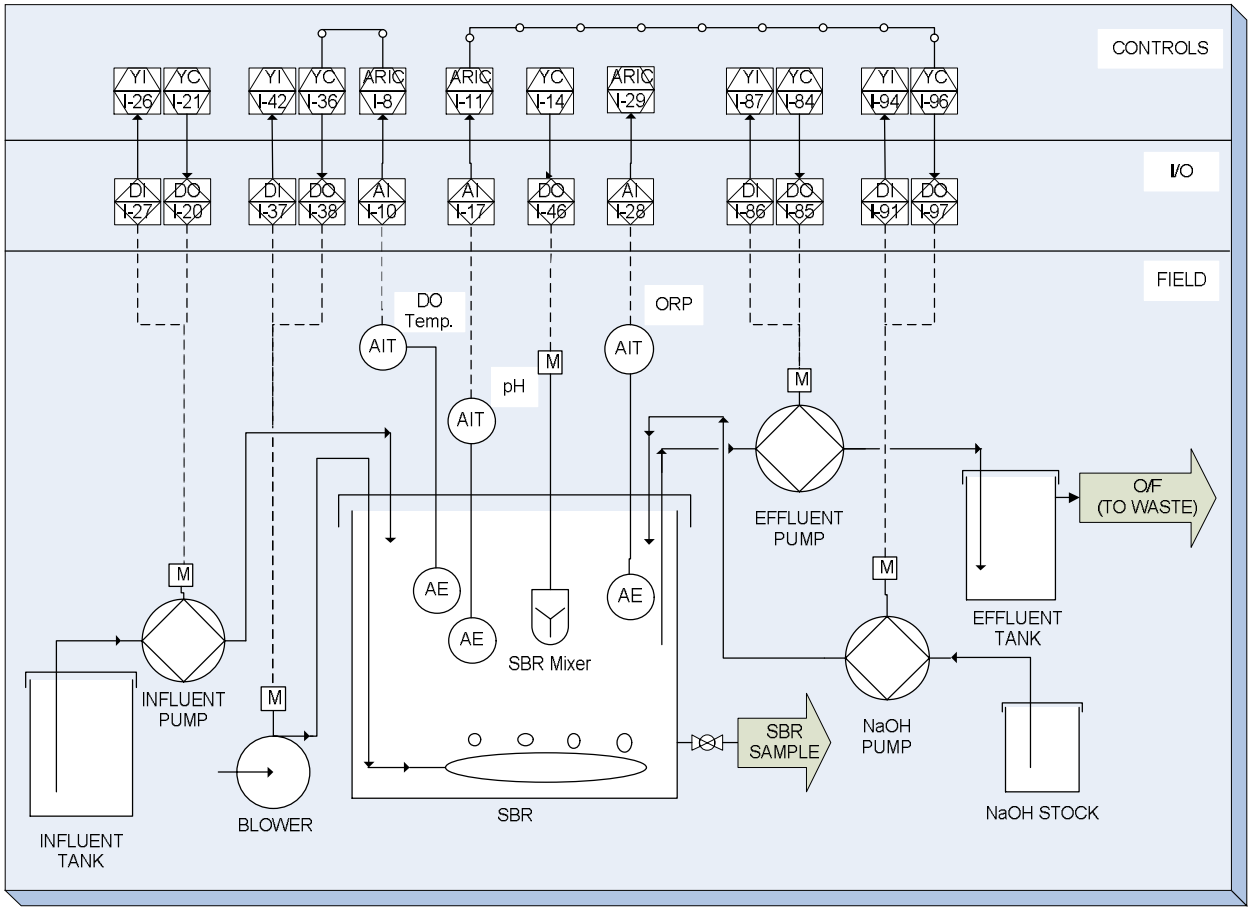

Figure V-1: Process flow diagram for lab scale nitrification SBR

V.2.2.3. SBR Operation, Data Acquisition and Control

The nit-SBR was continuously operated using a data acquisition and control system developed in-house using Labview v.9 (National Instruments, Austin, TX). The minimum decant and maximum volumes of the SBR were 15 L and 38 L, respectively. The influent was pumped into the SBR during the fill period using a peristaltic pump (Chem tech, XPV 033 LVLX). The decant was pumped from the SBR during the decant period using a peristaltic pump (Masterflex, model 7523-60 with EasyLoad II 77200-62 head). The contents of the SBR were mixed during the fill and react phases (IKAWORKS, RW20 Digital).

Dissolved oxygen (DO), pH, temperature and redox-potential (ORP) were measured and recorded every 10 seconds (Table V-10). SBR aeration during the fill and react phases was controlled using the DO signal – air was supplied when the DO was below the Air ON setpoint (2.50 mg/L) and turned off when the DO was above the Air OFF set point (2.52 mg/L). Aeration was achieved using a positive displacement air blower (Hiflo, HB 60**.**) and a 4-inch PolyTetraFluoro Etyhylene (PTFE) fine bubble tube diffuser for air distribution (provided courtesy of Stamford Scientific International Inc., Poughkeepsie, NY). Supplemental alkalinity in the form of 70 g/L sodium hydroxide (Fisher Chemical, S320-50) was added to the SBR during the fill and react phases when the measured pH was lower than the Pump ON setpoint (7.60); addition was stopped when the pH increases above the Pump OFF setpoint (7.61). This control approach allows the pH in the SBR to be maintained within a narrow range suitable for nitrification. SBR temperature and ORP were only monitored and not used for control purposes. All analog signals were transmitted to the data acquisition systems using a device controller (HACH SC-100, LXV401.52.00002).

Table V-10: SBR online measurements and control

		Measurement Instrument Manufacturer & Model No.	Process Objective	Control Target	Control Setpoints	
					ON	OFF
DO	(mg/L)	HACH LDO probe (5790000)	Aeration Control	Blower	2.50	2.52
pH	(--)	HACH GLI pHD Differential pH digital sensor (DPD1P1)	Alkalinity control	NaOH feed pump	7.60	7.61
ORP	(mV)	HACH GLI pHD Differential ORP digital sensor (DRD1P5)	N/A	--		
Temp.	(^{o}C)	HACH LDO probe (5790000)	N/A	--		

V.2.3. Pharmaceutical Sorption Experiments Protocol

Wasted Mixed liquor (WML) from the Nitrification SBR was used for all sorption experiments. The WML was autoclaved, centrifuged and reconstituted to a suspended solids concentration of approximately 1,000 mg/L. The actual suspended solids (X_{TSS}, g/L) and volatile solids concentrations (X_{VSS}, g/L) were measured in each experiment. The pH of the reconstituted mixed liquor was corrected to between 7.6 and 7.8 (i.e., within the typical pH range of the nitrification batch experiments).

V.2.3.1 Equilibrium sorption evaluation

Batch sorption experiments were setup in 50 ml foil covered glass vials with teflon caps for each pharmaceutical at concentrations in the desired range of concentration. Sorption of the PhAC at each concentration was assessed in triplicate. Homogenous samples were collected at regular intervals. Equilibrium was considered to have been achieved when the measured aqueous PhAC concentration of three

successive samples were the same. Controls were included to ascertain PhAC sorption to the glass vial and cap liner.

Samples were centrifuged and PhAC concentration in the aqueous phase (S_{PhAC}, ug/L) was measured using high performance liquid chromatography (HPLC) with fluorescence detection (FLD) (for method details, see Section V.2.1.3). The sorbed PhAC concentration (W_{PhAC}, ug-PhAC/g-SS) was calculated as shown in Equation V-5. Sorption isotherms were developed using the equilibrium sorption data; the sorption coefficient (K_D) was calculated for each PhAC which sorbs.

$$W_{PhAC} = \frac{\left(S_{PhAC,t0} - S_{PhAC,t}\right)}{X_{TSS}} \quad \text{(V-5)}$$

V.2.4. Pharmaceutical Biodegradation Batch Experiments

V.2.4.1 Batch Experiments Overview

The batch experiments were conducted using a sequential protocol consisting of up to two separate experiments for each PhAC to evaluate the role of AOB and NOB in PhAC biodegradation. The first experiment was used to evaluate the occurrence, extent and kinetics of biodegradation of each PhAC during nitrification and was subsequently referred to as NIT-EXPTs. The second experiment was used differentiate the role of ammonia oxidation and nitrite oxidation for PhACs that were observed to degrade in the NIT-EXPTs and were subsequently referred to as NOX-EXPTs.

The NIT-EXPTs consist of four separate reactors (Table V-11). The four reactors include two controls and two experimental replicates. A control, Reactor 1, was included to quantify AOB and NOB kinetics in the absence of the PhAC and a separate control, Reactor 2, was used to assess PhAC biodegradation when nitrification was

inhibited using allylthiourea (ATU) (Ginestet et al., 1998). The two experimental reactors were referred to as Reactor 3 and Reactor 4. The NOX-EXPTs consist of three reactors. Reactor 5 was a control used to evaluate nitrite oxidation kinetics in the absence of the PhAC, while Reactors 6 and 7 were experimental reactors used to evaluate PhAC biodegradation under nitrite oxidation conditions. Inhibition of ammonia oxidation by AOB in Reactors 5 – 7 was achieved using allylthiourea (ATU) (Ginestet et al., 1998).

Table V-11: Experimental protocol for evaluation of biodegradation of each PhAC during Nitrification

	Experiment A	Experiment B
Experiment Target:	Evaluate PhAC biodegradation during Nitrification	Evaluate PhAC biodegradation during Nitrite Oxidation (Ammonia Oxidation Inhibited)
Control # 1	Reactor # 1 (Nitrification Control) B, NH_4, M	Reactor # 5 (Nitrite Oxidation Control) B, NO_2, M **ATU**
Control # 2	Reactor # 2 (Nitrification Inhibition Control) B, NH_4, M, **PhAC, ATU**	
Experiment A	Reactor # 3 (Nitrification Experiment) B, NH_4, M, **PhAC**	Reactor # 6 (Nitrite Oxidation Experiment) B, NO_2, M, **PhAC, ATU**
Experiment B	Reactor # 4 (Nitrification Experiment) B, NH_4, M, **PhAC**	Reactor # 7 (Nitrite Oxidation Experiment) B, NO_2, M, **PhAC, ATU**

Legend:

B = biomass (from nit-SBR)
NH_4 = ammonium chloride,
NO_2 = potassium nitrite,
HyS = hydroxylamine sulfate
M = potassium phosphate and micronutrients
PhAC = parent pharmaceutical
ATU = allylthiourea

Nit. = nitrification (ammonia and nitrite oxidation)
Nit-Ox = nitrite oxidation only
Am-Ox = ammonia oxidation only
Hy-Ox = Hydroxylamine sulfate oxidation only

V.2.4.2. Batch Experiments Protocol

Batch experiments were conducted in 4000 mL glass beakers (Kimble Chase, 14000-4000) (see Figure V-2). Reactor contents were mixed using one inch teflon coated stir bar (Fisherbrand, 1451360) and magnetic stir plate. Reactor mixing intensity (stir plate setting) was established based on tracer (sodium chloride) experiments conducted to evaluate mixing.

Reactor DO was measured regularly during the batch experiment (HACH, HdQ 40d multi) and adequate aeration was provided to maintain the DO above 4 mg/L (manual control) utilizing air blowers (Petco, Model 6003) and aeration stones (Petco, Bubbling Air Stone, SKU no. 1191055). Reactor pH was measured regularly during the batch experiment (Mettler Toledo, MultiSeven) and maintained in the range of 7.5 – 8.0 (manual control).

V.2.4.3. Biomass for Batch Experiments

Biomass for batch experiments was collected from the nitrification enrichment SBR. Mixed liquor from the SBR was collected in five hundred milliliter bottle (Nalgene 500 ml) and centrifuged at 5,000 rpm for 15 minutes (Avanti, JA 10). The supernatant was discarded and the pellet was washed with deionized water and resuspended to a final volume of four hundred milliliters (400 ml). The washed mixed liquor was centrifuged at 5,000 rpm for 15 minutes (Avanti, JA 10). The supernatant was discarded and the pellet was resuspended to a final volume of approximately 400 ml. This twice-washed, mixed liquor was added to the batch reactor.

The mass of mixed liquor added to the reactor was measured and DI water was added to the reactor to obtain a final mass (mixed liquor and DI water) of 3,200 g.

Where an inhibitor or biocide were required (i.e., inhibition control reactors) – the inhibitor was added to this diluted mixed liquor. The diluted mixed liquor solution was mixed for two hours prior to commencing the experiment.

V.2.4.4. Feed for Batch Experiment Reactors

Feed stock powder consisting of ammonium chloride, potassium phosphate, sodium bicarbonate and essential micronutrients (see Table V-12) were added to the reactor at the same time as the PhAC being investigated. For control reactors, the inhibitor (allylthiourea (ATU) for nitrification or ammonia oxidation inhibition; sodium azide (SA) for nitrite oxidation inhibition) was added to the reactor a minimum of two hours prior to commencing the experiment.

Figure V-2: Batch bioreactor experimental setup
Mixed liquor from the SBR was used as biomass seed in the batch experiments

Table V-12: Feed Composition for Reactors in PhAC Biodegradation Batch Experiments

Function	Name	Molecular Formula	Target Conc. mg/L	CAS Number	Manufacturer	Item Number
Nitrogen Source	Ammonium Chloride	$(NH_4)Cl$	76.4	12125-02-9	Fisher Chemicals, Fairlawn, NJ	A661-500
	Ammonia-Nitrogen		20			
Phosphorus Source	Potassium Phosphate	KH_2PO_4	6.1	7778-77-0	Acros Organics, Geel, Belgium	205920025
	Phosphate		4.3			
Alkalinity	Sodium Bicarbonate	$NaHCO_3$	31.3	144-55-8	Fisher Chemicals, Fairlawn, NJ	S233-500
Micronutrients	Magnesium Sulfate	$MgSO_4.7H_2O$	2.1	7487-88-9	Acros Organics, Geel, Belgium	124900010
	Copper (II) Sulfate	$CuSO_4.5H_2O$	2.9	7758-98-7	Acros Organics, Geel, Belgium	423615000
	Zinc Sulfate	$ZnSO_4.7H_2O$	1.9	7733-02-0	Fisher Chemicals, Fairlawn, NJ	Z68-500
	Calcium Chloride	$CaCl_2.2H_2O$	3.0	10043-52-4	Acros Organics, Geel, Belgium	207780010
	Iron (II) Sulfate	$FeSO_4.7H_2O$	2.8	7782-63-0	Fisher Chemicals, Fairlawn, NJ	I146-500
	Cobalt Nitrate	$Co(NO_3)_2.6H_2O$	3.1	10141-05-6	Acros Organics, Geel, Belgium	423585000
	Sodium Molybdate	$Na(MoO_2).2H_2O$	3.0	7631-95-0	Fisher Chemicals, Fairlawn, NJ	S336-500
Nitrification Inhibitor	Allylthiourea (ATU)	$C_4H_8N_2S$	35.0	109-57-9	Acros Organics, Geel, Belgium	148801000
	ATU used only in controls where ammonia oxidation inhibition was targeted					

V.2.4.5. Batch Experiments – Sampling and Sample Handling

Baseline samples were collected prior to addition of feedstock powder or PhAC. Samples were collected upon addition of feedstock and PhAC (between 45 – 90 seconds of addition) and at regular intervals thereafter for the duration of the experiment (approximately hourly for the first 12 hours and then once every three-four hours). Samples were collected using a five milliliter syringe (BD syringe, Fisher Scientific).

Samples for VSS/TSS analyses were collected in a 50-ml container weighed and refrigerated at 4^{o}C for up to 5-days prior to analyses [in accordance with *Standard Methods* (APHA et al., 1999)]. Samples used to determine solute concentrations and microbial analyses were collected in 2-ml centrifuge tubes (Fisherbrand microcentrifuge tubes), weighed and centrifuged (11,000 RPM, 15 minutes using Thermofisher, Microlite). The supernatant was used for ammonia, nitrite, nitrate, and PhAC analyses. The pellet was frozen at -80^{o}C for subsequent DNA extraction and microbial analyses using quantitative real-time polymerase chain reaction (qPCR). Sample handling protocols were summarized in the workflow shown in Figure V-3.

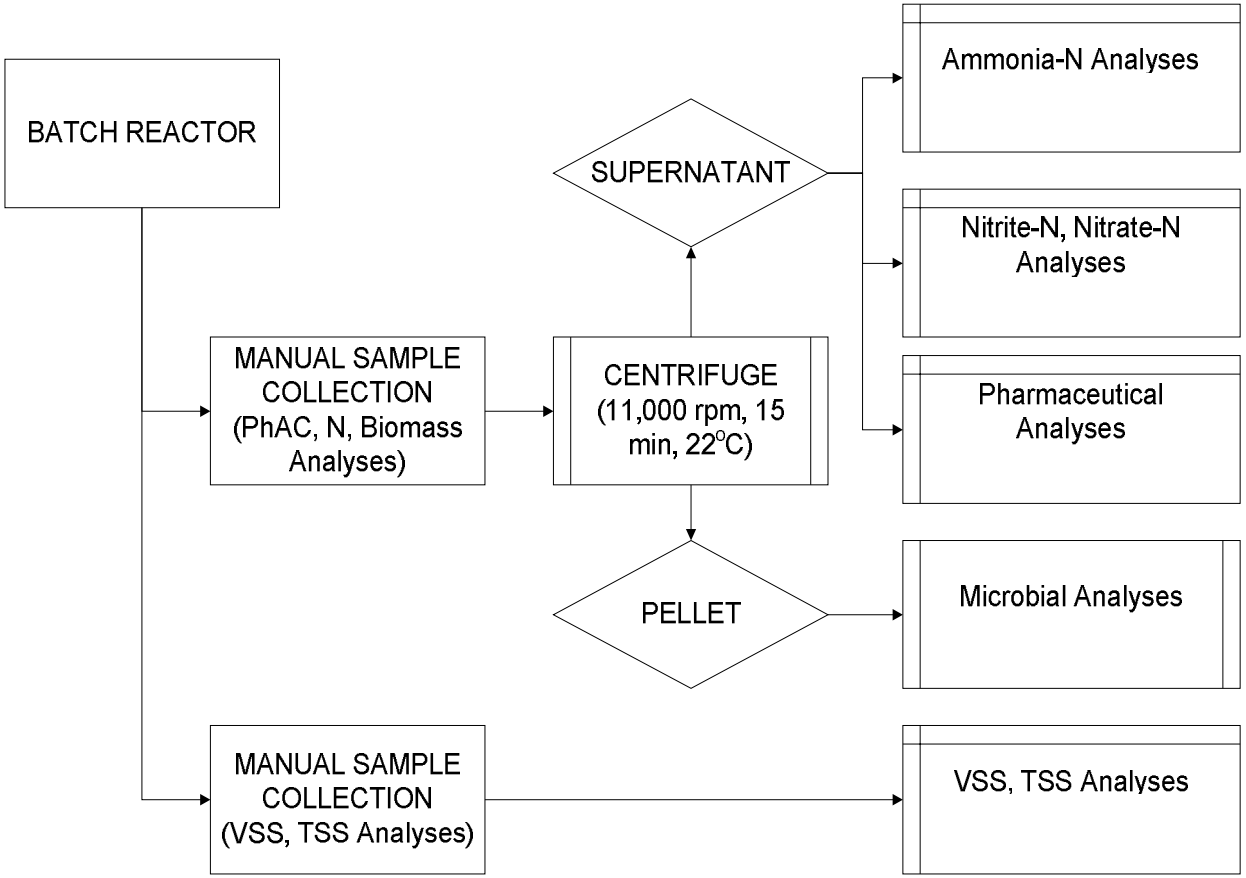

Figure V-3: PhAC Biodegradation Batch Experiments - Overview of Sample Handling and Analytical Protocols

V.3. Mathematical Modeling Methods

V.3.1. Regression Models to Predict Pharmaceutical Sorption

V.3.1.1. Single Parameter Models Assuming Hydrophobic Partitioning

The ability of log K_{OW} correlations (of the form shown in Equation V-6 to describe PhAC sorption to MLSS was examined.

$$\log K_{D,PhAC} = \alpha \log K_{OW,PhAC} + \beta \quad \text{(V-6)}$$

To use the largest possible data set in the assessment, K_D rather than K_{OC} was considered since the fraction of organic carbon (f_{OC}) for suspended solids was not regularly reported with values of K_D. The existing correlations considered here include those for sorption of microconstituents and trace organics based upon log K_{OW} (Stevens-Garmon et al., 2011; Hyland et al., 2012), as well as correlations previously developed to describe the sorption of largely uncharged organic contaminants (e.g., microconstituents, pesticides, chlorinated aromatics and PAHs) to activated sludge (Matter-Müller et al., 1980) and soils (Sabljic et al., 1995; Huuskonen, 2003). The models developed by Sabljic et al. (1995), Huuskonen (2003), Stevens-Garmon et al. (2011) and Hyland et al. (2012) describe sorption in terms of log K_{OC}, where K_{OC} defined in units of L/kg-OC. To show these models with the K_D data, an f_{OC} = 0.50 was assumed. This was consistent with reported f_{OC} values for activated sludge that fall within the range of 0.45 - 0.55 (Dickenson et al., 2010; Ottmar et al., 2010; Hyland et al., 2012).

Also assessed were models for K_D based on the apparent partition coefficients (D). Correction of K_{OW} to D for monoprotic PhACs was straightforward (Sangster, 1989). D for multiprotic PhACs was calculated using Marvin 5.6.0.4, 2011, (ChemAxon, http://www.chemaxon.com). For details on the calculation methods, the reader was

referred to Viswanadhan et al. (1989); Klopman et al. (1994); Szegezdi and Csizmadia (2004).

V.3.1.2. Polyparameter Models for Prediction of K_D

Numerous polyparameter models were available in the literature for estimation of sorption of environmental pollutants derived using structurally derived parameters, fragment contributions or linear solvation energy relationships (Doucette, 2003). Here Linear Free Energy Relationships (LFER)s employing Abraham predictors (Abraham, 1993) and polyparameter quantitative structural activity relationship (QSAR) models were evaluated.

The LFER model employing Abraham predictors (Abraham, 1993) to describe the sorption of uncharged PhACs was shown in Equation V-7. The predictors used in the model were as follows: E is the excess molar refraction (cm^3/mol), S is the dipolarity/polarizability, A is the solute hydrogen bond (H-bond) acidity, B is the solute H-bond basicity and V is the McGowan volume (cm^3/mol) divided by 100. Abraham predictor values for PhACs were calculated using Absolv module in ACD/Percepta (ACD Labs, http://www.acdlabs.com/products/percepta/).

$$\log K_{D,PhAC} = c + eE + sS + aA + bB + vV \quad \text{(V-7)}$$

QSAR models of the general form shown in Equation V-8 were developed specifically for PhAC sorption during biological wastewater treatment. Predictors in the QSAR models were selected to describe the variety of possible sorbate-sorbent interactions (Table V-13) and by the practicability and accessibility of the predictor within both the environmental engineering and PhAC development communities.

$$\begin{aligned}\log K_{D,PhAC} = \chi &+ a\left[\log K_{OW,PhAC} \text{ or } \log D_{PhAC}\right] + b\left[\left(\log MW \text{ or } \log MV\right)\right] \\ &+ c\left[\log(vdWSA)\right] + d\left[\log(TPSA)\right] + e\left(nAroC\right) + f\left(Pi.Energy\right) \\ &+ g\left(nHBD\right) + h\left(nHBA\right) + i\left(nRB\right) \\ &+ j\left(Dom.Species\right) + k\left(\alpha_{+}\right) + l\left(\alpha_{-}\right)\end{aligned} \quad \text{(V-8)}$$

Polyparameter QSARs of increasing complexity were systematically developed by addition of a new predictor to the previously *best* model until the addition of another predictor was not statistically significant (i.e., $p > 0.05$). A leading coefficient (χ) was included in models evaluated – omission of the leading coefficient would imply that the sorption mechanism can be entirely described by the predictor variables, which has limited physical meaning. For each model, the statistical significance of predictors was evaluated at $p < 0.05$, residuals were checked for homoscedasticity, and multicollinearity between predictors was evaluated.

V.3.1.3. Model Development and Evaluation

All models were developed and evaluated using Minitab 16.1.1. Models were assessed using a suite of statistics. The ability of each model to capture the variance in the data set used to develop the model was evaluated using the correlation coefficient (R^2, see Equation V-28) and adjusted-R^2 (adj-R^2, see Equation V-29). The predictive capability of models was assessed through predicted-R^2 (pred-R^2) (see Equation V-30) and Nash-Sutcliffe Efficiency (NSE) (see Equation V-31).

Table V-13: Molecular descriptors considered as predictor variables in polyparameter QSAR models developed for estimation of pharmaceutical sorption coefficients

Molecular Descriptor Predictor		Comments
Octanol water partitioning coefficient	log K_{OW}	
pH corrected octanol water partitioning coefficient	log D	Octanol water partitioning coefficients (log K_{OW}) were corrected using reported experimental pH (Schwarzenbach et al., 2003)
log of molecular weight (MW, g/mol)	log MW	
log of molecular volume (MV, $Å^3$)	log MV	The MV was selected to increase the sophistication of the molecular size descriptor. Others have employed McGowan (Abraham, 1993) or the molar volume (Nguyen et al., 2005) as a measure of solute size. Molecular volume calculated using group contribution methods via online *Molinspiration* property calculator (*www.molinspiration.com*). Considering the high colinearity between MW and MV, where one or the other enters the models, the other was excluded from models of increasing complexity.
Number of hydrogen bond donors	nHBD	determined via online *Molinspiration* property calculator (*www.molinspiration.com*).
Number of hydrogen bond acceptors	nHBA	determined via online *Molinspiration* property calculator (*www.molinspiration.com*).
Number of rotatable bonds	nRB	determined via online *Molinspiration* property calculator (*www.molinspiration.com*).
log of Van der Waals surface area	log vdWSA	van der Waals surface area (vdWSA) encodes information that was specific to London, Debye, and Keesom interactions between the PhAC and the sludge surface. vdWSA was obtained using Marvin 5.6.0.4, 2011, ChemAxon (http://www.chemaxon.com)).

Molecular Descriptor Predictor		Comments
log of topological polar surface area (TPSA, $Å^2$)	log TPSA	PSA encodes information related to and affecting hydrogen-bonding, polarity and solubility (Mannhold, 2008). It reflects the portion of the molecule that was polar, accounting for the oxygen and nitrogen atoms on the surface, including the hydrogen atoms bonded to them. PSA was calculated using the topological polar surface area (TPSA) based on fragment contributions and molecular topology (Ertl et al., 2000). TPSA for the PhACs employed was obtained using the *Molinspiration* online interface (*www.molinspiration.com*).
Aromaticity – Percentage of aromatic carbon atoms in molecule	%Aro-C	Aromaticity can be calculated using a number of techniques (Cyrañski et al., 2002), but for the purposes of this analysis a simple definition was employed that was consistent with that used by PhAC manufacturers - the percentage of aromatic carbon atoms in the molecule (Ritchie and Macdonald, 2009).
Charge of PhAC species which was dominant at the experimental conditions	Dom.Species	For monoprotic PhACs Dom.Species was calculated using the acid dissociation constant (pK_A). For multiprotic PhACs, Dom.Species was obtained using Marvin 5.6.0.4, 2011, ChemAxon (http://www.chemaxon.com)).
Fraction of PhAC in solution as negatively charged species	α_-	For monoprotic PhACs α_- was calculated using the acid dissociation constant (pK_A). For multiprotic PhACs, Dom.Species was obtained using Marvin 5.6.0.4, 2011, ChemAxon (http://www.chemaxon.com)).
Fraction of PhAC in solution as positively charged species	α_+	For monoprotic PhACs α_+ was calculated using the acid dissociation constant (pK_A). For multiprotic PhACs, Dom.Species was obtained using Marvin 5.6.0.4, 2011, ChemAxon (http://www.chemaxon.com)).
Fraction of PhAC in solution as uncharged species	α_0	For monoprotic PhACs α_0 was calculated using the acid dissociation constant (pK_A). For multiprotic PhACs, Dom.Species was obtained using Marvin 5.6.0.4, 2011, ChemAxon (http://www.chemaxon.com)).
log of Energy associated with aromatic ring system(s) of PhAC molecule	Pi.Energy	Pi energy provides an estimate of the total energy associated with the aromatic rings of the PhAC. Pi.Energy was determined using calculated using Marvin 5.6.0.4, 2011, ChemAxon (http://www.chemaxon.com)).

V.3.2 Modeling PhAC Biodegradation

Two approaches to model PhAC biodegradation were evaluated in this research: (i) a pseudo-first-order model based upon the reactor VSS concentration; and (ii) a cometabolic process-based model.

V.3.2.1. Pseudo-First-Order Model

The pseudo-first-order (PFO) approach (Equation V-9) was frequently used to model microconstituent degradation despite its lack of mechanistic or process significance(Urase and Kikuta, 2005; Joss et al., 2006; Fernandez-Fontaina et al., 2012; Helbling et al., 2012).

$$\frac{dS_{PhAC}}{dt} = -(k_{BIO} X_{TOT}) S_{PhAC} \qquad \text{(V-9)}$$

Here S_{PhAC} is the PhAC concentration [$M_{PhAC}L^{-3}$], k_{BIO} [$L^3M_{BIOMASS}^{-1}T^{-1}$] is a biomass normalized pseudo-first-order degradation rate coefficient, X_{TOT} [$M_{BIOMASS}L^{-3}$] is the biomass concentration and t [T] is time.

V.3.2.2. Cometabolic Process Based Model

V.3.2.2.1. Description of Model Framework

To address the aforementioned shortcomings of the PFO models, existing approaches for cometabolic biodegradation modeling (Criddle, 1993; Ely et al., 1995; Alvarez-Cohen and Speitel, 2001) were adapted herein to link PhAC biodegradation to biomass biokinetics. The resulting cometabolic process-based (CPB) model was developed and integrated into the Activated Sludge Models (ASM) framework(Henze et

al., 2000) with nitrification modeled as a two-step process(Chandran and Smets, 2000; Hiatt and Grady, 2008) (Table 1).

V.3.2.2.1.1. Biomass Concentration

The biomass community in the batch experiments was modeled as consisting of heterotrophic bacteria (HET), ammonia oxidizing bacteria (AOB) and nitrite oxidizing bacteria (NOB). The concentrations of AOB (X_{AOB}) and NOB (X_{NOB}) (in mg-biomass-COD/L) through time was described by Equations V-10 and V-11, respectively. Note that μ_{max} [T^{-1}] and b [T^{-1}] represent the maximum specific growth rate and decay coefficient of a population, respectively; and *S* [$M_{SOLUTE}L^{-3}$] and *K* [$M_{SOLUTE}L^{-3}$] represent the concentration and half saturation of a particular solute, respectively.

$$\frac{dX_{AOB}}{dt} = \left[\mu_{MAX,AOB} * \left(\frac{S_{NH}}{K_{NH} + S_{NH}} \right) - b_{AOB} \right] X_{AOB} \qquad \text{(V-10)}$$

$$\frac{dX_{NOB}}{dt} = \left[\mu_{MAX,NOB} * \left(\frac{S_{NO2}}{K_{NO2} + S_{NO2}} \right) - b_{NOB} \right] X_{NOB} \qquad \text{(V-11)}$$

Given the focus of this research on nitrification, the growth of heterotrophs was not modeled. Instead, it was assumes heterotrophic growth over the experimental period in the batch experiments was small enough that X_{HET} remained approximately constant over the course of the experiment. This assumption was supported by the fact that the nitrification enrichment SBR (source of the biomass used in the experiments, see Section V.2.2 for details) was operated with no addition of exogenous carbon and the only exogenous organic carbon added to the batch reactors was the PhAC at microgram per liter concentrations. Furthermore, the rate at which endogenous organic carbon becomes available in the batch experiments was effectively constrained by the rate of biomass decay.

V.3.2.2.1.2. Nitrogen Species Concentration

Nitrification was modeled as a 2-step process. S_{NH}, S_{NO2}, S_{NO3} were modeled as shown in Equations V-12 – V-14 ($i_{N,BM}$ [$M_N M_{COD}^{-1}$] represents the fraction of nitrogen in the biomass and Y [$M_{COD} M_N^{-1}$] indicates a yield coefficient for a particular biomass consortium).

$$\frac{dS_{NH}}{dt} = \left\{ -\left[i_{N,BM} + \frac{1}{Y_{AOB}} \right] \left[\mu_{MAX,AOB} \left(\frac{S_{NH}}{K_{NH} + S_{NH}} \right) \right] X_{AOB} \right\} + \left\{ \left[-i_{N,BM} \right] \left[\mu_{MAX,NOB} \left(\frac{S_{NO2}}{K_{N02} + S_{NO2}} \right) \right] X_{NOB} \right\} \quad \text{(V-12)}$$

$$\frac{dS_{NO2}}{dt} = \left\{ \left[\frac{1}{Y_{AOB}} \right] \left[\mu_{MAX,AOB} * \left(\frac{S_{NH}}{K_{NH} + S_{NH}} \right) \right] X_{AOB} \right\} + \left\{ \left[-\frac{1}{Y_{NOB}} \right] \left[\mu_{MAX,NOB} \left(\frac{S_{NO2}}{K_{N02} + S_{NO2}} \right) \right] X_{NOB} \right\} \quad \text{(V-13)}$$

$$\frac{dS_{NO3}}{dt} = \left\{ \left[\frac{1}{Y_{NOB}} \right] \left[\mu_{MAX,NOB} \left(\frac{S_{NO2}}{K_{N02} + S_{NO2}} \right) \right] X_{NOB} \right\} \quad \text{(V-14)}$$

V.3.2.2.3. Pharmaceutical Concentration

The cometabolic biodegradation of PhACs in this research was modeled based on the transformation capacity approach forwarded by Criddle (1993). The Criddle model describes the Transformation Capacity as the mass of nongrowth substrate transformed per unit mass of (growth) substrate consumed during growth [$M_{NGS}M_{GS}^{-1}$]. This transformation capacity was modified by a Monod expressions for the nongrowth and growth substrates (c.f., Equation 8 in Criddle (1993)) as shown in Equation V-15, below.

$$q_C = \left(T_C^g q_g + k_C\right)\frac{S_C}{\left(K_{SC} + S_C\right)} \qquad \text{(V-15)}$$

where: q_C = specific rate of utilization of nongrowth substrate [$M_C M_b^{-1} T^{-1}$]

T_C^g = growth substrate transformation capacity [$M_C M_g^{-1}$]

q_g = specific rate of utilization of growth substrate [$M_g M_b^{-1} T^{-1}$]

k_C = maximum specific rate of utilization of the nongrowth substrate in the absence of growth substrate [$M_C M_b^{-1}$]

S_C = concentration of nongrowth substrate [$M_C L^{-3}$]

K_{SC} = half-saturation coefficient of the nongrowth substrate [$M_C L^{-3}$]

Recognizing that: $q_g = \frac{\mu}{Y}$ (V-16)

and $q_C = -\frac{1}{X}\frac{dS_C}{dt}$ (V-17)

Equation V-15 can be rewritten as Equation V-18:

$$-\frac{dS_C}{dt} = \left(T_C^g \frac{\mu}{Y} + k_C\right) X \frac{S_C}{\left(K_{SC} + S_C\right)} \qquad \text{(V-18)}$$

Application of this model to cometabolic degradation of PhACs (i.e., where subscript C = PhAC) by AOB (i.e., X = X_{AOB}) results in Equation V-19:

$$-\frac{dS_{PhAC}}{dt}=\left(\frac{T_{PhAC}^{g}\mu_{AOB}}{Y_{AOB}}+k_{PhAC}\right)\frac{S_{PhAC}}{\left(K_{S,PhAC}+S_{PhAC}\right)}X_{AOB} \quad \text{(V-19)}$$

It was assumed that the PhAC concentration (S_{PhAC}) used in the batch experiments conducted in this research were lower than the half saturation value ($K_{S,PhAC}$) and Equation V-19 was modified to Equation V-24. This assumption is consistent with the fact that batch experiments were conducted at microgram per liter levels and typical half saturation values for solutes in environmental systems are several orders of magnitude greater (Orhon and Artan, 1994; Grady et al., 1999; Alvarez-Cohen and Speitel, 2001). The PhAC biodegradation rate was therefore assumed to be first order with respect to the PhAC concentration (Equation V-20).

$$-\frac{dS_{PhAC}}{dt}=\left(\frac{T_{PhAC}^{g}}{Y_{AOB}K_{S,PhAC}}\mu_{AOB}+\frac{k_{PhAC}}{K_{S,PhAC}}\right)X_{AOB}S_{PhAC} \quad \text{(V-20)}$$

let:

$$\frac{T_{PhAC}^{g}}{Y_{AOB}K_{S,PhAC}}=T_{PhAC-AOB} \quad \text{(V-21)}$$

and $$\frac{k_{PhAC}}{K_{S,PhAC}}=k_{PhAC-AOB} \quad \text{(V-22)}$$

Then, Equation V-20 can be modified to Equation V-23 which was used to describe cometabolic PhAC biodegradation by AOB.

$$-\frac{dS_{PhAC}}{dt}=\left(T_{PhAC-AOB}\mu_{AOB}+k_{PhAC-AOB}\right)X_{AOB}S_{PhAC} \quad \text{(V-23)}$$

Here $T_{PhAC\text{-}AOB}$ is a cometabolic PhAC transformation coefficient linked to AOB growth [$L^3M_{COD}^{-1}$], μ_{AOB} is the AOB growth rate [T^{-1}], $k_{PhAC\text{-}AOB}$ is a biomass normalized PhAC degradation rate coefficient in the absence of AOB growth [$L^3M_{COD}^{-1}T^{-1}$] and X_{AOB} is

the AOB concentration [$M_{COD}^{3}L^{-1}$]. In the absence of AOB growth, biodegradation of PhACs due to AOB activity is described by Equation V-24:

$$-\frac{dS_{PhAC}}{dt} = k_{PhAC-AOB} X_{AOB} S_{PhAC} \quad \text{(V-24)}$$

with $$\frac{dX}{dt} = -bX_{AOB} \quad \text{(V-25)}$$

The resulting cometabolic model (Equation V-23) was used with the ASM framework to assess three processes contributing to PhAC biodegradation: (i) cometabolic biodegradation linked to AOB growth (ii) biodegradation by AOB in the absence of growth; and (iii) biodegradation due to heterotrophs (HET) present in the mixed culture as shown in Equation V-26.

$$\frac{dS_{PhAC}}{dt} = -\left\{\begin{matrix}[\{[T_{PhAC-AOB}\mu_{AOB}]+[k_{PhAC-AOB}]\}X_{AOB}]+ \\ [\{[T_{PhAC-HET}\mu_{HET}]+[k_{PhAC-HET}]\}X_{HET}]\end{matrix}\right\} S_{PhAC} \quad \text{(V-26)}$$

Here $T_{PhAC-AOB}$ is a cometabolic PhAC transformation coefficient linked to AOB growth [$L^{3}M_{COD}^{-1}$], μ_{AOB} is the AOB growth rate [T^{-1}], $k_{PhAC-AOB}$ is a biomass normalized PhAC degradation rate coefficient in the absence of AOB growth [$L^{3}M_{COD}^{-1}T^{-1}$] and X_{AOB} is the AOB concentration [$M_{COD}^{3}L^{-1}$]. Similarly, $T_{PhAC-HET}$ is a cometabolic PhAC transformation coefficient linked to HET growth [$L^{3}M_{COD}^{-1}$], μ_{HET} is the HET growth rate [T^{-1}], $k_{PhAC-HET}$ is a biomass normalized PhAC degradation rate coefficient in the absence of HET growth [$L^{3}M_{COD}^{-1}T^{-1}$] and X_{HET} is the HET concentration [$M_{COD}^{3}L^{-1}$]. S_{PhAC} is the PhAC concentration [$M_{PhAC}L^{-3}$].

Based upon the assumption of negligible heterotrophic growth during the batch experiments (see discussion related to biomass modeling in Section V.3.2.2.1.1, above), Equation V-26 was modified to utilize a single biomass normalized rate coefficient $\alpha_{PhAC-HET}$ [$L^{3}M_{COD}^{-1}T^{-1}$] to describe the contribution of X_{HET} to PhAC biodegradation

(Equation V-27). Use of Equation V-27 assumes that all heterotrophic bacteria contribute equally to PhAC biodegradation. Furthermore, while use of this approach is generalizable across biological systems, the value of $\alpha_{PhAC\text{-}HET}$ may be system specific and dependent on the consortia of heterotrophs present. Therefore, caution is recommended when using $\alpha_{PhAC\text{-}HET}$ values determined utilizing the experimental approach described in Section V.2.4 with biomass from a given source to biological processes at other WWTPs.

$$\frac{dS_{PhAC}}{dt} = -\left\{\begin{matrix}\left[\left\{\left[T_{PhAC-AOB}\,\mu_{AOB}\right]+\left[k_{PhAC-AOB}\right]\right\}X_{AOB}\right]+ \\ \left[\left\{\alpha_{PhAC-HET}\right\}X_{HET}\right]\end{matrix}\right\}S_{PhAC} \qquad \text{(V-27)}$$

It is important to note that the model framework proposed here is flexible and readily adapted as estimates for $T_{PhAC\text{-}HET}$ and $k_{PhAC\text{-}HET}$ become available.

Table V-14: Component mass balance and process rates for integrated nitrification-pharmaceutical degradation process model.

Process	Nitrogen			Biomass			PhAC	Process Rate
	S_{NH}	S_{NO2}	S_{NO3}	X_{AOB}	X_{NOB}	X_{HET}	S_{PhAC}	
Growth of AOB	$-\left(i_{NBM}+\left(\frac{1}{Y_{AOB}}\right)\right)$	$\left(\frac{1}{Y_{AOB}}\right)$		1			$-T_{PhAC-AOB}S_{PhAC}$	$\left[\mu_{MAX,AOB}\left(\frac{S_{NH}}{K_{NH}+S_{NH}}\right)\right]X_{AOB}$
Decay of AOB				-1				$b_{AOB}X_{AOB}$
Transformation of Nongrowth Substrate							$-S_{PhAC}$	$k_{PhAC-AOB}X_{AOB}$
Growth of NOB	$-i_{NBM}$	$\left(\frac{1}{Y_{AOB}}\right)-\left(\frac{1}{Y_{NOB}}\right)$	$\left(\frac{1}{Y_{NOB}}\right)$		1			$\left[\mu_{MAX,NOB}\left(\frac{S_{NO2}}{K_{N02}+S_{NO2}}\right)\right]X_{NOB}$
Decay of NOB					-1			$b_{NOB}X_{NOB}$
Growth of HET	***Not explicitly modeled in this research***						$-\alpha_{PhAC-HET}S_{PhAC}$	X_{HET}
Decay of HET								

V.3.2.2.2. Model Solution and Parameter Estimation

The modeling objective in this research was estimation of values for $T_{PhAC-AOB}$, $k_{PhAC-AOB}$ and $\alpha_{PhAC-HET}$ for the selected pharmaceuticals. The mathematical model used in this research (Table V-14) comprises six, coupled, ordinary differential equations (ODEs) - one for each for X_{AOB}, $X_{NOB}$$S_{NH}$, S_{NO2}, S_{NO3} and S_{PhAC} - and 17 parameters (Table V-15). AOB and NOB biokinetic parameters were selected from the range of literature values noted in Table V-15. Parameter estimation was accomplished in MATLAB (Mathworks, release 2010b) using the *lsqnonlin* routine with a Levenberg-Marquardt algorithm in a sequential solution strategy as described below. In each model run, the model equations were solved using an explicit time discretized Runge-Kutta 1 method with a time-step of 30 seconds implemented in MATLAB. The 95% confidence intervals for all estimated parameters were determined using the *nlparci* routine.

To minimize the number of adjustable parameters in any one fit, the initial concentrations of AOB ($X_{AOB,t0}$) and NOB ($X_{NOB,t0}$) were first independently estimated for each experiment (e.g.,. ATN, MET, SOT). To accomplish this nitrogen data from the nitrification control reactor (i.e., Reactor 1) were used and X_{AOBt0} and X_{NOBt0} were adjusted to minimize the sum of square errors (SSE) between measured and modeled values of S_{NH}, S_{NO2} and S_{NO3}. Values of X_{AOBt0} and X_{NOBt0} were constrained between 1 and the COD equivalent of the measured VSS concentration. The fits producing the lowest SSE determined X_{AOBt0} and X_{NOBt0} used for the subsequent simulations using Reactors 2-4 for a given PhAC.

Values of $\alpha_{PhAC-HET}$ were independently estimated for each experiment using data from the nitrification inhibition control reactor (Reactor 2). Here X_{HET} was fixed as the difference between the total bacteria and nitrifying bacteria concentrations

produced from the qPCR results. Nitrogen and PhAC data from Reactor 2 were fit by adjusting values of $\alpha_{PhAC-HET}$ with $T_{PhAC\text{-}AOB}$ and $k_{PhAC\text{-}AOB}$ set to zero such that the SSE between the measured and modeled S_{PhAC} was minimized. It was recognized that assuming $T_{PhAC\text{-}AOB}$ and $k_{PhAC\text{-}AOB}$ were zero here means any residual degradation capacity of the inhibited ammonia oxidizers will be lumped into the estimate of heterotrophic degradation. The influence of this assumption was negligible since ATU binds with copper at the AMO active site to inhibit its activity (Bedard and Knowles, 1989) and thus dramatically limits residual activity.

Estimates of X_{AOBt0} and X_{NOBt0} and $\alpha_{PhAC-HET}$ obtained Reactors 1 and 2, respectively, were then employed with nitrogen and PhAC concentration data from Reactors 3 and 4 to estimate PhAC transformation. Data from the replicate reactors (Reactors 3 & 4) were used together in a single fit to produce values of $T_{PhAC\text{-}AOB}$ and $k_{PhAC\text{-}AOB}$ by minimizing the SSE between the measured and modeled S_{PhAC}. Model performance was measured using the metrics described in Section V.3.3, below.

Table V-15: Model parameters used in the Cometabolic Process Model

Description	Variable	Unit of Measure	Literature Values (where applicable) Range	Refs.
Common				
Nitrogen fraction of biomass	i_{NBM}	(mg-N·mg-COD^{-1})	0.07	(Grady et al., 1999; Henze et al., 2000)
Biomass VSS to Biomass COD ratio	f_{CV}	(mg-COD·mg-VSS^{-1})	1.42	(Grady et al., 1999; Henze et al., 2000)
AOB kinetics and stoichiometry				
max. specific growth rate	$\mu_{max,AOB}$	(day^{-1})	0.2 – 1.6	(Munz et al., 2011)
decay rate	b_{AOB}	(day^{-1})	0.06 – 0.4	(Marsili-Libelli et al., 2001; Munz et al., 2011)
half saturation value for S_{NH}	K_{NH}	(mg-N·L^{-1})	0.14 – 2.3	(Manser et al., 2005; Chandran et al., 2008)
Ammonia-N yield	Y_{AOB}	(mg-COD·mg-N^{-1})	0.11 – 0.21	(Hiatt and Grady, 2008; Sin et al., 2008; Munz et al., 2011)
PhAC inhibition coefficient	$K_{I,PhAC-AOB}$	(?gL^{-1})	NA	
NOB kinetics and stoichiometry				
max. specific growth rate	$\mu_{max,NOB}$	(day^{-1})	0.2 – 2.6	(Ahn et al., 2008)
decay rate	b_{NOB}	(day^{-1})	0.08-1.7	(Ahn et al., 2008; Munz et al., 2010)
half saturation value for S_{NO2}	K_{NO2}	(mg-N·L^{-1})	0.05 – 3	(Marsili-Libelli et al., 2001; Jones et al., 2007; Kampschreur et al., 2007)
Nitrite-N yield	Y_{NOB}	(mg-COD·mg-N^{-1})	0.06 – 0.10	(Sin et al., 2008)

Table V-15: Model parameters used in the Cometabolic Process Model

Description	Variable	Unit of Measure	Literature Values (where applicable) Range	Refs.
Initial Biomass Concentrations				
AOB	$X_{AOB,t0}$	(mg-COD·L^{-1})	NA	NA
NOB	$X_{NOB,t0}$	(mg-COD·L^{-1})	NA	NA
HET	$X_{HET,t0}$	(mg-COD·L^{-1})	NA	NA
PhAC Biodegradation				
AOB growth-related transformation Coefficient	$T_{PhAC-AOB}$	(L·g-COD^{-1})	NA	NA
AOB non-growth related transformation coefficient	$k_{PhAC-AOB}$	(L·g-COD^{-1}·d^{-1})	NA	NA
HET lumped biodegradation coefficient	$\alpha_{PhAC-HET}$	(L·g-COD^{-1}·d^{-1})	NA	NA

Notes:

i. $X_{AOB,t0}$ and $X_{NOB,t0}$ – independent, fit using the nitrification control (Reactor 1) data

ii. $T_{PhAC-AOB}$, $k_{PhAC-AOB}$ and $K_{I,PhAC-AOB}$ – independent, fit using the nitrification experiments (Reactor 3 & 4) data

iii. $\alpha_{PhAC-HET}$ – independent, fit using the nitrification inhibition control (Reactor 2) data

V.3.2.3. Uncertainty Analysis using Monte Carlo Simulations

In the model solution described above, the values for AOB and NOB biokinetic parameters were selected from the range of typical literature values as noted in Table V-15 in order to limit the number of variables estimated in this research. Furthermore, model uncertainty estimated using the *nlparci* routine in MATLAB does not account for uncertainties associated with selection of the values of biokinetic parameters from the range of literature values (see Table V-15).

Monte Carlo (MC) simulations were utilized herein evaluate the influence of uncertainty in the following six parameters $\mu_{MAX,AOB}$, b_{AOB}, K_{NH}, $\mu_{MAX,NOB}$, b_{NOB} and K_{NO2} on model inferences. Parameter sets for the MC simulations were selected using a Latin hypercube sampling method (McKay et al., 1979) from uniform distributions based on the interval corresponding to the range of literature values noted in Table V-15 (e.g., $\mu_{MAX,AOB}$: U(0.2,1.6)). There was no *a priori* basis to assume any cross correlation between these biokinetic parameters; no parameter combinations were excluded from the MC simulations. The MC simulation process used herein is as follows.

$X_{AOB,t0}$ and $X_{NOB,t0}$ were estimated as described in Section 3.2.2.2 utilizing the randomly selected set of AOB and NOB parameters in addition to parameters not modified as part of the sensitivity analysis process. Subsequently, nitrification performance using each biokinetic parameter set (i.e., MC simulation) was predicted and pharmaceutical degradation parameters were estimated in the replicate experimental reactors as described in Section V.3.2.2.2. An overview of the uncertainty analysis protocol is shown in Figure V-4.

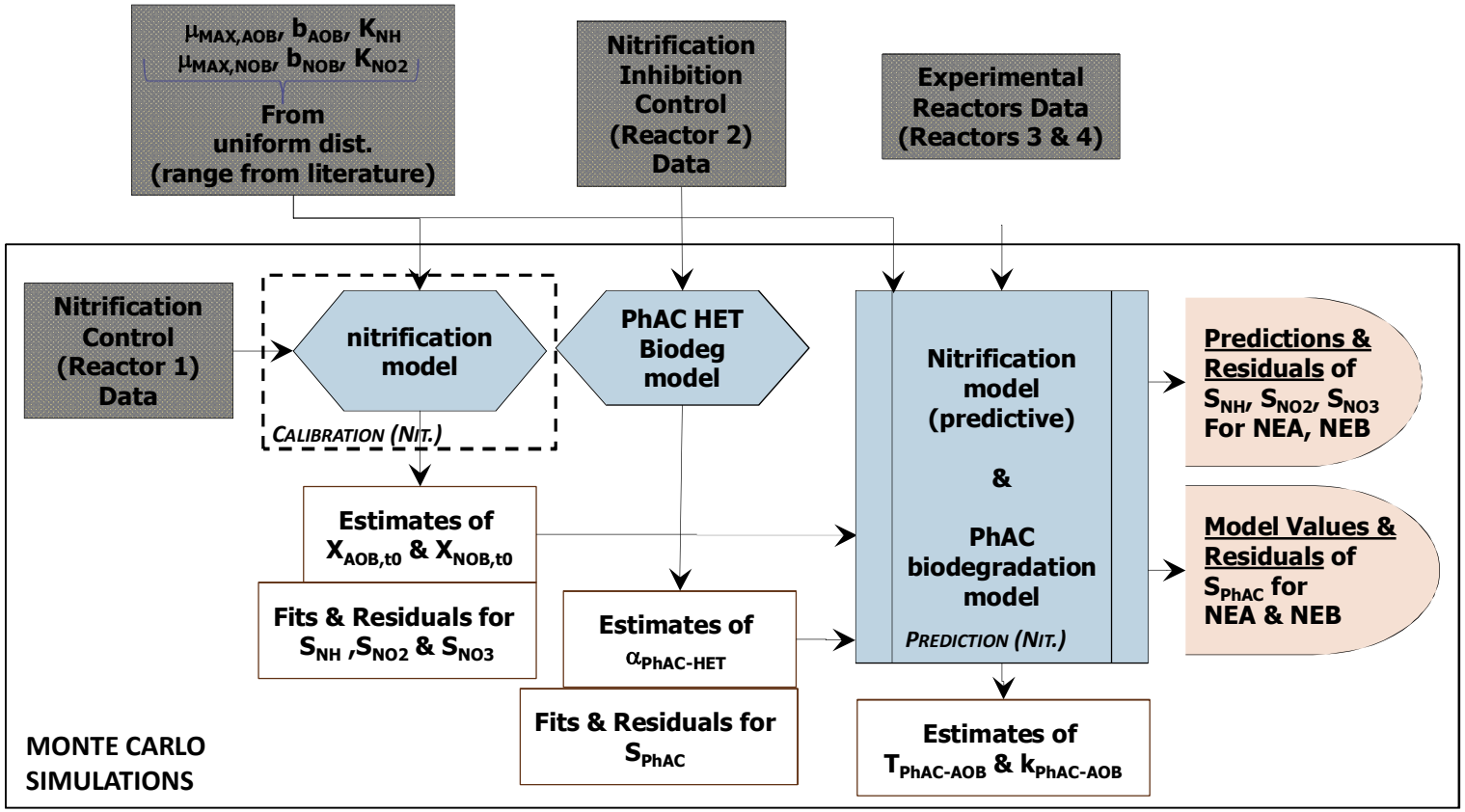

Figure V-4: Overview of the Monte Carlo analysis procedure utilized in this research for uncertainty and sensitivity analysis.

V.3.3. Goodness of Fit Metrics Used in this Research

A summary of goodness of fit metrics utilized in this research to measure model performance of regression models (developed in Chapter VI for PhAC sorption) and process models to describe PhAC biodegradation (Chapters VII – IX) is provided here. The correlation coefficient (R^2, Equation V-28) i used in this research to capture how well a model was able to capture the variance in sample data. In Chapter VI adjusted-R^2 (adj-R^2, Equation V-29) is also used to measure model fitting performance.

$$R^2 = 1 - \frac{SSE}{SST} \quad \text{(V-28)}$$

$$adj - R^2 = 1 - (1 - R^2)\frac{N-1}{N-P-1} \quad \text{(V-29)}$$

where:
SSE = the sum of square errors
SST = the total sum of squares
R^2 = is the correlation coefficient
N = the sample size
P = is the number of model parameters.

The predictive capability of models was assessed through predicted-R^2 (pred-R^2) (Equation V-30) and Nash-Sutcliffe Efficiency (NSE) (Equation V-31) (Nash and Sutcliffe, 1970). Unlike R^2 which describes the goodness of correlation, pred-R^2 was a goodness of prediction statistic based upon the prediction residuals of sum squares (Myers et al., 2010). The NSE ranges from $-\infty$ to 1 and is typically greater than 0. Negative values of NSE indicate that the mean of the measured values is a better predictor than the model. Strong predictive capability is generally characterized by pred-R^2 > 0.7 and NSE > 0.7 (McCuen et al., 2006; Moriasi et al., 2007).

$$\mathrm{p}red - \mathrm{R}^2 = 1 - \frac{SSE_{PRED}}{SST} \quad \text{(V-30)}$$

SSE_{PRED} is the prediction sum of square errors and SST is the total sum of squares.

$$NSE = \left(1 - \frac{\sigma_e^2}{\sigma_o^2}\right) \quad \text{(V-31)}$$

$\sigma_{e,i}^2$ is the variance of the residuals and $\sigma_{o,i}^2$ is the variance of the measurements

Chapter VI. Assessment of Quantitative Structural Property Relationships for Prediction of Pharmaceutical Sorption during Biological Wastewater Treatment

The contents of this chapter have been published as:

Sathyamoorthy, S. and Ramsburg, C.A. (2013). Assessment of quantitative structural property relationships for prediction of pharmaceutical sorption during biological wastewater treatment. *Chemosphere* 92(6): 639-646

Following is the graphical abstract from the manuscript:

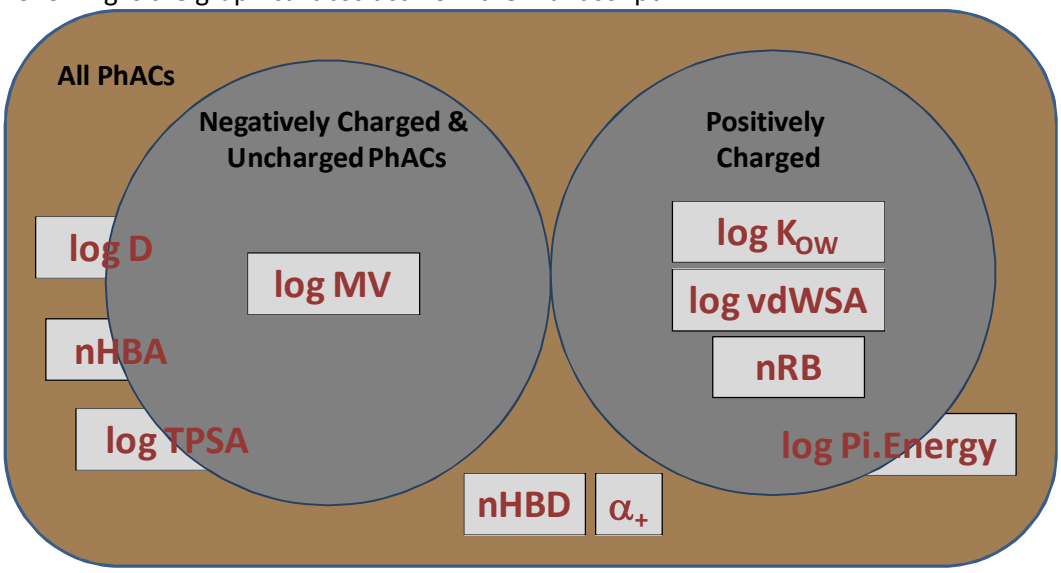

Assessment of QSPRs for PhAC Sorption

VI.1. Introduction

The occurrence of microconstituents in the environment has received significant attention in recent years. There is an increasing body of evidence that suggests the influence of microconstituents on aquatic ecosystems may include impaired embryo development and modified feeding behavior of biota (Cleuvers, 2004; Kostich and Lazorchak, 2008; Quinn et al., 2009). Consequently, managing the potential environmental risk posed by the burgeoning list of microconstituents has come to the forefront of environmental science and engineering (Schwarzenbach et al., 2006). The influence of pharmaceuticals (PhACs) on the environment is particularly concerning given the explosion in development and use of these chemicals over the last 30 yr (Robinson et al., 2007).

Wastewater treatment plants (WWTPs) provide a direct route for PhACs to enter the environment. Although WWTPs are not specifically designed to treat PhACs, recent studies highlight the potential for attenuation and degradation of some PhACs within the treatment processes (Gomez et al., 2007). The evidence suggests that the bulk of PhAC removal occurs during the biological treatment process(es) with sorption and biodegradation being the mechanisms primarily responsible for PhAC attenuation (e.g., Ternes et al., 2004; Onesios et al., 2009). The relative importance of these two attenuation mechanisms depends on PhAC properties and operating conditions.

The extent of sorption in biological treatment units is typically characterized using a distribution coefficient (K_D), which implies a linear equilibrium relationship based upon the concept of solute partitioning. Where the K_D of a PhAC is known *a priori*, assessment of the influence of sorption on PhAC attenuation may be evaluated using a mass balance approach for membrane bioreactors (MBRs), conventional activated

sludge (CAS) systems, and lab-scale reactors (lab) (see Section III.4, Chapter III). One way to assess the influence of sorption across the different treatment processes is to identify the K_D for which the PhAC mass evenly distributed between the aqueous and solid phases. For a CAS system operating at a mixed liquor suspended solids (MLSS) concentration of 3,000 mg/L this K_D is 0.37 Lg^{-1}-SS. For an MBR operating at 11,000 mgL^{-1} MLSS the same point occurs at K_D = 0.10 Lg^{-1}-SS. Thus, the number of PhACs for which sorption is relevant may be greater in MBR systems because fraction of PhAC mass sorbed may exceed 50% for PhACs having a K_D at or above 0.10 Lg^{-1}-SS.

The variation in the values of K_D (even for a single PhAC, see data in Appendix C) however, makes difficult any prediction of K_D within a given treatment system. There is therefore a need to better understand what factors influence PhAC sorption to develop a predictive capability for PhAC K_D values so that the influence of sorption can be better assessed when considering the attenuation of PhACs through the biological treatment process. The objective of this study is to develop and assess single and polyparameter models for the prediction of PhAC sorption in activated sludge systems. Included in the analysis described herein are all existing PhACs sorption data (see Appendix C) reported from studies conducted within the context of biological wastewater treatment (c.f. Appendix B for the list of studies included in this evaluation).

VI.2. Overview of Evaluation Approach

Predictive models for PhAC sorption are developed herein utilizing univariate and multivariate regression techniques described in Section V.3.1 (Chapter V, Materials and Methods). Models are evaluated using the suite of goodness of fit metrics described in Section V.3.3 (Materials and Methods).

VI.3. Results and Discussion

VI.3.1. Evaluation of the Sorption Coefficients Data Set

Assessment of the studies evaluating sorption of PhACs in biological treatment processes initially produced a total of 388 K_D measurements for 66 PhACs from peer reviewed studies (Appendix B for a list of studies and Appendix C for sorption data for each PhAC). This set of 66 PhACs certainly does not constitute all the PhACs currently on the market or in the production pipeline as sorption data for most PhACs to MLSS do not exist. Comparison of the 66 PhACs for which sorption studies have been conducted with the top 200 lists for generic PhACs in 2009 and 2010 (Drug-Topics, 2010, 2011) suggests that the sorption to MLSS has been evaluated for less than 10% of the most used PhACs. There has been a particular emphasis on few of these 66 PhACs across these studies. For example, more than five reported K_D values are available for only 21 of the 66 PhACs for which sorption data are available. Data from only 13 of these 21 PhACs include multiple measurement techniques (batch versus continuous) conducted under many experimental conditions (TOC, pH, suspended solids concentration, etc.). These 13 PhACs are: atenolol (ATN), carbamazepine (CBZ), clofibric acid (CLA), diclofenac (DCF), gemfibrozil (GMF), glibenclamide (GLC), ibuprofen (IBP), ketopofen (KET), metoprolol (MET), naproxen (NAP), propranolol (PRO) sulfamethaxazole (SMX) and trimethoprim (TMP). While the reason for an emphasis on these PhACs are unclear, it likely relates to patterns in the production and use of these PhACs coupled with the development of experimental and analytical methods.

Assessment of QSPRs for PhAC Sorption

Sorption of PhACs in environmental systems can result from a diverse range of mechanisms including non-specific hydrophobic interactions, columbic interactions or hydrogen bonding (Khunjar and Love, 2011). Given the types of possible sorbate-sorbent interactions, the charge of the PhAC becomes critical to modeling the observed sorption. The K_D measurements are therefore grouped based on the charge of dominant species at the experimental conditions. Separate models are developed and evaluated for negatively charged, uncharged, and positively charged PhACs. This type of charge-based classification necessitates the application of a threshold which defines the class (e.g., what fraction of PhAC mass is uncharged before it is labeled as such). Here the experimental pH relative to the pKa is employed with threshold of 50% for the uncharged group, thereby also defining the other two classes.

Only four studies report the experimental pH permitting calculation of the charge of the dominant species (Urase and Kikuta, 2005; Abegglen et al., 2009; Horsing et al., 2011; Stevens-Garmon et al., 2011). Thus, the overall number of available data are limited to 217 measurements for 54 PhACs. K_D values for these 217 measurements range from 0.03 L g^{-1} SS (5^{th} percentile) to 13.4 L g^{-1} SS (95^{th} percentile), with a median value of 0.60 L g^{-1} SS (see Figure VI-1). The Distribution of K_D values for negatively charged PhACs (25^{th}, 50^{th} and 75^{th} percentiles are 0.05, 0.14 and 0.40 L g^{-1} SS, respectively) is lower than that of uncharged PhACs (25^{th}, 50^{th} and 75^{th} percentiles are 0.15, 0.54 and 2.00 L g^{-1} SS, respectively). Also, the distribution of K_D values for uncharged PhACs is lower than that for positively charged PhACs (25^{th}, 50^{th} and 75^{th} percentiles are 0.55, 1.49 and 4.01, respectively) as shown in Figure VI-2. On average therefore, sorption may play a more important role in determining the fate of uncharged and positively charged PhACs than negatively charged PhACs. At the median

K_D of 0.60 Lg^{-1}-SS the fraction of PhAC sorbed to MLSS in CAS and MBR systems range from 48% to 70% and 83% to 90%, respectively, depending on the MLSS concentration employed for each process (refer to the discussion on PhAC sorption in different unit operations in Section III.4.2, Chapter III).

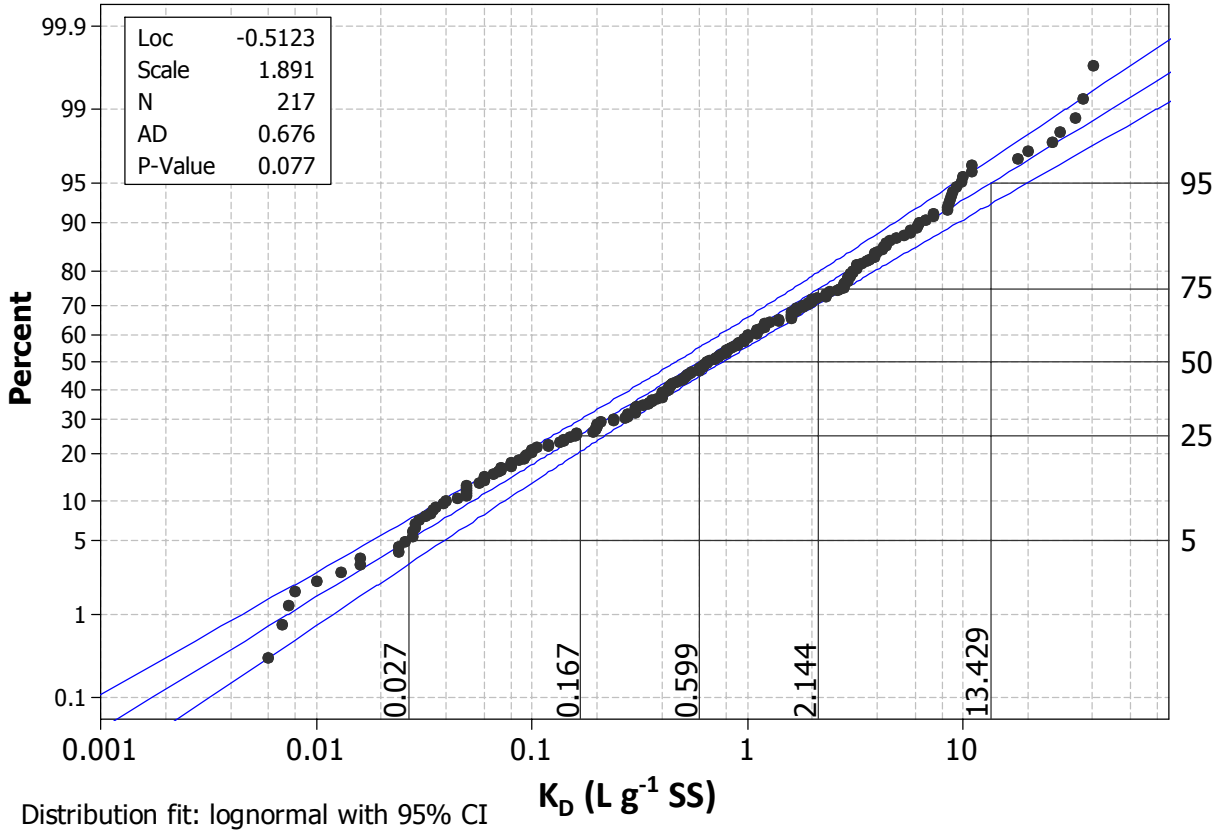

Figure VI-1: Distribution of PhAC sorption coefficients (KD) for the 217 data (for 54 PhACs) where experimental pH is available enabling calculation of PhAC charge at experimental conditions. Data are fit with 2-parameter log normal distribution. Shown for reference are 5th, 25th, 50th (median), 75th and 95th percentile K_D values.

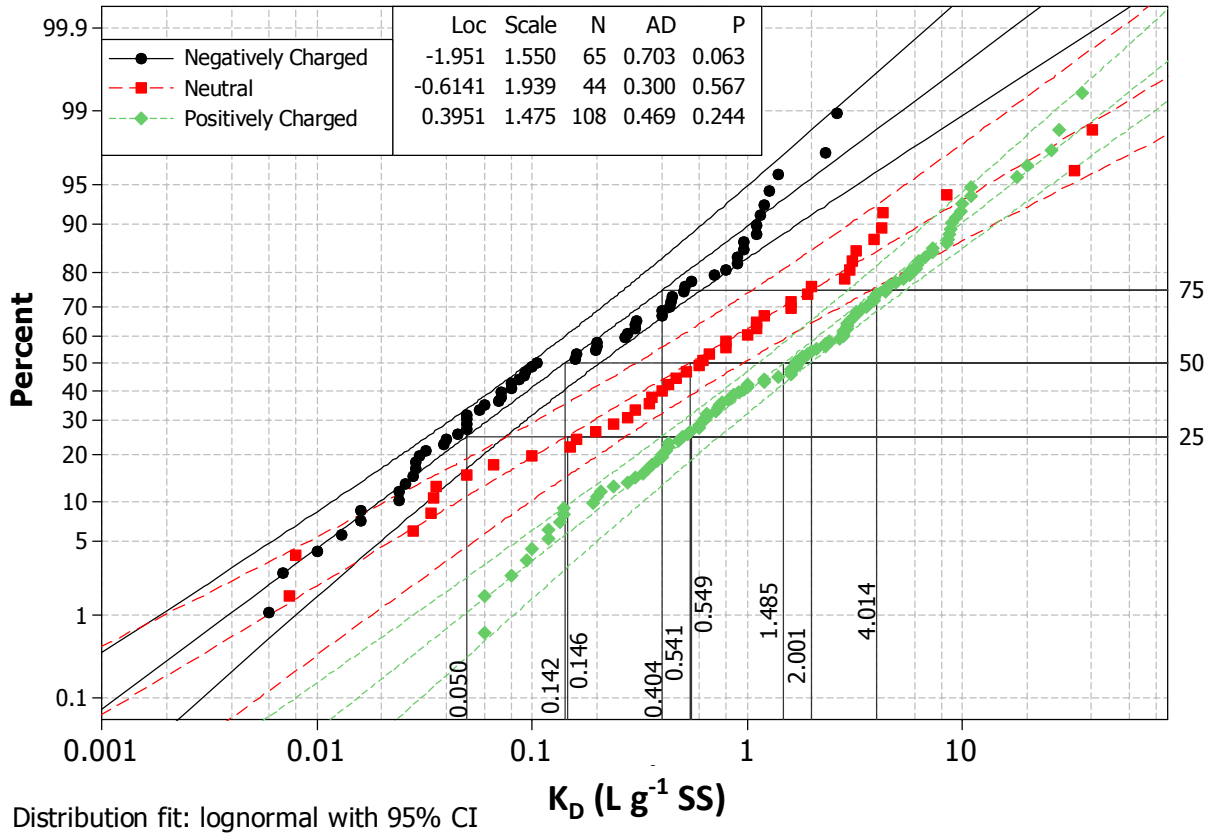

Figure VI-2: Distribution of PhAC sorption coefficients (KD) for PhACs where the dominant species is negatively charges (black circles), uncharged (red squares) and positively charged (green diamonds). Each data set is fit with 2-parameter log normal distribution; shown for reference are 25th, 50th (median) and 75th percentile KD values for each data set – values for negatively charged PhACs are shown at the lowest level, values for uncharged PhACs are shown at a level above and values for positively charged PhACs are shown at the highest level.

VI.3.2. Results of Single Parameter log K_{OW} and log D Models

Results suggest that log K_{OW} based models are generally ineffective at describing sorption of negatively-charged, uncharged, and positively-charged PhACs during biological treatment (Figure VI-3 and Table VI-1). The fact that regressions for the uncharged and positively-charged PhAC data offer higher values of pred-R^2 and NSE highlight that charge-based classification of PhACs is well aligned with the conceptualization of physical-chemical processes that result in sorption. This is particularly true for hydrophobic partitioning, where the uncharged species partitioning dominates the solid-liquid distribution, and can be seen in the performance of the models based upon hydrophobic compounds (Table VI-2). Existing models for sorption to activated sludge and soils shown in Figure VI-3 are restricted to values of log K_{OW} that fall within the range employed in developing each particular model (See Table VI-2 for ranges of applicability and summary statistics). Note that the best fit model produced in this work for the full range of K_{OW} (pred-R^2 = 0.29, NSE = 0.40) cannot achieve the predictive performance of some of the previous models, particularly that of Matter-Müller et al. (1980) (pred-R^2 = 0.57, NSE = 0.56). Correlations developed by Matter-Müller et al. (1980), Stevens-Garmon et al. (2011) and (Hyland et al., 2012) have a lower bound for log K_{OW} of 2. This restricts the data set to those PhACs for which hydrophobic interactions may be most important. When the range of K_{OW} in the best fit model is restricted to be consistent with that of Matter-Müller et al. (1980) (i.e., $2 < \log K_{OW} < 7$) performance increases to a level which is remarkably similar to that of the Matter-Müller et al. correlation (pred-R^2 = 0.57, NSE = 0.60, Table 2). This result highlights the robustness of the Matter-Müller et al. correlation in describing hydrophobic interactions.

Table VI-1: Influence of charge-based classification on the ability of one parameter log K_{OW} and log D based models to describe PhAC sorption

Data Set			Model Summary			Model Performance				
PhAC Grouping	N_{PhACs}	N_{DATA}	Predictor	Coeff.	SE. Coeff.	S	R^2	adj-R^2	pred-R^2	NSE
uncharged PhACs	19	44	Constant	-1.705	0.287	0.66	0.40	0.39	0.29	0.40
			log K_{OW}	0.409	0.077					
			Constant	-2.065	0.303	0.61	0.48	0.47	0.42	0.48
			log D	0.527	0.084					
negatively charged PhACs	16	65	Constant	-1.089	0.222	0.67	0.02	0.06	0.00	0.02
			log K_{OW}	0.062	0.053					
			Constant	-1.261	0.102	0.56	0.33	0.31	0.29	0.32
			log D	0.255	0.046					
positively charged PhACs	32	108	Constant	-0.738	0.128	0.51	0.36	0.36	0.34	0.36
			log K_{OW}	0.237	0.031					
			Constant	-0.108	0.082	0.58	0.17	0.17	0.14	0.17
			log D	0.144	0.030					

Table VI-1: Influence of charge-based classification on the ability of one parameter log K_{OW} and log D based models to describe PhAC sorption

Data Set			Model Summary			Model Performance				
PhAC Grouping	N_{PhACs}	N_{DATA}	Predictor	Coeff.	SE. Coeff.	S	R^2	adj-R^2	pred-R^2	NSE
Grouped Classification										
uncharged & negatively charged PhACs	30	109	Constant	-1.151	0.201	0.77	0.07	0.06	0.04	0.07
			log K_{OW}	0.144	0.050					
			Constant	-1.379	0.101	0.60	0.44	0.44	0.42	0.44
			log D	0.327	0.036					
uncharged & positively charged PhACs	43	152	Constant	-1.013	0.125	0.59	0.36	0.35	0.34	0.36
			log K_{OW}	0.282	0.031					
			Constant	-0.250	0.094	0.70	0.09	0.09	0.07	0.09
			log D	0.124	0.031					
all PhACs	54	217	Constant	-0.988	0.136	0.76	0.15	0.14	0.13	0.15
			log K_{OW}	0.202	0.033					
			Constant	-0.640	0.081	0.75	0.17	0.17	0.15	0.17
			log D	0.194	0.029					

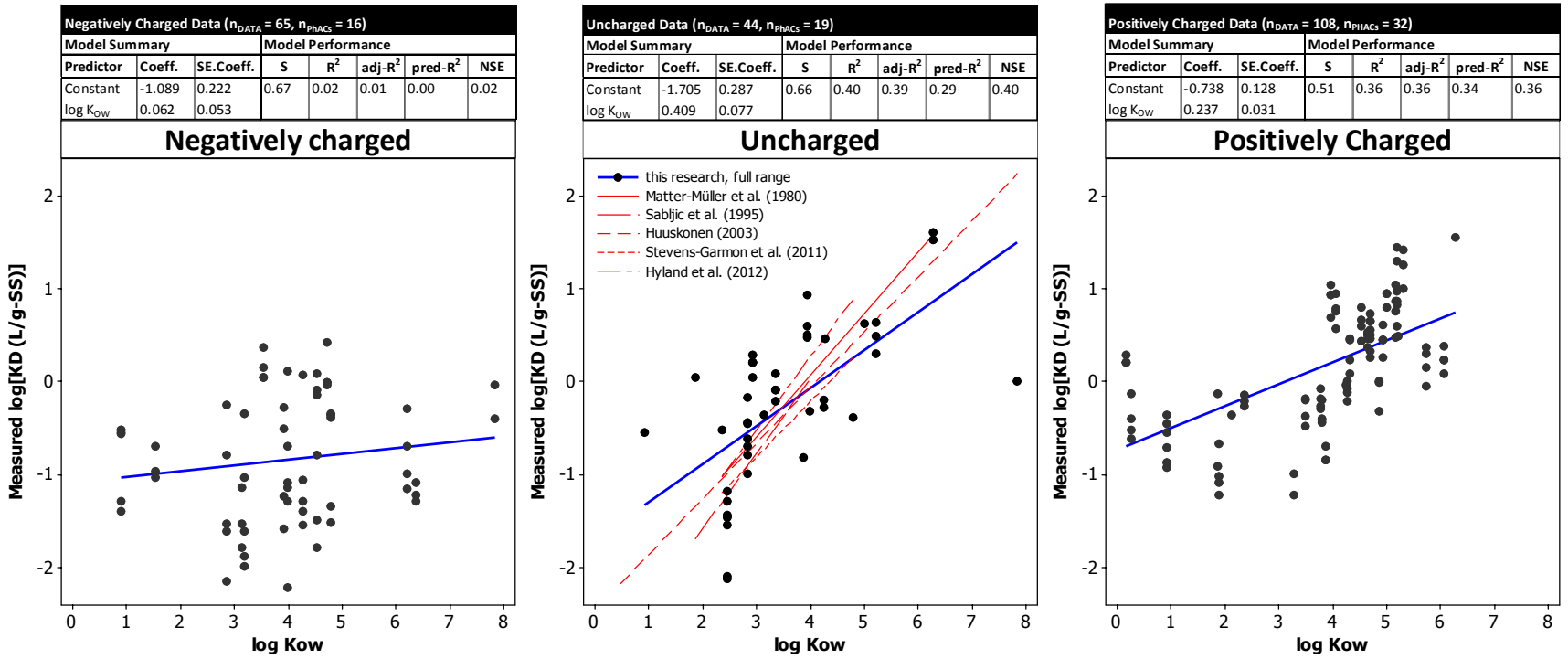

Figure VI-3: Reported log K_D values shown with predictions using one-predictor models based on log K_{OW} for negatively charged (left), uncharged (center) and positively charged (right) PhACs. Model coefficients and performance is shown in each overlying table. Also included on the uncharged plot are the models of (Matter-Müller et al., 1980)), Sabljic et al. (1995), Huuskonen (2003), Stevens-Garmon et al. (2011) and Hyland et al. (2012). K_{OC}-based models assume f_{OC} of biomass is 50%. Each of the existing models is only shown over the range of K_{OW} values used to develop the correlation (see Table 2 for range and performance statistics)

Table VI-2: Assessment of the performance of one-parameter log K_{OW} based models to describe sorption of uncharged pharmaceuticals included in this study in biological treatment processes

Reference	Correlation	Model Performance					Range of Applicability	No. of Data (& PhACs) in range
		S	R^2	adj-R^2	pred-R^2	NSE		
Literature Models:								
Matter-Müller et al. (1980)	$\log K_D = -2.61 + (0.67)\log K_{OW}$	0.56	0.60	0.59	0.57	0.56	$2 \le \log K_{OW} \le 7$	41 (15)
Sabljic et al. (1995)	$\log K_{OC} = 0.10 + (0.81)\log K_{OW}$	0.61	0.40	0.38	0.29	0.26	$1 \le \log K_{OW} \le 7.5$	32 (11)
Huuskonen (2003)	$\log K_{OC} = 0.84 + (0.60)\log K_{OW}$	0.66	0.40	0.39	0.29	0.31	$0 \le \log K_{OC} \le 6$	44 (19)
Stevens-Garmon et al. (2011)	$\log K_{OC} = 0.695 + (0.602)\log K_{OW}$	0.59	0.41	0.39	0.32	0.35	$2 \le \log K_{OW} \le 5$	35 (13)
Hyland et al. (2012)	$\log K_{OC} = [(0.47\pm0.46)] + [(0.79\pm0.13)\log K_{OW}]$	0.59	0.41	0.39	0.32	0.44	$2 \le \log K_{OW} \le 5$	35 (13)
Models developed in this Research:								
full range	$\log K_D = [-1.71\pm0.29] + [(0.41\pm0.08)\log K_{OW}]$	0.66	0.40	0.39	0.29	0.40	$1 \le \log K_{OW} \le 8$	44 (19)
limited K_{OW} range	$\log K_D = [-2.49\pm0.30] + [(0.63\pm0.08)\log K_{OW}]$	0.56	0.60	0.59	0.57	0.60	$2 \le \log K_{OW} \le 7$	41 (15)

Log D based models offer a substantial improvement in pred-R^2 for negatively charged PhACs and, as expected, marginal improvement for uncharged PhACs (Figure VI-4). For positively charged PhACs the log K_{OW} based model has significantly better predictive ability that the analogous log D based model (pred-$R^2_{\log Kow\ model}$ = 0.34; pred-$R^2_{\log D\ model}$ = 0.14). This can be explained by recognizing that K_{OW} and D are parameters which describe hydrophobic partitioning, while the positive charge species also have electrostatic interactions (Hyland et al., 2012; MacKay and Vasudevan, 2012; Schaffer et al., 2012) with the typically net-negative surfaces of MLSS (e.g., Schafer et al., 2002).

Negatively Charged Data (n_{DATA} = 65, n_{PhACs} = 16)

Model Summary			Model Performance				
Predictor	Coeff.	SE.Coeff.	S	R^2	adj-R^2	pred-R^2	NSE
Constant	-1.089	0.222	0.67	0.02	0.01	0.00	0.02
log K_{OW}	0.062	0.053					
Constant	-1.261	0.102	0.56	0.33	0.31	0.28	0.32
log D	0.255	0.046					

Uncharged Data (n_{DATA} = 44, n_{PhACs} = 19)

Model Summary			Model Performance				
Predictor	Coeff.	SE.Coeff.	S	R^2	adj-R^2	pred-R^2	NSE
Constant	-1.705	0.287	0.66	0.40	0.39	0.29	0.40
log K_{OW}	0.409	0.077					
Constant	-2.065	0.303	0.61	0.48	0.47	0.42	0.48
log D	0.527	0.084					

Positively Charged Data (n_{DATA} = 108, n_{PhACs} = 32)

Model Summary			Model Performance				
Predictor	Coeff.	SE.Coeff.	S	R^2	adj-R^2	pred-R^2	NSE
Constant	-0.738	0.128	0.51	0.36	0.36	0.34	0.36
log K_{OW}	0.237	0.031					
Constant	-0.108	0.082	0.58	0.17	0.17	0.14	0.17
log D	0.144	0.030					

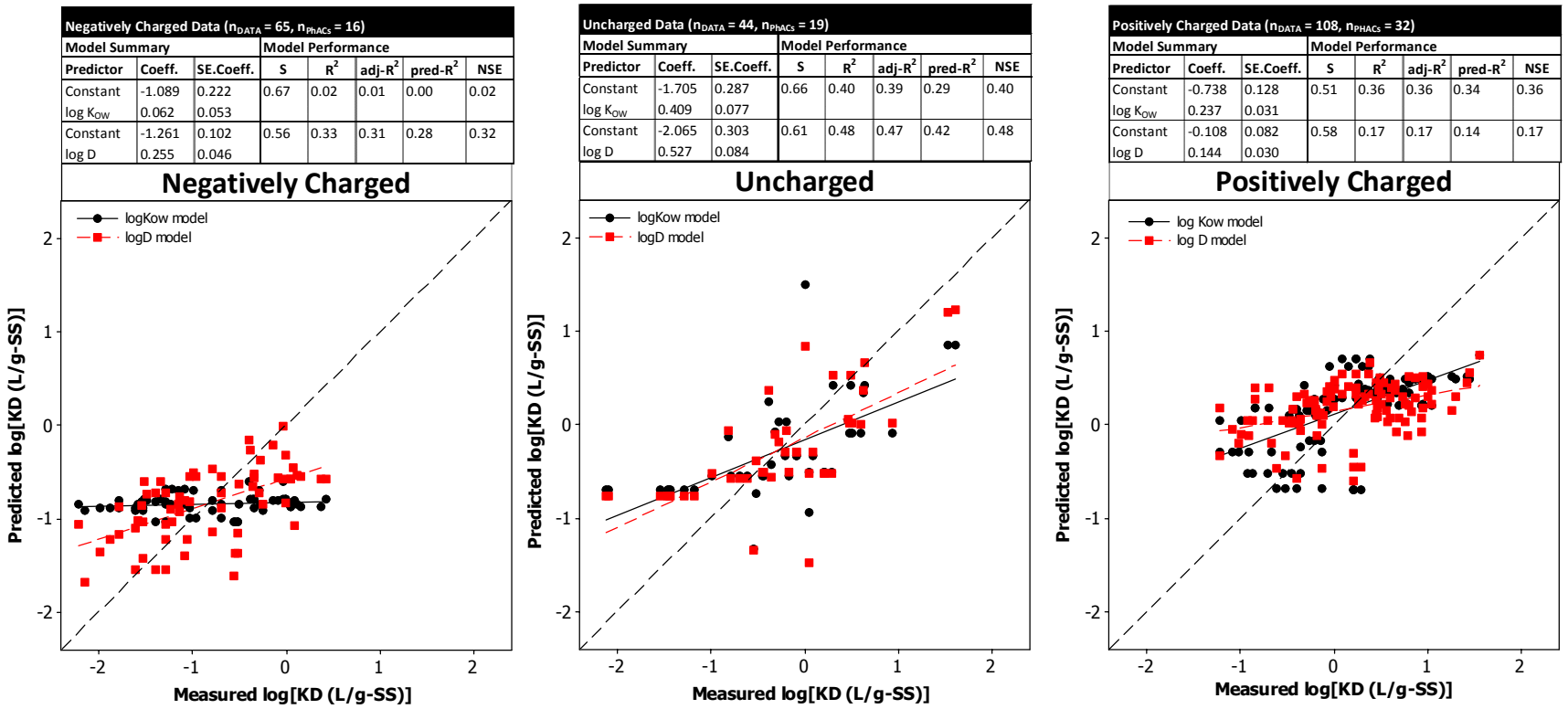

Figure VI-4: Reported log K_D values with predictions using one-parameter models based on log K_{OW} (black) and log D (red) for negatively charged (left), uncharged PhACs (middle) and positively charged PhACs (right). Model coefficients and performance is shown in the overlying tables

Assessment of QSPRs for PhAC Sorption

It is interesting to consider the effect of the threshold used to define the uncharged PhACs within the context of hydrophobic partitioning and single predictor models. The predictive capability of log D or log K_{OW} based models only becomes meaningful when the faction of uncharged PhAC (α_0) is >99% (Table VI-3). That is where electrostatic interactions are negligible, log D and low K_{OW} models may become applicable for PhAC sorption on MLSS. There are, however, only five PhACs (i.e., ~10% of the PhACs examined to date) for which the fraction of uncharged species was >99% suggesting caution should be exercised when considering predictive models for PhAC sorption predicated strictly on non-specific hydrophobic interactions. Such models are limited in application and highly dependent upon the selected threshold.

Table VI-3: Influence of the threshold used to define an uncharged pharmaceutical

Data Set			Model Summary			Model Performance				
Uncharged Threshold	**N_{PhACs}**	**N_{DATA}**	**Predictor**	**Coeff.**	**SE. Coeff.**	**S**	**R^2**	**adj-R^2**	**pred-R^2**	**NSE**
≥50% uncharged	19	44	Constant	-1.705	0.287	0.66	0.40	0.39	0.29	0.40
			log K_{OW}	0.409	0.077					
			Constant	-2.065	0.303	0.61	0.48	0.47	0.42	0.48
			log D	0.527	0.084					
≥85% uncharged	12	34	Constant	-2.446	0.331	0.61	0.59	0.57	0.53	0.65
			log K_{OW}	0.644	0.096					
			Constant	-2.661	0.333	0.58	0.63	0.62	0.58	0.63
			log D	0.710	0.097					
≥99% uncharged	5	22	Constant	-4.945	0.594	0.47	0.74	0.72	0.69	0.76
			log K_{OW}	1.483	0.198					
			Constant	-4.946	0.594	0.47	0.74	0.72	0.69	0.76
			log D	1.483	0.198					

Assessment of QSPRs for PhAC Sorption

The lack of predictive power of models based upon log D and log K_{OW} (best pred-R^2 and NSE are 0.42 and 0.44, respectively) highlights the importance of considering the type of solutes and sorbents that are more frequently employed to develop these types of relationships. Models such as Equation V-6 (shown here as Equation VI-1) are strictly valid only where there is a linear relationship between the Gibbs free energy of partitioning in the octanol-water system ($\Delta G_{PhAC,OW}$) and the partitioning in the environmental system ($\Delta G_{PhAC,env}$).

$$\log K_{D,PhAC} = \alpha \log K_{OW,PhAC} + \beta \quad \text{(VI-1)}$$

Theoretically, linearity in the Gibbs free energy occurs when the sorbent properties are identical to those of 1-octanol, and all solutes within the correlation data set offer the same extent of hydrogen bonding. Therefore linear models may offer good approximations for the partitioning of molecules that are apolar (i.e., only Van der Waals interaction) and monopolar (i.e., hydrogen bond donation *or* acceptance) such as pesticides and PAHs, but breakdown for molecules having more complex interactions. Indeed, most PhACs are designed to have specific interactions that often result in the compound being polar and pH active (Jjemba, 2008), which explains the poor predictive power of these single-predictor, linear models (Schwarzenbach et al., 2003).

VI.3.3. Results of Polyparameter Models

VI.3.3.1. Uncharged PhACs

The LFER model employing all of Abraham's five predictors (Abraham, 1993) was utilized to describe the sorption of uncharged PhACs (i.e., PhACs for which the fraction of uncharged species was >50% at the pH of the experiment). There are 44 data from 16 PhACs in this uncharged group. McGowan Volume (V) was the only statistically significant predictor ($p < 0.05$) as shown in Table VI-4. The performance of the LSER model using V is poor even when compared to a single parameter log K_{OW} or log D models (see Table VI-3 for $\alpha_0 > 50\%$).

Table VI-4: Summary of LSER models developed using Abraham predictors to describe the sorption of Uncharged PhACs to suspended solids during biological treatment

	Model Summary				Model Performance				
$N_{PRED.}$	Predictor	Coeff.	SE. Coeff.	p-value	S	R^2	adj-R^2	pred-R^2	NSE
5	Constant	-1.31	0.54	0.021					
	E	-0.27	0.31	0.388					
	S	0.23	0.40	0.572					
	A	-0.63	0.45	0.171					
	B	-0.36	0.52	0.485					
	V	0.78	0.32	0.019					
1	Constant	-1.11	0.42	0.012	0.81	0.09	0.07	0.01	0.08
	V	0.35	0.17	0.043					

Exploration of polyparamter QSAR models using the 13 predictors listed in Table VI-5 suggests that the best one predictor model to describe the K_D values for the 44 data from 16 PhACs in the group containing the uncharged PhACs is the log D based model (see Table VI-6 for all models related to uncharged PhACs). The best two predictor model, using log D and nHBA, improves pred-R^2 by 20%. The significant improvement

through the addition of nHBA relative to the 1-parameter log D model (Table VI-8 and Figure VI-4) highlights the importance of hydrogen bonding in the sorption of uncharged PhACs. The addition of the third predictor – a stereochemistry parameter in the form of nRB – further improves pred-R^2 by a modest 3%. This 3-parameter model, which includes log D, nHBA and nRB as the only statistically-significant predictors provides the best performance (Table VI-8) when describing K_D data for the uncharged PhACs.

Table VI-5: Molecular descriptors considered as predictor variables in polyparameter QSAR models developed for estimation of pharmaceutical sorption coefficients

Molecular Descriptor	**Predictor**
Octanol water partitioning coefficient	log K_{OW}
pH corrected octanol water partitioning coefficient	log D
log of molecular weight (MW, g/mol)	log MW
log of molecular volume (MV, $Å^3$)	log MV
Number of hydrogen bond donors	nHBD
Number of hydrogen bond acceptors	nHBA
Number of rotatable bonds	nRB
log of Van der Waals surface area	log vdWSA
log of topological polar surface area (TPSA, $Å^2$)	log TPSA
Aromaticity – Percentage of aromatic carbon atoms in molecule	%Aro-C
Charge of PhAC species which is dominant at the experimental conditions	Dom.Species
Fraction of PhAC in solution as negatively charged species	α_-
Fraction of PhAC in solution as positively charged species	α_+
Fraction of PhAC in solution as uncharged species	α_0
log of Energy associated with aromatic ring system(s) of PhAC molecule	Pi.Energy

Table VI-6: Summary of polyparameter QSAR models developed to describe the sorption of Uncharged PhACs to suspended solids during biological treatment

$N_{PRED.}$	Model Summary: $\log[K_D(L\ g^{-1}\ SS)] =$	Model Performance				
		S	R^2	adj-R^2	pred-R^2	NSE
1	[-2.07±0.30] + [(0.53±0.08)logD]	0.61	0.48	0.47	0.42	0.47
2	[-2.88±0.28] + [(0.58±0.07)logD] + [(0.20±0.03)nHBA]	0.48	0.69	0.68	0.62	0.69
3	[-3.12±0.29] + [(0.63±0.07)log D] + [(0.30±0.06)nHBA] + [(-0.07±0.03)nRB]	0.45	0.73	0.71	0.65	0.73

Parameter values are reported with the standard error of the estimate. See Table 1 for definition of the predictors.

The performance of the three-predictor model for uncharged PhACs was also found to be dependent upon the threshold (α_0) used to define the class (Table VI-7). To evaluate the influence of threshold selection on model performance – polyparameter QSAR models were developed for uncharged PhACs with $\alpha_0 \geq 85\%$ and $\alpha_0 \geq 90\%$. The same predictors which are included in the best fit model for the data set where $\alpha_0 \geq 50\%$ was used at the two higher thresholds. However, the models were refit to produce new coefficients. At a threshold of 50%, predictive performance is limited (pred-R^2 < 0.70). Increasing the threshold to 85% uncharged produces a model with meaningful predictive power (pred-R^2 > 0.85), though somewhat limited applicability (12 of the 66 PhACs tested to date were examined under this condition).

Table VI-7: Influence of the threshold used to define an uncharged pharmaceutical on three predictor QSAR models

Data Set			Model Summary	Model Performance				
α_0	N_{PhACs}	N_{DATA}	$\log[K_D(L\ g^{-1}\ SS)] =$	S	R^2	adj-R^2	pred-R^2	NSE
≥50%	19	44	[-3.12±0.29] + [(0.63±0.07)log D] + [(0.30±0.06)nHBA] + [(-0.07±0.03)nRB]	0.45	0.73	0.71	0.65	0.73
≥85%	12	34	[3.68 ± 0.26] + [(0.78 ± 0.07)log D] + [(0.34 ± 0.05)nHBA] + [(0.09±0.03)nRB]	0.37	0.86	0.84	0.82	0.85
≥90%	5	22	[11.41±1.49] + [(3.92±0.61)log D] + [(0.21±0.06)nHBA] + [(0.71±0.13)nRB]	0.25	0.94	0.93	0.91	0.94

Table VI-8: Summary of best fit polyparameter QSAR models developed to describe the sorption of pharmaceuticals to suspended solids biological treatment

$N_{PRED.}$	Model Summary: $\log[K_D(L/g\text{-}SS)]$ =	Model Performance				
		S	R^2	adj-R^2	pred-R^2	NSE
Uncharged PhACs (n_{DATA} = 44; n_{PhACs} = 19)						
3	QSAR Model: [-3.12±0.29] + [(0.63±0.07)log D] + [(0.30±0.06)nHBA] + [(-0.07±0.03)nRB]	0.45	0.73	0.71	0.65	0.73
Negatively Charged PhACs (n_{DATA} = 65; n_{PhACs} = 16)						
3	[5.88±1.69] + [(0.37±0.05)logD] + [(0.30±0.05)nHBA] + [(- 3.56±0.78)logMV]	0.44	0.60	0.58	0.56	0.61
Positively Charged PhACs (n_{DATA} = 108; n_{PhACs} = 32)						
4	(7.65±2.24) + [(0.34±0.04)]log(K_{OW})] + [(1.65±0.31)]log(PiEnergy)] + [(-4.34±0.94)]log(vdWSA)] + [(0.05±0.02)]log(nRB)]	0.44	0.54	0.52	0.49	0.54
Models for Grouped PhACs						
Negatively Charged and Uncharged PhACs (n_{DATA} = 109; n_{PhACs} = 16)						
4	[4.54±1.36) + [(0.39±0.04)logD] + [(0.32±0.04)nHBA] + [(-2.41±0.59)logMV] + [(-0.86±0.25)log(TPSA)]	0.48	0.64	0.63	0.61	0.64
All PhACs (n_{DATA} = 217; n_{PhACs} = 54)						
6	(-1.74±0.46) + [(0.22±0.03)logD] + [(0.92±0.10)α_+] + [(0.99±0.28)log(Pi.Energy)] + [(-0.85±0.17)log(TPSA)] + [(0.14±0.05)nHBD] + [(0.08±0.03)nHBA]	0.53	0.59	0.58	0.56	0.59

Parameter values are reported with the standard error of the estimate. See Table VI-5 for definition of the predictors.

VI.3.3.2. Negatively Charged PhACs

The best single parameter model (using any of the predictors in Table VI-8) to describe the K_D values for the 65 data from 16 PhACs in the group containing the negatively charged PhACs is the log D based model. The best two parameter model, using log D and nHBA, improves pred-R^2 14.0%. The inclusion of nHBA in describing K_D suggests that the formation of hydrogen bonds may be an important interaction for both uncharged and negatively charged species. The best-fit polyparameter QSAR to describe this class (65 K_D data for 16 PhACs) includes log D, nHBA and log MV as the only statistically-significant predictors (Table VI-9). The first two predictors are identical to the model for uncharged PhACs, though the fitted coefficient for log D is smaller in the model developed for negatively charged PhACs (Table VI-8). The diminished importance of log D as a predictor for negatively charged PhACs is consistent with the concept that electron donating groups generally decrease hydrophobic interactions (Schwarzenbach et al., 2003). The addition of the third predictor – size in the form of MV – further improves pred R^2 by 14.0%. Given that (i) MV is the principle difference in the predictors between the uncharged and negatively charged PhACs; (ii) all but two measurements within the negatively charged grouping were conducted under conditions in which the charge of the dominant species was -1 (refer to Appendix B for a summary of experimental conditions for all studies evaluated as part of this research); and (iii) the negative fitted coefficient for log MV suggests an inverse relationship, it is hypothesized that surface charge density may have a role in the sorption in a way where relatively smaller, negatively charged PhACs can more readily access localized positive surface charge or divalent cations incorporated within within the MLSS floc

structure. The addition of the third predictor – size in the form of MV – further improves pred-R^2 by 14.0%.

Table VI-9: Summary of polyparameter QSAR models developed to describe the sorption of negatively Charged PhACs to suspended solids during biological treatment

$N_{PRED.}$	Model Summary: $\log[K_D(L\ g^{-1}\ SS)]$ =	Model Performance				
		S	R^2	adj-R^2	pred-R^2	NSE
1	[-1.26±0.10] + [(0.26±0.04)logD]	0.56	0.33	0.31	0.28	0.33
2	[-1.78±0.16] + [(0.23±0.04)logD] + [(0.12±0.03)nHBA]	0.50	0.47	0.45	0.42	0.47
3	[5.88±1.69] + [(0.37±0.05)log D] + [(0.30±0.05)nHBA] + [(-3.56±0.78)log MV]	0.43	0.60	0.58	0.56	0.60

Parameter values are reported with the standard error of the estimate. See Table 1 for definition of the predictors.

VI.3.3.3. Positively Charged PhACs

The evaluation of models for positive PhACs is based on 108 K_D measurements for 32 PhACs from two studies (Horsing et al., 2011; Stevens-Garmon et al., 2011), with the vast majority of the data from the study of Horsing et al. (2011) (105 measurements). One would anticipate that interaction between positively charged PhACs and the solid phase would be electrostatic in nature, but even the best two parameter model includes variables related to hydrophobic partitioning (log K_{OW}) and aromaticity (%AroC). Hyland et al. (2012) attributed a lack of correlation between cation exchange capacity (CEC) of sludges and values of K_D to the fact that the CECs of the eight sludges examined had limited variation 61.0 ± 7.4 meq $(100\text{-g})^{-1}$. The emphasis on hydrophobic interactions is thought to be a result of the tight distribution in the fraction of positive charge for these 108 data. The fraction of positively charged species (α_+) during the sorption experiment(s) is >85% for 88 of the 108 measurements, the mean value of $\alpha_+$is 0.923 with a variance of 0.017. Consequently, the model is not able to attribute the variance in the log K_D data to the α_+ predictor. Note that the importance of charge as a predictor is more important when all PhAC data are simultaneous modeled (see Section VI.2.3.4, below).

In this analysis, the predictors in the best model relate to dipole-dipole interactions, hydrophobicity and molecular stereochemistry (Table VI-8, Table VI-10). It is hypothesized that the selection of PiEnergy and vdWSA as predictors instead of %AroC in the best three and four parameter models occurs because vdWSA represents a size that is associated with molecular interactions that are not included in the PiEnergy descriptor or in the TPSA descriptor (e.g., London, Debye and Keesom forces). %AroC and PiEnergy are related parameters, but %AroC also encodes information on size,

albeit indirectly. That selection of vdWSA in the three-predictor model allows the aromatic descriptor to become more specific. The best model includes four predictors: log K_{OW}, PiEnergy, vdWSA and nRB (Table VI-10). Inclusion of nRB as the fourth predictor in the model suggests molecular conformation may be important to the interaction. The best model for positively charged PhACs (four predictor) also represents improved, but insufficient, predictive power.

Table VI-10: Summary of polyparameter models developed to describe the sorption of positively charged pharmaceuticals to suspended solids biological treatment

$N_{PRED.}$	Model Summary: $\log[K_D(L\ g^{-1}\ SS)] =$	Model Performance				
		S	R^2	adj-R^2	pred-R^2	NSE
Positively Charged PhACs (n_{DATA} = 108; n_{PhACs} = 32)						
1	(-0.74±0.13) + [(0.24±0.03)]log(K_{OW})]	0.51	36.1%	35.5%	33.4%	0.36
2	(-1.46±0.17) + [(0.23±0.03)]log(K_{OW})] + [(1.42±0.26)]%AroC]	0.46	50.0%	49.1%	46.8%	0.50
3	(3.97±1.52) + [(0.28±0.03)]log(K_{OW})] + [(1.44±0.30)]log(PiEnergy)] + [(-2.59±0.59)]log(vdWSA)]	0.45	51.5%	50.1%	47.0%	0.52
4	(7.65±2.24) + [(0.34±0.04)]log(K_{OW})] + [(1.65±0.31)]log(PiEnergy)] + [(-4.34±0.94)]log(vdWSA)] + [(0.05±0.02)]log(nRB)]	0.44	53.7%	51.9%	48.6%	0.54

Parameter values are reported with the standard error of the estimate. See Table 1 for definition of the predictors.

VI.3.3.4. Utility of Grouping PhACs

The similarity in the predictors in the best fit polyparameter QSARs for uncharged and negatively charged PhACs (Table VI-8) suggests there may be utility in developing a single model for both uncharged and negatively charged PhACs. Grouping the negatively charged PhACs with the uncharged PhACs has an important practical

implication - it eliminates the need to define what is an arbitrary threshold thereby potentially increasing both the generalizability and practicability of all subsequent models. It should be noted here that establishing an arbitrary threshold to differentiate uncharged and positively charged PhACs has less practical implication given that most PhACs that can become positively charged are at circa neutral pH (see description of the α_+ distribution in sec 3.3.3). The best QSAR model to describe the K_D values for the 109 data from 30 PhACs in the combined uncharged and negatively charged group includes four statistically-significant predictors: - log D, nHBA, MV and TPSA (Table VI-8). The first three predictors are the same as was determined when considering only the negatively charged PhACs. The addition of the negative dependence of log K_D on log TPSA suggests that PhACs for which polar atoms (e.g., oxygen, nitrogen) contribute significantly to the exposed surface area tend to sorb to a lesser extent. This is consistent with design concepts for PhAC partitioning within the human body (Palm et al., 1997). While the final model offers improvement in predictive power when compared the results for negatively charge PhACs (Table VI-8), the goodness of prediction statistics coupled with the uncertainties associated with model coefficients suggests that caution should be exercised when considering such a model as a predictive tool for PhAC sorption. Moreover, the increase in model performance for the negatively charged PhACs comes at a nearly comparable expense in performance of the best model developed for only the uncharged PhACs (Table VI-8).

The performance of polyparameter models developed using all the data (i.e., a single data set consisting of uncharged, positively charged and negatively charged PhACs) is also explored. Interestingly, the best single predictor for the entire set of PhAC data is the charge of the dominant species (Dom.Species) at the pH of the

experiments (Table VI-11: pred-R^2 = 0.28 compared to 0.15 for log D based model). This reinforces the importance of the influence that the charge of a PhAC has on sorption in environmental systems.

The best model to describe the aggregate data set is a six parameter model using as predictors: logD, fraction of positively charged species (α_+), PiEnergy, TPSA, nHBD and nHBA. Note here that in moving from one to multiple predictors Dom.Species becomes irrelevant (effectively replaced by the combination of α_+ and log D). The inclusion of hydrophobic interactions here is expected based upon the results previously described for the grouped PhACs, since the influence of positive charge is incorporated (at least to some extent) by α_+. The utility of log(TPSA) and hydrogen bonding to describe the sorption of the aggregate data set is also consistent with results for the subgroups. It is interesting to note how the addition of a descriptor as simple as α_+ in the two-parameter model substantially improves the predictive capability of the model.

Table VI-11: Summary of polyparameter models developed to describe the sorption of pharmaceuticals to suspended solids biological treatment.

$N_{PRED.}$	Model Summary: $\log[K_D(L\ g^{-1}\ SS)]$ =	Model Performance				
		S	R^2	adj-R^2	pred-R^2	NSE
All PhACs (n_{DATA} = 217; n_{PhACs} = 54)						
1	(-0.32±0.05) + [(0.50±0.05)Dom.Species]	0.69	0.29	0.29	0.28	0.29
2	(-1.18±0.08) + [(0.24±0.02)logD] + [(0.99±0.09)α_+]	0.59	0.48	0.48	0.47	0.48
3	(-2.94±0.38) + [(0.23±0.02)logD] + [(1.07±0.09)α_+] + [(1.16±0.24)log(Pi.Energy)]	0.57	0.53	0.53	0.52	0.53
4	(-2.65±0.38) + [(0.19±0.03)logD] + [(0.93±0.09)α_+] + [(1.48±0.26)log(Pi.Energy)] + [(-0.40±0.12)log(TPSA)]	0.55	0.56	0.55	0.54	0.56
5	(-2.35±0.38) + [(0.23±0.03)logD] + [(0.99±0.09)α_+] + [(1.28±0.26)log(Pi.Energy)] + [(-0.61±0.13)log(TPSA)] + [(-0.17±0.05)nHBD]	0.54	0.58	0.57	0.56	0.58
6	(-1.74±0.46) + [(0.22±0.03)logD] + [(0.92±0.10)α_+] + [(0.99±0.28)log(Pi.Energy)] + [(-0.85±0.17)log(TPSA)] + [(0.14±0.05)nHBD] + [(0.08±0.03)nHBA]	0.53	0.59	0.58	0.56	0.59

Parameter values are reported with the standard error of the estimate. See Table 1 for definition of the predictors.

VI.4. Implications

The analyses described in this research demonstrate that K_{OW} is not an effective predictor of PhAC sorption in biological treatment units, even when K_{OW} is corrected to the experimental pH. Polyparameter models based on PhAC characteristics improve the predictive capability and increasing model complexity improves the predictive capability. However, most of the polyparameter models evaluated here appear to approach a plateau in predictive performance with pred-R^2 in the range of 0.50 to 0.60. The addition of more predictors to each model has increasingly little influence on the predictive power (Figure VI-5). Importantly, QSAR models with a higher degree of predictive capability (pred-R^2 >0.80) can be developed for scenarios where the uncharged species is greater than 85% of the total PhAC mass present in a system. The suite of molecular descriptors employed here as potential predictors capture the range of interactions between PhACs and the mixed liquor solids. The richness of set of molecular descriptors considered here coupled with the plateau in model performance for all classifications suggests that models for PhAC sorption relying solely on sorbate parameters may be incapable of achieving a level of predictive capability required to effectively assess the interplay between sorption and biodegradation. Knowledge of whether or not sorption of PhACs renders PhACs unavailable for biodegradation may have important implications when evaluating process options to reduce the discharge of PhACs into the environment.

Together the inability of experimental procedure to explain the observed variability in measure K_D and the inability of polyparameter QSARs incorporating only solute descriptors to predict K_D suggest that specific characteristics of the sludge are required to enhance the predictive capability of such models. This requires careful

characterization of each sludge employed for PhAC sorption studies. This research suggests that a good *baseline* level of information on the sludges employed in sorption studies includes: (i) experimental conditions (e.g., pH, ionic strength, dissolved oxygen, oxidation-reduction potential, and possibly even the concentration of metals), (ii) *bulk* sludge characteristics (e.g., source SRT, suspended solids, and volatile solids) and (iii) solids composition characteristics (e.g., organic carbon content, carbohydrates, EPS, proteins, CEC, etc.). It should be emphasized that some of these parameters are currently reported in sorption studies and others are more generally available in studies reporting on sludge setting and MBR fouling. Thus, the measurement techniques exist and should not represent a barrier to more thorough solids characterization.

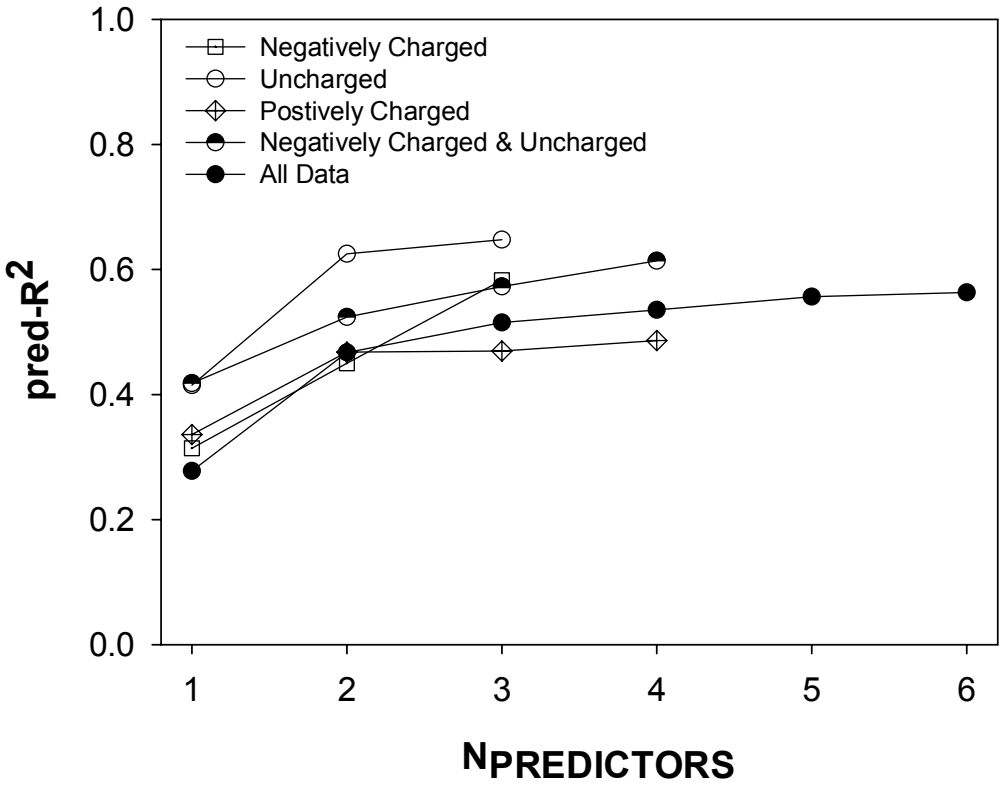

Figure VI-5: Predictive capability (pred-R^2) of the polyparameter QSAR models with increasing number of statistically significant predictors. Model details and summary statistics are provided in Table VI-8

Chapter VII. Degradation of Selected Beta Blockers during Ammonia Oxidation

The results presented in this chapter have been submitted for publication as:

Sathyamoorthy, S. Chandran, K.C. and Ramsburg, C.A. Evaluating the Degradation of Selected Beta Blockers during Ammonia Oxidation, *Environmental Science and Technology*, in review.

Following the graphical abstract from the manuscript:

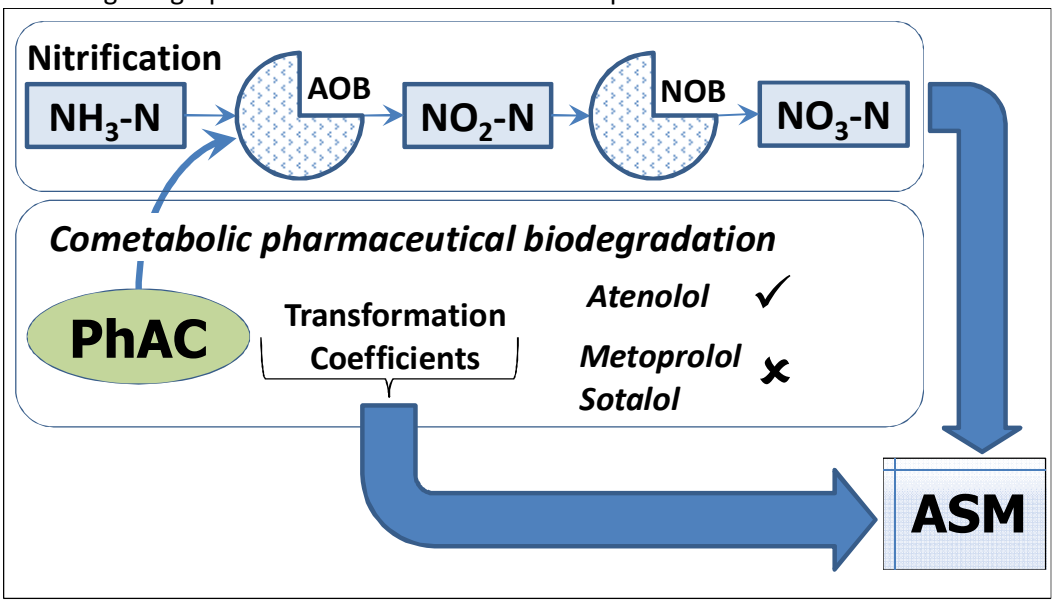

VII.1. Introduction

Reports of contemporary pharmaceuticals (PhACs) in the natural environment have engendered scientific concern related how these emerging contaminants may influence ecosystem health (Daughton and Ternes, 2000). Initial toxicological studies suggest that chronic exposure to PhACs at microgram per liter levels may decrease embryo hatching, reduce growth rates in fish and impact endocrine system activity in aquatic species (Massarsky et al., 2011; Ings et al., 2012). Wastewater treatment plants (WWTPs) are a primary pathway by which PhACs enter the aquatic environment. While WWTPs are not specifically designed to treat PhACs, several studies highlight attenuation across biological treatment processes (Andreozzi et al., 2003; Bendz et al., 2005; Chefetz et al., 2008). These studies, however, indicate that PhAC removals are highly variable - ranging from recalcitrance to effective removal depending on the PhAC and operating conditions.

Some reports have linked greater PhAC attenuation with longer solids retention times (SRTs ≥ 8-10 day) (Kreuzinger et al., 2004; Clara et al., 2005; Joss et al., 2006). The notion of greater removal at longer SRTs is interesting because it could overlay two emerging concerns - removal of microconstituents and nutrients - and, in doing so, raise interesting questions about the role of nitrifying organisms in PhAC attenuation. It should be recognized, however, that PhAC attenuation in WWTPs operated with longer SRTs could be due to either the presence of slow-growing nitrifying bacteria or more general changes in microbial diversity (Shi et al., 2004; Batt et al., 2006; Reif et al., 2008; Tran et al., 2009; Suarez et al., 2010; Falas et al., 2012; Fernandez-Fontaina et al., 2012). Many previous studies do not discriminate between PhAC attenuation (i.e., removal) and degradation. Moreover, where degradation is implied, there is often a critical lack

of evidence linking PhAC biodegradation to specific bacterial consortia. Therefore there is a need for research which elucidates and quantifies the influence of specific bacterial populations on PhAC degradation.

The overall objective of this research was to assess the biodegradation of three beta blockers– atenolol (ATN), metoprolol (MET) and sotalol (SOT) during nitrification. To accomplish this objective a combination of batch experiments and mathematical modeling is employed to evaluate and link rates of PhAC degradation and ammonia oxidizing bacteria (AOB) growth. It is hypothesized that if biodegradation of these beta blockers was observed in the batch experiments there would be a link between the PhAC degradation and ammonia oxidation activity. This hypothesis was based upon the fact that AOB are known to catalyze the oxidation of a wide array of aliphatic, aromatic and chlorinated organic compounds (Keener and Arp, 1994; Hooper et al., 1995), as well as endocrine disrupting compounds (Gaulke et al., 2009; Skotnicka-Pitak et al., 2009). The ability of AOB to catalyze non-specific oxidation of several compounds stems from the broad substrate range of ammonia monooxygenase (AMO) (Hooper et al., 1997). While AOB rely on AMO for ammonia oxidation as part of its energy metabolism (Arp and Stein, 2003), the oxidation of organic compounds by AMO does not result in energy generation. In fact organic compounds undergoing cometabolic oxidation may reduce the rate of ammonia oxidation by competitively binding to the same catalytic site (Arp et al., 2007) or an allosteric alternate site (Taher and Chandran, 2013) on AMO.

VII.2. Overview of Experimental and Modeling Approach

The biodegradation of each beta blocker was evaluated as described in Section V.2.4.1 (Chapter V, Materials and Methods). In brief, the biodegradation of the

beta blocker under consideration was first evaluated under nitrification conditions utilizing a set of four reactors: a control to evaluate AOB and NOB biokinetics in the absence of the beta blocker (Reactor 1), a control to evaluate biodegradation of the beta blocker under nitrification inhibition conditions (Reactor 2) and two experimental replicates to evaluate beta blocker biodegradation resulting from nitrification (Reactors 3 and 4). A follow up experiment (NOX-EXPT) was conducted where the beta blocker was observed to degrade to a greater extent in Reactors 3 and 4. In the NOX-EXPT, three reactors were utilized as follows. Reactor 5 was used a control evaluate NOB kinetics in the absence of the beta blocker. Reactors 6 and 7 were experimental replicates used to elucidate the biodegradation of the beta blocker under nitrite oxidation conditions. Data from these experiments were described utilizing the models described in Section V.3.2 Chapter V, Materials and Methods).

VII.3. Results and Discussion

VII.3.1. Microbial Community Structure

Gene copy concentrations (Figure VII-1) are used to determine estimates for biomass concentrations related to all bacteria (using EUB), AOB (using amoA) and NOB (using NOB-Nb and NOB-Ns). Estimates of HET concentrations are determined as the difference between all bacteria and nitrifying bacteria. Note that biomass from the nitrification enrichment SBR is collected for all reactors of a given experiment at the same time. Therefore the initial biomass concentrations in each reactor are expected to be statistically the same. This is assumed in the mathematical modeling in this research. Estimated biomass concentrations from each reactor are therefore averaged across all

reactors from a given experiment (4 reactors in the NIT-EXPTs and 3 reactors in the NOX-EXPTs).

Estimated biomass concentrations (for HET, NOB and AOB) for each experiment determined using gene copy concentrations suggest that AOB are dominant in the enrichment community and represent between 75% and 85% of the nitrifying population (i.e., AOB + NOB) (Figure VII-2). These data are consistent with previous studies of nitrifying populations in systems treating high nitrogen loads (Dytczak et al., 2008). *Nitrobacter* spp. are dominant NOB, effectively accounting for the remainder of the nitrifying population. *Nitrospira* spp. account for less than 0.1% of the nitrifying population. This observation can be explained due to the high S_{NH} concentrations used in the nitrification enrichment SBR which was the seed biomass source for these experiments. High levels of S_{NH} result in high S_{NO2} levels during the SBR cycle which favors *Nitrobacter* over *Nitrospira* NOB (Schramm et al., 2000). Comparison the model average value of X_{AOB} and X_{NOB} with the estimated value based on qPCR measurements for each experiment is provided in Table VII-1.

Table VII-1: Comparison of model average XAOB and XNOB with values estimated using qPCR for NIT-EXPTs.

	X_{AOB}		X_{NOB}	
	qPCR	**model**	**qPCR**	**model**
Atenolol	60 ± 17	50 ± 1	16 ± 2	29 ± 1
Metoprolol	29 ± 9	40 ± 6	11 ± 2	30 ± 11
Sotalol	65 ± 5	42 ± 9	11 ± 3	21 ± 8

Estimates of HET using the qPCR analyses suggest they represent <25% of the community. These estimates for X_{HET} fraction were compared to those determined

based on the active heterotroph fraction at the operating SRT of the nitrification enrichment SBR at the time of each experiment (Grady et al., 1999). SRT values for the MET, ATN and SOT experiments were 244, 297 and 338 day. Recall that the nit-SBR feed was a biomass free synthetic medium with no exogenous organic carbon. Under these conditions, and using 0.45 d^{-1} for the heterotropic decay coefficient (Henze et al. 2000), the active heterotroph fraction was estimated to be approximately 10% which is consistent with qPCR results. .

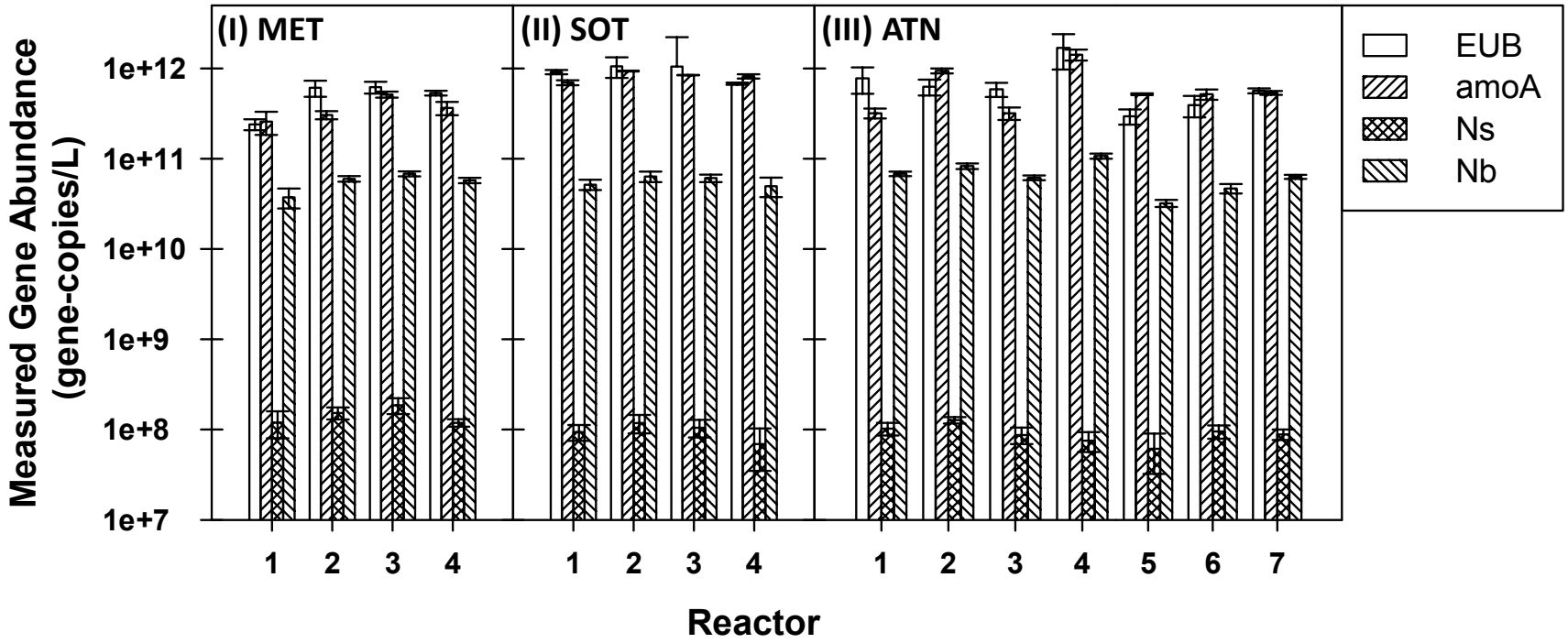

Figure VII-1: Abundance of gene copies from qPCR measurements for EUB, amoA, Ns and Nb from MET NIT-EXPT (panel I), SOT NIT-EXPT (panel II) and ATN NIT-EXPT and ATN NOX-EXPT (panel III).

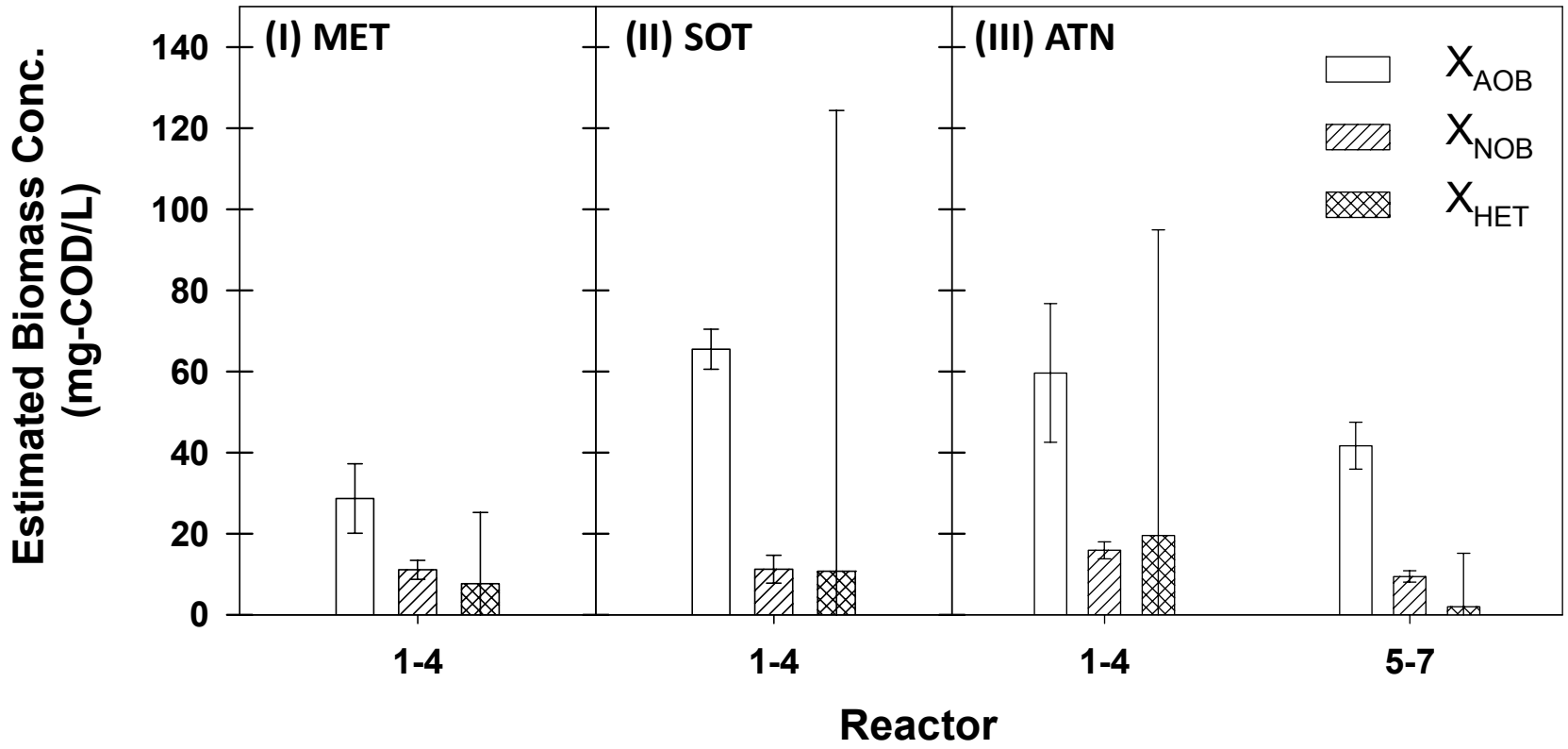

Figure VII-2: Estimated biomass concentrations for XAOB , XNOB and XHET utilizing gene abundance measurements from qPCR from MET NIT-EXPT (panel I), SOT NIT-EXPT (panel II) and ATN NIT-EXPT and ATN NOX-EXPT (panel III).

VII.3.2 Beta Blocker Degradation

Measured concentrations of ATN, MET and SOT during the first 12 hr of NIT-EXPTs are shown in Figure VII-3. Note that the MET experiment was terminated after 12 hr, while the duration of the ATN and SOT experiments was 25 hr. Results indicate that neither MET or SOT were attenuated in the presence of this nitrification enrichment community (Figure VII-3, panels I and II). In contrast, ATN was attenuated by approximately 30% in the experimental reactors (Reactors 3 & 4) before S_{NH} fell below 0.2 mg-N/L around 4 hr (panel III). Interestingly, ATN was further attenuated by approximately 50% after nitrification was complete (i.e., ~80% of the ATN was attenuated after 25 hr) (Figure VII-4). In comparison, the extent of ATN attenuation in the nitrification inhibition control (Reactor 2) at the completion of the 25 h experiment reactor is 30% (Figure VII-4). Attenuation of ATN during nitrite oxidation (NOX-EXPTs) was also explored in an attempt to elucidate the biochemical processes in nitrification that may contribute to the observed attenuation. Results from this NOX-EXPT (Reactors 6 and 7 in Panel III, Figure VII-3) indicate that ATN attenuation was approximately 30% over the 25 hour experimental duration.

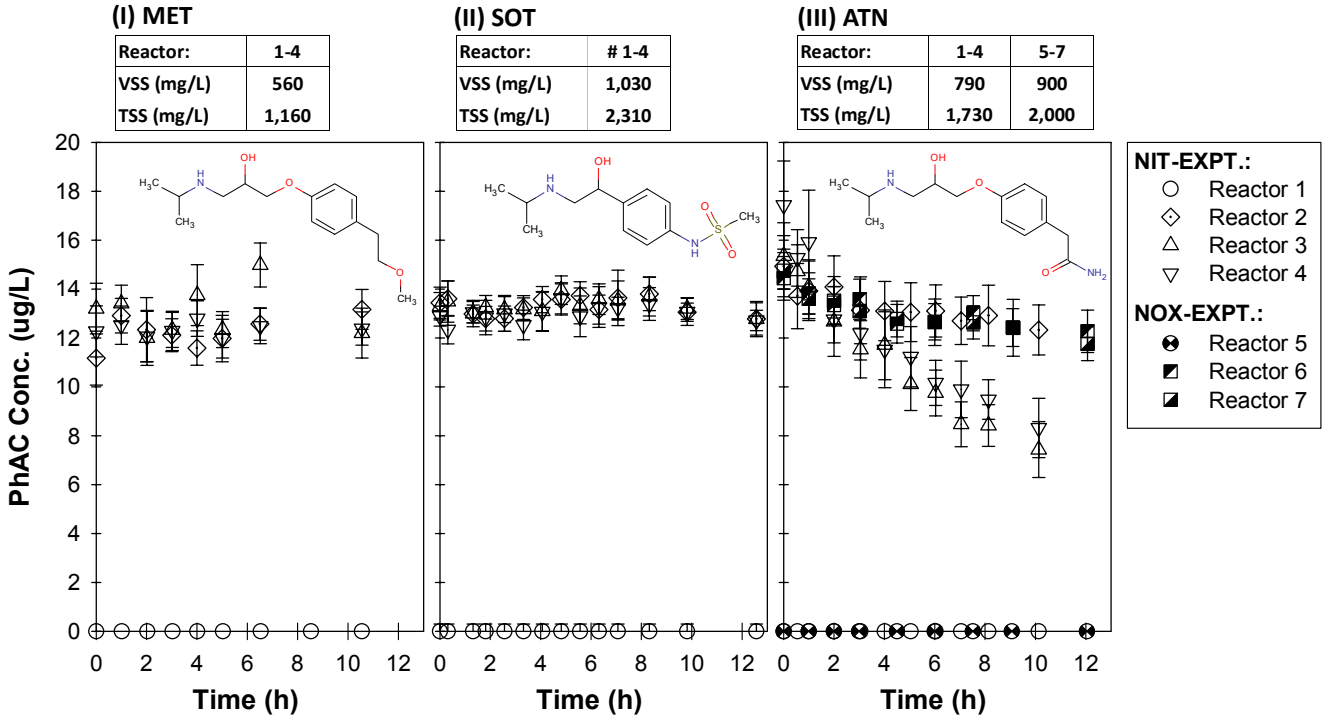

Figure VII-3: PhAC concentration in batch experiments conducted to independently evaluate the degradation of the selected beta blockers during nitrification processes. For each PhAC results are shown from each of the four NIT-EXPT reactors a nitrification control (Reactor 1), a nitrification inhibition control (Reactor 2), and replicate experimental reactors (Reactors 3 and 4). For ATN, data are also shown from the NOX-EXPT for a nitrite-oxidation control (Reactor 5) and replicate experimental reactors (Reactors 6 and 7). Note that data for each experiment are shown up to 12 hours to provide a consistent comparison. Complete time course PhAC data with data for nitrogen species for each PhAC experiment is provided in Figure VII-5 (MET), Figure VII-6 (SOT), Figure VII-7 (ATN, NIT-EXPT) and Figure VII-8 (ATN,NOX-EXPT).

Pseudo first order model fits (solids lines)

$k_{BIO\text{-}ATN,NIT}$	$L \cdot g\text{-}COD^{-1} \cdot d^{-1}$	1.7 ± 0.2
$k_{BIO\text{-}ATN,NIT\text{-}INH}$	$L \cdot g\text{-}COD^{-1} \cdot d^{-1}$	0.4 ± 0.1

Cometabolic process -based model fits (dashed lines)

$T_{ATN\text{-}AOB}$	$L \cdot g\text{-}COD^{-1}$	71.5 ± 22.7
$k_{ATN\text{-}AOB}$	$L \cdot g\text{-}COD^{-1} \cdot d^{-1}$	16.1 ± 5.6
$\alpha_{ATN\text{-}HET}$	$L \cdot g\text{-}COD^{-1} \cdot d^{-1}$	22.3 ± 4.4
$\Delta SSE_{Reactor3\&4}$= -9.1	$\Delta AIC_{C,Reactor3\&4}$= -19.5	

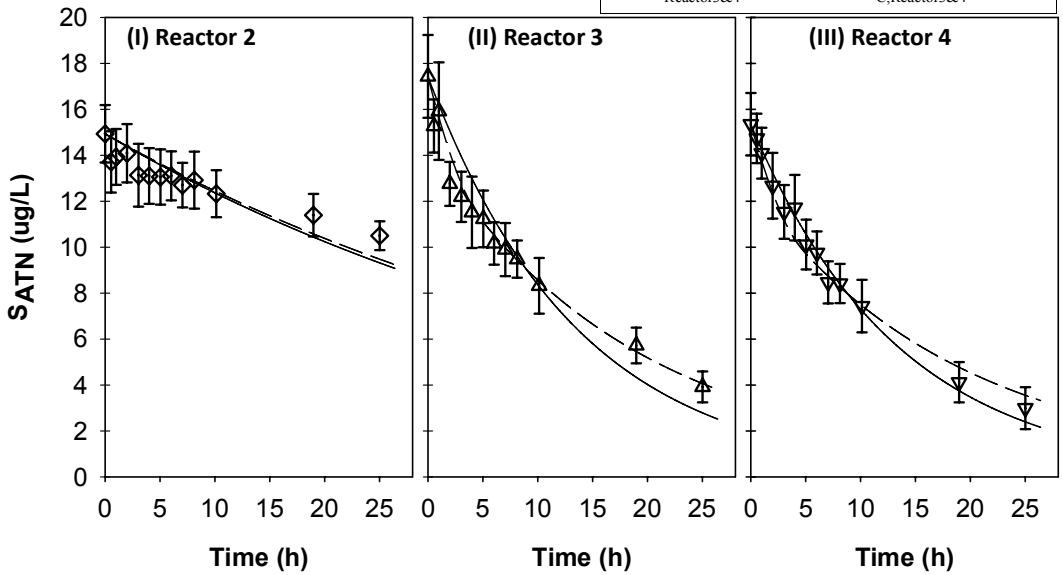

Figure VII-4: ATN concentration in batch nitrification experiments. Data from experimental replicates (Reactors 3 and 4, middle and right, respectively) and nitrification inhibition control (Reactor 2, left) are shown with model fits using the pseudo-first-order (PFO) model (solid line) and the cometabolic process-based (CPB) model (dashed line). ATN biodegradation parameters for each model are provided in the overlying tables. Also shown is the improvement in model performance for the experimental reactors when using CPB (as described by decreases in SSE and AICc).

The lack of quantifiable attenuation in the SOT and MET NIT-EXPTs is consistent with measured distribution coefficients for all three beta blockers (SOT, MET, and ATN) that indicate sorption has a negligible influence on attenuation (Maurer et al., 2007; Sathyamoorthy and Ramsburg, 2013). Thus, ATN attenuation was attributed to biological activity even in the absence of direct evidence (i.e., observation of degradation products). Taken in concert these results suggest: (i) ammonia oxidation may have a role in supporting ATN degradation, and (ii) the biodegradability of PhACs from the same therapeutic family or having similar chemical structures by nitrifying bacteria may be substantially different.

ATN biodegradation was modeled using the pseudo-first-order (PFO) approach (see Equation V-13, Section V.3.2.1., Chapter V) in order to compare biodegradation rates with literature values where the PFO approach is often used for microconstituent degradation (Urase and Kikuta, 2005; Joss et al., 2006; Fernandez-Fontaina et al., 2012; Helbling et al., 2012). The biomass normalized, pseudo-first-order biodegradation rate coefficient for ATN degradation in Reactors 3 and 4, $k_{BIO\text{-}ATN,NIT}$ is 2.39 ± 0.21 $L \cdot g\text{-}VSS^{-1} \cdot d^{-1}$ (1.68 ± 0.15 $L \cdot g\text{-}COD^{-1} \cdot d^{-1}$) (Figure VII-4). The analogous coefficient under nitrification inhibition conditions in Reactor 2 ($k_{BIO\text{-}ATN,NIT\text{-}INH}$) is 0.56 ± 0.10 $L \cdot g\text{-}VSS^{-1} \cdot d^{-1}$ (0.40 ± 0.07 $L \cdot g\text{-}COD^{-1} \cdot d^{-1}$). The biodegradation rate of ATN when nitrification is not inhibited is therefore approximately four times greater than when nitrification is inhibited by ATU. This is consistent with the hypothesis that the activity of nitrifying bacteria controls the degradation of ATN in this nitrification enrichment community. Although such a formulation is convenient, it was of limited value when comparing systems with different design or operating conditions. The principal shortfall of this approach is that it does not link PhAC degradation to a specific consortium (e.g., AOB,

NOB, HET) or specific processes occurring within the mixed community (e.g., ammonia oxidation). It is important to note here that the highest nitrite concentration observed was less than 5 mg-N/L, which suggests nitration reactions are not relevant in the batch experiments described herein (Gaulke et al., 2008). No production of either nitrite or nitrate was observed in the nitrification inhibition controls (Reactors 2) which indicates the utility of the ATU addition. The biomass normalized pseudo-first-order order degradation rate coefficient for ATN during nitrite oxidation (Reactors 6 & 7, in the absence of ammonia oxidation) is 0.39 ± 0.05 $L \cdot g\text{-}VSS^{-1} \cdot d^{-1}$. This is less than rate coefficient obtained from the nitrification experiments (2.39 ± 0.21 $L \cdot g\text{-}VSS^{-1} \cdot d^{-1}$, Reactors 3 & 4) and consistent with that observed when nitrification was inhibited with ATU (0.56 ± 0.10 $L \cdot g\text{-}VSS^{-1} \cdot d^{-1}$, Reactor 2).

The rate coefficient for ATN degradation during nitrification (Reactors 3 and 4), when converted to a suspended solids normalized value (1.09 ± 0.10 $L \cdot g\text{-}SS^{-1} \cdot d^{-1}$) is comparable to those reported by (Maurer et al., 2007) (0.98 $L \cdot g\text{-}SS\text{-}^{1} \cdot d^{-1}$ in batch experiments using biomass from an MBR operated at 20 day SRT) and Wick et al. (2009) (1.90 and 1.10 $L \cdot g\text{-}SS^{-1} \cdot d^{-1}$ in batch experiments using sludge from a suspended growth system operated at 18 day SRT). The similarity between these reported rate coefficients is noteworthy considering that the comparison includes experiments conducted with biomass from a nitrification enrichment (SBR operated at > 100 d SRT) containing a relatively low fraction of heterotrophs (~20%), and biomass from WWTPs operating at 18 – 20 d SRT. Neither Maurer et al. nor Wick et al. however report concentrations of nitrogen species, or attempt to link PhAC biodegradation to specific biological processes. Interestingly, and in contrast to the results presented herein, both Maurer et al. and Wick et al. reported attenuation of MET (0.82 $L \cdot g\text{-}SS^{-1} \cdot d^{-1}$, and 0.38 $L \cdot g\text{-}SS^{-1} \cdot d^{-1}$,

respectively) and SOT (0.41 $L \cdot g\text{-}SS^{-1} \cdot d^{-1}$ and 0.42 $L \cdot g\text{-}SS^{-1} \cdot d^{-1}$, respectively) as resulting from nitrification processes.

A preliminary assessment of the ATN biodegradation rate during and after nitrification suggests that two distinct processes may be occurring - a faster rate occurring during ammonia oxidation and slower rate occurring over the entire duration of the experiment. This hypothesis was explored by extending the pseudo-first order model to dual rate models as described below.

First, the pseudo-first-order (PFO) model was modified to a dual rate pseudo-first-order (DRPFO) model (Chapra, 2008) using a fast biodegradation rate related to AOB activity ($k_{BIO,FAST}$) and a slower process primarily due to HET activity ($k_{BIO,SLOW}$) (Equation VII-1).

$$\frac{dS_{PhAC}}{dt} = -(k_{BIO,FAST} + k_{BIO,SLOW}) X_{TOT} S_{PhAC} \qquad \text{(VII-1)}$$

Mathematically, this would be similar to the original one parameter fit of a pseudo-first-order degradation rate coefficient if it were not for the fact that the influence of the heterotrophs can be independently assessed using data from Reactor 2 (nitrification inhibition control). Results of this approach suggest $k_{BIO,FAST}$ is 1.83 ± 0.21 $L \cdot g\text{-}VSS^{-1} \cdot d^{-1}$ (1.29 ± 0.15 $L \cdot g\text{-}COD^{-1} \cdot d^{-1}$) and $k_{BIO,SLOW.}$ is 0.56 ± 0.10 $L \cdot g\text{-}VSS^{-1} \cdot d^{-1}$ (0.39 ± 0.07 $L \cdot g\text{-}COD^{-1} \cdot d^{-1}$). The statistically significant difference in these rate coefficients ($p < 0.05$) provides another line of evidence suggesting that ATN biodegradation in this enrichment is linked to ammonia oxidation.

A further modification of the PFO model tested herein incorporates biomass specific biodegradation rate coefficients for AOB and HET (Equation VII-2) to produce a population-specific, dual rate pseudo-first order (PS-DRPFO) model. Here $k_{BIO,HET}$ was fit

to the ATN degradation data obtained in the absence of AOB activity (i.e., Reactor 2). X_{AOB} was obtained by fitting nitrogen data from Reactor 1 and X_{HET} was determined using the estimated X_{AOB} value and qPCR data as described in the Materials and Methods Chapter.

$$\frac{dS_{PhAC}}{dt} = -(k_{BIO,AOB}X_{AOB} + k_{BIO,HET}X_{HET})S_{PhAC} \quad \text{(VII-2)}$$

Results of this analysis suggest that $k_{BIO,AOB}$ is 29.5 ± 3.4 $L{\cdot}g\text{-}COD^{-1}{\cdot}d^{-1}$ and $k_{BIO,HET}$ is 12.8 ± 2.4 $L{\cdot}g\text{-}COD^{-1}{\cdot}d^{-1}$. Here the rate coefficients are reported normalized to biomass COD consistent with the ASM modeling framework. The statistically significant difference in these biomass specific rate coefficients ($p < 0.05$) provides further evidence that ATN biodegradation in this enrichment is linked to AOB activity. A review of the literature suggests that this is the first such implementation of biomass specific PFO biodegradation rate coefficients for PhACs in mixed culture systems. A summary of the estimated biodegradation rate coefficients from each of the PFO models is provided in Table VII-2 along with biodegradation parameters from the cometabolic process based (CPB) model (see results in Section VII.2.3, below).

Table VII-2: ATN biodegradation parameters from the models evaluated in this research

Pseudo first order (PFO) model	$k_{BIO\text{-}ATN,NIT}$	1.68 ± 0.15	$L.g\text{-}COD^{-1}.d^{-1}$
	$k_{BIO\text{-}ATN,NIT\text{-}INH}$	0.40 ± 0.07	$L.g\text{-}COD^{-1}.d^{-1}$
Dual rate, psuedo-first-order (DRPFO) model	$k_{BIO,FAST}$	1.29 ± 0.15	$L.g\text{-}COD^{-1}.d^{-1}$
	$k_{BIO,SLOW}$	0.39 ± 0.07	$L.g\text{-}COD^{-1}.d^{-1}$
Population-specific, dual ratepseudo-first order (PS-DRPFO) model	$k_{BIO,AOB}$	29.5 ± 3.4	$L.g\text{-}COD^{-1}.d^{-1}$
	$k_{BIO,HET}$	12.8 ± 2.4	$L.g\text{-}COD^{-1}.d^{-1}$
Cometabolic process based (CPB) model	$T_{ATN\text{-}AOB}$	71.5 ± 22.7	$L.g\text{-}COD^{-1}$
	$k_{ATN\text{-}AOB}$	16.1 ± 5.6	$L.g\text{-}COD^{-1}.d^{-1}$
	$\alpha_{ATN\text{-}HET}$	22.3 ± 4.4	$L.g\text{-}COD^{-1}.d^{-1}$

The performance of the models employed here is assessed using three goodness of fit metrics: sum of square errors (SSE), Nash-Sutcliffe Efficiency (NSE) (defined by Equation V-12 in Section V.3.1.3, Chapter V) and the Akaike Information Criterion (AIC) (Akaike, 1973 and 1974).

The Akaike Information Criterion (AIC) ranks the ability of models to explain a particular data set incorporating goodness of fit, model precision and a penalty adding fitting parameters (Ludden et al., 1994; Poeter and Anderson, 2005; Saffron et al., 2006; Hemsi et al., 2010). AIC values are not bounded and use of this metric is strictly relative (i.e., there is not absolute limit to indicate a "good" AIC). For a given set of models, the model producing the lowest AIC is most effective in explaining that particular data set. Given the sample size of the data sets, the small-sample corrected AIC (Sugiura, 1978; Hurvich and Tsai, 1991; Burnham and Anderson, 2002) (AIC_C, Equation VII-3) is used herein.

$$AIC_C = \left[n \cdot \ln\left(\frac{SSE}{n} \right) + 2K \right] + \frac{2K(K+1)}{(n-K-1)} \qquad \text{(VII-3)}$$

Here n is the sample size (12), K is the number of estimated model parameters which includes the number of fitting parameters (P) and one model variance parameter (i.e., K = P+1).

Shown in Table VII-3 are summaries of SSE, NSE and AIC_C for the experimental reactors (Reactors 3 and 4) and the inhibition control reactor (Reactor 2). Extended PFO models (i.e., DRPFO and PS-DRPFO) offer little to no advantage relative to the PFO model based on the comparisons of SSE and NSE. Inspection of the AIC_C values for these models suggests that inclusion of the second rate parameter is not warranted.

Table VII-3: Goodness of fit statistics for ATN biodegradation models when fitting data from the nitrification inhibition control (Reactor 2) and nitrification experiments (Reactors 3 & 4)

Metric	Model	Reactor 2	Reactors 3 & 4 combined data
Sum of Square Errors (SSE)	PFO	4.68	14.07
	DRPFO	4.68	14.07
	PS-DRPFO	4.68	14.12
	CPB	4.68	4.95
Nash Sutcliffe Efficiency (NSE)	PFO	0.84	0.94
	DRPFO	0.84	0.94
	PS-DRPFO	0.84	0.94
	CPB	0.84	0.97
Small sample corrected Akaike Information Criteria (AIC_C)	PFO	-5.97	-8.24
	DRPFO	-5.97	-5.61
	PS-DRPFO	-5.97	-5.52
	CPB	-5.97	-27.76

It is important to recognize the extended pseudo first order models (Equations 2 and 3) assume that AOB remain active over the duration of the experiment. As noted above, this may be inappropriate (S_{NH} is < 0.2 mg-N/L after 4 hr) and highlights the need for a process based model.

VII.3.3. Cometabolic Process-Based Model

VII.3.3.1. Application of the Cometabolic Process Based Model

Data from Reactor 1 in each experiment were used to estimate the initial AOB and NOB concentrations ($X_{AOB,t0}$ and $X_{NOB,t0}$). Model fit values of $X_{AOB,t0}$ and $X_{NOB,t0}$ (SI: Table S-6) appear to fall within the generally accepted level of accuracy for biomass concentrations estimated using qPCR (i.e., up to ± 100%) (Harms et al., 2003; Ahn et al., 2008). Complete time course data for S_{NH}, S_{NO2}, S_{NO3} and S_{PhAC} with model simulations from Reactors 1 – 4 for MET, SOT and ATN are shown in Figure VII-5, Figure VII-6 and Figure VII-7, respectively. Note that for each beta blocker only the nitrification control data sets are fit (Reactor 1 in each panel). Simulations shown for Reactors 2-4 for each PhAC are predictions using the fitted initial biomass concentration and model parameters shown in Table VII-4. Data from Reactors 5 – 7 (from the NIT-OX experiments) for ATN are shown in Figure VII-8.

Table VII-4: Model parameters used in the process model developed in this research.

Description	Variable	Unit of Measure	Literature Values (where applicable)		Selected value
			Range	Refs.	
Common					
Nitrogen fraction of biomass	i_{NBM}	(mg-N·mg-COD^{-1})	0.07	(Grady et al., 1999; Henze et al., 2000)	0.07
Biomass VSS to Biomass COD ratio	f_{CV}	(mg-COD·mg-VSS^{-1})	1.42	(Grady et al., 1999; Henze et al., 2000)	1.42
AOB kinetics and stoichiometry					
max. specific growth rate	$\mu_{max,AOB}$	(day^{-1})	0.2 – 1.6	(Munz et al., 2011)	0.50
decay rate	b_{AOB}	(day^{-1})	0.06 – 0.4	(Marsili-Libelli et al., 2001; Munz et al., 2011)	0.15
half saturation value for S_{NH}	K_{NH}	(mg-N·L^{-1})	0.14 – 2.3	(Manser et al., 2005; Chandran et al., 2008)	0.50
Ammonia-N yield	Y_{AOB}	(mg-COD·mg-N^{-1})	0.11 – 0.21	(Hiatt and Grady, 2008; Sin et al., 2008; Munz et al., 2011)	0.15
PhAC inhibition coefficient	$K_{I,PhAC-AOB}$	(μgL^{-1})	NA	NA	*fit*[(ii)]
NOB kinetics and stoichiometry					
max. specific growth rate	$\mu_{max,NOB}$	(day^{-1})	0.2 – 2.6	(Ahn et al., 2008)	0.50
decay rate	b_{NOB}	(day^{-1})	0.08-1.7	(Ahn et al., 2008; Munz et al., 2010)	0.15
half saturation value for S_{NO2}	K_{NO2}	(mg-N·L^{-1})	0.05 – 3	(Marsili-Libelli et al., 2001; Jones et al., 2007; Kampschreur et al., 2007)	0.50
Nitrite-N yield	Y_{NOB}	(mg-COD·mg-N^{-1})	0.06 – 0.10	(Sin et al., 2008)	0.09

Table VII-4: Model parameters used in the process model developed in this research.

Description	Variable	Unit of Measure	Literature Values (where applicable)		Selected
Initial Biomass Concentrations					
AOB	$X_{AOB,t0}$	(mg-COD·L^{-1})	NA	NA	*fit*[(i)]
NOB	$X_{NOB,t0}$	(mg-COD·L^{-1})	NA	NA	*fit*[(i)]
HET	$X_{HET,t0}$	(mg-COD·L^{-1})	NA	NA	*calculated*
PhAC Biodegradation					
AOB Transformation Coefficient	$T_{PhAC-AOB}$	(L·g-COD^{-1})	NA	NA	*fit*[(ii)]
AOB endogenous transformation coefficient	$k_{PhAC-AOB}$	(L·g-COD^{-1}·d^{-1})	NA	NA	*fit*[(ii)]
HET lumped biodegradation coefficient	$\alpha_{PhAC-HET}$	(L·g-COD^{-1}·d^{-1})	NA	NA	*fit*[(iii)]

Notes:

i. $X_{AOB,t0}$ and $X_{NOB,t0}$ – independent, fit using the nitrification control (Reactor 1) data
ii. $T_{PhAC-AOB}$, $k_{PhAC-AOB}$ and $K_{I,PhAC-AOB}$ – independent, fit using the nitrification experiments (Reactor 3 & 4) data
iii. $\alpha_{PhAC-HET}$ – independent, fit using the nitrification inhibition control (Reactor 2) data

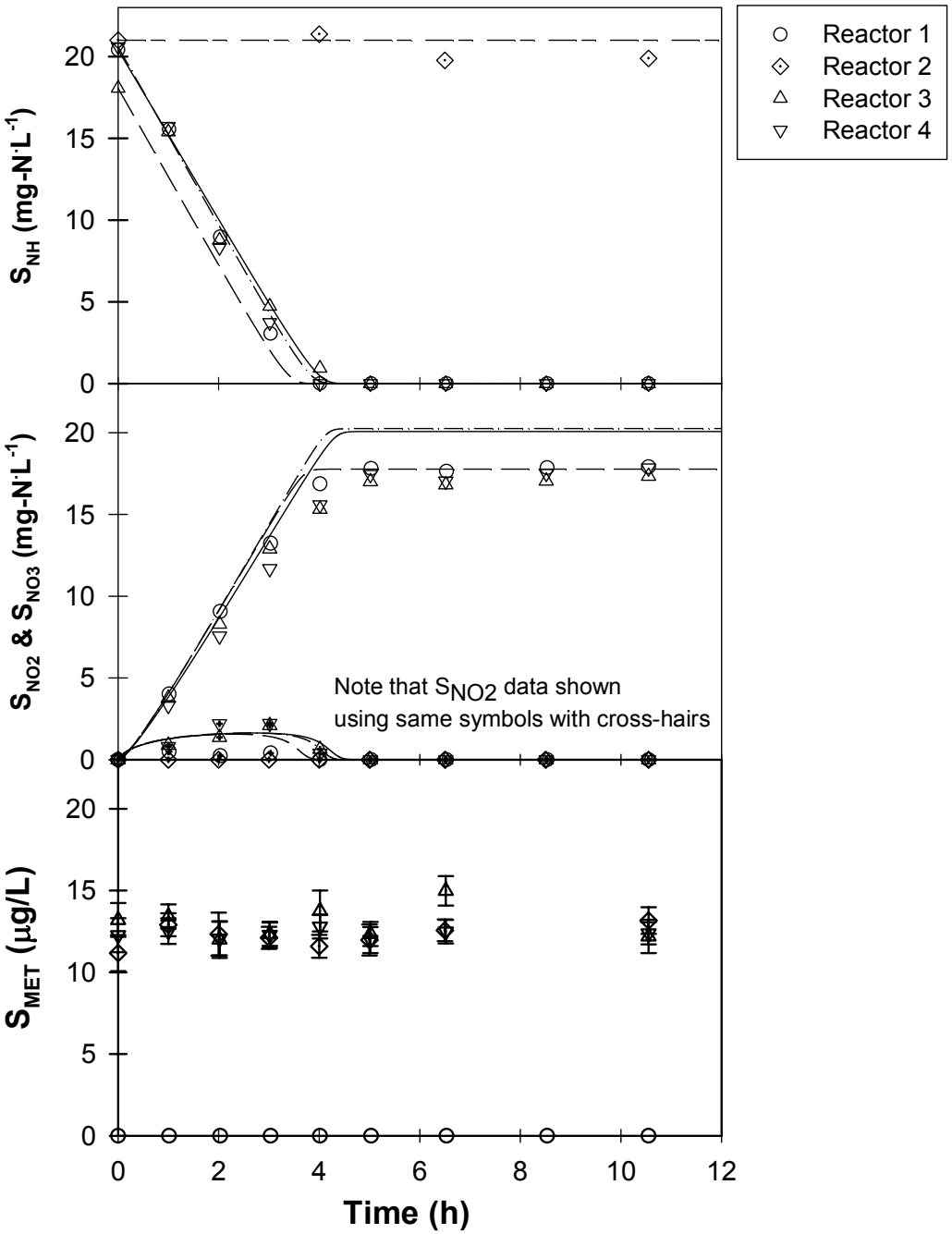

Figure VII-5: Observed and modeled concentrations of ammonia (top panel), nitrite and nitrate (middle panel) and MET (bottom panel) for nitrification batch experiments conducted with MET. Results are shown from each of the four NIT-EXPT reactors a nitrification control (Reactor 1), a nitrification inhibition control (Reactor 2), and replicate experimental reactors (Reactors 3 and 4).

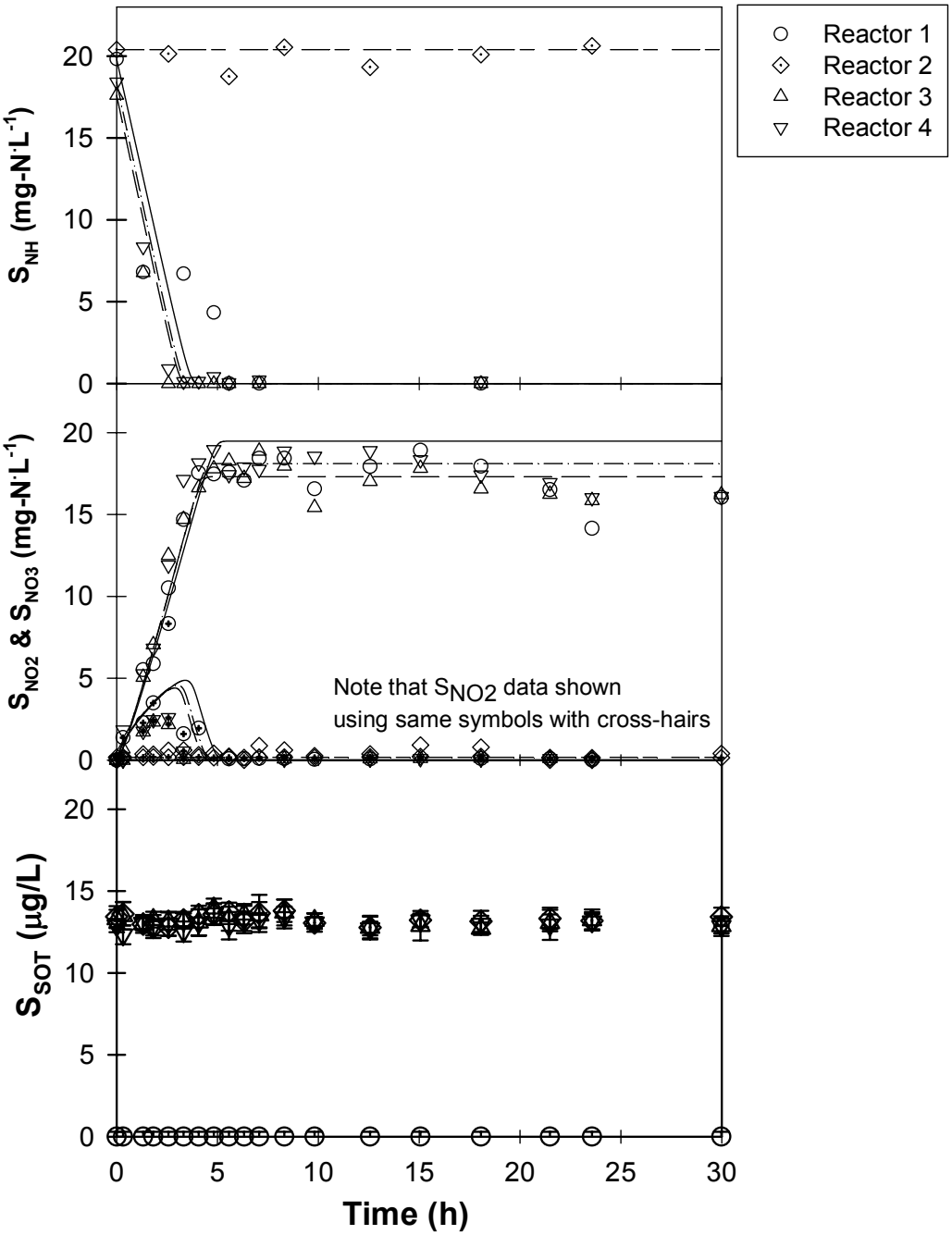

Figure VII-6: Observed and modeled concentrations of ammonia (top panel), nitrite and nitrate (middle panel) and SOT (bottom panel) for nitrification batch experiments conducted with SOT. Results are shown from each of the four NIT-EXPT reactors a nitrification control (Reactor 1), a nitrification inhibition control (Reactor 2), and replicate experimental reactors (Reactors 3 and 4).

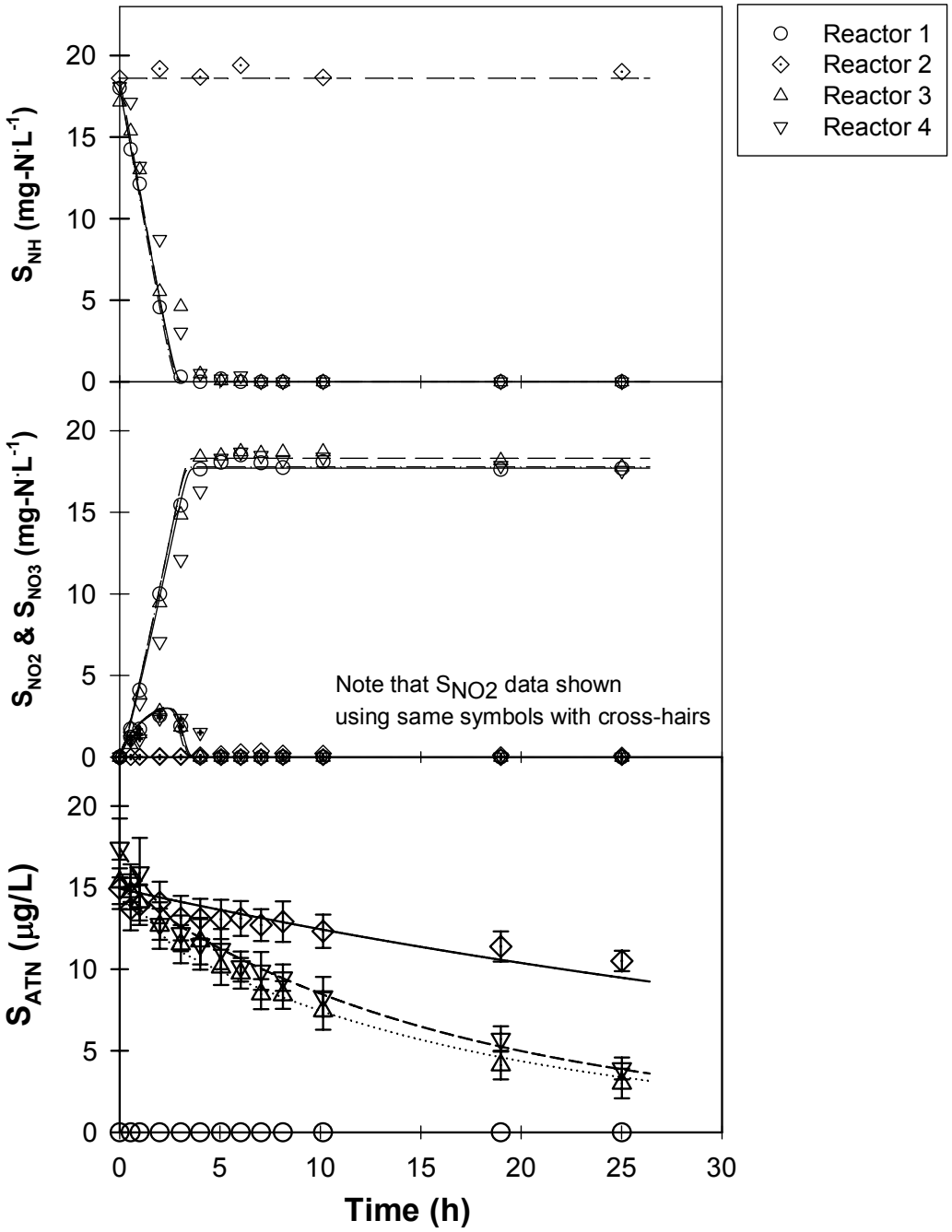

Figure VII-7: Observed and modeled concentrations of ammonia (top panel), nitrite and nitrate (middle panel) and ATN (bottom panel) for nitrification batch experiments conducted with ATN. Results are shown from each of the four NIT-EXPT reactors a nitrification control (Reactor 1), a nitrification inhibition control (Reactor 2), and replicate experimental reactors (Reactors 3 and 4).

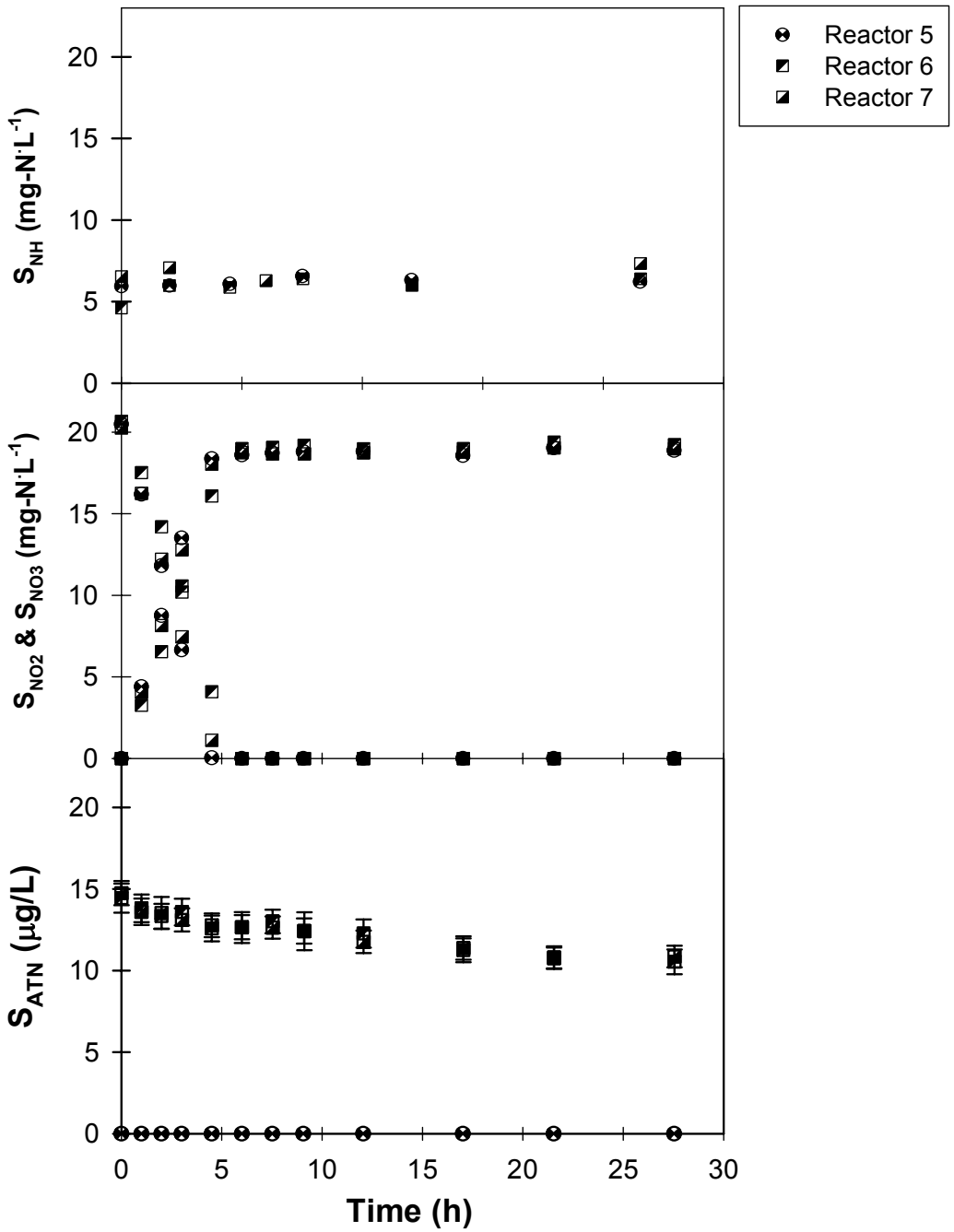

Figure VII-8: Observed and modeled concentrations of ammonia (top panel), nitrite and nitrate (middle panel) and ATN (bottom panel) for nitrite oxidation batch experiments conducted with ATN. Results are shown from each of the three NOX-EXPT reactors a nitrite oxidation control (Reactor 5), and replicate experimental reactors (Reactors 6 and 7).

S_{NH} residuals for experimental reactors containing ATN were observed to be larger at low S_{NH}, suggesting that the model may be unable to satisfactorily predict S_{NH} oxidation as S_{NH} approaches the half saturation value. This effect was not observed with MET or SOT. To explore the hypothesis that ATN exerts a competitive inhibition on AOB growth, the AOB growth process rate ($r_{G,X_{AOB}}$) was modified as shown in Equation VII-4 (Bailey and Ollis, 1986) and the nitrification data from the experimental reactors (NIT-EXPT Reactors 3 & 4) from the ATN experiment were fit by adjusting a single parameter, $K_{I,ATN\text{-}AOB}$.

$$r_{G,X_{AOB}} = \left[\mu_{MAX,AOB} \left(\frac{S_{NH}}{K_{NH}\left(1 + \frac{S_{ATN}}{K_{I,ATN-AOB}}\right) + S_{NH}} \right) \right] X_{AOB} \qquad \text{(VII-4)}$$

Application of the competitive inhibition model significantly improved model performance when $K_{I,ATN\text{-}AOB}$ = 1.84 ± 0.39 μg/L (Figure VII-9, SSE reduced to 39% and 15% and AIC_C reduced to 37% and 79% of the base case values for Reactors 3 & 4, respectively. These data and simulations strongly suggest that ATN may competitively inhibit the ammonia oxidation process, which is consistent with the hypothesis of cometabolic degradation due to AMO. That notwithstanding, the possibility that degradation products contribute to the observed inhibition cannot be eliminated even though none were observed in the batch experiments. A review of the available peer-reviewed literature suggests that this is the first report of possible PhAC inhibition of ammonia oxidation.

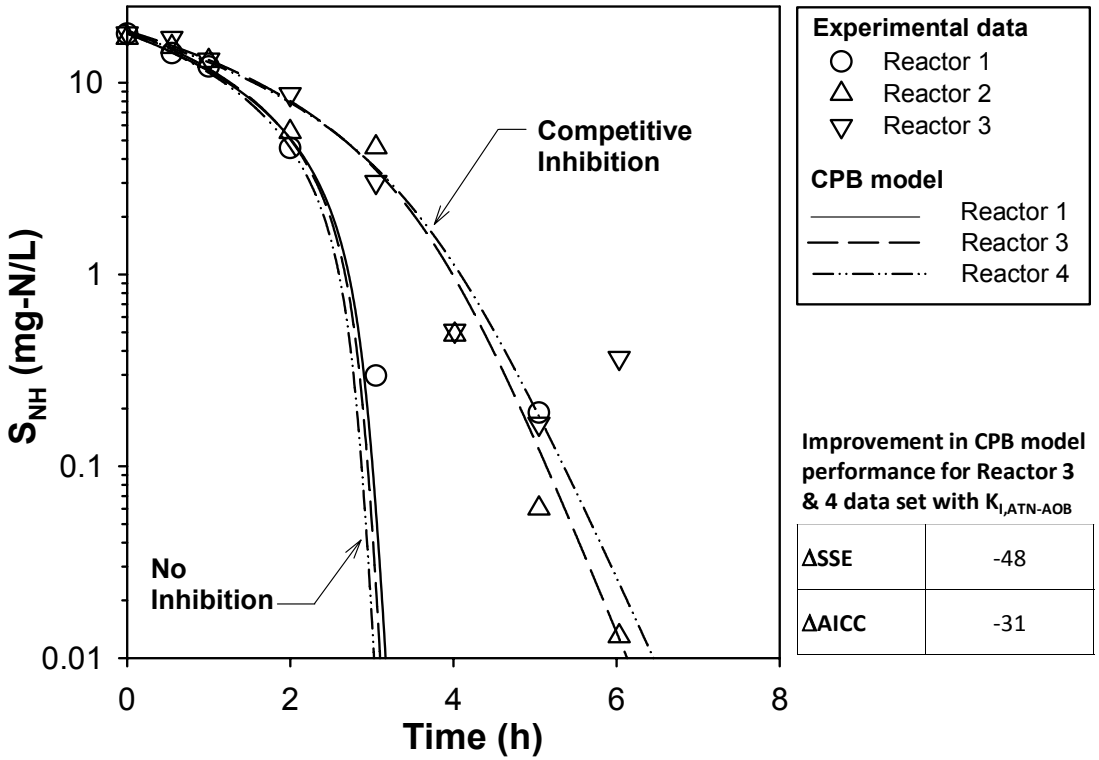

Figure VII-9: Observed and modeled concentration of ammonia during the ATN experiment. Data are shown for a nitrification control reactor (Reactor 1) and experimental replicates (Reactors 3 & 4). Note that minor differences between the simulations for Reactors 3 & 4 (in both the inhibition or no inhibition simulations) entirely result from subtle differences in the measured initial SNH concentrations in each reactor. Simulations shown include the two-step nitrification model with and without competitive inhibition. The competitive inhibition is described by Equation 5 with $K_{I,ATN-AOB}$ = 1.84 ± 0.39 μg/L. The combined improvement in the fit for data from Reactors 3 and 4 when using the competitive inhibition modelis shown by the decreases in SSE and AICC from those obtained when the data are modeled without competitive inhibition

With the ammonia oxidation model in place, the transformation capacity for ATN can be assessed. To accomplish this, the process model was first fit to the nitrification inhibition data (Reactor 2) to determine that $\alpha_{ATN\text{-}HET} = 22.3 \pm 4.4$ L·g-COD^{-1}·d^{-1}. Best fit values of $T_{ATN\text{-}AOB}$ and $k_{ATN\text{-}AOB}$ were subsequently determined using the replicate experimental reactors (Reactors 3 & 4) to be 71.5 ± 22.7 L·g-COD^{-1} and 16.1 ± 5.6 L·g-COD^{-1}·d^{-1}, respectively. Comparison of the values of $T_{ATN\text{-}AOB}$ or $k_{ATN\text{-}AOB}$ to similarly estimated values for other PhACs is not currently possible due to the nearly universal practice of modeling PhAC attenuation using a single, pseudo-first order reaction rate coefficient. Note, however, that the performance of cometabolic process rate model is markedly greater than any pseudo first order approach (see goodness of fit metrics in Table VII-3) and illustrates the merit of linking PhAC degradation to specific biochemical processes. Since this is the first known cometabolic modeling of PhAC degradation the results for ATN are compared with reported cometabolic biodegradation of conventional organic pollutants by AOB in axenic or mixed nitrifying communities (Ely et al., 1997; Kocamemi and Cecen, 2005 and 2010b and a). It is, however, important note here that the nomenclature within the cometabolic literature is quite diverse as a result of: (i) differences in bases for normalization (e.g., biomass normalized vs. growth substrate normalized), and, more importantly, (ii) similarity in terminology used to describe different mechanisms (e.g., transformation capacity is used to describe degradation in the presence and absence of growth). This makes difficult the direct comparison of measured transformation coefficients from this research ($T_{ATN\text{-}AOB}$ and $k_{ATN\text{-}AOB}$) to previous studies.

One study that is conducive to comparison is that of Kocamemi and Cecen (2010a) related to the cometabolic biodegradation of TCE by AOB in a mixed biomass

community. Kocamemi and Cecen (2010a) present data related to the cometabolism of TCE by nitrifying organisms. In order to compare the cometabolic parameters with those produced in this research, Figure 1 in Kocamemi and Cecen (2010a) which presents data for multiple initial concentrations of TCE was reexamined. The plot is shown on a theoretical basis in Figure VII-10.

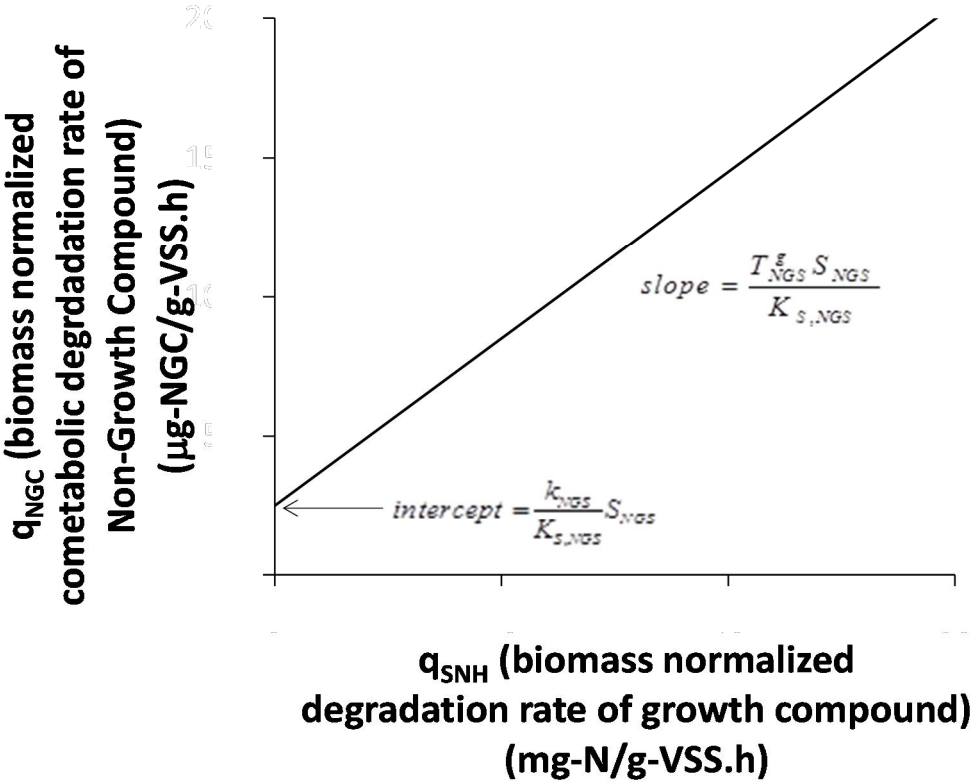

Figure VII-10: Theoretical relationship between biomass normalized degradation rate of growth compound and cometabolic degradation rate of non-growth compound.

Starting with Equation VII-5 (see Cometabolic Process Model Development in the Materials and Methods chapter for details related to derivation of Equation VII-5) for any non-growth substrate (NGS),

$$-\frac{dS_{PhAC}}{dt}=\left(\frac{T_{PhAC}^{g}}{Y_{AOB}K_{S,PhAC}}\mu_{AOB}+\frac{k_{PhAC-AOB}}{K_{S,PhAC}}\right)X_{AOB}S_{PhAC} \quad \text{(VII-5)}$$

and recognizing: $$\frac{\mu_{AOB}}{Y_{AOB}}=q_{SNH}$$ in Figure VII-10 (VII-6)

and $$\frac{1}{X_{AOB}}\left(-\frac{dS_{NGS}}{dt}\right)=q_{NGC}$$ in Figure VII-10 (VII-7)

Equation 6 can therefore be rewritten as shown in Equation 10:

$$q_{NGS}=\left(\frac{T_{NGS}^{g}}{K_{S,NGS}}q_{SNH}+\frac{k_{NGS}}{K_{S,NGS}}\right)S_{NGS} \quad \text{(VII-8)}$$

Inspection of Equation 9 indicates that a plot of q_{NGS} versus q_{SNH} at a fixed S_{NGS} produces a straight line with a slope = $\frac{T_{NGS}^{g}S_{NGS}}{K_{S,NGS}}$ and intercept = $\frac{k_{NGS}}{K_{S,NGS}}S_{NGS}$ assuming $K_{s,c} >> S_{NGS}$. Thus, the analysis of the Kocamemi and Cecen (2010a) data set is restricted to initial concentrations of TCE that were below 350 μg/L The growth-related transformation coefficient ($T_{NGS\text{-}AOB}$) used in the research described herein can be obtained from the slope using Equation VII-9:

$$\frac{slope}{S_{NGS}Y_{AOB}}=\frac{T_{NGS}^{g}}{Y_{AOB}\cdot K_{S,NGS}}=T_{NGS-AOB} \quad \text{(VII-9)}$$

The cometabolic biodegradation rate under endogenous (i.e., non-growth conditions) can be estimated by Equation VII-10:

$$\frac{intercept}{S_{NGS}K_{S,NGS}} = \frac{k_{NGS}}{K_{S,NGS}} = k_{NGS-AOB} \qquad \text{(VII-10)}$$

It is important to note that there is a theoretical basis for, and evidence of, a non-zero intercept based upon cometabolic degradation when there is no growth (Ely et al., 1997). Kocamemi and Cecen (2010a) effectively assumed each line passed through the origin when they estimated transformation capacities using only the data point corresponding to the highest TCE degradation rate for each initial TCE concentration. Fitting their data to Equation 9 and applying Equations 10-11 produces the values shown in Table VII-5. Here a yield coefficient for AOB of 0.15 mg-COD.mg-N^{-1} is assumed.

Table VII-5: Evaluating the Transformation Coefficients (T and k) for cometabolic biodegradation of TCE by AOB using the data presented by Kocamemi and Cecen (2010a).

TCE conc. (μg/L)	Model fits (using Equation 9)		Cometabolic Coefficients	
	Slope (μg-TCE.mg-N-1)	Intercept (μg-TCE.g-VSS^{-1} h^{-1})	TTCE-AOB (L.g-COD-1)	kTCE-AOB (L.g-COD-1 d-1)
325	2.34 ± 0.29	57.48 ± 8.17	48 ± 6	3.0 ± 0.42
110	0.98 ± 0.26	43.46 ± 2.58	60 ± 16	6.7 ± 1.2
40	0.25 ± 0.17	25.55 ± 5.76	42 ± 29	10.8 ± 2.4
Average ± SD:			50 ± 17	6.8 ± 1.3

It is interesting to observe that the values of $T_{ATN-AOB}$ (71.5 ± 22.7 L.g-COD^{-1}) and $k_{ATN-AOB}$ (16.1 ± 5.6 L·g-COD^{-1}·d^{-1}) obtained for ATN are similar to those obtained for TCE ($T_{TCE-AOB}$ ~50 ± 17 L.g-COD^{-1} and $k_{ATN-AOB}$ ~7 ± 1 L·g-COD^{-1}·d^{-1}).

VII.3.3.2. Sensitivity Analysis using Monte Carlo Simulations

A total of 2,000 Monte Carlo (MC) simulations were conducted to evaluate the sensitivity of the fitted values of $X_{AOB,t0}$, $X_{NOB,t0}$, $\alpha_{ATN-HET}$, $T_{ATN-AOB}$, $k_{ATN-AOB}$ and $K_{I,ATN-AOB}$ on the selected values of the biokinetic parameters $\mu_{MAX,AOB}$, b_{AOB}, K_{NH}, $\mu_{MAX,NOB}$, b_{NOB} and K_{NO2}. Parameter sets were selected using a Latin hypercube sampling technique (McKay et al., 1979) from the range of literature values noted in Table VII-4. No constraints were placed on parameter combinations because there is no a priori basis to assume cross correlation between the biokinetic parameters. $X_{AOB,t0}$ and $X_{NOB,t0}$ were estimated by fitting the nitrogen species data from Reactor 1 utilizing the randomly selected set of AOB and NOB parameters in addition to those parameters not included in the sensitivity analysis process. The resulting estimates of $X_{AOB,t0}$ and $X_{NOB,t0}$ were then used to fit $\alpha_{ATN-HET}$, $T_{ATN-AOB}$, $k_{ATN-AOB}$ and $K_{I,ATN-AOB}$.

Results suggest that the range (5^{th} -95^{th} percentile values) of $T_{ATN-AOB}$ and $k_{ATN-AOB}$ are 66.3 – 73.0 $L \cdot g\text{-}COD^{-1}$ and 8.6 to 45.5 $L \cdot g\text{-}COD^{-1} \cdot d^{-1}$, respectively (see Table VII-6). $T_{ATN-AOB}$ is therefore relatively insensitive to selection of AOB growth parameters (Figure VII-11). The greater variation in $k_{ATN-AOB}$ can be explained by the role of $\mu_{MAX,AOB}$ in the model (Figure VII-12). At high values of $\mu_{MAX,AOB}$, the duration over which $T_{ATN-AOB}$ contributes to ATN degradation is shorter (i.e., shorter period for ammonia oxidation). Thus, it is hypothesized that the apparent relationship between $k_{ATN-AOB}$ and $\mu_{MAX,AOB}$ reflects the need for higher $k_{ATN-AOB}$ (at higher $\mu_{MAX,AOB}$) when fitting the experimental data. The ATN inhibition constant ($K_{I,ATN-AOB}$) varies from 1.18 to 8.86 $\mu g \cdot L^{-1}$ (recall that for the CPB model with inhibition $K_{I,ATN-AOB}$ = 1.84 ± 0.39 $\mu g \cdot L^{-1}$). The estimated range of $K_{I,ATN-AOB}$ (~4 – 33 nM) is significantly lower than inhibition coefficients reportedly exerted by chlorinated solvents in pure *N.europaea* cultures (~12 – 1,000 μM)

suggesting that the affinity of AMO for ATN may be significantly greater. Results from the MC sensitivity analysis suggest that CPB model developed in this research may hold more general utility for describing PhAC degradation, especially given the widespread usage of the ASM modeling framework in industrial WWTP process simulators (e.g., Biowin, GPSx, etc.).

Table VII-6: Summary of Results from Monte Carlo Sensitivity Analysis using the Cometabolic Process-Based Model with Ammonia Oxidation inhibition for ATN Experiment.

	X_{AOBt0} mg–COD·L^{-1}	X_{NOBt0} mg–COD·L^{-1}	$K_{I,ATN-AOB}$ µg·L^{-1}	$T_{ATN-AOB}$ L·g-COD^{-1}·	$k_{ATN-AOB}$ L·g-COD^{-1}·d^{-1}
From MC Simulations:					
5th Percentile	16.6	6.3	1.2	66.3	8.6
Median	28.7	15.0	5.2	69.7	27.8
95th Percentile	97.6	68.0	8.9	73.0	45.4
CPB model with AOB growth inhibition by ATN:	49.6 ± 0.9	29.4 ± 1.1	1.84 ± 0.39	71.5 ± 22.7	16.1 ± 5.58

Note that $\alpha_{ATN-HET}$ is fit using the ATN data from the nitrification inhibition reactor (Reactor 2) with X_{HET} constrained to the value determined using qPCR. Therefore, the value of $\alpha_{ATN-HET}$ in all 2,000 MC simulations remains constant (22.3 L·g-COD^{-1}·d^{-1}).

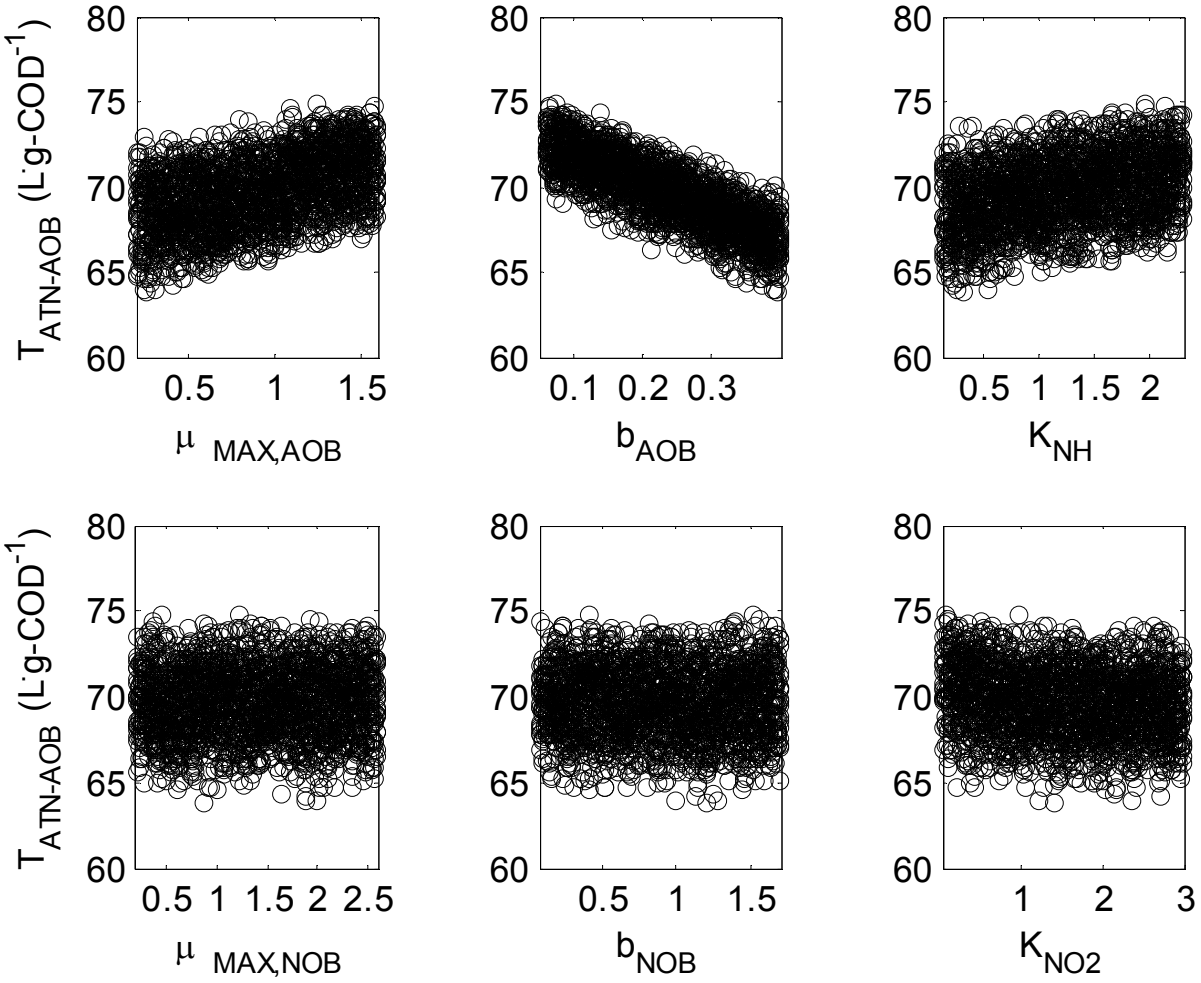

Figure VII-11: Estimated value of TATN-AOB from the 2,000 Monte Carlo simulations as a function of the AOB (top panels) and NOB (bottom panels) biokinetic parameters in each simulation.

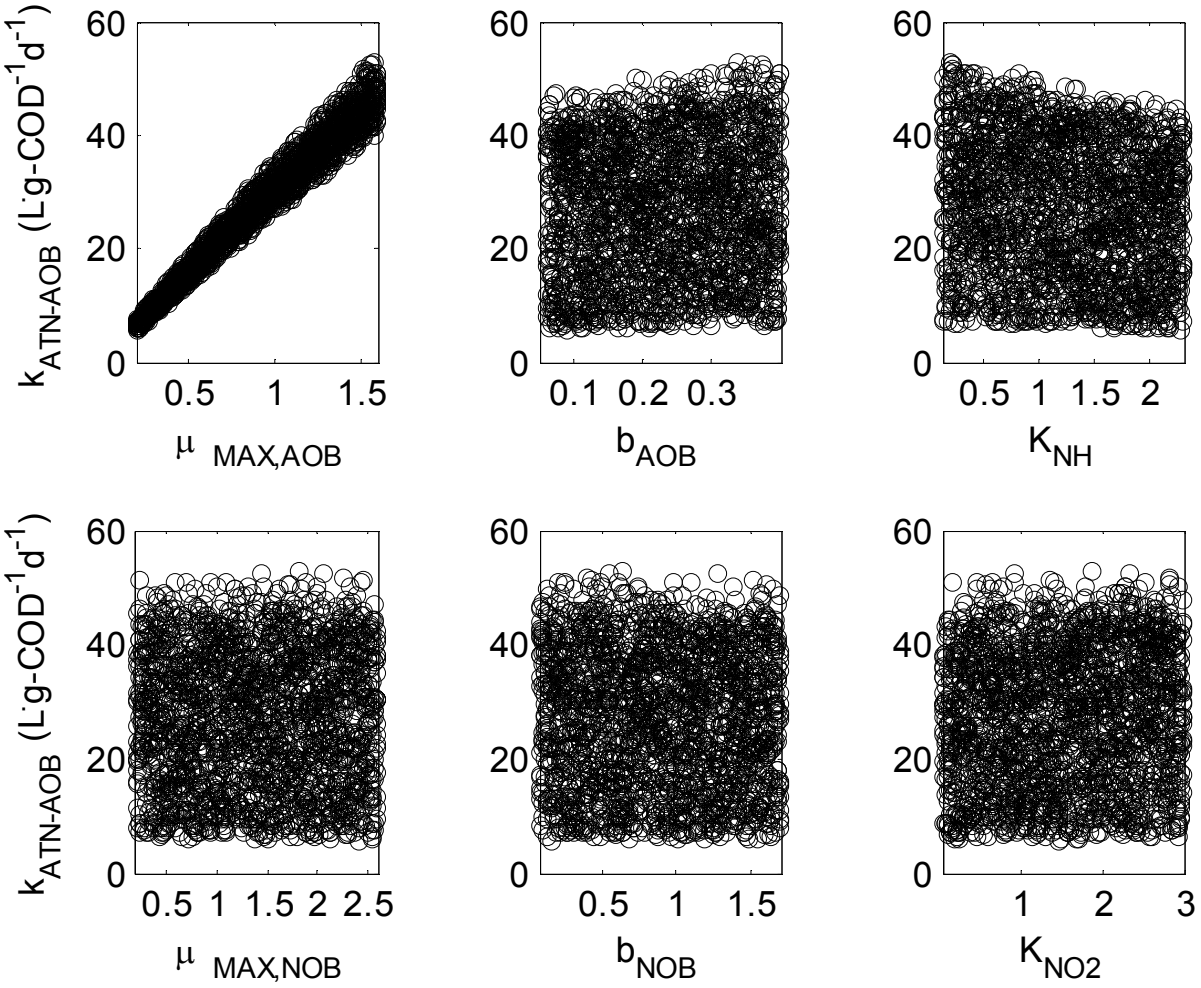

Figure VII-12: Estimated value of $k_{ATN-AOB}$ from the 2,000 Monte Carlo simulations as a function of the AOB (top panels) and NOB (bottom panels) biokinetic parameters in each simulation.

VII.3.4. Implications

Results of the experiments described herein indicate that ATN degradation resulted from ammonia oxidation. If ATN degradation rates prove to be representative of other PhACs degraded under ammonia oxidizing conditions, the role of AOB in PhAC biodegradation may be more relevant than previously estimated. It is conventionally assumed that the role of nitrifying bacteria in PhAC biodegradation is limited by the small number fraction of these organisms in the biomass at a WWTP. This research suggests that even when AOB make up 5% of the total biomass in a WWTP reactor, they contribute between 7% - 17% to the biodegradation rate of ATN (Figure VII-13, left panel). That is to say, their contribution outweighs their proportion in the biomass. This implication may be particularly relevant for partial nitrification processes (e.g., SHARON) where AOB make up greater than 10% of the biomass (Mota et al., 2005). Note here that it is assumed that PhAC degradation due to heterotrophs present in these batch experiments is more generally representative of rates of PhAC degradation by heterotrophs.

Equally important is the inhibition of AOB observed in these experiments. Where PhACs are present, even at half the inhibition coefficient value, the maximum achievable growth rates are significantly reduced (Figure VII-13, right panel). Moreover, the influence may need to be summed over multiple inhibitors given the additive nature of this type of inhibition (Bedard and Knowles, 1989) and the many microconstituents present in wastewater. Therefore, based on this study, any inhibition of AOB not only reduces the ability of WWTPs to meet stringent effluent nitrogen targets – a significant focus of modern WWTPs - but also negatively influences PhAC biodegradation due to the reduction in the growth rate of AOB (Figure VII-13, right panel).

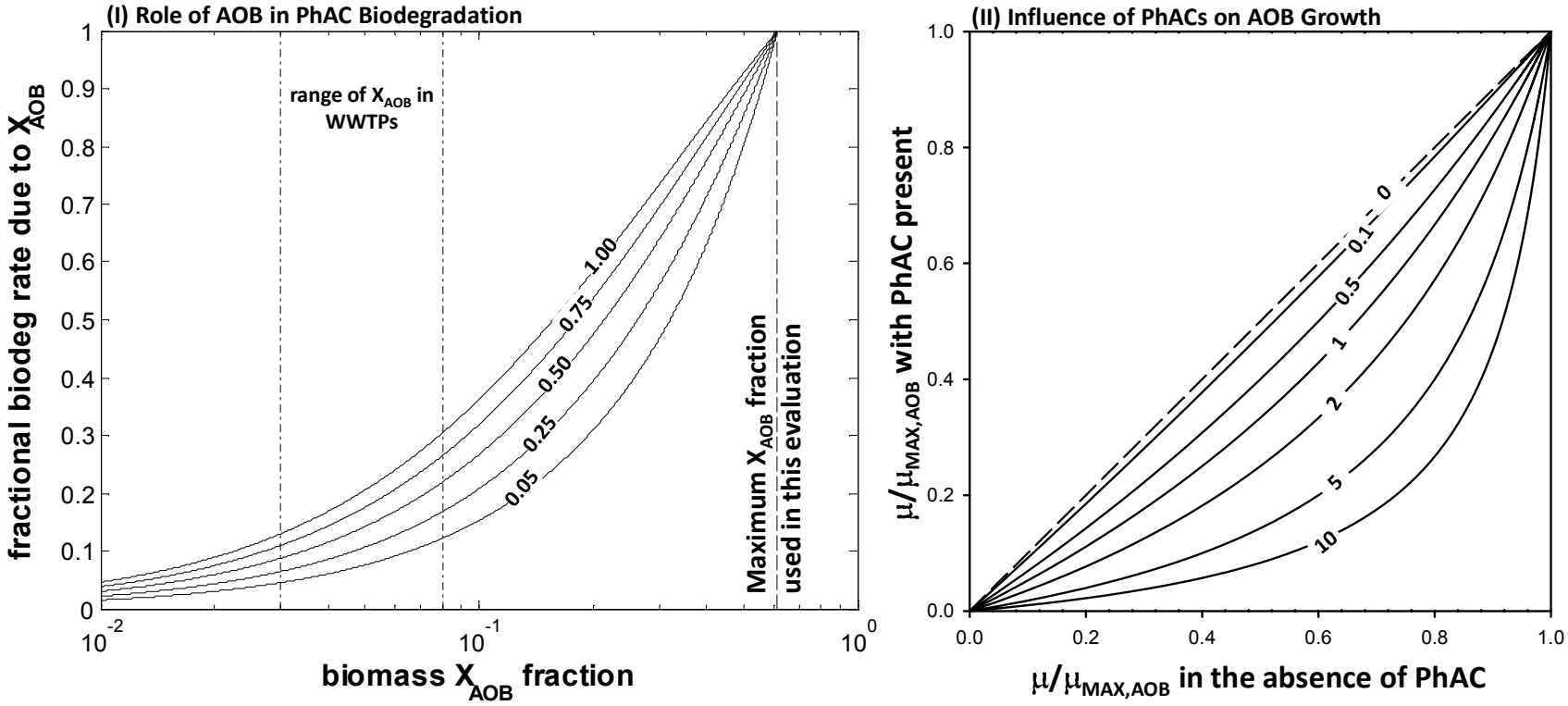

Figure VII-13: Left: Contribution of ammonia oxidizing bacteria to the rate of ATN biodegradation (i.e., fractional biodegration rate resulting due to X_{AOB}) as a function of fraction of AOB in the biomass. Each curve represents a specific condition related to ammonia concentration (and operating conditions) resulting in a given AOB growth rate relative to the maximum specific growth rate. Note that AOB are assumed to constitute approximately 60% of the nitrifying bacteria, which is therefore the maximum X_{AOB} fraction (vertical dashed line) when all the biomass is made up of nitrifying bacteria Right: Influence of PhAC inhibition on AOB growth. Each curve represents the ratio of the PhAC concentration to the inhibition coefficient ($K_{I,PhAC-AOB}$).

Chapter VIII. Uncertainty and Sensitivity Anlaysis using GLUE when Modeling Inhibition and Pharmaceutical Cometabolism during Nitrification

The results presented in this chapter are in preparation for submission to *Environmental Modeling and Software* as:

Sathyamoorthy, S., Vogel, R.M., Chapra, S.C. and Ramsburg, C.A. Uncertainty and Sensitivity Analysis using GLUE when Modeling Inhibition and Pharmaceutical Cometabolism during Nitrification

VIII.1. Introduction

The unified activated sludge model (ASM) framework, has been extensively used for wastewater treatment process modeling since its development by the International Water Association task group (Henze et al., 2000). One of the reasons for the success of the ASM framework is its adaptability - the framework allows new descriptions of processes to be easily incorporated into the model structure, albeit at the expense of simplicity. The original ASM1 model had eight processes, thirteen components and nineteen parameters (Henze et al., 1987). In comparison, a recent updated model proposed by Hiatt and Grady (2008) relies on 18 processes, 20 components and 54 parameters. While some parameters are easily transferable from one system to another, application of the ASM model typically requires a significant number of assumptions related to biokinetics (e.g., maximum specific growth rate and half saturation values) and wastewater composition (e.g., COD fractionation). Understanding the uncertainty and sensitivity related to these assumptions is critical for the meaningful application of ASM in complex dynamic biological systems (Saltelli et al., 2005; Rieger et al., 2013). Both confidence intervals (associated with uncertainties in model parameters) and prediction intervals (which further incorporate model error) are important considerations when using ASM in wastewater treatment process design. Yet, industrial process simulators, as well as many research studies using aspects of the ASM framework found in these simulators, do not adequately account for uncertainties in model inputs (Flores-Alsina et al., 2008; Belia et al., 2009). Important exceptions to this generalization include recent studies which employ Monte Carlo (MC) analyses (Flores-Alsina et al., 2008; Benedetti et al., 2011), couple MC analyses with Global Sensitivity Analyses (Flores-Alsina et al. (2012) and apply the Generalized Likelihood

Uncertainty Estimation (GLUE) technique (Mannina et al., 2010; Mannina et al., 2011; Mannina et al., 2012).

GLUE was developed over 20 years ago for hydrologic modeling problems by Beven and Binley (1992) as an extension to the Global Sensitivity Analysis method (Hornberger and Spear, 1981). It has since been extensively used in a wide range of environmental science and engineering applications including modeling fate of emerging pollutants (Vezzaro et al., 2012; Vezzaro and Mikkelsen, 2012) and wastewater treatment processes (Sin et al., 2005; Di Bella et al., 2008; Mannina et al., 2010; Mannina et al., 2012; Cosenza et al., 2013). The GLUE technique relies on the output of numerous MC simulations each conducted with input parameters selected at random from a particular distribution (uniform distributions of model input parameters are most commonly used). Model outputs are used to determine a value of the likelihood function, which is then compared to an arbitrarily selected threshold value. Simulations producing a likelihood function below the threshold are termed non-behavioral and discarded from future consideration, while those simulations producing a likelihood function greater than the threshold are termed behavioral, and retained to generate confidence intervals associated with behavioral models (Beven and Binley, 1992).

Critical to the use of GLUE is the concept of equifinality. Equifinality acknowledges that many different model parameter combinations can result in equally plausible model outcomes (Beven and Binley, 1992; Freer et al., 1996; Beven and Freer, 2001). In other words, all possible parameter sets in the posterior distribution are equally likely. The attractiveness of the GLUE technique lies in its ease of application, coupled with the claim that there is no need for assumptions related to the probability

distribution of the residuals. Furthermore, Beven and Binley (1992) suggest that use of GLUE comprehensively reflects all sources of error including that arising from: (i) model selection (i.e., model structural error); (ii) parameter uncertainty; and (iii) model calibration (i.e., model error). Use of the GLUE technique, however, has been severely criticized. For example, Stedinger et al. (2008), argue that use of GLUE without a formal specification of the probability distribution of model error will in general, lead to results not suitable for scientific work. They further argue against implementation of a user-selected behavioral threshold on the basis that this selection is arbitrary and is not necessary when a formal likelihood function is used within a Bayesian context. Formal likelihood functions, however, can be difficult to develop for models describing complex processes, and for this reason are often replaced with informal (i.e., arbitrary) likelihood functions based upon goodness-of-fit metrics (e.g., Freer et al., 1996)

While GLUE has been extensively used and scrutinized within the hydrology community, there has not been a rigorous examination of its applicability for uncertainty analysis in biological process modeling. Such an examination is needed given that the use of GLUE within industrial process models may hold potential for communicating uncertainty in model outputs. Notably absent is an evaluation of the influence of model selection on uncertainty and sensitivity analysis outcomes when using GLUE to generate confidence intervals associated with fitted models. Assessing the influence of model selection is a particularly important area of research when considering applying GLUE with ASM given the flexibility of the ASM model framework to readily incorporate new or updated models.

The objective of this chapter is to assess the effectiveness of GLUE in capturing uncertainties associated with assumed biokinetic parameters when using ASM modules

that may also contain model structural errors. Focus is placed on a subset of the complete ASM framework describing nitrification using a two-step model and a new process that describes cometabolic pharmaceutical (PhAC) degradation by ammonia oxidizing bacteria (AOB). Uncertainty analyses build upon experimental data and mathematical models developed when evaluating the biodegradation of selected beta blockers during nitrification (Sathyamoorthy et al., submitted). Importantly, the selected experimental data sets provide an opportunity to evaluate confidence intervals using GLUE. Thus, the research reported herein offers an important step toward considering uncertainty in industrial process model simulators based on the ASM framework (e.g., GPSx, Biowin, SIMBA, etc.). Moreover, should GLUE provide meaningful insights for these experiments, it could be applied with ASM to quantify uncertainty in complex biological systems.

VIII.2. Overview of Methods

Monte Carlo (MC) simulations utilized in this chapter were implemented as described in V.3.2.3 (Chapter V, Materials and Methods). Results of the MC simulations were evaluated using metrics based on the Nash Sutcliffe Efficiency (NSE, as defined previously in Equation V-31, Section V.3.3) and the small-sample Akaike Information Criteria (AIC_C, as defined previously in Equation VII-3, Section VII.2.2, Chapter VII).

VIII.3. Results and Discussion

VIII.3.1. Monte Carlo Analyses and GLUE Implementation

In this research, 2,000 Monte Carlo (MC) simulations were used with the application of GLUE. The implementation of GLUE relies on the definition of the likelihood function. It is important to note here that in this research, as in many others, it was found that the model errors exhibit extremely complex stochastic structure including serial correlation, heteroscedasticity and nonnormality. For this reason, similar to hundreds of other studies using GLUE, GLUE was employed with an informal likelihood function. It is in this way that the GLUE uncertainty analysis presented herein reflects parameter uncertainty without giving attention to the important aspect of model error. Given that the lack of a statistically meaningful description of model errors, the uncertainty analysis and application of GLUE presented herein prohibits the development of prediction intervals.

Goodness of fit metrics used for the likelihood function have typically been based on the sum of square residuals or the ratio of the sum of square residuals to the variance of the observed data (i.e., the Nash Sutcliffe Efficiency, NSE) (Beven and Binley, 1992; Freer et al., 1996; Mannina et al., 2011). Here the average NSE for S_{NH}, S_{NO2} and S_{NO3} are used to evaluate the likelihood function (L_M) for the model description of nitrification (Equation VIII-1). Note that the formulation of L_M shown in Equation VIII-1 equally weights the NSE for each of the nitrogen species evaluated.

$$L_M(\theta_k \mid Y_k) = \frac{1}{3}\left(1 - \frac{\sigma^2_{e,S_{NH},k}}{\sigma^2_{o,S_{NH}}}\right) + \frac{1}{3}\left(1 - \frac{\sigma^2_{e,S_{NO2},k}}{\sigma^2_{o,S_{NO2}}}\right) + \frac{1}{3}\left(1 - \frac{\sigma^2_{e,S_{NO3},k}}{\sigma^2_{o,S_{NO3}}}\right) \qquad \text{(VIII-1)}$$

where:

for the k^{th} simulation:

$\sigma^2_{e,S_{NH},k}$ = variance of the residuals for S_{NH}

$\sigma^2_{e,S_{NO2},k}$ = variance of the residuals for S_{NO2}

$\sigma^2_{e,S_{NO3},k}$ = variance of the residuals for S_{NO3}

for the experimental data:

$\sigma^2_{o,S_{NH}}$ = variance of the measured values of S_{NH}

$\sigma^2_{o,S_{NO2}}$ = variance of the measured values of S_{NO2}

$\sigma^2_{o,S_{NO3}}$ = variance of the measured values of S_{NO3}

Each of the 2,000 L_M values are compared with the behavioral threshold ($L_{M,BEV}$) in order to determine which simulations are behavioral and retained for the uncertainty analysis. As Beven and Binley (1992) and others have noted the selection of $L_{M,BEV}$ is inherently subjective. However, the development of an L_M based upon NSE permits us to select a $L_{M,BEV}$ that is consistent with good model performance (i.e., NSE > 0.70, e.g., McCuen et al. (2006); Moriasi et al. (2007). This criterion effectively ensures that the production of confidence intervals is based upon meaningful descriptions of the data. Following rejection of the non-behavioral simulations, L_M values for the behavioral simulations are rescaled to produce $L_{M,UPDATED}$ such that $\sum L_{M,UPDATED} = 1$. The behavioral simulations are sorted on the basis of $L_{M,UPDATED}$ and desired quantiles are selected. Confidence and prediction intervals are then developed by identifying those parameter sets that correspond to the 5th and 95th percentile values of $L_{M,UPDATED}$ for the nitrification control reactors.

VIII.3.1.1 Nitrification in Absence of Pharmaceuticals

Data from two nitrification control experiments were employed herein - those from the control during biodegradation experiments conducted with atenolol (denoted here as set I), and those from the control during biodegradation experiments conducted with sotalol (denoted here as set II). Details related to complete experimental results are presented in Chapter VII. Recall that these control experiments were used to assess ammonia oxidation and nitrite oxidation kinetics in the absence of the pharmaceutical as part of an experimental matrix designed to examine the degradation of atenolol or sotolol (see Chapter VII). It is in this way that these two sets of data provide an insight into how the microbial community in the nitrification enrichment culture was functioning over time, as the data sets were developed 60 days apart.

1,994 and 1,987 of the 2,000 simulations for data sets I and II, respectively, result in $L_M > 0$. $L_M < 0$ suggests that a given set of parameter results in behavior uncharacteristic of the system and therefore these parameter sets are discarded from further consideration (Beven and Binley, 1992; Chin, 2009). Note that only a small fraction of the total simulations are discarded (i.e., 0.3% and 0.7%, respectively). For each data set, there is no statistically significant correlation between the posterior distributions of parameters varied in the MC simulations. The lack of a statistically significant correlation between the parameters and their resulting values of L_M was also confirmed (see Table VIII-1 and Table VIII-2).

Table VIII-1: Correlation matrix for posterior distributions of AOB and NOB biokinetic parameters from the behavioral simulations for SOT experiment. Also provided are correlations between biokinetic parameters and GLUE likelihood function values for behavioral Monte Carlo Simulations.

$N_{BEHAV.SIM.}$ = 1,980

	$\mu_{MAX,AOB}$	b_{AOB}	K_{NH}	$\mu_{MAX,NOB}$	b_{NOB}	K_{NO2}
$\mu_{MAX,AOB}$	1					
b_{AOB}	-0.027	1				
K_{NH}	-0.022	0.005	1			
$\mu_{MAX,NOB}$	0.004	-0.049	-0.032	1		
b_{NOB}	-0.017	0.015	0.029	0.006	1	
K_{NO2}	**0.061***	0.028	0.008	0.000	0.023	1
GLUE L_M	-0.003	-0.004	0.02	-0.018	0.000	-0.012

Note: p-value < 0.05 only for values with asterisk(*)

Table VIII-2: Correlation matrix for posterior distributions of AOB and NOB biokinetic parameters from the behavioral simulations for ATN experiment. Also provided are correlations between biokinetic parameters and GLUE likelihood function values for behavioral Monte Carlo Simulations.

$N_{BEHAV.SIM.}$ = 1,993

	$\mu_{MAX,AOB}$	b_{AOB}	K_{NH}	$\mu_{MAX,NOB}$	b_{NOB}	K_{NO2}
$\mu_{MAX,AOB}$	1					
b_{AOB}	0.032	1				
K_{NH}	0.004	-0.007	1			
$\mu_{MAX,NOB}$	0.017	-0.02	0.001	1		
b_{NOB}	0.029	0.008	-0.04	-0.002	1	
K_{NO2}	-0.001	0.013	0.012	0.027	**-0.046***	1
GLUE L_M	-0.019	-0.003	0.018	0.013	0.007	0.002

Note: p-value < 0.05 only for values with asterisk(*)

The positive L_M values (1,994) for data set I are tightly clustered between 0.91 and 0.99; all but one of the L_M values are greater than 0.91. The median value of L_M for these simulations is 0.96, and the 25^{th} and 75^{th} percentile values are 0.95 and 0.97, respectively. Interestingly, simulations for data set II all produce $L_M < 0.90$. The 1,987 positive L_M values for data set II range from 0.13 to 0.85. The median value of L_M is 0.84, and the 25^{th} and 75^{th} percentile values are 0.83 and 0.85, respectively. These metrics suggest that while there are some parameter sets that produce low values of L_M for set II, most simulations are tightly clustered around the median value of 0.84. Simulations for the nitrification control experiments suggest that two step nitrification model and range of biokinetic parameters provide reasonable descriptions of the measured concentrations of nitrogen species.

As noted previously the selection of the behavioral threshold is inherently subjective and is unnecessary when one uses a Bayesian approach to GLUE as recommended by Stedinger et al. (2008). This suggests that modelers must often look to compromise between the competing demands of retaining the maximum number of simulations and improving the perceived quality of these simulations through goodness of fit metrics. To consider the influence of the behavioral threshold on the number of simulations retained when using GLUE, $L_{M,BEV}$ was varied between 0.70 and 1.00 for sets I and II (Figure VIII-1). Selection of $L_{M,BEV} = 0.70$, based on the generally accepted criteria for NSE, results in 1,993 and 1,980 behavioral simulations ($N_{BEH.SIM}$) for data sets I and II, respectively. In fact, for $0.70 \leq L_{M,BEV} \leq 0.95$ the difference in $N_{BEH.SIM}$ is one (i.e., $1,993 \geq N_{BEH.SIM} \geq 1,992$). It is only when $L_{M,BEV}$ exceeds 0.95 that the number of behavior simulations decreases substantially with increasing $L_{M,BEV}$. For set II $N_{BEH.SIM}$ remains the same (i.e,. 1,980) over the range $0.70 \leq L_{M,BEV} \leq 0.82$, but begins to decrease

substantially if $L_{M,BEV}$ exceeds 0.82. These results suggest that $L_{M,BEV}$ = 0.82 produces a similar interpretation of uncertainty to that produced using $L_{M,BEV}$ = 0.70 in these nitrification control reactors. The results also demonstrate that a criterion of $L_{M,BEV}$ = 0.80, rather than 0.70, may be a more meaningful representation of model performance since L_M is tied back to NSE and larger NSEs are indicate better model performance. Thus, a value of 0.80 is used for $L_{M,BEV}$ throughout the remaining analyses as this is indicative of good model performance while preserving diversity in the parameter sets (i.e., 1,993 and 1,980 behavioral simulations for data set I and II, respectively).

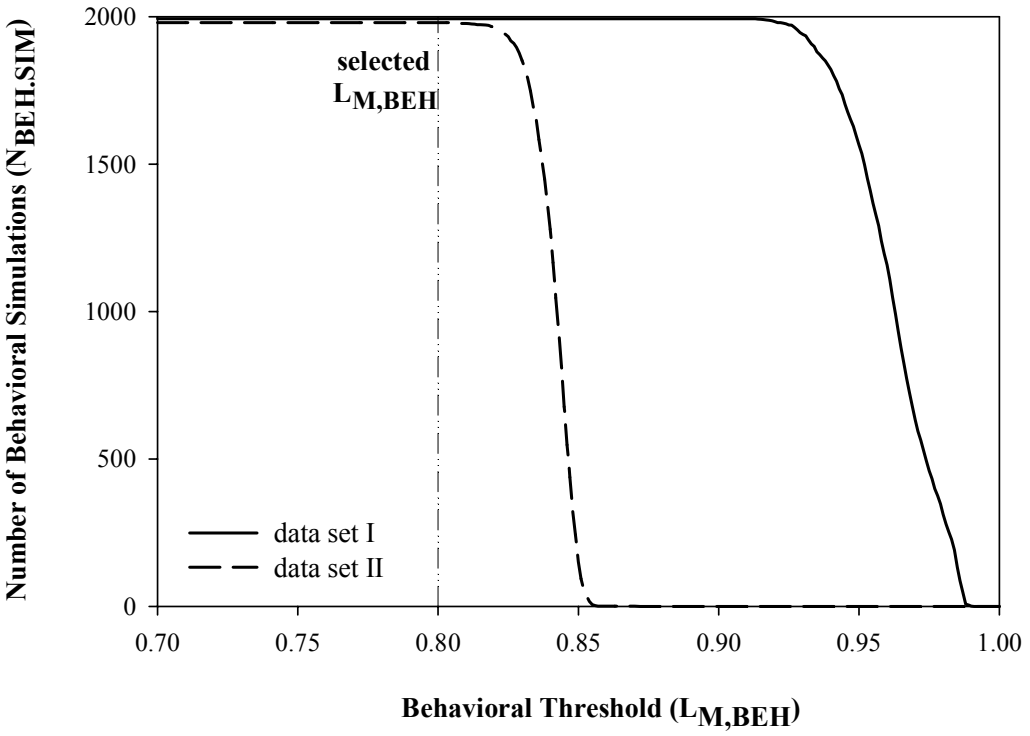

Figure VIII-1: Reduction in the number of behavioral simulations as a function of the selected behavioral threshold ($L_{M,BEH}$) for data sets I and II. Selected $L_{M,BEH}$ of 0.80 is shown as the vertical line.

Shown in Figure VIII-2 are the best fit estimates for $X_{AOB,t0}$ and $X_{NOB,t0}$ produced using the behavioral MC simulations for data sets I and II. Estimates of the AOB and NOB biomass concentrations (and ratios) obtained in the behavioral simulations are compared to those obtained from quantitative real time polymerase chain reaction (qPCR) in Sathyamoorthy et al. (submitted, and presented herein as Chapter VII) . Interestingly in both experiments, the qPCR values for X_{AOB} fall in the range of 80^{th} to 90^{th} percentile, while the values for X_{NOB} are at the 55^{th} percentile. It should be noted here that order of magnitude variability in biomass concentrations obtained using qPCR is commonly acknowledged (Harms et al., 2003; Ahn et al., 2008). Also shown in Figure VIII-2 are biomass ratios of NOB to AOB for each of the behavioral simulations. Experimental values X_{NOB}/X_{AOB} typically fall within the range of 0.20 to 0.55 (Chandran and Smets, 2000; Li et al., 2006; Dytczak et al., 2008; Winkler et al., 2012). Interestingly, many of the values for produced using the behavioral simulations exceed the theoretical upper bound of 0.625 (as determined using yield considerations). Enforcing this constraint using a modified L_M function with an $L_{M,BEV}$ = 0.8 reduces the number of behavioral simulations to 1,191 and 1,384 for Sets I and II, respectively. However, as will be shown in section 3.1.2 the reduction in the number of behavioral simulations does not enhance the predictive capability when using GLUE.

Quantile	X_{AOB}	X_{NOB}	X_{NOB}/X_{AOB}
5th	17	6	0.12
50th	29	15	0.51
95th	99	68	2.44

Quantile	X_{AOB}	X_{NOB}	X_{NOB}/X_{AOB}
5th	14	5	0.09
50th	24	10	0.39
95th	85	44	2.05

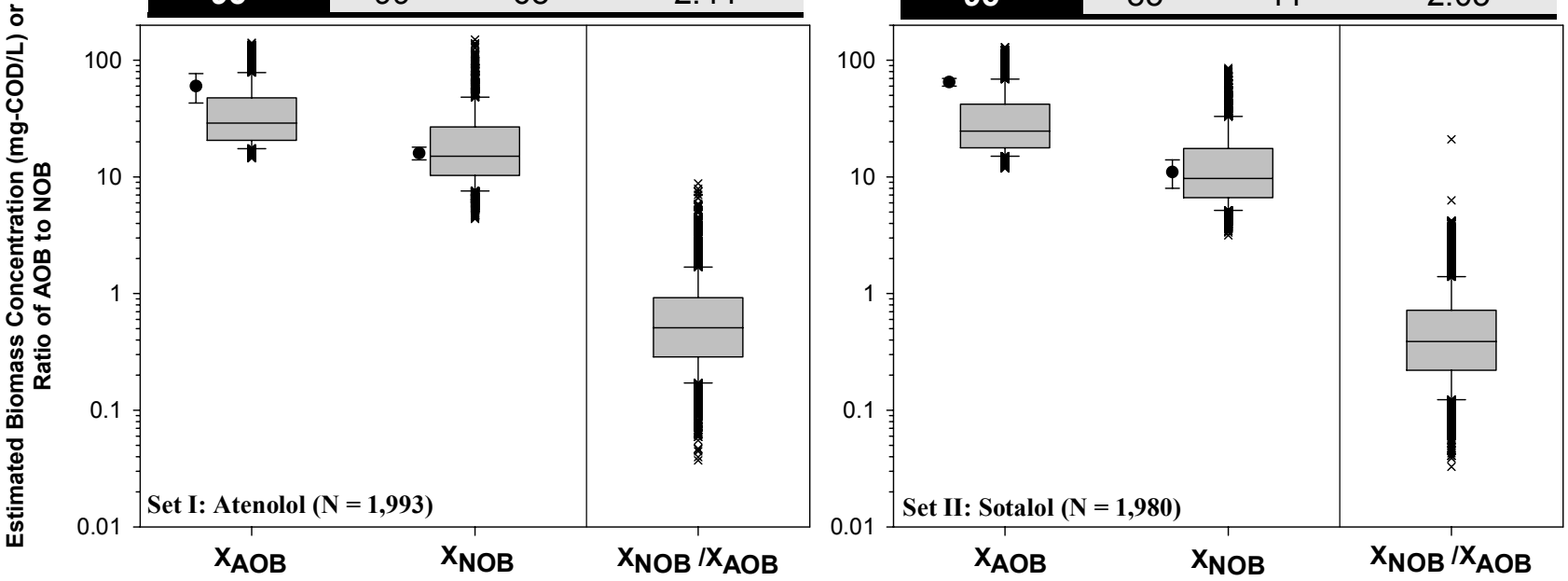

Figure VIII-2: Biomass concentrations and ratios estimated from the behavioral MC simulations for data sets I (left) and II (right). Estimated biomass concentrations using qPCR from Sathyamoorthy *et al.*, submitted are shown for comparison to the estimates from the behavioral simulations. Provided in the overlying tables are 5th, 50th and 95th percentile values of each concentration and ratio.

VIII.3.1.2 Nitrification in Presence of Pharmaceuticals

Nitrification data from two sets of experiments containing ATN and SOT are used here to assess the ability of GLUE to account for model structural errors. In this section the simulation of nitrification when the batch reactors also contain 15 μg/L ATN or SOT is first described (Sathyamoorthy et al., submitted). These simulations then form the basis for the assessment of GLUE while considering structural error of the underlying model.

Simulation of nitrification in the presence of ATN or SOT was conducted using parameter sets that produced behavioral simulations ($L_{M,BEV}$ = 0.80) in the nitrification controls (i.e., set I for atenolol and set II for sotalol). For the simulation of the replicate experiments containing atenolol, values of L_M for range from 0.69 to 0.97 (Figure VIII-3). For the replicate experiments with sotalol, values of L_M range from 0.55 to 0.77 (Figure VIII-3). The lower L_M values produced with simulating nitrification in the reactors containing pharmaceutical results from poor prediction of S_{NO2}. While L_M values can be improved by increasing the weight associated with S_{NO2} (see Equation VIII-1), this modification does not improve the predictive performance for S_{NO2}. Furthermore, such a modification suggests that particular emphasis should be placed on S_{NO2} even though the experimental methods and protocols do not justify such emphasis. Thus, any adjustment would only reinforce the criticism that the informal likelihood function is arbitrary (Mantovan and Todini, 2006; Stedinger et al., 2008).

Also shown in (Figure VIII-3) are the effects of modifying L_M to include the theoretical upper bound on X_{NOB}/X_{AOB}. Results suggest that there are no statistical differences in the sets of L_M values produced when the theoretical bound is enforced or unenforced based on a 5% Mann-Whitney test. In addition, constraining the biomass

ratio does not enhance the goodness of fit ability (as defined by an increase in L_M) for either replicate conducted for either PhAC.

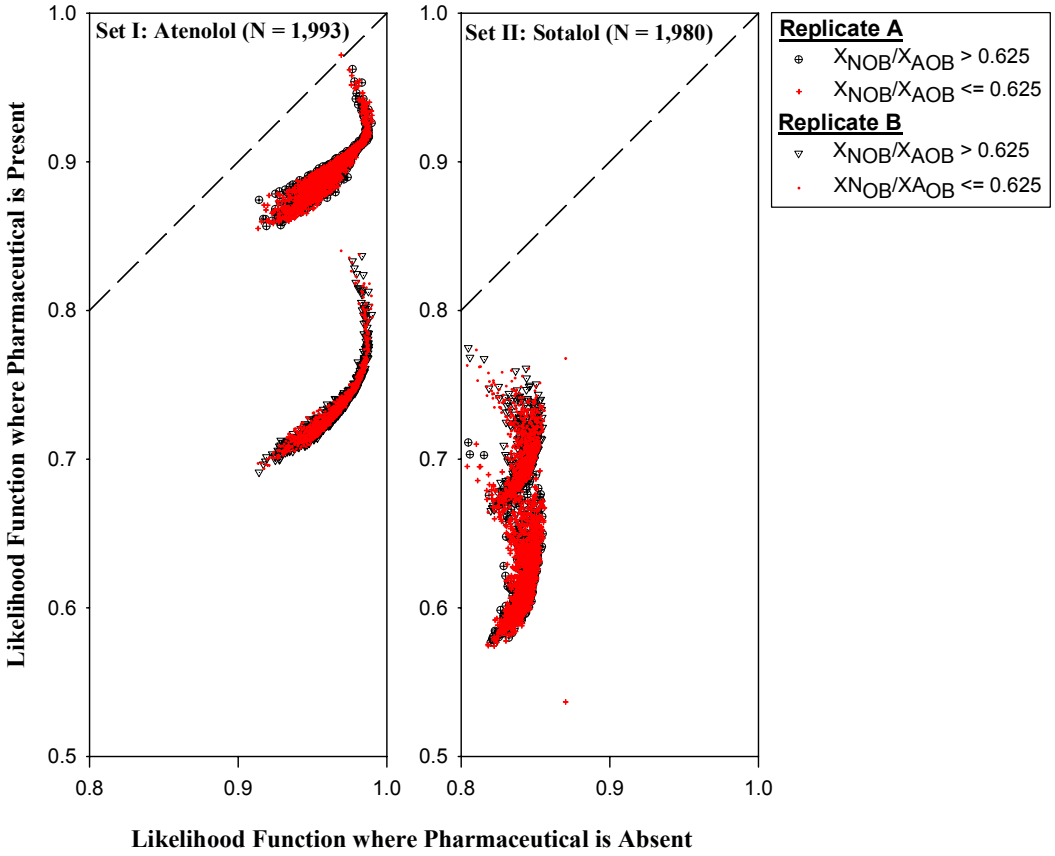

Figure VIII-3: Relationship between the likelihood function values produced from behavioral simulations describing nitrification in the presence and absence of atenolol (left) and sotolol (right). Note that the abscissa describes the nitrification control experiments, described in the text as Sets I and II, and is restricted to the behavioral range ($L_M \geq 0.8$) Values shown are separated into two groups based upon whether or not X_{NOB}/X_{AOB} exceeds the theoretical ratio of 0.625.

Sathyamoorthy et al. (submitted, and presented here as Chapter VII) report that atenolol exerts a competitive inhibition on AOB growth. No inhibition was observed in experiments conducted with SOT. This difference provides an opportunity to assess how well GLUE can account for model structural errors. To accomplish this, nitrification data from the atenolol experiments were simulated using an AOB growth rate that accounts for competitive inhibition (Bailey and Ollis, 1986) as shown in Equation VII-4 (Section VII.2.3.1, Chapter VIII).

Note the use of a competitive inhibition model for AOB growth introduces a new parameter, $K_{I,ATN}$ that cannot be independently evaluated using the experimental data. Thus, $K_{I,ATN}$ must be fit to the nitrification data of the replicate atenolol experiments. Fitting $K_{I,ATN}$ in the competitive inhibition case enables development of confidence intervals based on the fitted inhibition model. Thus, GLUE was utilized to compare the confidence intervals produced using behavioral simulations when implementing the competitive inhibition model with the confidence intervals produced from the behavioral simulations obtained for the model that does not include inhibition (described in Section VIII.2.1.1). If model structural errors are accounted for by GLUE, the confidence intervals for the fitted and generated models should be statistically similar.

To use the GLUE to assess the uncertainty resulting from use of the competitive-inhibition hypothesis, a modified likelihood function (L_{M2}) is employed. L_{M2} is based upon equally weighting the two replicate reactors (A and B) when considering S_{NH}, S_{NO2}, and S_{NO3} as shown in Equation VIII-2.

$$L_{M2}(\theta_k \mid Y_k) = \left[0.5 * \sum_i \omega_i \left(1 - \frac{\sigma^2_{e,A,i,k}}{\sigma^2_{o,A,i}}\right)\right] + \left[0.5 * \sum_i \omega_i \left(1 - \frac{\sigma^2_{e,B,i,k}}{\sigma^2_{o,B,i}}\right)\right] \quad \text{(VIII-2)}$$

$$i = S_{NH}, S_{NO2}, S_{NO3}$$

The efficacy of the original and competitive-inhibition models are compared using the small-sample Akaike Information Criteria (AIC_C, as defined previously in Equation VII-3, Section 2.2, Chapter VII). The threshold for determining behavioral simulations in this analysis is noted $L_{M2,BEV}$ and set to 0.80 to be consistent with the analysis above. This value of $L_{M2,BEV}$ results in 1,970 behavioral simulations for the competitive inhibition model compared to 1,993 for the model with no inhibition. Implementation of the competitive inhibition model lowers both the SSE and AIC_C for S_{NH} of the behavioral simulations confirming the utility of the competitive inhibition model (Table VIII-3).

Table VIII-3: Comparison of GLUE likelihood function L_{M2} and goodness of fit metrics when using a monod model for AOB growth (no inhibition) versus competitive inhibition model for the combined data sets from experimental reactors with atenolol

metric	quantile	no inhibition	Competitive inhibition
$N_{BEH.SIM}$		1,993	1,970
L_{M2}	5th	0.79	0.82
	50th	0.81	0.84
	95th	0.85	0.86
S_{NH} NSE	5th	11.06	5.68
	50th	11.40	6.13
	95th	11.56	7.13
S_{NH} AIC_C	5th	-11.39	-24.48
	50th	-10.68	-22.65
	95th	-10.33	-19.04

Use of the competitive inhibition model with any of the biokinetic parameter sets producing a behavioral simulation lowers AIC_C values by at least 10. This decrease in the AIC_C suggests that the data do not support use of the no-inhibition model. Furthermore, the distribution of L_{M2} for the competitive inhibition model is statistically different than that calculated for the no inhibition model at a 5% significance level using a Mann-Whitney test. Thus, GLUE appears to be unable to account for the model structural error resulting from competitive inhibition of AOB growth by atenolol in this scenario.

VIII.3.2. Parameter Sensitivity Analysis

The use of GLUE is extended herein to parameter sensitivity analysis by extracting parameter elasticity coefficients of AOB and NOB biokinetic parameters from the behavior simulations. Focus is placed on the ATN data set as ATN was the only beta blocker evaluated in this research that was observed to degrade during ammonia oxidation (Sathyamoorthy et al., submitted). Estimates for $T_{ATN\text{-}AOB}$, $k_{ATN\text{-}AOB}$ and $K_{I,ATN\text{-}AOB}$ were developed using the MC procedure outlined in Section V.3.2.3 (Materials and Methods) using the competitive-inhibition model for AOB growth. Confidence intervals for atenolol biodegradation are subsequently determined using a protocol identical to that described in Section VIII.2.1.1 for the nitrification process with the likelihood function shown as Equation VIII-3.

$$L_{M-ATN}(\theta_k \mid Y_k) = \left[\frac{1}{2}\left(1 - \frac{\sigma^2_{e,A,k}}{\sigma^2_{o,A}}\right)\right] + \left[\frac{1}{2}\left(1 - \frac{\sigma^2_{e,B,k}}{\sigma^2_{o,B}}\right)\right] \qquad \text{(VIII-3)}$$

Here $\sigma^2_{e,A,k}$ and $\sigma^2_{e,B,k}$ are the variance of the residuals from the replicate experiments A and B for a particular simulation *k*. And $\sigma^2_{o,A}$ and $\sigma^2_{o,B}$ are the variance of the S_{ATN} values measured in each of the replicate experiments.

All 1,970 behavioral simulations obtained using the competitive inhibition model (when evaluated using L_M as shown in Equation VIII-1) are also behavioral when considering $L_{M\text{-}PhAC}$ as all $L_{M\text{-}PhAC}$ values are greater than 0.95. The high values of $L_{M\text{-}PhAC}$ indicate the simulations using CPB are extremely good representations of the PhAC data. Values of $T_{ATN\text{-}AOB}$ and $k_{ATN\text{-}AOB}$ are weakly correlated with each other ($R^2 = 0.33$). The ranges of these parameters are $63.8 \leq T_{ATN\text{-}AOB} \leq 74.8$ L.g-COD^{-1} and $5.6 \leq k_{ATN\text{-}AOB} \leq 52.7$ L.g-COD^{-1}d^{-1}.

VIII.3.2.1. Development of Elasticity Coefficients for Sensitivity Analysis

Parameter sensitivity is assessed by quantifying and comparing elasticity coefficients (Louca, 2007). An elasticity coefficient ($\varepsilon_{X/Y}$) is defined as shown in Equation VIII-4 and represents the fractional change in an output variable *y* given a 1 percent change in a particular model parameter *x*.

$$\varepsilon_{X/Y} = \frac{\partial Y / Y}{\partial X / X} \qquad \text{(VIII-4)}$$

While popular in economics (Louca, 2007), elasticity coefficients have been used in fields ranging from hydrology (Sankarasubramanian et al., 2001; Chiew, 2006) to biochemistry and metabolic engineering (Fell, 1992). Here a dimensionless formulation for elasticity is used (Sankarasubramanian et al., 2001) and elasticity coefficients are estimated about the mean value of the behavioral simulations. The derivation is

described below using the AOB-growth related transformation coefficient of a pharmaceutical ($T_{PhAC\text{-}AOB}$).

The total derivative of the model output ($T_{PhAC\text{-}AOB}$ here) resulting from changes in each of the biokinetic parameters is calculated through application of the chain rule as shown in Equation VIII-5. Note here that no assumptions are required about the underlying data as is normally necessary when estimating elasticities.

$$dT_{PhAC-AOB} = \frac{\partial T_{PhAC-AOB}}{\partial \mu_{MAX,AOB}} d\mu_{MAX,AOB} + \frac{\partial T_{PhAC-AOB}}{\partial b_{AOB}} db_{AOB} + \frac{\partial T_{PhAC-AOB}}{\partial K_{NH}} dK_{NH} + \frac{\partial T_{PhAC-AOB}}{\partial \mu_{MAX,NOB}} d\mu_{MAX,AOB} + \frac{\partial T_{PhAC-AOB}}{\partial b_{NOB}} db_{AOB} + \frac{\partial T_{PhAC-AOB}}{\partial K_{NO2}} dK_{NO2} \quad \text{(VIII-5)}$$

Taking the differentials at the mean value with respect to each biokinetic parameter results in Equation VIII-6:

$$\begin{aligned}\left(T_{PhAC-AOB} - \overline{T}_{PhAC-AOB}\right) = {} & \frac{\partial T_{PhAC-AOB}}{\partial \mu_{MAX,AOB}} \left(\mu_{MAX,AOB} - \overline{\mu}_{MAX,AOB}\right) + \\ & \frac{\partial T_{PhAC-AOB}}{\partial b_{AOB}} \left(b_{AOB} - \overline{b}_{AOB}\right) + \\ & \frac{\partial T_{PhAC-AOB}}{\partial K_{NH}} \left(K_{NH} - \overline{K}_{NH}\right) + \\ & \frac{\partial T_{PhAC-aOB}}{\partial \mu_{MAX,NOB}} \left(\mu_{MAX,NOB} - \overline{\mu}_{MAX,NOB}\right) + \\ & \frac{\partial T_{PhAC-AOB}}{\partial b_{NOB}} \left(b_{NOB} - \overline{b}_{NOB}\right) + \\ & \frac{\partial T_{PhAC-AOB}}{\partial K_{NO2}} \left(K_{NO2} - \overline{K}_{NO2}\right)\end{aligned} \quad \text{(VIII-6)}$$

Dividing each term in Equation VIII-11 by $\overline{T}_{PhAC-AOB}$ and multiplying each term on the right hand side by 1 (in the form of the mean of the parameter divided by itself) results in Equation VIII-7.

$$\frac{\left(T_{PhAC-AOB}-\overline{T}_{PhAC-AOB}\right)}{\overline{T}_{PhAC-AOB}}=\frac{\left(\partial T_{PhAC-AOB}/\overline{T}_{PhAC-AOB}\right)}{\left(\partial\mu_{MAX,AOB}/\overline{\mu}_{MAX,AOB}\right)}\frac{\left(\mu_{MAX,AOB}-\overline{\mu}_{MAX,AOB}\right)}{\overline{\mu}_{MAX,AOB}}+\frac{\left(\partial T_{PhAC-AOB}/\overline{T}_{PhAC-AOB}\right)}{\left(\partial b_{AOB}/\overline{b}_{AOB}\right)}\frac{\left(b_{AOB}-\overline{b}_{AOB}\right)}{\overline{b}_{AOB}}+\frac{\left(\partial T_{PhAC-AOB}/\overline{T}_{PhAC-AOB}\right)}{\left(\partial K_{NH}/\overline{K}_{NH}\right)}\frac{\left(K_{NH}-\overline{K}_{NH}\right)}{\overline{K}_{NH}}+\frac{\left(\partial T_{PhAC-AOB}/\overline{T}_{PhAC-AOB}\right)}{\left(\partial\mu_{MAX,AOB}/\overline{\mu}_{MAX,NOB}\right)}\frac{\left(\mu_{MAX,NOB}-\overline{\mu}_{MAX,NOB}\right)}{\overline{\mu}_{MAX,NOB}}+\frac{\left(\partial T_{PhAC-AOB}/\overline{T}_{PhAC-AOB}\right)}{\left(\partial b_{NOB}/\overline{b}_{NOB}\right)}\frac{\left(b_{NOB}-\overline{b}_{NOB}\right)}{\overline{b}_{NOB}}+\frac{\left(\partial T_{PhAC-AOB}/\overline{T}_{PhAC-AOB}\right)}{\left(\partial K_{NH}/\overline{K}_{NO2}\right)}\frac{\left(K_{NO2}-\overline{K}_{NO2}\right)}{\overline{K}_{NO2}} \quad \text{(VIII-7)}$$

Inspection of the right hand side of Equation VIII-12 indicates that the ratio of deviation of each parameter from the mean to the mean value was multiplied by the elasticity coefficient of that parameter (ε_i) for the estimated parameter. Thus, Equation VIII-7 can be rewritten as a multivariate, ordinary least-squares regression model relating the fractional change in $T_{ATN\text{-}AOB}$ about the mean value to the elasticities of each of the biokinetic parameters varied in the analysis (Equation VIII-8). Note that this functional definition of elasticity is specific to the use of a linear model in the OLS regression.

Other model formulations such as a log-log and log-linear models have also been applied to estimate elasticities in economics (Wooldridge, 2008).

$$T^*_{PhAC-AOB} = \varepsilon_{\mu_{MAX,AOB}/T_{PhAC-AOB}} \mu^*_{MAX,AOB} + \varepsilon_{b_{AOB}/T_{PhAC-AOB}} b^*_{AOB} + \varepsilon_{K_{NH}/T_{PhAC-AOB}} K^*_{NH} + \varepsilon_{\mu_{MAX,NOB}/T_{PhAC-AOB}} \mu^*_{MAX,NOB} + \varepsilon_{b_{NOB}/T_{PhAC-AOB}} b^*_{NOB} + \varepsilon_{K_{NO2}/T_{PhAC-AOB}} K^*_{NO2} \quad \text{(VIII-8)}$$

Here the asterisk denotes deviations from the mean values of the data from the Monte Carlo simulations.

VIII.3.2.2. Assessment of Elasticities for Atenolol Biodegradation Parameters

Shown in Table VIII-4 is the elasticity evaluation for $T_{ATN\text{-}AOB}$, $k_{ATN\text{-}AOB}$ and $K_{I,ATN\text{-}AOB}$ based on the parameter sets and estimates in the 1,970 behavioral simulations considered here. All parameters which are included in the elasticity regression model are statistically significant at the 0.05-level, unless otherwise noted. Also provided for each parameter is the standard error and percentage of the model sum of square errors attributable to its elasticity. The goodness of fit of each of the elasticity models is indicated using the NSE, in lieu of the coefficient of determination (R^2), as these are no-intercept models, in which case R2 lacks meaning. Model residuals were found to be well approximated by a homoscedastic normal distribution.

Some general observations are warranted related to the multivariate regression model used to develop these elasticities. All the models have high NSEs suggesting that the ordinary least squares models used herein effectively describe the distributions of $T_{ATN\text{-}AOB}$, $k_{ATN\text{-}AOB}$ and $K_{I,ATN\text{-}AOB}$. Variances in $T_{ATN\text{-}AOB}$, $k_{ATN\text{-}AOB}$ and $K_{I,ATN\text{-}AOB}$ are nearly explained by the AOB biokinetic parameters alone (see %model SSEs), suggesting NOB biokinetic parameters contribute little sensitivity these parameters. This is not

surprising as $T_{ATN\text{-}AOB}$, $k_{ATN\text{-}AOB}$ and $K_{I,ATN\text{-}AOB}$ all relate to ammonia oxidation, not nitrite oxidation.

Table VIII-4: Elasticity coefficients (ε_i) of biokinetic parameters for atenolol biodegradation parameters using estimated values from 1,970 behavioral simulations employing the competitive inhibition model for AOB growth.

	Elasticity Values (with Standard Errors); % of Model Sum of Square Errors explained by each elasticity term						
	$\varepsilon_{\mu_{MAX-AOB}}$	$\varepsilon_{b_{AOB}}$	$\varepsilon_{K_{NH}}$	$\varepsilon_{\mu_{MAX-NOB}}$	$\varepsilon_{b_{NOB}}$	$\varepsilon_{K_{NO2}}$	Model NSE
$T^*_{ATN-AOB}$	0.030 (0.000) 20.6%	-0.056 (0.000) 64.5%	0.020 (0.000) 12.2%	0.000 (0.000) 0%	-0.001 (0.000) 0%	-0.009 (0.000) 2.6%	0.991
$k^*_{ATN-AOB}$	0.945 (0.001) 97.1%	0.090 (0.002) 0.8%	-0.108 (0.001) 1.6%	*N/A (p > 0.05)*	*N/A (p > 0.05)*	0.006 (0.001) 0%	0.995
$K^*_{I,ATN-AOB}$	-0.010 (0.002) 0.1%	0.013 (0.002) 0%	0.924 (0.001) 98.8%	-0.006 (0.001) 0%	0.005 (0.001) 0%	0.072 (0.001) 0.7%	0.996

The elasticities shown in Table VIII-4 suggest that small deviations in $T_{ATN\text{-}AOB}$ (coefficient of variation of $T_{ATN\text{-}AOB}$ = 3%) are primarily linked to deviations in b_{AOB} through a weak inverse relationship ($\varepsilon_{b_{AOB}-T_{ATN-AOB}}$ = -0.06). $T_{ATN\text{-}AOB}$, however, is sensitive the AOB net growth rate (i.e., all three AOB growth parameters) which corresponds to the physical interpretation of $T_{ATN\text{-}AOB}$ as representing atenolol cometabolism during AOB growth. In contrast, deviations in $k_{ATN\text{-}AOB}$ appear related to

deviations in $\mu_{MAX,AOB}$ ($\varepsilon_{\mu_{MAX-AOB}-k_{ATN-AOB}}$ = 0.95). It is hypothesized that the sensitivity of $k_{ATN-AOB}$ to $\mu_{MAX,AOB}$ results from the fact $k_{ATN-AOB}$ controls the model fit after ammonia oxidation is complete. That is, higher $\mu_{MAX,AOB}$ results in faster completion of ammonia oxidation, and consequently greater influence of $k_{ATN-AOB}$. Deviations in the AOB growth inhibition coefficient ($K_{I,ATN-AOB}$) are well explained by deviations in K_{NH} ($\varepsilon_{K_{NH}-K_{I,ATN-AOB}}$ = 0.92, see Table VIII-4) given that $K_{I,ATN-AOB}$ effectively increases K_{NH} (Equation 6). While this may appear to suggest there is a less pronounced inhibitory effect for larger values of K_{NH}, it is important to recognize that the range of $K_{I,ATN-AOB}$ values reported here is similar to the range of environmentally relevant concentrations of atenolol (< 10 μgL^{-1}).

VIII.4. Conclusions and Implications

The application of GLUE using an informal likelihood function for constructing confidence intervals for model estimates when modeling nitrification has been evaluated in this chapter. The findings suggest that confidence intervals based on GLUE for nitrification models, in cases where parameter uncertainty is the primary source of errors, satisfactorily encompass experimental data and provide a good estimate of the uncertainty resulting from parameter uncertainty alone. However, where model structural errors may arise due to inhibition, GLUE cannot produce confidence intervals large enough to explain variations in models estimates. These results strongly suggest that where an inappropriate model basis is used to develop confidence intervals, GLUE, used as prescribed, is incapable of producing meaningful degrees of model uncertainty. This is a particularly important finding as GLUE continues to gain popularity in the

wastewater treatment process modeling community. Epistemic uncertainty due a range of factors including changing influent quality or potential influx of inhibitory pollutants, are commonplace in wastewater treatment plants. Therefore, from the perspective of wastewater treatment process modeling, these results suggest that caution should be exercised when using GLUE with an informal likelihood function to develop confidence intervals pertaining to the effectiveness of treatment.

It is worth reiterating that the development of a formal likelihood function for this analysis was made impracticable by the complexity observed in the stochastic structure of the model residuals. This is very often the case for models describing complex phenomena (Liu and Gupta, 2007). Thus, the analysis presented herein cannot and does not reflect the full uncertainty associated with particular model output (Stedinger et al., 2008). The use of an informal likelihood function means that the analysis neglects model error and is restricted to parameter uncertainty (reflected in confidence intervals). In effect, use of GLUE in this manner cannot produce prediction intervals. While it is likely to be common practice to continue to use GLUE without a formal likelihood function, future research where the stochastic structure of model residuals in more fully interrogated is recommended. Such research may result in approximations of a formal likelihood function that support development of meaningful prediction intervals using GLUE.

The multivariate elasticity approach introduced to assess model sensitivity is based on the chain rule and the use of multivariate linear regression. The method is unique because it is completely nonparametric in the sense that it does not require any model assumptions. Results from the sensitivity analysis suggest that the cometabolic transformation coefficient for atenolol biodegradation linked to AOB growth is relatively

inelastic to AOB biokinetics. On the other hand, the non-growth related transformation coefficient is elastic. Quantification of these elasticities has important implications for understanding PhAC biodegradation by AOB in WWTPs. Principally, it allows utilization of lab-derived biodegradation coefficients when attempting to characterize PhAC biodegradation in full-scale systems. As an example, the influence of 10°C fluctuation in water temperature (e.g., seasonal variation) on the degradation of atenolol by AOB in a WWTP in considered here. The variation in $T_{ATN\text{-}AOB}$, $k_{ATN\text{-}AOB}$ and $K_{I,ATN\text{-}AOB}$ were estimated using AOB and NOB biokinetics and the temperature dependencies proposed by Manser et al. (2006) and Kaelin et al. (2009) (Table VIII-5). The analysis suggests that $T_{ATN\text{-}AOB}$ and $K_{I,ATN\text{-}AOB}$ are insensitive to temperature (Figure VIII-4, left). In contrast, $k_{ATN\text{-}AOB}$ varies by significantly over the 10^{o}C range in temperature. The variation in $k_{ATN\text{-}AOB}$ with temperature is a direct result of the variation in $\mu_{MAX,AOB}$ in this scenario.. The influence of this variation in $k_{ATN\text{-}AOB}$ is shown by considering the change in the rate of cometabolism (due to temperature effects) relative to the mean rate of cometabolism for this range in temperature. This is metric is shown in Figure VIII-4 for conditions indicative of WWTPs that produce: (a) near complete nitrification (S_{NH} = 0.01 mg-N/L); and, (b) a near incomplete nitrification (S_{NH} = 10 mg-N/L). In both cases the atenolol concentration is assumed to be 1 μg/L, although this only influences the variation in the rate through the inhibition of AOB. This simplified analysis suggests that changes in temperature may result in large variations to the rate of atenolol cometabolism by AOB (Figure VIII-4, right). Interestingly, the degree of nitrification has minimal influence on variations in atenolol degradation due to temperature changes. Thus, the ability to maintain nitrification will only impart substantial variations in the rate of cometabolism when AOB biomass concentrations begin to fluctuate (which is not accounted for in

these simplified simulations). A review of the literature suggests that this is the first evaluation of temperature related sensitivity of PhAC biodegradation in biological wastewater treatment processes. It is important recall that elasticities developed herein are specific to the range of parameter values utilized in the MC simulations. While the selected parameter ranges utilized in the MC simulations (see Table V-15, Chapter V, Materials and Methods) are representative of most nitrification processes, care should be taken to reassess elasticities for outlying biokinetic behavior observed in a natural or engineered process.

Table VIII-5: AOB and NOB biokinetic parameters proposed by Manser et al. (2006) and by Kaelin et al. (2009)

		Value at (20°C)	Temp. Correction Factor (θ)
$\mu_{MAX,AOB}$	d^{-1}	0.47	0.12
b_{AOB}	d^{-1}	0.15	0.12
K_{NH}	mg-NL^{-1}	0.14	--
$\mu_{MAX,NOB}$	d^{-1}	0.65	0.078
b_{NOB}	d^{-1}	0.22	0.078
K_{NO2}	mg-NL^{-1}	0.28	--

Table VIII-6: Correlation matrix for posterior distributions of AOB and NOB biokinetic parameters from the behavioral simulations for ATN experiment using the competitive-inhibition model. Also provided are correlations between biokinetic parameters and GLUE likelihood function values for behavioral Monte Carlo Simulations.

$N_{BEHAV.SIM.}$ = 1,970

	$\mu_{MAX,AOB}$	b_{AOB}	K_{NH}	$\mu_{MAX,NOB}$	b_{NOB}	K_{NO2}
$\mu_{MAX,AOB}$	1					
b_{AOB}	-0.025	1				
K_{NH}	-0.024	0.001	1			
$\mu_{MAX,NOB}$	0.001	-0.047	-0.037	1		
b_{NOB}	-0.019	0.016	0.036	0.002	1	
K_{NO2}	**0.072***	0.022	0.066	-0.012	0.027	1
GLUE L_M	0.002	-0.002	0.025	-0.018	-0.003	-0.021

Note: p-value < 0.05 only for values with asterisk(*)

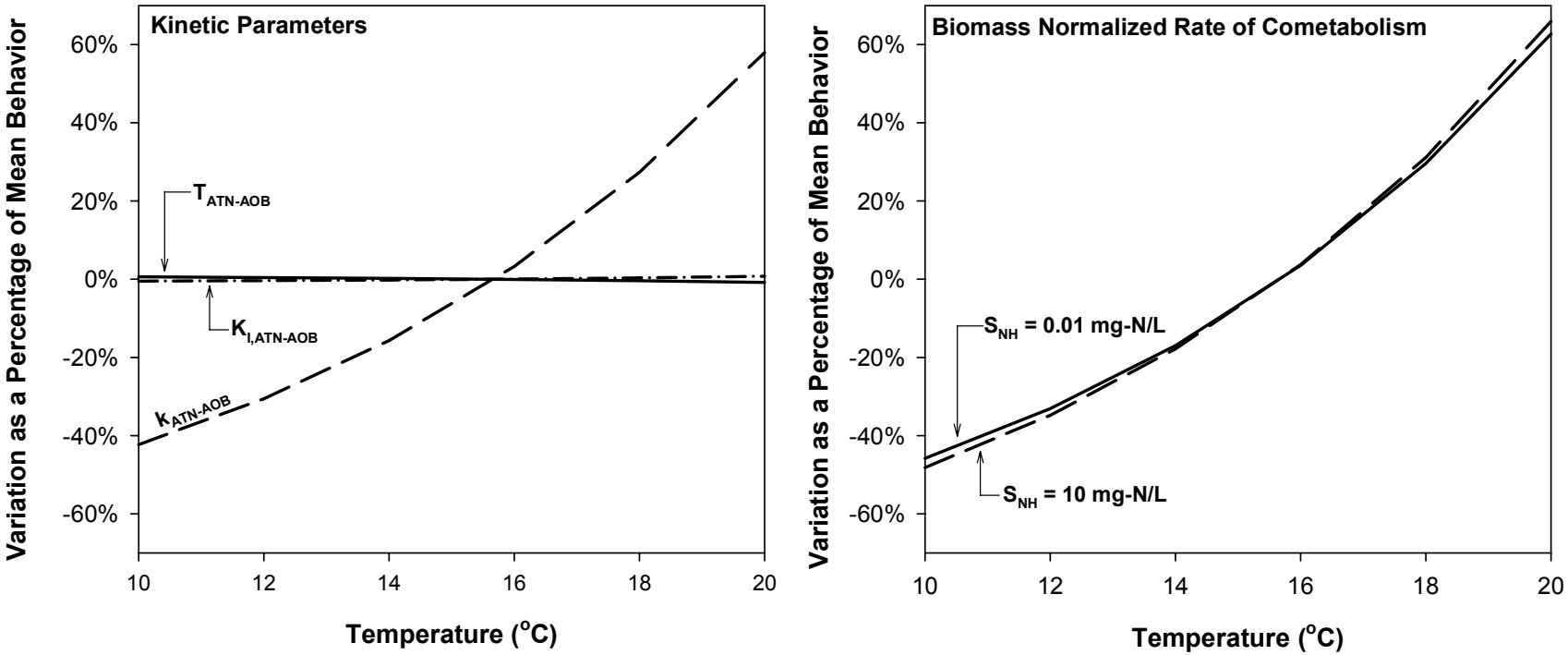

Figure VIII-4: Influence of wastewater temperature on the biodegradation of atenolol. Variation of kinetic parameters (left) and rate of cometabolic biodegradation by AOB (right). The rate plot assumes 1 µg/L atenolol, though it should be noted that atenolol concentration only influences the variation in rate through AOB inhibition.

Chapter IX. Cometabolic Degradation of Naproxen by Ammonia Oxidizing Bacteria

IX.1. Introduction

The discharge of pharmaceuticals (PhACs) into the natural environment via wastewater treatment plant (WWTP) effluents is now well established (Ternes, 1998; Kolpin et al., 2002; Andreozzi et al., 2003; Metcalfe et al., 2003; Bendz et al., 2005; Waiser et al., 2011; Onesios and Bouwer, 2012). In conventional WWTPs, the majority of PhAC attenuation occurs during biological treatment through biodegradation and sorption. The role of WWTP operating conditions on PhAC these attenuation processes has not been elucidated to a degree permitting effective predictive modeling of PhACs during biological wastewater treatment. PhAC attenuation is too often modeled assuming pseudo first order (PFO) kinetics. Application these simple attenuation models results in orders of magnitude variation in the PFO rate coefficient (k_{BIO}) reported some PhACs (see Section II.5). Hypotheses to explain the variation in k_{BIO} values include that they are related to operating conditions of the biological treatment process or related to the diversity of biomass within the biological treatment process. In fact, the observed variability in k_{BIO} data suggests that more mechanistic approaches are required to effectively model the biodegradation of PhACs during biological wastewater treatment.

Sathyamoorthy et al. (submitted, reflected here in Chapter VII) have recently developed a consortium-level process-based model for cometabolic PhAC biodegradation by ammonia oxidizing bacteria (AOB) which can be integrated into the

activated sludge model (ASM) framework (Henze et al., 2000). The cometabolic process-based (CPB) model was utilized to model biodegradation of atenolol (ATN, at a concentration of 15 μg/L) in batch experiments using an enriched nitrifying culture. The objective of this chapter is to explore molecular properties of the PhACs that may be used to interrogate rates of cometabolism by AOB. This objective was achieved using batch experiments to evaluate the biodegradation of naproxen (NAP) by enriched nitrifying cultures. NAP is useful model-PhAC candidate, considering it is one of most ubiquitously found in WWTP influents and effluents and among the most well studied in both engineered (Paxeus, 2004; Carballa et al., 2007; Quintana et al., 2010; Sarp et al., 2011; Falas et al., 2012; Schroder et al., 2012) and natural environmental systems (Ternes, 1998; Topp et al., 2008a; Topp et al., 2008b; Edwards et al., 2009; Waiser et al., 2011). Furthermore, it is particularly relevant when evaluating models for PhAC biodegradation by AOB since it is known to degrade in nitrifying systems (Suarez et al., 2005; Tran et al., 2009; Fernandez-Fontaina et al., 2012).

IX.2. Overview of Experimental and Modeling Approach

IX.2.1. Description of the Batch Experiments

The batch experiments described in this chapter (referred to as Experiments A, B and C) were conducted using biomass from two nitrification enrichment cultures (see Table IX-1). Experiments A and B consisted of the four NIT-EXPT reactors included in this research to evaluate the biodegradation of a PhAC during nitrification (see Section V.2.4.1 in the Materials and Methods for a description of reactors). Experiment C did not include a nitrification inhibition control (i.e., Reactor 2), as the objective therein was to evaluate the impact of PhAC exposure during growth on PhAC biodegradation after nitrification was complete. Therefore, an important distinction between the experimental reactors (i.e., Reactors 3 and 4, see reactor nomenclature in Section V.2.4.1 in the Materials and Methods) in Experiment C is the time in the experiment when NAP was added to the reactor. In the case of Reactor 3, NAP was added at the start of the experiment, as is the case in all these batch experiments. However, in Reactor 4, NAP was added 41.7 hr after addition of S_{NH} with an objective to assess the biodegradation of NAP by AOB entering endogenous respiration using biomass that had not been exposed to NAP during the growth phase. In the absence of real-time S_{NH} data, changes in reactor pH (which was manually monitored) were used as guide to assess the extent of nitrification in this reactor.

Experiment A utilized biomass enriched from that in the nitrification stage of a WWTP operating a two-stage biological treatment process (BOD removal followed by nitrification, see details in Section V.2.2.1, Chapter V). Experiments B and C were conducted utilizing biomass enriched from that in a WWTP operating a single-sludge

biological treatment process that achieves complete nitrification at a solids retention time of 8 to 11 day. In all cases, the minimum level of enrichment was a three-fold increase in the specific nitrification rate (mg-N/g-VSS·h) (i.e., no experiments were conducted until the specific nitrification rate of the enrichment was at least three times greater than the original biomass seed).

Both initial ammonia and experimental biomass concentrations were varied in the batch experiments described herein (see Table IX-1). Volatile solids concentration in the batch experiments ranged from 15 mg/L to ~400 mg/L, $S_{NH,t0}$ ranged from 40 to 60 mg-N/L and $S_{NAP,t0}$ ranged from ~300 to 1,300 μg/L. This difference in the experiments can be exploited to assess whether or not the CPB model coefficients hold general utility or are a function of WWTP bioreactor operating conditions.

IX.2.2. Application of Cometabolic Process Based Model

The CPB model developed by Sathyamoorthy et al. (submitted, and described here in Section V.3.2.2) was applied to the describe the data from Experiments A - C. For each experiment data from Reactor 1 (nitrification control) was utilized to estimate values of initial AOB and nitrite oxidizing bacteria (NOB) concentrations ($X_{AOB,t0}$ and $X_{NOB,t0}$) by reducing the sum of square errors for nitrogen species. AOB and NOB biokinetic parameters utilized herein were the same as those used in the beta-blocker experiments (see Table VII-4 for a summary of biokinetic parameters). For Experiment A, nitrogen species quantified included S_{NH}, S_{NO2} and S_{NO3}, whereas for Experiments B and C, only S_{NO2} and S_{NO3} were quantified.

Table IX-1: Summary of experimental conditions for batch experiments evaluating the degradation of naproxen during nitrification.

Expt.	Reactor	MLVSS (mg/L)	MLSS (mg/L)	$S_{NH,t0}$ (mg-N/L)	$S_{NAP,t0}$ (ng/L)	$\frac{S_{NH,t0}}{S_{NAPT,t0}}$ (ng-N/ng)	$\frac{MLVSS}{S_{NAPT,t0}}$ (ng-VSS/ng)	$\frac{X_{AOB,t0}}{S_{NAPT,t0}}$ (ng-COD/ng)
A[a]	1 (Nit. Control)	369	556	39	--	--	--	--
	2 (Nit. Inhibition Control)	398	587	39	501	0.8×10^5	7.9×10^5	0.46×10^5
	3 (Nit. Expt.)	404	568	37	506	0.7×10^5	8.0×10^5	0.45×10^5
	4 (Nit. Expt.)	372	510	36	504	0.7×10^5	8.4×10^5	0.46×10^5
B[b]	1 (Nit. Control)	420	1,054	68	--	--	--	--
	2 (Nit. Inhibition Control)	411	1,032	68	322	1.9×10^5	12.8×10^5	2.55×10^5
	3 (Nit. Expt.)	411	1,032	68	301	2.0×10^5	13.7×10^5	2.72×10^5
	4 (Nit. Expt.)	411	1,032	68	301	2.3×10^5	13.7×10^5	2.72×10^5
C[b]	1 (Nit. Control)	15	54	50	--	--	--	--
	2 (Nit. Inhibition Control)	*not included*						
	3 (Nit. Expt.)	17	54	50	389	1.3×10^5	0.4×10^5	0.10×10^5
	4 (Nit. Expt.)[c]	15	54	50	391	1.3×10^5	0.4×10^5	0.10×10^5

[a] Biomass seed for Experiment A from two-stage WWTP
[b] Biomass seed for Experiments B and C from single-stage WWTP
[c] Naproxen added to Reactor 4 at 41.7 hr

The concentration of heterotrophic biomass (X_{HET}) was not independently measured in these experiments. X_{HET} was therefore estimated as follows. The active biomass fraction for a given experiment was determined based on the SRT of the nit-SBR at the time when biomass was harvested for the experiment (Grady et al., 1999) and literature values for the heterotrophic decay coefficient (Henze et al., 2000). The influent COD was assumed to be zero since no exogenous organic carbon is provided with the nit-SBR feed. X_{HET} was subsequently calculated as the difference between the active biomass fraction and the nitrifier population ($X_{AOB,t0} + X_{NOB,t0}$) estimated using data from Reactor 1 (nitrification in the absence of NAP). Given the uncertainty included in this estimation of X_{HET}, fits of NAP biodegradation in Reactor 2 (nitrification control reactor) are described using $\alpha_{NAP\text{-}HET}X_{HET}$ [T^{-1}] rather than $\alpha_{NAP\text{-}HET}$, as was previously done for ATN (see Chapter VII). That is to say, the uncertainty in the calculation of X_{HET} did not enter the fitting of the degradation in the control reactor.

For each experiment NAP AOB-biodegradation coefficients were estimated using data from Reactors 3 and 4. As indicated in Table IX-1 a nitrification inhibition control (i.e., Reactor 2) was not included in Experiment C. Experiments B and C were conducted only seven days apart with the nit-SBR having been operational as an enrichment culture for 362 days prior to Experiment B. It was therefore assumed that the heterotrophic community in these two experiments is effectively identical, supporting the use of a single $\alpha_{NAP\text{-}HET}$. Thus the value of that $\alpha_{NAP\text{-}HET}$ estimated from Experiment B data was utilized when fitting $T_{NAP\text{-}AOB}$ and $k_{NAP\text{-}AOB}$ to data in Experiment C.

IX.3. Results and Discussion

IX.3.1. Modeling Nitrification and Estimation of Biomass Concentrations

Shown in Figure IX-1 are the time course data and CPB model fits for S_{NH} (top panel), S_{NO2} (middle panel), and S_{NO3} (middle panel) for the four NIT-EXPT reactors from Experiment A. The analogous data for Experiments B and C are shown in Figure IX-2 and Figure IX-3, respectively (recall that S_{NH} data are not available in Experiments B and C). Nitrification in Experiment A proceeds such that nitrite concentrations remain low (<5 mg-N/L). Nitrite concentrations in Experiments B and C, however, reach as high as ~20 – 30 mg-N/L due to the higher initial concentration of ammonia employed in these experiments($S_{NH,t0,Expt.B}$ = 50 mg-N/L and $S_{NH,t0,Expt.C}$ = 68 mg-N/L). The ammonia oxidation rate remains relatively constant in Experiments A and B, increasing by less than 10% during the course of the experiment. In Experiment C, however, the initial ammonia oxidation rate is 0.58 mg-N/L·h and increases to a maximum value of 1.10 mg-N/L·h, when S_{NH} = 6.24 mg-N/L (at 52.6 hr) and then decreases to 0 mg-N/L·h once all the S_{NH} is oxidized (61 h). Therefore, the maximum ammonia oxidation rate is 1.9 times greater than the initial oxidation rate in this experiment. This large increase in the ammonia oxidation rate in Experiment C resulted from the significant AOB growth relative to the estimated initial concentration. $X_{AOB,t0}$ is 4.4 mg-COD/L, which increased to a maximum value of 9.4 mg-COD/L (59 hr).

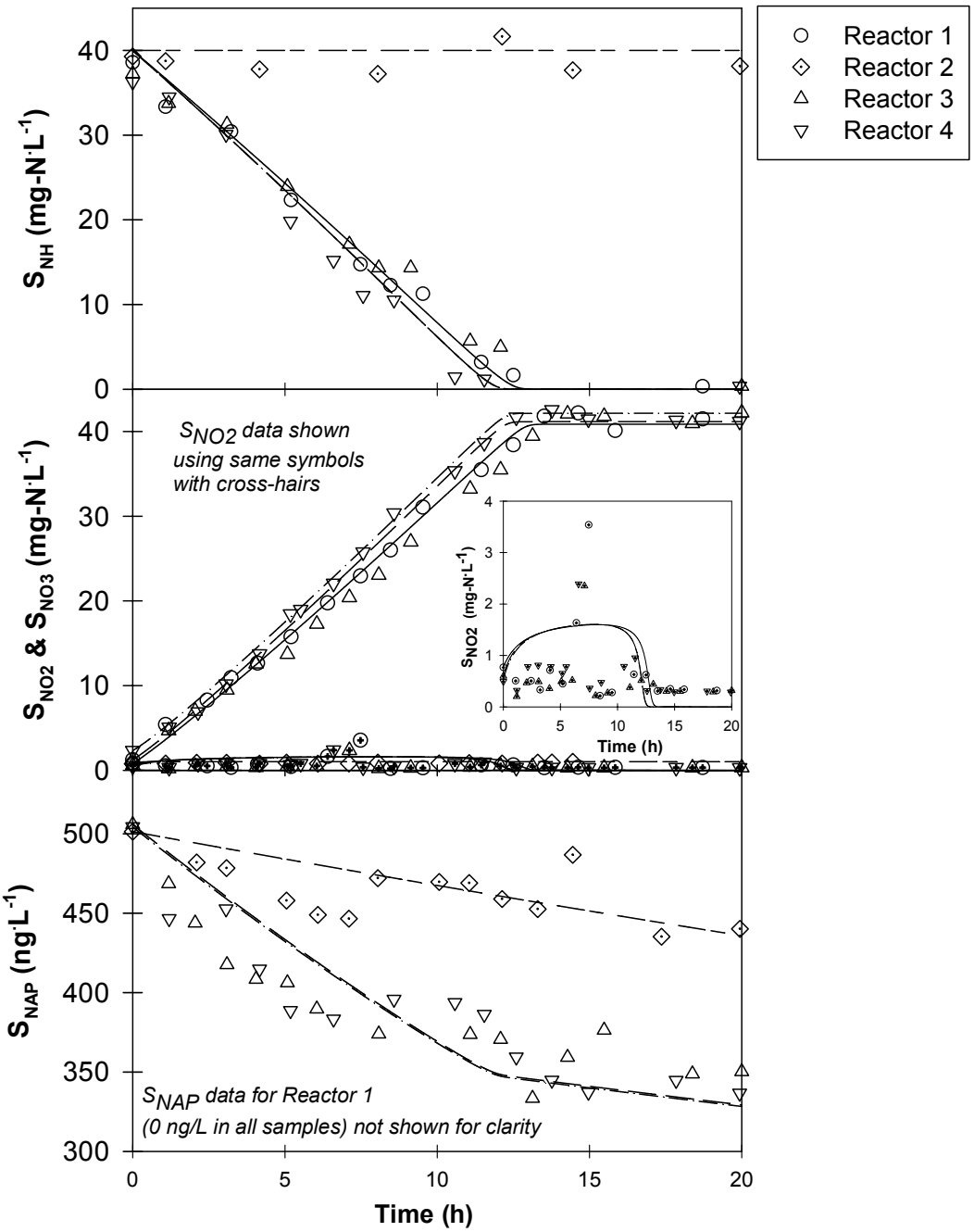

Figure IX-1: Observed and modeled concentrations of ammonia (top panel), nitrite and nitrate (middle panel) and NAP (bottom panel) for nitrification Experiment A conducted with NAP. Results are shown from each of the four NIT-EXPT reactors a nitrification control (Reactor 1), a nitrification inhibition control (Reactor 2), and replicate experimental reactors (Reactors 3 and 4).

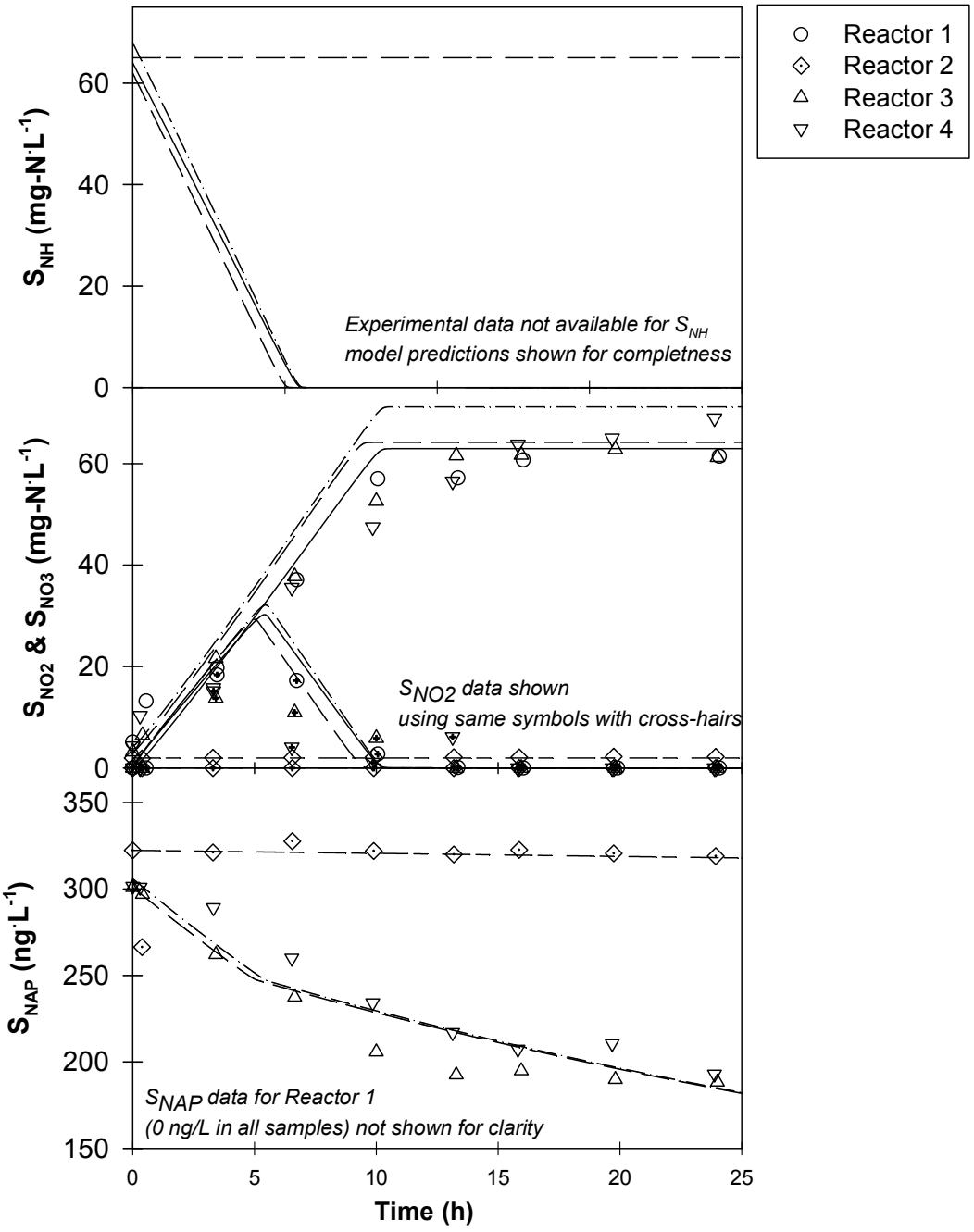

Figure IX-2: Observed and modeled concentrations of nitrite and nitrate (middle panel) and NAP (bottom panel) for nitrification Experiment B conducted with NAP. Results are shown from each of the four NIT-EXPT reactors a nitrification control (Reactor 1), a nitrification inhibition control (Reactor 2), and replicate experimental reactors (Reactors 3 and 4). Note that ammonia-nitrogen data were not collected for this experiment, model predictions are shown in the top panel for completeness.

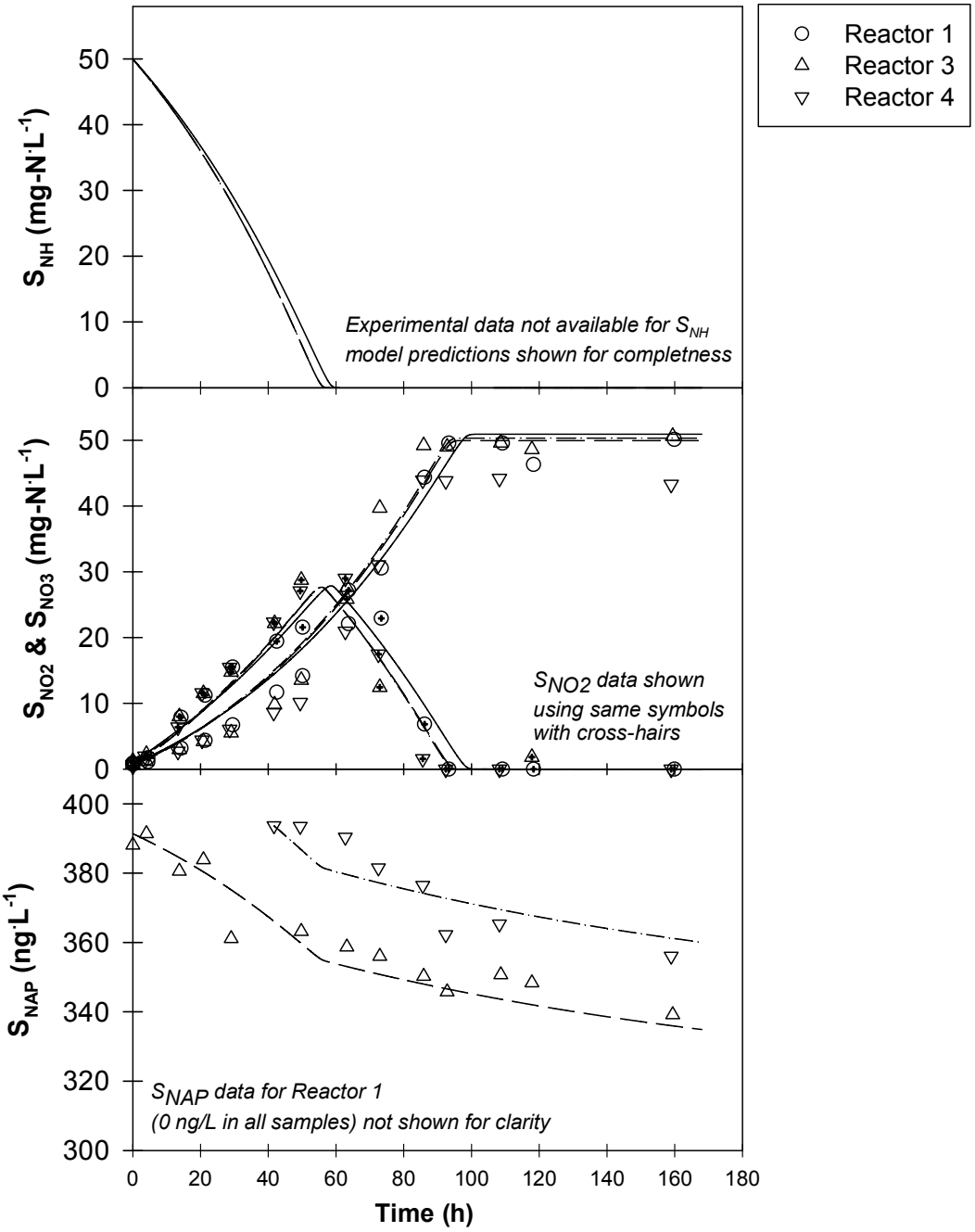

Figure IX-3: Observed and modeled concentrations of nitrite and nitrate (middle panel) and NAP (bottom panel) for nitrification Experiment C conducted with NAP. Results are shown from each of the three NIT-EXPT reactors included in this experiment - a nitrification control (Reactor 1), and replicate experimental reactors (Reactors 3 and 4). Note that ammonia-nitrogen data were not collected for this experiment, model predictions are shown in the top panel for completeness. Note also that NAP was added to Reactor 4 at 41.7 hr.

Fitted values of X_{AOB} and X_{NOB} are provided in Table IX-2 along with calculated values of X_{HET}. Fits of initial nitrifying biomass concentrations suggest that the NOB to AOB ratios at time zero for Experiment A, B and C are 0.78, 0.35 and 0.25, respectively. While the ratios for Experiments B and C are similar (recall these experiments were separated by seven days), they illustrate that nitrifying populations can be different even when specific rates of nitrification appear temporally stable for a given culture (Dytczak et al., 2008; Wang et al., 2010). The temporal stability in the specific rate of nitrification is, however, a good marker a relatively stable fraction of heterotrophs (i.e., the fraction heterotrophs was 0.17 in both Experiments B and C, see below). The estimated X_{NOB}:X_{AOB} ratios for Experiments B and C fall within the range of typical literature values - 0.20 to 0.55 (Chandran and Smets, 2000; Li et al., 2006; Dytczak et al., 2008; Winkler et al., 2012). The estimate for Experiment A however, is above this range and also above the theoretical value of 0.625 determined using yield considerations. While the reason for this is not clear, it is hypothesized to result from the relatively poor performance of the model in describing the nitrite data in this experiment (note that the model does not capture the little accumulation of nitrite observed around 7 hr, see inset in Figure IX-1).

The fraction of heterotrophs in Experiments B and C are identical (0.17) and comparable to that estimated using qPCR in the experiments conducted with the beta blockers atenolol (0.20), metoprolol (0.16) and sotalol (0.12) (see Section VII.2.1 and Table IX-2). However, the fraction of heterotrophs in Experiment A is significantly higher (0.61). Recall that these fractions were determined using the estimated operational SRT of the nitrification enrichment SBR and fitted values of X_{AOB} and X_{NOB} from the simulations. The higher fraction of heterotrophs for Experiment A is likely the

result of the shorter period of enrichment (40 day when Experiment A was conducted compared to 362 and 369 day for Experiments B and C). Moreover, the seeds for the two enrichments were from different WWTPs (see Table IX-1 and Section V.2.2.1 in the Materials and Methods).

Table IX-2: Estimated AOB, NOB and HET biomass concentrations and coefficients for cometabolic biodegradation of NAP by AOB from application of the cometabolic process based model to describe nitrification and NAP biodegradation in batch experiments A – C evaluating NAP biodegradation. A summary of experimental conditions is provided in Table IX-1.

		Experiment A	Experiment B	Experiment C
Fitted Biomass Concentrations[c]	$X_{AOB,t0}$ (mg-COD.L^{-1})	23 ± 1	82 ± 32	4 ± 0.1
	$X_{NOB,t0}$ (mg-COD.L^{-1})	18 ± 2	29 ± 3	1 ± 0.1
	$X_{NOB,t0}/X_{AOB,t0}$	0.78	0.35	0.25
	X_{HET} (mg-COD.L^{-1})	64	23	1
	Fraction X_{HET}	0.61	0.17	0.17
Fitted NAP Biodegradation Coefficients[c]	$T_{NAP-AOB}$ (L.g-COD^{-1})	49.0 ± 23.9	13.6 ± 6.0	9.4 ± 3.1
	$k_{NAP-AOB}$ (L.g-COD^{-1} d^{-1})	0.001 ± 0.2	4.3 ± 1.1	1.8 ± 0.7
	$\alpha_{NAP-AOB}X_{HET}$ (d^{-1})	0.17 ± 0.05	0.01 ± 0.01	N/F[a]
	$\alpha_{NAP-AOB}$ (L.g-COD^{-1} d^{-1})[b]	2.6 ± 0.7	0.4 ± 0.4	N/F[a]
NAP Goodness of Fit	Reactor 2 (Nit. Inhib. control)	0.30	0.80	--
	Reactor 3	0.88	0.93	0.80
	Reactor 4	0.86	0.90	0.78

[a] N/F = not fit. $\alpha_{NAP-AOB}$ from Expt. B used to model data in Experiment C

[b] $\alpha_{NAP-AOB}$ is calculated using the estimated value of $\alpha_{NAP-AOB}X_{HET}$ and estimated X_{HET}

[c] Values provided are best fit estimates with 95% confidence intervals

IX.3.2. Naproxen Biodegradation

NAP degradation was observed in all three experiments (Figure IX-1 - Figure IX-3). The extent of NAP biodegradation from these three experiments fall into two clusters, one where the VSS to $S_{NAP,t0}$ is ~$0.4x10^5$ ng-VSS/ng (Table IX-1) and another were the ratio is $0.7x10^5 – 1.4x10^5$ ng-VSS/ng. Experiments conducted at higher VSS to $S_{NAP,t0}$ ratios exhibit NAP removals of 32% - 39%, whereas removals at the lower ratios were 10% - 14%. That is to say, higher mixed liquor concentrations appear to produce greater removal in these experiments. In light of the high S_{NO2} levels observed in Experiments B and C, there is a potential for nitration reactions to be responsible for NAP degradation (Gaulke et al., 2008; Chiron et al., 2010). This was not explored as part of this research. Note that batch sorption experiments conducted with NAP at similar concentrations suggest that the extent of sorption of NAP is not significant (data not shown).

Interestingly, when evaluated on the basis of fitted X_{AOB} concentration (see Section IX.2.2.1 for description of biomass fits) it appears that higher X_{AOB} concentrations appear to enhance the extent of NAP removal (Figure IX-4). Thus, the $X_{AOB,t0}$ to $S_{NAP,t0}$ ratios explored here suggest that the availability of enzyme for NAP biodegradation has a role in determining the extent of NAP biodegradation. Recall that two separate seed biomass were used for these experiments, and that the experiments were conducted at different points in the enrichment process suggesting that the observation related to $S_{NAP,t0}$ to X_{AOB} ratio may be more broadly applicable. That notwithstanding, caution is warranted when trying to generalize this result until additional studies can verify the observed trend. Also, it should be noted here that there was no apparent relationship between the $S_{NAP,t0}/S_{NH,t0}$ ratio and NAP attenuation

for the data shown in Figure IX-1. Comparison of the observed NAP attenuation in Experiments A – C with those from ATN biodegradation (see Chapter VII) suggest that the influence of AOB is PhAC specific. ATN was biodegraded to a greater extent even at a much lower $X_{AOB,t0}/S_{ATN,t0}$.

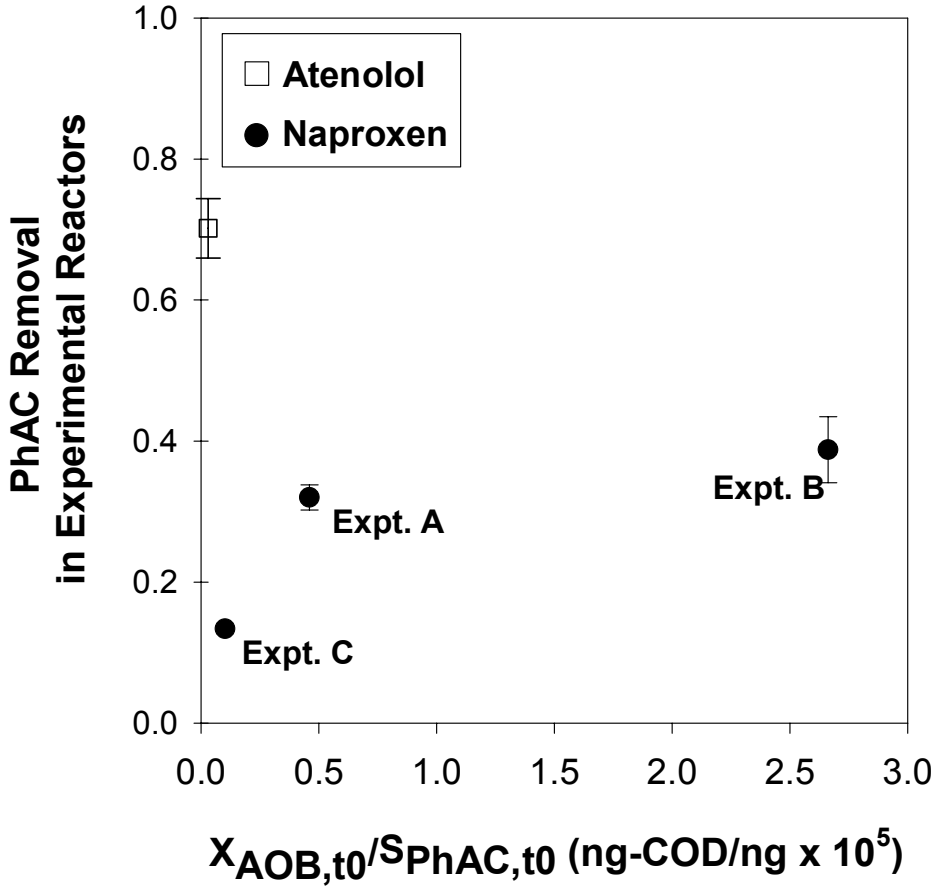

Figure IX-4: Influence of the ratio of AOB and NAP concentrations ($X_{AOB,t0}/S_{PhAC,t0}$) on the observed removal of the pharmaceuticals evaluated in this research which biodegraded in batch experiments - naproxen (filled circle) and atenolol (open square).

A summary of the CPB model parameters for cometabolic biodegradation of NAP by AOB from Experiments A, B and C are provided in Table IX-2. The value of $T_{NAP\text{-}AOB}$ for Experiment A (49.0 ± 23.9) is higher than that for Experiments B or C (12.6 ± 6.0 and 13.8 ± 2.9, respectively). On the other hand, the value of $k_{NAP\text{-}AOB}$ is effectively zero for Experiment A but 4.3 ± 1.1 and 1.8 ± 0.7 Lg-COD^{-1}·d^{-1} for Experiments B and C, respectively. The low value fitted for $k_{NAP\text{-}AOB}$ using the data from Experiment A is a result of the high value fitted value of $\alpha_{NAP\text{-}AOB}X_{HET}$ (fit to data from Reactor 2). Inspection of the fit for Reactor 2 in Experiment A (Figure IX-1, bottom panel) and the Nash-Sutcliffe Efficiency (NSE) value of 0.30) suggests that use of a single fitting parameter ($\alpha_{NAP\text{-}HET}X_{HET}$) is not satisfactory to describe the observed trend in these data. It should be noted here that a model with more fitting parameters, such as the modified PFO models discussed in Chapter VII, may provide a better description of the data. However, such an approach is not considered here in order to retain the same mechanistic significance of the CPB model in all applications of the model. The fits of NAP concentration for Reactors 3 and 4 from Experiment A are both acceptable having NSE values of 0.88 and 0.86, respectively. Note that NSE > 0.70 is generally considered to be acceptable for time-series data (Moriasi et al., 2007). NSE values for the NAP fits in Experiments B and C are greater than 0.75 (Table IX-1). The high level of uncertainty in the estimate of T coupled with the near zero value of k from Experiment A suggests that caution should be exercised in using these estimates as being representative of the NAP-AOB interaction.

IX.3.3. Influence of PhAC properties on T and k

The objective here is to assess potential links between PhAC properties and CPB model coefficients T and k utilizing data for NAP and ATN (Sathyamoorthy et al. (submitted), presented here as Chapter VII). Given the uncertainty in establishing the rate of NAP by heterotrophs in Experiment A (see Section IX.2.3), the fitted values of T and k are not included in the subsequent analysis. This leaves results from Experiments B and C with NAP to be compared those obtained for ATN. Recall that the enrichment durations for the nit-SBR are very similar for these three experiments (Experiment B = 362 days, Experiment C = 369 days and ATN Experiment = 294 days).

Here, the estimates from the three experiments are compared using z-scores calculated as recommended by Paternoster et al. (1998) and Brame et al. (1998). In brief, z-scores are calculated utilizing the mean value of the estimates and the standard error of the estimate calculated from the 95% confidence intervals generated through the fitting process. Comparisons of $T_{PhAC\text{-}AOB}$ and $k_{PhAC\text{-}AOB}$ for the three experiments are shown in Table IX-3 and IX-4, respectively. At the 1% level, the estimated values of $T_{NAP\text{-}AOB}$ are similar to each other, but different from $T_{ATN\text{-}AOB}$. This is true as well for $k_{PhAC\text{-}AOB}$, though at the 2% level. These data suggest that under both growth and non-growth conditions, AOB appear more effective in biotransformation of ATN than NAP.

Table IX-3: Summary of p-values at which $T_{PhAC-AOB}$ estimates from Experiments B and C (NAP) and atenolol are the same

	NAP.Expt.B	NAP.Expt.C	ATN
$T_{PhAC-AOB}$ ($L \cdot g\text{-}COD^{-1}$)	13.6 ± 6.0	9.4 ± 3.1	71.5 ± 22.7
NAP.Expt.B			
NAP.Expt.C	0.207		
ATN	0.009	0.007	

Table IX-4: Summary of p-values at which $k_{PhAC-AOB}$ estimates from Experiments B and C (NAP) and atenolol are the same

	NAP.Expt.B	NAP.Expt.C	ATN
$k_{PhAC-AOB}$ ($L \cdot g\text{-}COD^{-1}$)	4.3 ± 1.1	1.8 ± 0.7	16.1 ± 5.6
NAP.Expt.B			
NAP.Expt.C	0.076		
ATN	0.017	0.004	

It is useful to compare these AOB related transformation coefficients based on a conceptualization of the cometabolic biodegradation process in order to evaluate what differences in the PhAC properties contribute to the differences in $T_{PhAC-AOB}$. Such an analysis may be relevant to development of future Quantitative Structure Property Relationships (QSPRs) for PhAC biodegradation by AOB. QSPRs have been used to predict PFO rate constants for biodegradation of other organic compounds (e.g., phenol, benzene and aniline) in activated sludge systems with varying degrees of success (e.g., Okey and Stensel, 1993 and 1996). These types of relationships often employ molecular properties. Chemometrics are often used in the early phases of PhAC development/screening to evaluate the ADMET properties of a compound (adsorption, distribution, metabolism, excretion and toxicity) (Mannhold, 2008). For example,

Lipinski's rule of 5 is frequently used to qualitatively screen the potential ADMET properties and *design* of new drugs (Lipinski et al., 1997). PhAC properties are therefore readily available and the ability to link these properties to cometabolic biodegradation holds significant predictive utility to the environmental engineering/science community.

AOB derive the energy required for metabolism by the oxidation of ammonia to nitrite in a two-step process. First ammonia is oxidized to hydroxylamine utilizing AMO (a membrane-bound protein) followed by oxidation of hydroxylamine to nitrite by hydroxylamine oxidoreductase (HAO) located in the periplasm membrane-bound protein (see Section II.1.1 and Arp and Stein (2003), Sayavedra-Soto and Arp (2011)). Transport of these PhACs to the AMO active site, the presumed first step in the degradation process, therefore requires passage across the cell walls and to the periplasmic membrane.

AOB, exemplified by the well-studied *Nitrosomonas Europaea spp.*, have very few transport proteins dedicated to uptake of organic molecules (Chain et al., 2003). It is therefore reasonable to assume that PhAC transport across the cell membrane occurs via passive transport, and that the hydrophobic nature of a PhAC is an important factor in determining that transport efficiency. Values of the octanol-water partition coefficient (log K_{OW}) for ATN and NAP indicate that NAP is more hydrophobic than ATN (Table IX-5), even when using log D at the experimental pH of ca. 7 – 8 (Sangster, 1989). While the environmental science and engineering community has typically relied on log K_{OW} and log D as indicators for transport across cell membranes (e.g., Wammer and Peters, 2005), the pharmaceutical development community has made significant use of polar surface area (PSA) as a surrogate for passive transport. The PSA encodes information related to and affecting hydrogen-bonding, polarity and solubility

(Mannhold, 2008). It reflects the portion of the molecule that is polar, accounting for Van der Waals surface area of the molecule resulting from oxygen and nitrogen atoms on the surface, including the hydrogen atoms bonded to them. Compounds having higher PSA generally exhibit lower fractional absorption in the human body (Palm et al., 1997; Clark, 1999). The calculation of PSA requires the determination of 3-D structures is complex and computationally intensive. Therefore, researchers in pharmaceutical community instead use topological polar surface area (TPSA), which makes use of fragment contributions and molecular topology based on a large database of structures (Ertl et al., 2000). NAP has a lower TPSA than ATN (Table IX-5) suggesting that it should be more readily transported (albeit passively) into the bacterial cell. The difference in $T_{PhAC\text{-}AOB}$ values therefore does not likely result from differences in PhAC transport to AMO.

With the PhAC at AMO, attachment to the active site is the next step in the biodegradation process. It is hypothesized that attachment to the active site pocket is linked to the PhAC size and stereochemistry. PhAC size, however, cannot readily explain the observed difference in cometobolic rate parameters as there is only a 36 Da difference in molecular weight and a 47 $Å^3$ difference in molecular volume between ATN and NAP (see Table IX-5). Stereochemistry is therefore interrogated using the surrogate metric of the number of rotatable bonds (nRB). While this simple nRB metric does not capture entropic penalties for specific binding orientations, it can be easily identified for each PhAC molecule based upon the molecular structure. Indeed, inspection of this nRB suggests that ATN, with eight potential rotatable bonds compared to only three for NAP, may have increased flexibility and ability to bind to multiple amino acid moieties at the AMO active site. Note that nRB values for NAP and ATN are at the 25^{th} and 80^{th}

percentiles, respectively, when evaluating the 200 most frequently used PhACs suggesting that there may be some merit to considering this a more general indicator of degradation by AOB. However, SOT and MET, which were not biodegraded by nitrifiers (see results in Chapter VII) have nRB values of 6 and 9, respectively. This emphasizes the complex of nature of the biodegradation process and therefore, caution is warranted when using a such predictors to develop QSPR models.

Hydrogen bonding has been shown to also be an important factor in the interaction between proteins or enzyme pockets and substrates (Kubinyi, 2001). Here, hydrogen bonding impacts the orientation of interaction between the PhAC and the enzyme pocket as well as the affinity of binding site to the active ligand of the PhAC (Davis and Teague, 1999; Kubinyi, 2001). Histidine is thought to play a role in the active site for ammonia oxidation on AMO (Norton et al., 2002; Gilch et al., 2009), which is capable of both hydrogen bond donation and acceptance, with the number of hydrogen bond acceptors increasing with increasing pH (calculated using Chemaxon). At the low pH in the periplasmic space (4 – 6) (Schmidt et al., 2004; Weidinger et al., 2007), Histidine has an equal number of both hydrogen bond donors and acceptors. As shown in Table IX-5 ATN has the ability to make seven total hydrogen bonds than NAP (four). Indeed, it may be the interplay between the ability to form hydrogen bonds with AMO and the flexibility of the molecule to conveniently be located at the active site which influences the efficiency of interaction between the PhAC and the enzymatic pocket.

Once a PhAC is bound at the AMO active site, biochemical transformation can proceed. Here, energetics will impact the cometabolic transformation of the PhAC. A comparison of the pi energy of these two PhACs suggests that the pi energy of NAP is in fact greater than that of ATN (Table IX-5). However, the difference is very small (< 2 eV),

it therefore seems less likely that this is a critical factor when considering ATN and NAP. The use of energetics in explaining differences in cometabolic PhAC biodegradation by AOB may still hold general utility, when used in poly parameter QSPR models especially considering that the Pi Energy values for ATN and NAP are at approximately the 30th percentile for the top 200 most used drugs. Therefore additional research is certainly warranted evaluating the biodegradation of PhACs with lower Pi Energy values.

Table IX-5: Chemometric Properties of Atenolol and Naproxen

	Atenolol	Naproxen
Chemical Formula	$C_{14}H_{22}N_2O_3$	$C_{14}H_{14}O_3$
Fraction of aromatic carbon atoms (f_{AroC})	0.43	0.71
MW (g/mol)	266.3	230.3
MV (A^3)	260.9	214.0
Van der Waals Surface Area (vdWSA)	440	344
pK_A	9.60	4.15
Log K_{OW}	0.16	3.18
Log D (@ expt. pH ~ 7.5)	-1.94	-0.17
TPSA (A^2)	84.60	46.53
No. of Rot. Bonds	8	3
Hydrogen bond donors	3	1
acceptors	4	3
Randic Index	9.0	8.1
Pi Energy (eV)	26.8	28.1

IX.4. Conclusions

Results from a set of experiments evaluating the biodegradation of NAP, a non-steroidal anti-inflammatory have been presented here. The utility of the cometabolic process model for NAP biodegradation linked to AOB to describe the experimental data under differing experimental conditions has been demonstrated. The data suggest that AOB are less effective at cometabolic biodegradation of NAP relative to ATN, the only other PhAC for which analogous estimates of cometabolic biodegradation coefficients are available. Interestingly, an analysis of potential PhAC properties which could help to explain these differences lead to the preliminary inference that PhAC transport to membrane-bound AMO may not be the rate limiting step in PhAC biodegradation by AOB. Rather, stereochemistry, hydrogen bonding and potentially molecular orbital pi-energies may have a more important role in determining the efficacy of cometabolic PhAC biodegradation by AOB. Firm conclusions here are premature given the limited number of data at present. A broader study of numerous PhACs which are cometabolically biodegraded by AOB is warranted providing an opportunity to interrogate the role of specific PhAC chemometric properties.

Chapter X. Conclusions and Recommendations for Future Research

X.1. Conclusions

With more than 3,000 potentially harmful microconstituents in the environment, an exclusive focus on a single objective, such as nutrient removal, is not only problematic but also irresponsible environmental stewardship. The ecotoxicological impact of pharmaceuticals (PhACs) is particularly concerning given the explosion in development and use of these chemicals over the last thirty years and incomplete attenuation of these chemicals in wastewater treatment plants (WWTPs). Biological treatment processes are responsible for the majority of this attenuation in conventional WWTPs, with biodegradation and sorption being the two primary attenuation mechanisms.

A review of the available data for PhAC removal during biological treatment in WWTPs which included 51 PhACs, suggests that PhAC removal varies significantly, even for single PhAC, from highly recalcitrant to almost complete removal. This is the first such comprehensive evaluation of PhAC removal across WWTPs and a range of unit operations. The analysis suggests that typical WWTP design and operating parameters such as SRT and biomass concentration (using MLVSS as a surrogate) are incapable of serving as effective predictors for PhAC removal performance. *In fact, operation of biological treatment processes at long SRTs (typically utilized to achieve biological nutrient removal) should not be considered a prerequisite or predictor for PhAC removal.* The review also highlights that the capabilities of biological wastewater treatment

processes may be limited when considering complete attenuation of PhACs in wastewater. Additional process options integrating both physical-chemical and biological treatment may ultimately be required where high degrees of PhAC attenuation are necessary. Examples of such approaches include incorporation of powdered activated carbon (e.g., PACT) within the biological treatment process to increase the potential for PhAC sorption, coupled with side-stream oxidation or ultrasonic treatment of sludge.

A comparison of PhAC removal in MBR and suspended growth processes indicates no clear trend in PhAC removal - suggesting both types of processes can be used effectively for treatment of PhACs at the low concentrations typically present in domestic wastewater. The advantages of MBR systems, such as small footprint and higher effluent quality, must be measured on a case by case basis against the disadvantages of higher cost, greater energy consumption and greater operational complexity. Interestingly, a review of the available data suggests that the pseudo-first-order rate coefficients for the attenuation PhACs are higher in suspended growth processes than they are in MBRs for many PhACs. The role of sorption on the other hand, is much more relevant in MBRs, where the sorbed fraction of a PhAC may account for up to 80% of the total PhAC mass in a given reactor.

There is however a wide variation in PhAC K_D values, even for a single PhAC, making it difficult to predict the extent of PhAC sorption *a priori*. A broader evaluation of PhAC sorption, across a range of processes and unit operations, using existing values of the PhAC distribution coefficient was therefore explored in Chapter VI. This analysis suggests *that the conventional use of single-parameter models based on octanol-water partition coefficients has limited predictive capability. Rather, polyparameter models*

developed in this research utilizing chemometric properties of PhACs as predictors offers significantly improved predictive capability. These polyparameter models suggest that the single best predictor for PhAC sorption is the charge of the dominant species. Other important predictors include molecular weight (MW), molecular volume (MV), aromaticity, number of rotatable bonds (nRB), hydrogen bonding capacity (hydrogen bond donors- nHBD and acceptors- nHBA) and polar surface area (PSA).

This research (Chapter III) also highlighted the limited number of studies where the role of nitrifiers in PhAC removal has been evaluated. Therefore, laboratory experiments were coupled with mathematical modeling in this research to evaluate the role of nitrifying bacteria in PhAC biodegradation, focusing on the beta blockers atenolol, metoprolol and sotalol. Results from these experiments (described in Chapter VII) indicate that only ATN is readily biodegraded by the nitrification enrichment culture used herein. Thus, care should therefore be taken to avoid assuming that the occurrence of nitrification leads to biodegradation of PhACs. *Furthermore, results from this research casts considerable doubt on the utility of PhAC therapeutic class (e.g., NSAID or beta blocker) for understanding or predicting environmental fate and transport in natural and engineered environments.* Results from the biodegradation experiments conducted with ATN (Chapter VII) and NAP (Chapter IX) indicate that *biodegradation of these PhACs occurred cometabollically during ammonia oxidation.* In fact, the ATN and NAP results suggest that the role of ammonia oxidizing bacteria in PhAC biodegradation may be more relevant than previously estimated. It is conventionally assumed that the role of nitrifying bacteria in PhAC biodegradation is limited by the fact that these organisms represent only a small fraction of the biomass in a wastewater treatment plant. This research suggests that the contribution of AOB to PhAC biodegradation

outweighs their proportion in the biomass. Note that this conclusion is predicated on the assumption that the capability of heterotrophs in WWTP bioreactors to degrade PhACs is comparable to that of the heterotrophs present within the enrichment cultures employed in this research. This assumption is supported by reports of comparable degradation rates of the endocrine disrupting compound 17α-Ethinylestradiol obtained utilizing heterotrophs grown on primary effluent and complex synthetic carbon sources (Clark et. al, 2009).

ATN and NAP degradation was effectively described using a cometabolic process-based (CPB) model. In the CPB model PhAC biodegradation is linked to AOB during growth and non-growth conditions using the cometabolic transformation coefficients $T_{PhAC\text{-}AOB}$ and $k_{PhAC\text{-}AOB}$, respectively. *The CPB model represents a novel use of an integrated cometabolic biodegradation module within the activated sludge model (ASM) framework.* This approach is particularly relevant considering the widespread utility of the ASM modeling framework in industrial WWTP process simulators (e.g., Biowin, GPSx, etc.). Consortium level assessments of PhAC biodegradation offer increased sophistication and greater generalizability over pseudo first order biodegradation rate coefficients which offer no mechanistic insight. *Results from this research also suggest that ATN competitively inhibits AOB growth (with an inhibition coefficient $K_{I,ATN\text{-}AOB}$ = 1.84 ± 0.39 μg/L). This is the first reported inhibition of AOB by PhACs during nitrification during biological wastewater treatment.*

The influence of biokinetic parameter selection on model inferences was explored (Chapter VIII) using the Generalized Likelihood Uncertainty Estimation (GLUE) technique. Results from experiments with ATN and SOT were utilized to evaluate the applicability of GLUE when modeling nitrification using a two-step model within the

ASM framework. The difference in the inhibitory impact of these PhACs on AOB was utilized to assess the ability of GLUE to generate meaningful confidence intervals for the nitrification process where competitive inhibition was present (ATN) or absent (SOT). *Results suggest that where model structural errors are unaccounted for, GLUE is unable to adequately provide confidence intervals. This finding is particularly important considering the growing popularity of GLUE in wastewater treatment process modeling and the relative ease of implementing GLUE within industrial biological process modeling tools.* GLUE was subsequently utilized with the correct model describing nitrification to evaluate the sensitivity of ATN-AOB competabolic biodegradation coefficients (T, k and K_I) to AOB and NOB biokinetics. *The sensitivity analysis was conducted using a novel application of elasticity coefficients.* Results suggest that the coefficient describing cometabolic degradation of atenolol during the growth of ammonia oxidizing bacteria (AOB) is relatively insensitive to variation in ammonia and nitrite oxidizing biokinetic parameters. In contrast, the parameter describing cometabolic degradation of atenolol by AOB entering or undergoing endogenous respiration appears to be sensitive to the specific growth rate of ammonia oxidizing bacteria. The elasticities were used to assess whether estimates of atenolol-AOB cometabolic biodegradation coefficients from lab-scale experiments could be used more generally. *The application of elasticities to biological wastewater process modeling suggests that seasonal temperature variations may be an important factor in pharmaceutical biodegradation during biological wastewater treatment.*

Results from Chapter IX, where the CPB model was utilized to describe biodegradation of naproxen, suggest that the CPB model holds utility more generally to describe the biodegradation of PhACs during nitrification. These results suggest that

specific PhAC chemometric properties, such as molecular orbital energy and stereochemistry may, in part, explain the differences in PhAC biodegradation by AOB.

X.2. Recommendations for Future Research

The work performed in this research largely focused on evaluating the biodegradation of PhACs during nitrification, with an emphasis on a small group of PhACs. Two important conclusions from this research are (i) nitrification is not a relevant biodegradation mechanism for all the PhACs evaluated and (ii) ammonia oxidation has an important role where PhAC biodegradation is observed. In order to generalize the role of nitrification in PhAC biodegradation, additional studies are recommended for to examine a broad range of PhACs utilizing the protocol established in this research. A broader investigation will provide an opportunity to explore the role of PhAC properties in determining the propensity for biodegradation by AOB during nitrification. Furthermore, such research will provide a framework for predictive models for the PhAC-AOB biodegradation coefficients (T,k and where relevant K_I) integrating PhAC chemometric properties.

Additional research is also recommended to investigate and quantify the mechanisms of PhAC biodegradation by heterotrophic bacteria (HET) in WWTP biological processes. It remains an open question whether or not a subset of *specialized heterotrophs* have the ability to utilize PhACs, at environmentally relevant concentrations, as a carbon source for growth. Investigations such as these would expand the utility of the CPB model through the replacement of the lumped biomass normalized coefficient related to the role of HET with biomass specific growth and non-growth rate coefficients. Given the adaptability and flexibility of the activated

sludge model framework, these coefficients and processes can readily be implemented and employed as more emphasis is placed on the management of microconstituents in WWTP effluents.

The above recommendations build upon, and expand the utility of, the CPB model developed herein. It would be beneficial to expand such research to elucidate which bacteria or consortia are responsible for PhAC biodegradation in mixed populations. Batch experiments such as those conducted here, coupled with gene sequencing tools available today allow interrogation of the microbiome at relatively low cost.

Additional research is also recommended to improve the predictive capability for PhAC sorption during biological wastewater treatment. The research presented here indicates that the use of polyparameter predictive model developed herein significantly enhance the predictive capability relative to traditional log K_{OW} based models. However, even the best models developed herein can only explain approximately 60% of the variance in the available PhAC sorption data. More research is therefore required to assess the role that biosolids surface properties have in PhAC sorption.

Finally, it is recommended that research be directed toward developing one of our most undervalued resources - treated wastewater. Publicly supported reuse requires that the environmental science and engineering community address concerns related to the occurrence of PhACs and other microconsitutents in the environment. Even more generally, the community needs to develop holistic solutions that address the ever increasing demand for water resources while understanding and managing environmental and ecological risk associated with both water quantity and quality. Traditionally, these priorities have been addressed separately. However, balancing

these multiple priorities, while challenging, is critical to achieve comprehensive environmental stewardship. Although it is expeditious to target removal of specific pollutants, emphasis must be equally placed on elucidating and addressing the impact on WWTP discharges, constituting mixtures and myriad compounds. It is imperative that scientists and engineers avoid applying a "one size fits all" solution to any of these problems. Moreover, the environmental engineering community should look beyond specific treatment options, process configurations, or unit operations, and toward more integrated water management strategies that aim to better balance treatment targets with the stewardship of both water and energy resources. Solutions based on sound science and engineering need to be tailored to site specific objectives, constraints and challenges. Furthermore, a crucial element of such research is effectively communicating not only to the scientific community but to the general public, the benefits of engineered solutions rather than placing focus on potentially catastrophic outcomes.

References

Abegglen, C., A. Joss, C. S. McArdell, G. Fink, M. P. Schlusener, T. A. Ternes and H. Siegrist (2009). "The fate of selected micropollutants in a single-house MBR." *Water Res* **43**(7): 2036-2046.

Abraham, M. H. (1993). "Application of solvation equations to Chemical and Biochemical Processes." *Pure Appl Chem* **65**(12): 2503-2512.

Adams, C., Y. Wang, K. Loftin and M. Meyer (2002). "Removal of antibiotics from surface and distilled water in conventional water treatment processes." *Journal of Environmental Engineering-Asce* **128**(3): 253-260.

Ahn, J. H., S. Kim, H. Park, B. Rahm, K. Pagilla and K. Chandran (2010). "N2O Emissions from Activated Sludge Processes, 2008-2009: Results of a National Monitoring Survey in the United States." *Environmental Science & Technology* **44**(12): 4505-4511.

Ahn, J. H., R. Yu and K. Chandran (2008). "Distinctive microbial ecology and biokinetics of autotrophic ammonia and nitrite oxidation in a partial nitrification Bioreactor." *Biotechnology and Bioengineering* **100**(6): 1078-1087.

Akaike, H. (1973). Information Theory and an Extension of the Maximum Likelihood Principle. F. Csáki and B. N. Petrov. Budapest, Hungary, Akademiai Kiado**:** 267-281.

Akaike, H. (1974). "A new look at the statistical model identification." *Automatic Control, IEEE Transactions on* **19**(6): 716-723.

Alvarez-Cohen, L. and P. L. McCarty (1991). "A Cometabolic Biotransformation Model for Halogenated Aliphatic Compounds Exhibiting Product Toxicity." *Environmental Science & Technology* **25**(8): 1381-1387.

Alvarez-Cohen, L. and G. E. Speitel (2001). "Kinetics of aerobic cometabolism of chlorinated solvents." *Biodegradation* **12**(2): 105-126.

Andreottola, G., G. Bortone and A. Tilche (1997). "Experimental validation of a simulation and design model for nitrogen removal in sequencing batch reactors." *Water Science and Technology* **35**(1): 113-120.

Andreozzi, R., M. Raffaele and P. Nicklas (2003). "Pharmaceuticals in STP effluents and their solar photodegradation in aquatic environment." *Chemosphere* **50**(10): 1319-1330.

Andrews, J. F. (1968). "A Mathematical Model for Continuour Culture of Microorganisms Utilizing Inhibitory Substrates." *Biotechnology and Bioengineering* **10**(6): 707-&.

Andrews, J. F. (1968). "A Mathematical Model for Continuous Culture of Microorganisms Utilizing Inhibitory Substances." *Biotechnology and Bioengineering* **10**(6): 707-&.

Andrews, J. H. and R. F. Harris (1986). "R-selection and K-selection and Microbial Ecology." *Advances in Microbial Ecology* **9**: 99-147.

References

APHA, AWWA and WEF (1999). Standard Methods for the Examination of Water and Wastewater.

Arcangeli, J. P. and E. Arvin (1997). "Modeling of the cometabolic biodegradation of trichloroethylene by toluene oxidizing bacteria in a biofilm system." *Environmental Science & Technology* **31**(11): 3044-3052.

Arcangeli, J. P., E. Arvin and H. M. Jensen (1995). Cometabolic biodegradation of trichloroethylene in a biofilm reactor. *Bioremediation of Chlorinated Solvents*. R. E. Hinchee, A. Leeson and L. Semprini. **3:** 203-211.

Arp, D. J., P. S. G. Chain and M. G. Klotz (2007). "The impact of genome analyses on our understanding of ammonia-oxidizing bacteria." *Annual Review of Microbiology* **61**: 503-528.

Arp, D. J., L. A. Sayavedra-Soto and N. G. Hommes (2002). "Molecular biology and biochemistry of ammonia oxidation by Nitrosomonas europaea." *Archives of Microbiology* **178**(4): 250-255.

Arp, D. J. and L. Y. Stein (2003). "Metabolism of inorganic N compounds by ammonia-oxidizing bacteria." *Critical Reviews in Biochemistry and Molecular Biology* **38**(6): 471-495.

Arp, D. J., C. M. Yeager and M. R. Hyman (2001). "Molecular and cellular fundamentals of aerobic cometabolism of trichloroethylene." *Biodegradation* **12**(2): 81-103.

Associated-Press. (2008). "An AP Investigation: Pharmaceuticals found in the drinking water." Retrieved 10/01/2010, 2010, from http://hosted.ap.org/specials/interactives/pharmawater_site/index.html.

Bailey, J. E. and D. F. Ollis (1986). *Biochemical Engineering Fundamentals*, McGraw-Hill.

Balakrishnan, S. and W. Eckenfelder (1969). "Nitrogen Relationships in Biological Treatment Processes. 1. Nitrification in Activated Sludge Process." *Water Research* **3**(1): 73-&.

Barnard, J. L. (2006). *Biological Nutrient Removal: Where have we been, Where are we going?* . Water Environment Federation Annual Technical Conference, Dallas, TX, Water Environment Federation.

Batt, A. L., S. Kim and D. S. Aga (2006). "Enhanced biodegradation of iopromide and trimethoprim in nitrifying activated sludge." *Environmental Science & Technology* **40**(23): 7367-7373.

Bedard, C. and R. Knowles (1989). "Physiology, Biochemistry and Specific Inhibitors of CH4, NH4+ and CO Oxidation by Methanotrophs and Nitrifiers." *Microbiological Reviews* **53**(1): 68-84.

Belia, E., Y. Amerlinck, L. Benedetti, B. Johnson, G. Sin, P. A. Vanrolleghem, K. V. Gernaey, S. Gillot, M. B. Neumann, L. Rieger, A. Shaw and K. Villez (2009). "Wastewater treatment modelling: dealing with uncertainties." *Water Science and Technology* **60**(8): 1929-1941.

Bendz, D., N. A. Paxeus, T. R. Ginn and F. J. Loge (2005). "Occurrence and fate of pharmaceutically active compounds in the environment, a case study: Hoje River in Sweden." *Journal of Hazardous Materials* **122**(3): 195-204.

References

Benedetti, L., F. Claeys, I. Nopens and P. A. Vanrolleghem (2011). "Assessing the convergence of LHS Monte Carlo simulations of wastewater treatment models." *Water Science and Technology* **63**(10): 2219-2224.

Bernhard, M., J. Muller and T. P. Knepper (2006). "Biodegradation of persistent polar pollutants in wastewater: comparison of an optimised lab-scale membrane bioreactor and activated sludge treatment." *Water Res* **40**(18): 3419-3428.

Beven, K. and A. Binley (1992). "The Future of Distributed Models - Model Calibration and Uncertainty Prediction." *Hydrological Processes* **6**(3): 279-298.

Beven, K. and J. Freer (2001). "A dynamic TOPMODEL." *Hydrological Processes* **15**(10): 1993-2011.

Bouwer, E. J., P. L. Mccarty, H. Bouwer and R. C. Rice (1984). "Organic Contaminant Behavior during Rapid Infiltration of Secondary Wastewater at the Phoenix 23rd Avenue Project." *Water Res* **18**(4): 463-472.

Boxall, A. B. A. (2004). "The environmental side effects of medication - How are human and veterinary medicines in soils and water bodies affecting human and environmental health?" *Embo Reports* **5**(12): 1110-1116.

Boxall, A. B. A., M. A. Rudd, B. W. Brooks, D. J. Caldwell, K. Choi, S. Hickmann, E. Innes, K. Ostapyk, J. P. Staveley, T. Verslycke, G. T. Ankley, K. F. Beazley, S. E. Belanger, J. P. Berninger, P. Carriquiriborde, A. Coors, P. C. DeLeo, S. D. Dyer, J. F. Ericson, F. Gagne, J. P. Giesy, T. Gouin, L. Hallstrom, M. V. Karlsson, D. G. J. Larsson, J. M. Lazorchak, F. Mastrocco, A. McLaughlin, M. E. McMaster, R. D. Meyerhoff, R. Moore, J. L. Parrott, J. R. Snape, R. Murray-Smith, M. R. Servos, P. K. Sibley, J. O. Straub, N. D. Szabo, E. Topp, G. R. Tetreault, V. L. Trudeau and G. Van Der Kraak (2012). "Pharmaceuticals and Personal Care Products in the Environment: What Are the Big Questions?" *Environmental Health Perspectives* **120**(9): 1221-1229.

Brame, R., R. Paternoster, P. Mazerolle and A. Piquero (1998). "Testing for the equality of maximum-likelihood regression coefficients between two independent equations." *Journal of Quantitative Criminology* **14**(3): 245-261.

Bruce, G. M., R. C. Pleus and S. A. Snyder (2010). "Toxicological Relevance of Pharmaceuticals in Drinking Water." *Environmental Science & Technology* **44**(14): 5619-5626.

Burnham, K. P. and D. R. Anderson (2002). *Model selection and multimodel inference : a practical information-theoretic approach*. New York, Springer-Verlag.

California Department of Public Health. (2007). "Groundwater Recharge Reuse - Draft Regulation."

Camacho-Munoz, D., J. Martin, J. L. Santos, E. Alonso, I. Aparicio, T. De la Torre, C. Rodriguez and J. J. Malfeito (2012). "Effectiveness of three configurations of membrane bioreactors on the removal of priority and emergent organic compounds from wastewater: comparison with conventional wastewater treatments." *Journal of Environmental Monitoring* **14**(5): 1428-1436.

Carballa, M., F. Omil and J. M. Lema (2005). "Removal of cosmetic ingredients and pharmaceuticals in sewage primary treatment." *Water Res* **39**(19): 4790-4796.

References

Carballa, M., F. Omil, T. Ternes and J. M. Lema (2007). "Fate of pharmaceutical and personal care products (PPCPs) during anaerobic digestion of sewage sludge." *Water Res* **41**(10): 2139-2150.

Carucci, A., G. Cappai and M. Piredda (2006). "Biodegradability and toxicity of pharmaceuticals in biological wastewater treatment plants." *Journal of Environmental Science and Health Part a-Toxic/Hazardous Substances & Environmental Engineering* **41**(9): 1831-1842.

Castiglioni, S., R. Bagnati, R. Fanelli, F. Pomati, D. Calamari and E. Zuccato (2006). "Removal of pharmaceuticals in sewage treatment plants in Italy." *Environmental Science & Technology* **40**(1): 357-363.

Chain, P., J. Lamerdin, F. Larimer, W. Regala, V. Lao, M. Land, L. Hauser, A. Hooper, M. Klotz, J. Norton, L. Sayavedra-Soto, D. Arciero, N. Hommes, M. Whittaker and D. Arp (2003). "Complete genome sequence of the ammonia-oxidizing bacterium and obligate chemolithoautotroph Nitrosomonas europaea." *Journal of Bacteriology* **185**(9): 2759-2773.

Chandran, K., Z. Hu and B. F. Smets (2005). "Applicability of an extant batch respirometric assay in describing dynamics of ammonia and nitrite oxidation in a nitrifying bioreactor." *Water Science and Technology* **52**(10-11): 503-508.

Chandran, K., Z. Q. Hu and B. F. Smets (2008). "A critical comparison of extant batch respirometric and substrate depletion assays for estimation of nitrification biokinetics." *Biotechnology and Bioengineering* **101**(1): 62-72.

Chandran, K. and B. F. Smets (2000). "Single-step nitrification models erroneously describe batch ammonia oxidation profiles when nitrite oxidation becomes rate limiting." *Biotechnology and Bioengineering* **68**(4): 396-406.

Chang, H. L. and L. Alvarez-Cohen (1995). "Model for the Cometabolic Biodegradation of Chlorinated Organics." *Environmental Science & Technology* **29**(9): 2357-2367.

Chang, W. K. and C. S. Criddle (1997). "Experimental evaluation of a model for cometabolism: Prediction of simultaneous degradation of trichloroethylene and methane by a methanotrophic mixed culture." *Biotechnology and Bioengineering* **56**(5): 492-501.

Chapra, S. C. (2008). *Surface Water-Quality Modeling*. Long Grove, IL, Waveland Press, Inc.

Chefetz, B., T. Mualem and J. Ben-Ari (2008). "Sorption and mobility of pharmaceutical compounds in soil irrigated with reclaimed wastewater." *Chemosphere* **73**(8): 1335-1343.

Chiew, F. H. S. (2006). "Estimation of rainfall elasticity of streamflow in Australia." *Hydrological Sciences Journal-Journal Des Sciences Hydrologiques* **51**(4): 613-625.

Chin, D. A. (2009). "Predictive Uncertainty in Water-Quality Modeling." *Journal of Environmental Engineering-Asce* **135**(12): 1315-1325.

Chiron, S., E. Gomez and H. Fenet (2010). "Nitration Processes of Acetaminophen in Nitrifying Activated Sludge." *Environmental Science & Technology* **44**(1): 284-289.

Cirja, M., P. Ivashechkin, A. Schäffer and P. F. X. Corvini (2008). "Factors affecting the removal of organic micropollutants from wastewater in conventional treatment plants (CTP) and membrane bioreactors (MBR)." *Reviews in Environmental Science and Biotechnology* **7**(1): 61-78.

Clara, M., N. Kreuzinger, B. Strenn, O. Gans and H. Kroiss (2005). "The solids retention time-a suitable design parameter to evaluate the capacity of wastewater treatment plants to remove micropollutants." *Water Research* **39**(1): 97-106.

Clara, M., B. Strenn, M. Ausserleitner and N. Kreuzinger (2004). "Comparison of the behaviour of selected micropollutants in a membrane bioreactor and a conventional wastewater treatment plant." *Water Science and Technology* **50**(5): 29-36.

Clara, M., B. Strenn, O. Gans and N. Kreuzinger (2003). "The elimination of selected pharmaceuticals in wastewater treatment - lab scale experiments with different sludge retention times." *Water Resources Management II* **8**: 227-236.

Clara, M., B. Strenn, O. Gans, E. Martinez, N. Kreuzinger and H. Kroiss (2005). "Removal of selected pharmaceuticals, fragrances and endocrine disrupting compounds in a membrane bioreactor and conventional wastewater treatment plants." *Water Res* **39**(19): 4797-4807.

Clark, D. E. (1999). "Rapid calculation of polar molecular surface area and its application to the prediction of transport phenomena. 1. Prediction of intestinal absorption." *Journal of Pharmaceutical Sciences* **88**(8): 807-814.

Clark, C.D., L. Gaulke and H.D. Stensel (2008). *Effect of Primary Substrate and Solids Retention Time on Biodegradation of 17α-Ethinylestradiol (EE2)*. WEFTEC 2009, Orlando, FL, WEF.

Cleuvers, M. (2004). "Mixture toxicity of the anti-inflammatory drugs diclofenac, ibuprofen, naproxen, and acetylsalicylic acid." *Ecotoxicol Environ Safe* **59**(3): 309-315.

Cosenza, A., G. Mannina, M. B. Neumann, G. Viviani and P. A. Vanrolleghem (2013). "Biological nitrogen and phosphorus removal in membrane bioreactors: model development and parameter estimation." *Bioprocess and Biosystems Engineering* **36**(4): 499-514.

Criddle, C. S. (1993). "The Kinetics of Cometabolism." *Biotechnology and Bioengineering* **41**(11): 1048-1056.

Cunningham, V. L., C. Perino, V. J. D'Aco, A. Hartmann and R. Bechter (2009). "Human health risk assessment of carbamazepine in surface waters of North America and Europe." *Regulatory Toxicology and Pharmacology* **56**(3): 343-351.

Cyrañski, M. K., T. M. Krygowski, A. R. Katritzky and P. v. R. Schleyer (2002). "To What extent Can aromaticity be defined uniquely?" *J Org Chem* **67**(4): 1333-1338.

Daims, H., J. L. Nielsen, P. H. Nielsen, K. H. Schleifer and M. Wagner (2001). "In situ characterization of Nitrospira-like nitrite oxidizing bacteria active in wastewater treatment plants." *Applied and Environmental Microbiology* **67**(11): 5273-5284.

Danish-Environmental-Protection-Agency (2002). Feminisation of fish - The effect of estrogenic compounds and their fate in sewage treatment plants and nature.

Daughton, C. G. (2010). Pharmaceutical Ingredients in Drinking Water: Overview of Occurrence and Significance of Human Exposure. *Contaminants of Emerging Concern in the Environment: Ecological and Human Health Considerations*. R. U. Halden. Washington, Amer Chemical Soc. **1048:** 9-68.

Daughton, C. G. and T. A. Ternes (1999). "Pharmaceuticals and personal care products in the environment: agents of subtle change?" *Environ Health Perspect* **107 Suppl 6**: 907-938.

Daughton, C. H. and T. A. Ternes (2000). "Special Report: Pharmaceuticals and personal care products in the environment: agents of subtle change? (vol 107, pg 907, 1999)." *Environmental Health Perspectives* **108**: 598-598.

Davis, A. M. and S. J. Teague (1999). "Hydrogen bonding, hydrophobic interactions, and failure of the rigid receptor hypothesis." *Angewandte Chemie-International Edition* **38**(6): 737-749.

De Gusseme, B., L. Vanhaecke, W. Verstraete and N. Boon (2011). "Degradation of acetaminophen by Delftia tsuruhatensis and Pseudomonas aeruginosa in a membrane bioreactor." *Water Res* **45**(4): 1829-1837.

De Wever, H., S. Weiss, T. Reemtsma, J. Vereecken, J. Muller, T. Knepper, O. Rorden, S. Gonzalez, D. Barcelo and M. Dolores Hernando (2007). "Comparison of sulfonated and other micropollutants removal in membrane bioreactor and conventional wastewater treatment." *Water Res* **41**(4): 935-945.

Degrémont S.A. (1991). *Water treatment handbook*. Paris, Degremont.

Deksissa, T., D. De Pauw and P. A. Vanrolleghem (2004). "Dynamic in-stream fate modeling of xenobiotic organic compounds: A case study of linear alkylbenzene sulfonates in the Lambro River, Italy." *Environmental Toxicology and Chemistry* **23**(9): 2267-2278.

Di Bella, G., G. Mannina and G. Viviani (2008). "An integrated model for physical-biological wastewater organic removal in a submerged membrane bioreactor: Model development and parameter estimation." *Journal of Membrane Science* **322**(1): 1-12.

Dickenson, E. R. V., J. Drewes, S. Khan and J. A. McDonald (2010). Evaluation of QPSR Techniques for Wastewater Treatment Processes. Alexandria, VA, Water Environment Research Foundation.

Dokianakis, S. N., M. E. Kornaros and G. Lyberatos (2004). "On the effect of pharmaceuticals on bacterial nitrite oxidation." *Water Science and Technology* **50**(5): 341-346.

Doucette, W. J. (2003). "Quantitative structure-activity relationships for predicting soil-sediment sorption coefficients for organic chemicals." *Environ Toxicol Chem* **22**(8): 1771-1788.

Drillia, P., K. Stamatelatou and G. Lyberatos (2005). "Fate and mobility of pharmaceuticals in solid matrices." *Chemosphere* **60**(8): 1034-1044.

Drug-Topics (2010). 2009 Top 200 generic drugs by total prescriptions, Advanstar Communications.

Drug-Topics (2011). 2010 Top 200 branded drugs by retail dollars, Advanstar Communications.

Drug-Topics (2011). 2010 Top 200 generic drugs by total prescriptions, Advanstar Communications.

Dytczak, M. A., K. L. Londry and J. A. Oleszkiewicz (2008). "Activated sludge operational regime has significant impact on the type of nitrifying community and its nitrification rates." *Water Research* **42**(8-9): 2320-2328.

Edwards, M., E. Topp, C. D. Metcalfe, H. Li, N. Gottschall, P. Bolton, W. Curnoe, M. Payne, A. Beck, S. Kleywegt and D. R. Lapen (2009). "Pharmaceutical and personal care products in tile drainage following surface spreading and injection of dewatered municipal biosolids to an agricultural field." *Science of the Total Environment* **407**(14): 4220-4230.

Ely, R. L., K. J. Williamson, R. B. Guenther, M. R. Hyman and D. J. Arp (1995). "A Cometabolic Kinetics Model Incorporating Enzyme-Inhibition, Inactivation, and Recovery.1.Model Development, Analysis and Testing." *Biotechnology and Bioengineering* **46**(3): 218-231.

Ely, R. L., K. J. Williamson, M. R. Hyman and D. J. Arp (1997). "Cometabolism of chlorinated solvents by nitrifying bacteria: Kinetics, substrate interactions, toxicity effects, and bacterial response." *Biotechnology and Bioengineering* **54**(6): 520-534.

Ensign, S. A., M. R. Hyman and D. J. Arp (1993). "Invitro Activation of Ammonia Monooxygease from Nitrosomonas Europaea by Copper." *Journal of Bacteriology* **175**(7): 1971-1980.

Ensign, S. A., M. R. Hyman and D. J. Arp (1993). "INVITRO ACTIVATION OF AMMONIA MONOOXYGENASE FROM NITROSOMONAS-EUROPAEA BY COPPER." *Journal of Bacteriology* **175**(7): 1971-1980.

Ertl, P., B. Rohde and P. Selzer (2000). "Fast calculation of molecular polar surface area as a sum of fragment-based contributions and its application to the prediction of drug transport properties." *J Med Chem* **43**(20): 3714-3717.

Falas, P., H. R. Andersen, A. Ledin and J. l. C. Jansen (2012). "Impact of solid retention time and nitrification capacity on the ability of activated sludge to remove pharmaceuticals." *Environmental Technology* **33**(8): 865-872.

Falas, P., A. Baillon-Dhumez, H. R. Andersen, A. Ledin and J. la Cour Jansen (2012). "Suspended biofilm carrier and activated sludge removal of acidic pharmaceuticals." *Water Research* **46**(4): 1167-1175.

Farges, B., L. Poughon, D. Roriz, C. Creuly, C. G. Dussap and C. Lasseur (2012). "Axenic Cultures of Nitrosomonas europaea and Nitrobacter winogradskyi in Autotrophic Conditions: a New Protocol for Kinetic Studies." *Applied Biochemistry and Biotechnology* **167**(5): 1076-1091.

Fell, D. A. (1992). "Metabolic Control Analysis - A Survey of Its Theoretical and Experimental Development." *Biochemical Journal* **286**: 313-330.

Fernandez-Fontaina, E., F. Omil, J. M. Lema and M. Carballa (2012). "Influence of nitrifying conditions on the biodegradation and sorption of emerging micropollutants." *Water Research* **46**(16): 5434-5444.

Fernandez-Fontaina, E., I. Pinho, M. Carballa, F. Omil and J. M. Lema (2013). "Biodegradation kinetic constants and sorption coefficients of micropollutants in membrane bioreactors." *Biodegradation* **24**(2): 165-177.

Ferrari, B., N. Paxeus, R. Lo Giudice, A. Pollio and J. Garric (2003). "Ecotoxicological impact of pharmaceuticals found in treated wastewaters: study of carbamazepine, clofibric acid, and diclofenac." *Ecotoxicology and Environmental Safety* **55**(3): 359-370.

Ferris, M. J., G. Muyzer and D. M. Ward (1996). "Denaturing gradient gel electrophoresis profiles of 16S rRNA-defined populations inhabiting a hot spring microbial mat community." *Applied and Environmental Microbiology* **62**(2): 340-346.

Flores-Alsina, X., L. Corominas, M. B. Neumann and P. A. Vanrolleghem (2012). "Assessing the use of activated sludge process design guidelines in wastewater treatment plant projects: A methodology based on global sensitivity analysis." *Environmental Modelling & Software* **38**: 50-58.

Flores-Alsina, X., I. Rodriguez-Roda, G. Sin and K. V. Gernaey (2008). "Multi-criteria evaluation of wastewater treatment plant control strategies under uncertainty." *Water Research* **42**(17): 4485-4497.

Freer, J., K. Beven and B. Ambroise (1996). "Bayesian estimation of uncertainty in runoff prediction and the value of data: An application of the GLUE approach." *Water Resources Research* **32**(7): 2161-2173.

Gälli, R. and P. L. McCarty (1989). "Kinetics of Biotransformation of 1,1,1-Trichloroethylene by Clostridium Sp Strain TCAIIB." *Applied and Environmental Microbiology* **55**(4): 845-851.

Gaulke, L. S., S. E. Strand, T. F. Kalhorn and H. D. Stensel (2008). "17 alpha-ethinylestradiol Transformation via Abiotic Nitration in the Presence of Ammonia Oxidizing Bacteria." *Environmental Science & Technology* **42**(20): 7622-7627.

Gaulke, L. S., S. E. Strand, T. F. Kalhorn and H. D. Stensel (2009). "Estrogen Biodegradation Kinetics and Estrogenic Activity Reduction for Two Biological Wastewater Treatment Methods." *Environmental Science & Technology* **43**(18): 7111-7116.

Gilch, S., O. Meyer and I. Schmidt (2009). "A soluble form of ammonia monooxygenase in Nitrosomonas europaea." *Biological Chemistry* **390**(9): 863-873.

Gilch, S., M. Vogel, M. W. Lorenz, O. Meyer and I. Schmidt (2009). "Interaction of the mechanism-based inactivator acetylene with ammonia monooxygenase of Nitrosomonas europaea." *Microbiology-Sgm* **155**: 279-284.

Ginestet, P., J. M. Audic, V. Urbain and J. C. Block (1998). "Estimation of nitrifying bacterial activities by measuring oxygen uptake in the presence of the metabolic inhibitors allylthiourea and azide." *Applied and Environmental Microbiology* **64**(6): 2266-2268.

Gobel, A., C. S. McArdell, A. Joss, H. Siegrist and W. Giger (2007). "Fate of sulfonamides, macrolides, and trimethoprim in different wastewater treatment technologies." *Science of the Total Environment* **372**(2-3): 361-371.

Gomez, M. J., M. J. M. Bueno, S. Lacorte, A. R. Fernandez-Alba and A. Aguera (2007). "Pilot survey monitoring pharmaceuticals and related compounds in a sewage treatment plant located on the Mediterranean coast." *Chemosphere* **66**(6): 993-1002.

Grady, C. P. L., G. T. Diagger and H. C. Lim (1999). *Biological Wastewater Treatment*. New York, Marcel Dekker.

Graham, D. W., C. W. Knapp, E. S. Van Vleck, K. Bloor, T. B. Lane and C. E. Graham (2007). "Experimental demonstration of chaotic instability in biological nitrification." *Isme Journal* **1**(5): 385-393.

Guisasola, A., I. Jubany, J. A. Baeza, J. Carrera and J. Lafuente (2005). "Respirometric estimation of the oxygen affinity constants for biological ammonium and nitrite oxidation." *Journal of Chemical Technology and Biotechnology* **80**(4): 388-396.

Gujer, W. (2010). "Nitrification and me - A subjective review." *Water Research* **44**(1): 1-19.

HACH Company (2008). Nitrogen, Ammonia Salicylate Method.

Halling-Sørensen, B., S. Nors Nielsen, P. F. Lanzky, F. Ingerslev, H. C. Holten Lützhøft and S. E. Jørgensen (1998). "Occurrence, fate and effects of pharmaceutical substances in the environment- A review." *Chemosphere* **36**(2): 357-393.

Harms, G., A. C. Layton, H. M. Dionisi, I. R. Gregory, V. M. Garrett, S. A. Hawkins, K. G. Robinson and G. S. Sayler (2003). "Real-time PCR quantification of nitrifying bacteria in a municipal wastewater treatment plant." *Environmental Science & Technology* **37**(2): 343-351.

Heberer, T. (2002). "Occurrence, fate, and removal of pharmaceutical residues in the aquatic environment: a review of recent research data." *Toxicology Letters* **131**(1-2): 5-17.

Helbling, D. E., D. R. Johnson, M. Honti and K. Fenner (2012). "Micropollutant Biotransformation Kinetics Associate with WWTP Process Parameters and Microbial Community Characteristics." *Environmental Science & Technology* **46**(19): 10579-10588.

Hemsi, P. S., C. D. Shackelford and L. A. Figueroa (2010). "Calibration of Reactive Transport Models for Remediation of Mine Drainage in Solid-Substrate Biocolumns." *Journal of Environmental Engineering-Asce* **136**(9): 914-925.

Henze, M., C. P. L. Grady, W. Gujer, G. V. R. Marais and T. Matsuo (1987). "A general model for single-sludge wastewater treatment systems." *Water Research* **21**(5): 505-515.

Henze, M., W. Gujer, T. Mino and M. V. Loosdrecht (2000). *Activated sludge models ASM1, ASM2, ASM2d and ASM3*. London, IWA Pub.

Henze, M., W. Gujer, T. Mino, T. Matsuo, M. C. Wentzel, G. V. R. Marais and M. C. M. Van Loosdrecht (1999). "Activated Sludge Model No.2d, ASM2d." *Water Science and Technology* **39**(1): 165-182.

Henze, M., W. Gujer, T. Mino, T. Matsuo, M. C. Wentzel and G. Vonmarais (1995). "Wastewater and Biomass Characterization for the Activated Slduge Model No 2 - Biological Phosphorus Removal." *Water Science and Technology* **31**(2): 13-23.

Hiatt, W. C. and C. P. L. Grady (2008). "An Updated Process Model for Carbon Oxidation, Nitrification, and Denitrification." *Water Environment Research* **80**(11): 2145-2156.

Hignite, C. and D. L. Azarnoff (1977). "Drugs and Drug Metabolites as Environmental Contaminants: Chlorophenoxyisobutyrate and Salicylic Acid in Sewage Water Effluent." *Life Sciences* **20**(2): 337-342.

Hockenbury, M. R. and C. P. L. Grady (1977). "Inibition of Nitrification - Effects of Selected Organic Compounds." *Journal Water Pollution Control Federation* **49**(5): 768-777.

Holbrook, R. D., K. A. Massie and J. T. Novak (2005). "A comparison of membrane bioreactor and conventional-activated-sludge mixed liquor and biosolids characteristics." *Water Environment Research* **77**(4): 323-330.

Hooper, A. B. and K. R. Terry (1973). "Specific Inhibitors of Ammonia Oxidation in Nitrosomonas." *Journal of Bacteriology* **115**(2): 480-485.

Hooper, A. B., T. Vannelli, D. J. Bergmann and D. M. Arciero (1995). *Enzymology of the oxidation of ammonia to nitrite by bacteria*. Beijerinck Centennial Symposium on Microbial Physiology and Gene Regulation - Emerging Principles and Applications, The Hague, Netherlands, Kluwer Academic Publ.

Hooper, A. B., T. Vannelli, D. J. Bergmann and D. M. Arciero (1997). "Enzymology of the oxidation of ammonia to nitrite by bacteria." *Antonie Van Leeuwenhoek International Journal of General and Molecular Microbiology* **71**(1-2): 59-67.

Hornberger, G. M. and R. C. Spear (1981). "An Approach to the Preliminary Analysis of Environmnetal Systems." *Journal of Environmental Management* **12**(1): 7-18.

Horsing, M., A. Ledin, R. Grabic, J. Fick, M. Tysklind, J. la Cour Jansen and H. R. Andersen (2011). "Determination of sorption of seventy-five pharmaceuticals in sewage sludge." *Water Res* **45**(15): 4470-4482.

Horvath, R. S. (1972). "Microbial Cometabolism and Degradation of Organic Compounds in Nature." *Bacteriological Reviews* **36**(2): 146-&.

Hurvich, C. M. and C. L. Tsai (1991). "Bias of the Corrected AIC Criterion for Underfitted Regression and Time Series Models." *Biometrika* **78**(3): 499-509.

Huuskonen, J. (2003). "Prediction of soil sorption coefficient of a diverse set of organic chemicals from molecular structure." *J Chem Inf Comput Sci* **43**(5): 1457-1462.

Hyland, K. C., E. R. Dickenson, J. E. Drewes and C. P. Higgins (2012). "Sorption of ionized and neutral emerging trace organic compounds onto activated sludge from different wastewater treatment configurations." *Water Research* **46**(6): 1958-1968.

Iacopozzi, I., V. Innocenti, S. Marsili-Libelli and E. Giusti (2007). "A modified Activated Sludge Model No. 3 (ASM3) with two-step nitrification-denitrification." *Environmental Modelling & Software* **22**(6): 847-861.

Igarashi, N., H. Moriyama, T. Fujiwara, Y. Fukumori and N. Tanaka (1997). "The 2.8 angstrom structure of hydroxylamine oxidoreductase from a nitrifying chemoautotrophic bacterium, Nitrosomonas europaea." *Nature Structural Biology* **4**(4): 276-284.

Ings, J. S., N. George, M. C. S. Peter, M. R. Servos and M. M. Vijayan (2012). "Venlafaxine and atenolol disrupt epinephrine-stimulated glucose production in rainbow trout hepatocytes." *Aquatic Toxicology* **106**: 48-55.

Isidori, M., M. Lavorgna, A. Nardelli, A. Parrella, L. Previtera and M. Rubino (2005). "Ecotoxicity of naproxen and its phototransformation products." *Science of the Total Environment* **348**(1-3): 93-101.

Janus, T. and B. Ulanicki (2010). "Modelling SMP and EPS formation and degradation kinetics with an extended ASM3 model." *Desalination* **261**(1-2): 117-125.

Jelic, A., F. Fatone, S. Di Fabio, M. Petrovic, F. Cecchi and D. Barcelo (2012). "Tracing pharmaceuticals in a municipal plant for integrated wastewater and organic solid waste treatment." *Science of the Total Environment* **433**: 352-361.

Jelic, A., M. Gros, A. Ginebreda, R. Cespedes-Sanchez, F. Ventura, M. Petrovic and D. Barcelo (2011). "Occurrence, partition and removal of pharmaceuticals in sewage water and sludge during wastewater treatment." *Water Res* **45**(3): 1165-1176.

Jjemba, P. K. (2008). *Pharma-Ecology: The Occurrence and Fate of Pharmaceuticals and Personal Care Products in the Environment*, Wiley.

Jones, R. M., P. Dold, I. Takacs, K. Chapman, B. Wett, S. Murthy and M. O'Shaughnessy (2007). Simulation for Operation and Control of Reject Water Treatment Processes. San Diego, CA, Water Environment Federation.

Joss, A., S. Zabczynski, A. Gobel, B. Hoffmann, D. Loffler, C. S. McArdell, T. A. Ternes, A. Thomsen and H. Siegrist (2006). "Biological degradation of pharmaceuticals in municipal wastewater treatment: proposing a classification scheme." *Water Research* **40**(8): 1686-1696.

Jubany, I., J. Carrera, J. Lafuente and J. A. Baeza (2008). "Start-up of a nitrification system with automatic control to treat highly concentrated ammonium wastewater: Experimental results and modeling." *Chemical Engineering Journal* **144**(3): 407-419.

Jubany, I., J. Lafuente, J. A. Baeza and J. Carrera (2009). "Total and stable washout of nitrite oxidizing bacteria from a nitrifying continuous activated sludge system using automatic control based on Oxygen Uptake Rate measurements." *Water Research* **43**(11): 2761-2772.

Juretschko, S., G. Timmermann, M. Schmid, K. H. Schleifer, A. Pommerening-Roser, H. P. Koops and M. Wagner (1998). "Combined molecular and conventional analyses of nitrifying bacterium diversity in activated sludge: Nitrosococcus mobilis and Nitrospira-like bacteria as dominant populations." *Applied and Environmental Microbiology* **64**(8): 3042-3051.

Kaelin, D., R. Manser, L. Rieger, J. Eugster, K. Rottermann and H. Siegrist (2009). "Extension of ASM3 for two-step nitrification and denitrification and its calibration and validation with batch tests and pilot scale data." *Water Research* **43**(6): 1680-1692.

Kagle, J., A. W. Porter, R. W. Murdoch, G. Rivera-Cancel and A. G. Hay (2009). Biodegradation of Pharmaceutical and Personal Care Products. *Advances in Applied Mircobiology, Vol 67*. **67:** 65-108.

Kampschreur, M. J., C. Picioreanu, N. Tan, R. Kleerebezem, M. S. M. Jetten and M. C. M. van Loosdrecht (2007). "Unraveling the source of nitric oxide emission during nitrification." *Water Environment Research* **79**(13): 2499-2509.

Keenan, J. E., S. E. Strand and H. D. Stensel (1994). Degradation Kinetics of Chlorinated Solvents by a Propane-Oxidizing Enrichment Culture. *Bioremediation of Chlorinated and Polycyclic Aromatic Hydrocarbon Compounds*. R. E. Hinchee, A. Leeson, L. Semprini and S. K. Ong. 1994, CRC Press. **2:** 1-13.

Keener, W. K. and D. J. Arp (1994). "Transformations of Aromatic-Compounds by Nitrosomonas Europaea." *Applied and Environmental Microbiology* **60**(6): 1914-1920.

Keith, L. H. (1976). *Identification & analysis of organic pollutants in water*. Ann Arbor, Ann Arbor Science Publishers.

Khunjar, W. O. and N. G. Love (2011). "Sorption of carbamazepine, 17 alpha-ethinylestradiol, iopromide and trimethoprim to biomass involves interactions with exocellular polymeric substances." *Chemosphere* **82**(6): 917-922.

Khunjar, W. O., S. A. Mackintosh, J. Skotnicka-Pitak, S. Baik, D. S. Aga and N. G. Love (2011). "Elucidating the Relative Roles of Ammonia Oxidizing and Heterotrophic Bacteria during the Biotransformation of 17 alpha-Ethinylestradiol and Trimethoprim." *Environmental Science & Technology* **45**(8): 3605-3612.

Kimura, K., H. Hara and Y. Watanabe (2005). "Removal of pharmaceutical compounds by submerged membrane bioreactors (MBRs)." *Desalination* **178**(1-3): 135-140.

Kindaichi, T., Y. Kawano, T. Ito, H. Satoh and S. Okabe (2006). "Population dynamics and in situ kinetics of nitrifying bacteria in autotrophic nitrifying biofilms as determined by real-time quantitative PCR." *Biotechnology and Bioengineering* **94**(6): 1111-1121.

Klappenbach, J. A., P. R. Saxman, J. R. Cole and T. M. Schmidt (2001). "rrndb: the Ribosomal RNA Operon Copy Number Database." *Nucleic Acids Research* **29**(1): 181-184.

Klopman, G., J. Y. Li, S. M. Wang and M. Dimayuga (1994). "Computer Automated Log P Calculations Based on an Extended Group-Contribution Approach." *J Chem Inf Comp Sci* **34**(4): 752-781.

Knackmuss, H. J. (1996). "Basic knowledge and perspectives of bioelimination of xenobiotic compounds." *Journal of Biotechnology* **51**(3): 287-295.

Kocamemi, B. A. and F. Cecen (2005). "Cometabolic degradation of TCE in enriched nitrifying batch systems." *Journal of Hazardous Materials* **125**(1-3): 260-265.

Kocamemi, B. A. and F. Cecen (2007). "Kinetic analysis of the inhibitory effect of trichloroethylene (TCE) on nitrification in cometabolic degradation." *Biodegradation* **18**(1): 71-81.

Kocamemi, B. A. and F. Cecen (2009). "Biodegradation of 1,2-dichloroethane (1,2-DCA) by cometabolism in a nitrifying biofilm reactor." *International Biodeterioration & Biodegradation* **63**(6): 717-726.

Kocamemi, B. A. and F. Cecen (2010). "Biological removal of the xenobiotic trichloroethylene (TCE) through cometabolism in nitrifying systems." *Bioresource Technology* **101**(1): 430-433.

Kocamemi, B. A. and F. Cecen (2010). "Cometabolic degradation and inhibition kinetics of 1,2-dichloroethane (1,2-DCA) in suspended-growth nitrifying systems." *Environmental Technology* **31**(3): 295-305.

Koch, G., M. Kühni, W. Gujer and H. Siegrist (2000). "Calibration and validation of activated sludge model no. 3 for Swiss municipal wastewater." *Water Research* **34**(14): 3580-3590.

Kolpin, D. W., E. T. Furlong, M. T. Meyer, E. M. Thurman, S. D. Zaugg, L. B. Barber and H. T. Buxton (2002). "Pharmaceuticals, hormones, and other organic wastewater contaminants in US streams, 1999-2000: A national reconnaissance." *Environ. Sci. Technol.* **36**(6): 1202-1211.

Kostich, M. S. and J. M. Lazorchak (2008). "Risks to aquatic organisms posed by human pharmaceutical use." *Sci Total Environ* **389**(2-3): 329-339.

Kraigher, B. and I. Mandic-Mulec (2011). "Nitrification activity and community structure of nitrite-oxidizing bacteria in the bioreactors operated with addition of pharmaceuticals." *Journal of Hazardous Materials* **188**(1-3): 78-84.

Kreuzinger, N., M. Clara, B. Strenn and H. Kroiss (2004). "Relevance of the sludge retention time (SRT) as design criteria for wastewater treatment plants for the removal of endocrine disruptors and pharmaceuticals from wastewater." *Water Science and Technology* **50**(5): 149-156.

Kubinyi, H. (2001). *Hydrogen bonding: The last mystery in drug design?*

Kumar, A., B. A. Chang and I. Xagoraraki (2010). "Human Health Risk Assessment of Pharmaceuticals in Water: Issues and Challenges Ahead." *International Journal of Environmental Research and Public Health* **7**(11): 3929-3953.

Larsen, M. C. (2009). Statement before the Committee on Natural Resources Subcommittee on Insular Affairs, Oceans, and Wildlife. www.usgs.gov/congressional/hearings/docs/larsen_09june09.doc.

Lee, Y. and J. A. Oleszkiewicz (2003). "Effects of predation and ORP conditions on the performance of nitrifiers in activated sludge systems." *Water Research* **37**(17): 4202-4210.

Li, B., S. Irvin and K. Baker (2006). *The variation of nitrifying bacterial population sizes in a sequencing batch reactor (SBR) treating low/mid/high concentrated wastewater*. WEFTEC 2006, New Orleans, LA, WEF.

Li, W. H., Y. L. Shi, L. H. Gao, J. M. Liu and Y. Q. Cai (2012). "Occurrence of antibiotics in water, sediments, aquatic plants, and animals from Baiyangdian Lake in North China." *Chemosphere* **89**(11): 1307-1315.

Lipinski, C. A., F. Lombardo, B. W. Dominy and P. J. Feeney (1997). "Experimental and computational approaches to estimate solubility and permeability in drug discovery and development settings." *Advanced Drug Delivery Reviews* **23**(1-3): 3-25.

Louca, F. (2007). *Years of High Econometrics*. London, Routledge.

Ludden, T. M., S. L. Beal and L. B. Sheiner (1994). "Comparison of the Akaike Information Criteria, The Schwarz Criterion and the F-Test as Guides to Model Selection." *Journal of Pharmacokinetics and Biopharmaceutics* **22**(5): 431-445.

MacKay, A. A. and D. Vasudevan (2012). "Polyfunctional ionogenic compound sorption: challenges and new approaches to advance predictive models." *Environ Sci Technol* **46**(17): 9209-9223.

Majewsky, M., T. Galle, V. Yargeau and K. Fischer (2011). "Active heterotrophic biomass and sludge retention time (SRT) as determining factors for biodegradation kinetics of pharmaceuticals in activated sludge." *Bioresource Technology* **102**(16): 7415-7421.

Mannhold, R. (2008). *Molecular Drug Properties: Measurement and Prediction*. Weinheim, Wiley-VCH.

Mannina, G., A. Cosenza, P. A. Vanrolleghem and G. Viviani (2011). "A practical protocol for calibration of nutrient removal wastewater treatment models." *Journal of Hydroinformatics* **13**(4): 575-595.

Mannina, G., A. Cosenza and G. Viviani (2012). "Uncertainty assessment of a model for biological nitrogen and phosphorus removal: Application to a large wastewater treatment plant." *Physics and Chemistry of the Earth* **42-44**: 61-69.

Mannina, G., G. Di Bella and G. Viviani (2010). "Uncertainty assessment of a membrane bioreactor model using the GLUE methodology." *Biochemical Engineering Journal* **52**(2-3): 263-275.

Manser, R., W. Gujer and H. Siegrist (2005). "Consequences of mass transfer effects on the kinetics of nitrifiers." *Water Research* **39**(19): 4633-4642.

Manser, R., W. Gujer and H. Siegrist (2006). "Decay processes of nitrifying bacteria in biological wastewater treatment systems." *Water Research* **40**(12): 2416-2426.

Mantovan, P. and E. Todini (2006). "Hydrological forecasting uncertainty assessment: Incoherence of the GLUE methodology." *Journal of Hydrology* **330**(1-2): 368-381.

Marsili-Libelli, Ratini P, Spagni A and Bortone G (2001). "Implementation, study and calibration of a modified ASM2d for the simulation of SBR processes." *Water Science and Technology* **43**(3): 69-76.

Massarsky, A., V. L. Trudeau and T. W. Moon (2011). "beta-Blockers as Endocrine Disruptors: The Potential Effects of Human beta-Blockers on Aquatic Organisms." *Journal of Experimental Zoology Part a-Ecological Genetics and Physiology* **315A**(5): 251-265.

Masse, A., M. Sperandio and C. Cabassud (2006). "Comparison of sludge characteristics and performance of a submerged membrane bioreactor and an activated sludge process at high solids retention time." *Water Research* **40**(12): 2405-2415.

Matter-Müller, C., W. Gujer, W. Giger and W. Stumm (1980). "Non-Biological Elimination Mechanisms in a Biological Sewage-Treatment Plant." *Prog Water Technol* **12**(6): 299-314.

Maurer, M., B. I. Escher, P. Richle, C. Schaffner and A. C. Alder (2007). "Elimination of beta-blockers in sewage treatment plants." *Water Research* **41**(7): 1614-1622.

McCuen, R. H., Z. Knight and A. G. Cutter (2006). "Evaluation of the Nash-Sutcliffe efficiency index." *J Hydrol Eng* **11**(6): 597-602.

McKay, M. D., R. J. Beckman and W. J. Conover (1979). "A Comparison of Three Methods for Selecting Values of Input Variables in the Analysis of Output from a Computer Code." *Technometrics* **21**(2): 239-245.

Metcalf & Eddy, I., G. Tchobanogolous, L. Burton and S. D.H. (2003). *Wastewater Engineering: Treatment and Reuse*, McGraw-Hill.

Metcalfe, C. D., B. G. Koenig, D. T. Bennie, M. Servos, T. A. Ternes and R. Hirsch (2003). "Occurrence of neutral and acidic drugs in the effluents of Canadian sewage treatment plants." *Environmental Toxicology and Chemistry* **22**(12): 2872-2880.

Metcalfe, C. D., X. S. Miao, B. G. Koenig and J. Struger (2003). "Distribution of acidic and neutral drugs in surface waters near sewage treatment plants in the lower Great Lakes, Canada." *Environmental Toxicology and Chemistry* **22**(12): 2881-2889.

Monteiro, S. C. and A. B. A. Boxall (2009). "Factors Affecting the Degradation of Pharmaceuticals in Agricultural Soils." *Environmental Toxicology and Chemistry* **28**(12): 2546-2554.

Monteiro, S. C. and A. B. A. Boxall (2010). Occurrence and Fate of Human Pharmaceuticals in the Environment. *Reviews of Environmental Contamination and Toxicology, Vol 202*. D. M. Whitacre. New York, Springer. **202:** 53-154.

Moriasi, D. N., J. G. Arnold, M. W. Van Liew, R. L. Bingner, R. D. Harmel and T. L. Veith (2007). "Model evaluation guidelines for systematic quantification of accuracy in watershed simulations." *Transactions of the Asabe* **50**(3): 885-900.

Mota, C., J. Ridenoure, J. Y. Cheng and F. L. de los Reyes (2005). "High levels of nitrifying bacteria in intermittently aerated reactors treating high ammonia wastewater." *Fems Microbiology Ecology* **54**(3): 391-400.

Mulder, A., A. A. Vandegraaf, L. A. Robertson and J. G. Kuenen (1995). "Anaerobic Ammonium Oxidation Discovered in a Denitryfying Fluidized Bed Reactor." *Fems Microbiology Ecology* **16**(3): 177-183.

Munz, G., C. Lubello and J. A. Oleszkiewicz (2011). "Factors affecting the growth rates of ammonium and nitrite oxidizing bacteria." *Chemosphere* **83**(5): 720-725.

Munz, G., C. Lubello and J. A. Oleszkiewicz (2011). "Modeling the decay of ammonium oxidizing bacteria." *Water Research* **45**(2): 557-564.

Munz, G., G. Mori, C. Vannini and C. Lubello (2010). "Kinetic parameters and inhibition response of ammonia- and nitrite-oxidizing bacteria in membrane bioreactors and conventional activated sludge processes." *Environmental Technology* **31**(14): 1557-1564.

Myers, R. H., D. C. Montgomery and G. G. Vining (2010). *Generalized Linear Models: With Applications in Engineering and the Sciences*. New York, Wiley-Interscience.

Nakada, N., T. Tanishima, H. Shinohara, K. Kiri and H. Takada (2006). "Pharmaceutical chemicals and endocrine disrupters in municipal wastewater in Tokyo and their removal during activated sludge treatment." *Water Res* **40**(17): 3297-3303.

Nash, J. E. and J. V. Sutcliffe (1970). "River flow forecasting through conceptual models. Part 1: A discussion of principles." *J Hydrol* **10**(3): 282-290.

National Academy of Engineering. (2010). "Grand Challenges for Engineering: Managing the Nitrogen Cycle." Retrieved October 20, 2010, 2010, from http://www.engineeringchallenges.org/cms/8996/9132.aspx.

Ng, H. Y. and S. W. Hermanowicz (2005). "Membrane bioreactor operation at short solids retention times: performance and biomass characteristics." *Water Research* **39**(6): 981-992.

Nguyen, T. H., K. U. Goss and W. P. Ball (2005). "Polyparameter linear free energy relationships for estimating the equilibrium partition of organic compounds between water and the natural organic matter in soils and sediments." *Environ Sci Technol* **39**(4): 913-924.

Norton, J. M., J. J. Alzerreca, Y. Suwa and M. G. Klotz (2002). "Diversity of ammonia monooxygenase operon in autotrophic ammonia-oxidizing bacteria." *Archives of Microbiology* **177**(2): 139-149.

Nowak, O., K. Svardal and P. Schweighofer (1995). "THE DYNAMIC BEHAVIOR OF NITRIFYING ACTIVATED-SLUDGE SYSTEMS INFLUENCED BY INHIBITING WASTE-WATER COMPOUNDS." *Water Science and Technology* **31**(2): 115-124.

Nowak, O., K. Svardal and P. Schweighofer (1995). "Thye Dynamic Behavior of Nitrifying Activated Sludge Systems Influenced by Inhibiting Wastewater Compounds." *Water Science and Technology* **31**(2): 115-124.

Okabe, S., H. Satoh and Y. Watanabe (1999). "In situ analysis of nitrifying biofilms as determined by in situ hybridization and the use of microelectrodes." *Applied and Environmental Microbiology* **65**(7): 3182-3191.

Okey, R. W. and H. D. Stensel (1993). "A QSBR Development Procedure for Aromatic Xenobiotic Degradation by Unacclimated Bacteria." *Water Environment Research* **65**(6): 772-780.

Okey, R. W. and H. D. Stensel (1996). "A QSAR-based biodegradability model - A QSBR." *Water Res* **30**(9): 2206-2214.

Onesios, K. M. and E. J. Bouwer (2012). "Biological removal of pharmaceuticals and personal care products during laboratory soil aquifer treatment simulation with different primary substrate concentrations." *Water Research* **46**(7): 2365-2375.

Onesios, K. M., J. T. Yu and E. J. Bouwer (2009). "Biodegradation and removal of pharmaceuticals and personal care products in treatment systems: a review." *Biodegradation* **20**(4): 441-466.

Oppenheimer, J., R. Stephenson and A. Burbano (2007). "Characterizing the passage of personal care products through wastewater treatment processes." *Water Environment Research* **79**(13): 2564-2577.

Orhon, D. and N. Artan (1994). *Modelling of Activated Sludge Systems*. Lancaster, Techmonic Publishing Company.

Ottmar, K. J., L. M. Colosi and J. A. Smith (2010). "Sorption of Statin Pharmaceuticals to Wastewater-Treatment Biosolids, Terrestrial Soils, and Freshwater Sediment." *J Environ Eng-ASCE* **136**(3): 256-264.

Oulton, R. L., T. Kohn and D. M. Cwiertny (2010). "Pharmaceuticals and personal care products in effluent matrices: A survey of transformation and removal during wastewater treatment and implications for wastewater management." *Journal of Environmental Monitoring* **12**(11): 1956-1978.

Palm, K., P. Stenberg, K. Luthman and P. Artursson (1997). "Polar molecular surface properties predict the intestinal absorption of drugs in humans." *Pharm Res* **14**(5): 568-571.

Park, H., A. Rosenthal, R. Jezek, K. Ramalingam, J. Fillos and K. Chandran (2010). "Impact of inocula and growth mode on the molecular microbial ecology of anaerobic ammonia oxidation (anammox) bioreactor communities." *Water Research* **44**(17): 5005-5013.

Paternoster, R., R. Brame, P. Mazerolle and A. Piquero (1998). "Using the correct statistical test for the quality of regression coefficients." *Criminology* **36**(4): 859-866.

Pauer, J. J. and M. T. Auer (2009). "Formulation and testing of a novel river nitrification model." *Ecological Modelling* **220**(6): 857-866.

Paxeus, N. (2004). "Removal of selected non-steroidal anti-inflammatory drugs (NSAIDs), gemfibrozil, carbamazepine, beta-blockers, trimethoprim and triclosan in conventional wastewater treatment plants in five EU countries and their

discharge to the aquatic environment." *Water Science and Technology* **50**(5): 253-260.

Peev, M., M. Schonerklee and H. De Wever (2004). "Modelling the degradation of low concentration pollutants in membrane bioreactors." *Water Science and Technology* **50**(5): 209-218.

Perez, S. and D. Barcelo (2008). "First Evidence for Occurrence of Hydroxylated Human Metabolites of Diclofenac and Aceclofenac in Wastewater Using QqLIT-MS and QqTOF-MS." *Analytical Chemistry* **80**(21): 8135-8145.

Plosz, B. G., K. H. Langford and K. V. Thomas (2012). "An activated sludge modeling framework for xenobiotic trace chemicals (ASM-X): Assessment of diclofenac and carbamazepine." *Biotechnology and Bioengineering* **109**(11): 2757-2769.

Plósz, B. G., H. Leknes and K. V. Thomas (2010). "Impacts of Competitive Inhibition, Parent Compound Formation and Partitioning Behavior on the Removal of Antibiotics in Municipal Wastewater Treatment." *Environmental Science & Technology* **44**(2): 734-742.

Poeter, E. and D. Anderson (2005). "Multimodel ranking and inference in ground water modeling." *Ground Water* **43**(4): 597-605.

Pomies, M., J. M. Choubert, C. Wisniewski and M. Coquery (2013). "Modelling of micropollutant removal in biological wastewater treatments: A review." *Science of the Total Environment* **443**: 733-748.

Prasse, C., M. Wagner, R. Schulz and T. A. Ternes (2011). "Biotransformation of the Antiviral Drugs Acyclovir and Penciclovir in Activated Sludge Treatment." *Environmental Science & Technology* **45**(7): 2761-2769.

Prosser, J. I. (1989). "Autrotrophic Nitrification in Bacteria." *Advances in Microbial Physiology* **30**: 125-181.

Quinn, B., F. Gagne and C. Blaise (2009). "Evaluation of the acute, chronic and teratogenic effects of a mixture of eleven pharmaceuticals on the cnidarian, Hydra attenuata." *Sci Total Environ* **407**(3): 1072-1079.

Quintana, J. B., R. Rodil, P. Lopez-Mahia, S. Muniategui-Lorenzo and D. Prada-Rodriguez (2010). "Investigating the chlorination of acidic pharmaceuticals and by-product formation aided by an experimental design methodology." *Water Res* **44**(1): 243-255.

Radjenovic, J., M. Petrovic and D. Barcelo (2007). "Analysis of pharmaceuticals in wastewater and removal using a membrane bioreactor." *Analytical and Bioanalytical Chemistry* **387**(4): 1365-1377.

Radjenovic, J., M. Petrovic and D. Barcelo (2009). "Fate and distribution of pharmaceuticals in wastewater and sewage sludge of the conventional activated sludge (CAS) and advanced membrane bioreactor (MBR) treatment." *Water Res* **43**(3): 831-841.

Reichert, P., D. Borchardt, M. Henze, W. Rauch, P. Shanahan, L. Somlyódy and P. A. Vanrolleghem (2001). *River Water Quality Model No. 1*. London, IWA Publishing.

Reif, R., S. Suarez, F. Omil and J. M. Lema (2008). "Fate of pharmaceuticals and cosmetic ingredients during the operation of a MBR treating sewage." *Desalination* **221**(1-3): 511-517.

Richardson, M. L. and J. M. Bowron (1985). "The Fate of Pharmaceutical Chemicals in the Aquatic Environment." *Journal of Pharmacy and Pharmacology* **37**(1): 1-12.

Rieger, L., S. Gillot, G. Langergraber, T. Ohtsuki, A. Shaw, I. Takacs and S. Winkler (2013). *Guidelines for Using Activated Sludge Models*. London, IWA Publishing.

Ritchie, T. J. and S. J. Macdonald (2009). "The impact of aromatic ring count on compound developability--are too many aromatic rings a liability in drug design?" *Drug Discov Today* **14**(21-22): 1011-1020.

Robinson, I., G. Junqua, R. Van Coillie and O. Thomas (2007). "Trends in the detection of pharmaceutical products, and their impact and mitigation in water and wastewater in North America." *Anal Bioanal Chem* **387**(4): 1143-1151.

Rossi-Marshall, E. J., D. W. Kincaid, H. A. Bechtold, T. V. Royer, M. Rojas and J. J. Kelly (2013). "Pharmaceuticals suppress algal growth and microbial respiration and alter bacterial communities in stream biofilms." *Ecological Applications* **23**(3): 583-593.

Rotthauwe, J. H., K. P. Witzel and W. Liesack (1997). "The ammonia monooxygenase structural gene amoA as a functional marker: Molecular fine-scale analysis of natural ammonia-oxidizing populations." *Applied and Environmental Microbiology* **63**(12): 4704-4712.

Sabljic, A., H. Gusten, H. Verhaar and J. Hermens (1995). "QSAR Modeling of Soil Sorption - Improvements and Systematics of log KOC vs. log KOW Correlations." *Chemosphere* **31**(11-12): 4489-4514.

Saez, P. B. and B. E. Rittmann (1991). "Biodegradation Kinetics of 4-Chlorophenol, An Inhibitory Cometabolite." *Research Journal of the Water Pollution Control Federation* **63**(6): 838-847.

Saez, P. B. and B. E. Rittmann (1991). "BIODEGRADATION KINETICS OF 4-CHLOROPHENOL, AN INHIBITORY CO-METABOLITE." *Research Journal of the Water Pollution Control Federation* **63**(6): 838-847.

Saffron, C. M., J.-H. Park, B. E. Dale and T. C. Voice (2006). "Kinetics of contaminant desorption from soil: Comparison of model formulations using the akaike information criterion." *Environmental Science & Technology* **40**(24): 7662-7667.

Saltelli, A., M. Ratto, S. Tarantola and F. Campolongo (2005). "Sensitivity analysis for chemical models." *Chemical Reviews* **105**(7): 2811-2827.

Sangster, J. (1989). "Octanol-Water Partition-Coefficients of Simple Organic-Compounds." *J Phys Chem Ref Data* **18**(3): 1111-1229.

Sankarasubramanian, A., R. M. Vogel and J. F. Limbrunner (2001). "Climate elasticity of streamflow in the United States." *Water Resources Research* **37**(6): 1771-1781.

Sarp, S., K. Chon, I. S. Kim and J. Cho (2011). "Advanced treatment of Membrane Bioreactor (MBR) effluents for effective wastewater reclamation." *Water Science and Technology* **63**(2): 303-310.

Sathyamoorthy, S., K. Chandran and C. A. Ramsburg (submitted). "Degradation of Beta Blockers during Ammonia Oxidation." *Environmental Science & Technology*.

Sathyamoorthy, S. and C. A. Ramsburg (2013). "Assessment of Quantitative Structural Property Relationships for Prediction of Pharmaceutical Sorption during Biological Wastewater Treatment." *Chemosphere* **In Press**.

Sato, C., J. L. Schnoor, D. B. McDonald and J. Huey (1985). "TEST MEDIUM FOR THE GROWTH OF NITROSOMONAS-EUROPAEA." *Applied and Environmental Microbiology* **49**(5): 1101-1107.

Sayavedra-Soto, L. A. and D. J. Arp (2011). *Ammonia Oxidizing Bacteria: Their Biochemistry and Molecular Biology*. Washington, Amer Soc Microbiology.

Schafer, A. I., M. Mastrup and R. L. Jensen (2002). *Particle interactions and removal of trace contaminants from water and wastewaters*. International Congress on Membranes and Membrane Processes (ICOM), Toulouse, France, Elsevier Science Bv.

Schaffer, M., N. Boxberger, H. Boernick, T. Licha and E. Worch (2012). "Sorption influenced transport of ionizable pharmaceuticals onto a natural sandy aquifer sediment at different pH." *Chemosphere* **87**(5): 513-520.

Schmidt, I., C. Look, E. Bock and M. S. M. Jetten (2004). "Ammonium and hydroxylamine uptake and accumulation in Nitrosomonas." *Microbiology-Sgm* **150**: 1405-1412.

Schmidt, S. K., S. Simkins and M. Alexander (1985). "Models for the Kinetics of Biodegradation of Organic Compounds Not Supporting Growth." *Applied and Environmental Microbiology* **50**(2): 323-331.

Schoenerklee, M., M. Peev, H. De Wever, S. Weiss and T. Reemtsma (2009). "Micropollutant Degradation in Wastewater Treatment: Experimental Parameter Estimation for an Extended Biokinetic Model." *Water Air and Soil Pollution* **206**(1-4): 69-81.

Schramm, A., D. De Beer, A. Gieseke and R. Amann (2000). "Microenvironments and distribution of nitrifying bacteria in a membrane-bound biofilm." *Environmental Microbiology* **2**(6): 680-686.

Schramm, A., D. de Beer, J. C. van den Heuvel, S. Ottengraf and R. Amann (1999). "Microscale distribution of populations and activities of Nitrosospira and Nitrospira spp. along a macroscale gradient in a nitrifying bioreactor: Quantification by in situ hybridization and the use of microsensors." *Applied and Environmental Microbiology* **65**(8): 3690-3696.

Schroder, H. F., J. L. Tambosi, R. F. Sena, R. Moreira, H. J. Jose and J. Pinnekamp (2012). "The removal and degradation of pharmaceutical compounds during membrane bioreactor treatment." *Water Science and Technology* **65**(5): 833-839.

Schwarzenbach, R. P., B. I. Escher, K. Fenner, T. B. Hofstetter, C. A. Johnson, U. von Gunten and B. Wehrli (2006). "The challenge of micropollutants in aquatic systems." *Science* **313**(5790): 1072-1077.

Schwarzenbach, R. P., P. M. Gschwend and D. M. Imboden (2003). *Environmental Organic Chemistry*. Hoboken, New Jersey, Wiley.

Semprini, L. and P. L. McCarty (1991). "Comparison between Model Simulations and Field Results for In-Situ Biorestoration of Chlorinated Aliphatics - Part 1. Biostimulation of Methanotrophic Bacteria." *Ground Water* **29**(3): 365-374.

Semprini, L. and P. L. McCarty (1992). "Comparison Between Model Simulations and Field Results for In-Situ Biorestoration of Chlorinated Aliphatics: Part 2. Cometabolic Transformations." *Ground Water* **30**(1): 37-44.

Shi, J., S. Fujisawa, S. Nakai and M. Hosomi (2004). "Biodegradation of natural and synthetic estrogens by nitrifying activated sludge and ammonia-oxidizing bacterium Nitrosomonas europaea." *Water Research* **38**(9): 2322-2329.

Siegrist, H., I. Brunner, G. Koch, L. C. Phan and V. C. Le (1999). "Reduction of biomass decay rate under anoxic and anaerobic conditions." *Water Science and Technology* **39**(1): 129-137.

Siegrist, H. and A. Joss (2012). "Review on the fate of organic micropollutants in wastewater treatment and water reuse with membranes." *Water Science and Technology* **66**(6): 1369-1376.

Siemens, J., G. Huschek, C. Siebe and M. Kaupenjohann (2008). "Concentrations and mobility of human pharmaceuticals in the world's largest wastewater irrigation system, Mexico City-Mezquital Valley." *Water Research* **42**(8-9): 2124-2134.

Sin, G., D. Kaelin, M. J. Kampschreur, I. Takacs, B. Wett, K. V. Gernaey, L. Rieger, H. Siegrist and M. C. M. van Loosdrecht (2008). "Modelling nitrite in wastewater treatment systems: a discussion of different modelling concepts." *Water Science and Technology* **58**(6): 1155-1171.

Sin, G., S. W. H. Van Hulle, D. J. W. De Pauw, A. van Griensven and P. A. Vanrolleghem (2005). "A critical comparison of systematic calibration protocols for activated sludge models: A SWOT analysis." *Water Research* **39**(12): 2459-2474.

Sipma, J., B. Osuna, N. Collado, H. Monclus, G. Ferrero, J. Comas and I. Rodriguez-Roda (2010). "Comparison of removal of pharmaceuticals in MBR and activated sludge systems." *Desalination* **250**(2): 653-659.

Skotnicka-Pitak, J., W. O. Khunjar, N. G. Love and D. S. Aga (2009). "Characterization of Metabolites Formed During the Biotransformation of 17α-Ethinylestradiol by Nitrosomonas europaea in Batch and Continuous Flow Bioreactors." *Environmental Science & Technology* **43**(10): 3549-3555.

Snyder, S. A., E. C. Wert, D. J. Rexing, R. E. Zegers and D. D. Drury (2006). "Ozone oxidation of endocrine disruptors and pharmaceuticals in surface water and wastewater." *Ozone-Science & Engineering* **28**(6): 445-460.

Sperandio, M., A. Masse, M. C. Espinosa-Bouchot and C. Cabassud (2005). "Characterization of sludge structure and activity in submerged membrane bioreactor." *Water Science and Technology* **52**(10-11): 401-408.

Spieck, E., S. Muller, A. Engel, E. Mandelkow, H. Patel and E. Bock (1996). "Two-dimensional structure of membrane-bound nitrite oxidoreductase from Nitrobacter hamburgensis." *Journal of Structural Biology* **117**(2): 117-123.

Stackelberg, P. E., J. Gibs, E. T. Furlong, M. T. Meyer, S. D. Zaugg and R. L. Lippincott (2007). "Efficiency of conventional drinking-water-treatment processes in removal of pharmaceuticals and other organic compounds." *Science of the Total Environment* **377**(2-3): 255-272.

Starkenburg, S. R., P. S. G. Chain, L. A. Sayavedra-Soto, L. Hauser, M. L. Land, F. W. Larimer, S. A. Malfatti, M. G. Klotz, P. J. Bottomley, D. J. Arp and W. J. Hickey (2006). "Genome sequence of the chemolithoautotrophic nitrite-oxidizing bacterium Nitrobacter winogradskyi Nb-255." *Applied and Environmental Microbiology* **72**(3): 2050-2063.

Stasinakis, A. S., C. I. Kordoutis, V. C. Tsiouma, G. Gatidou and N. S. Thomaidis (2010). "Removal of selected endocrine disrupters in activated sludge systems: Effect of sludge retention time on their sorption and biodegradation." *Bioresource Technology* **101**(7): 2090-2095.

Stedinger, J. R., R. M. Vogel, S. U. Lee and R. Batchelder (2008). "Appraisal of the generalized likelihood uncertainty estimation (GLUE) method." *Water Resources Research* **44**: 17.

Stein, L. Y. and D. J. Arp (1998). "Loss of ammonia monooxygenase activity in Nitrosomonas europaea upon exposure to nitrite." *Applied and Environmental Microbiology* **64**(10): 4098-4102.

Stephenson, R. and J. Oppenheimer (2007). Fate of Pharmaceuticals and Personal Care Products Through Municipal Wastewater Treatment Processes, WERF.

Stevens-Garmon, J., J. E. Drewes, S. J. Khan, J. A. McDonald and E. R. Dickenson (2011). "Sorption of emerging trace organic compounds onto wastewater sludge solids." *Water Res* **45**(11): 3417-3426.

Strand, S. E., M. D. Bjelland and H. D. Stensel (1990). "Kinetics of Chlorinated Hydrocarbon Degradation by Suspended Cultures of Methane-Oxidizing Bacteria." *Research Journal of the Water Pollution Control Federation* **62**(2): 124-129.

Strenn, B., M. Clara, O. Gans and N. Kreuzinger (2004). "Carbamazepine, diclofenac, ibuprofen and bezafibrate - investigations on the behaviour of selected pharmaceuticals during wastewater treatment." *Water Science and Technology* **50**(5): 269-276.

Suarez, S., J. M. Lema and F. Omil (2010). "Removal of pharmaceutical and personal care products (PPCPs) under nitrifying and denitrifying conditions." *Water Research* **44**(10): 3214-3224.

Suarez, S., J. M. Lerna and F. Omil (2009). "Pre-treatment of hospital wastewater by coagulation-flocculation and flotation." *Bioresource Technology* **100**(7): 2138-2146.

Suarez, S., M. Ramill, F. Omil and J. M. Lema (2005). "Removal of pharmaceutically active compounds in nitrifying-denitrifying plants." *Water Science and Technology* **52**(8): 9-14.

Suarez, S., R. Reif, J. M. Lema and F. Omil (2012). "Mass balance of pharmaceutical and personal care products in a pilot-scale single-sludge system: Influence of T, SRT and recirculation ratio." *Chemosphere* **89**(2): 164-171.

Sugiura, N. (1978). "Further Analysi of Akaike's Information Criterion and Finite Corrections." *Communications in Statistics Part a-Theory and Methods* **7**(1): 13-26.

Sui, Q., J. Huang, S. B. Deng, W. W. Chen and G. Yu (2011). "Seasonal Variation in the Occurrence and Removal of Pharmaceuticals and Personal Care Products in Different Biological Wastewater Treatment Processes." *Environmental Science & Technology* **45**(8): 3341-3348.

Sundermeyer-klinger, H., W. Meyer, B. Warninghoff and E. Bock (1984). "MEMBRANE-BOUND NITRITE OXIDOREDUCTASE OF NITROBACTER - EVIDENCE FOR A NITRATE REDUCTASE SYSTEM." *Archives of Microbiology* **140**(2-3): 153-158.

Suzuki, I., U. Dular and S. C. Kwok (1974). "Ammonia or Ammonium Ion as Substrate for Oxidation by Nitrosomonas-Europaea Cellsa and Extracts." *Journal of Bacteriology* **120**(1): 556-558.

Szegezdi, J. and F. Csizmadia (2004). "Prediction of distribution coefficient using microconstants." *Abstr Pap Am Chem S* **227**: U1019-U1019.

Tadkaew, N., F. I. Hai, J. A. McDonald, S. J. Khan and L. D. Nghiem (2011). "Removal of trace organics by MBR treatment: the role of molecular properties." *Water Res* **45**(8): 2439-2451.

Taher, E. and K. Chandran (2013). "High-Rate, High-Yield Production of Methanol by Ammonia-Oxidizing Bacteria." *Environmental Science & Technology* **47**(7): 3167-3173.

Tambosi, J. L., R. F. de Sena, M. Favier, W. Gebhardt, H. J. Jose, H. F. Schroder and R. Moreira (2010). "Removal of pharmaceutical compounds in membrane bioreactors (MBR) applying submerged membranes." *Desalination* **261**(1-2): 148-156.

Tanaka, Y., Y. Fukumori and T. Yamanaka (1983). "Purification of Cytochrome-A1C1 from Nitrobacter-Agilis and Characterization of Nitrite Oxidation System of the Bacterium." *Archives of Microbiology* **135**(4): 265-271.

Ternes, T. A. (1998). "Occurrence of drugs in German sewage treatment plants and rivers." *Water Research* **32**(11): 3245-3260.

Ternes, T. A. (2007). "The occurrence of micopollutants in the aquatic environment: a new challenge for water management." *Water Science and Technology* **55**(12): 327-332.

Ternes, T. A., M. Bonerz, N. Herrmann, B. Teiser and H. R. Andersen (2007). "Irrigation of treated wastewater in Braunschweig, Germany: An option to remove pharmaceuticals and musk fragrances." *Chemosphere* **66**(5): 894-904.

Ternes, T. A., N. Herrmann, M. Bonerz, T. Knacker, H. Siegrist and A. Joss (2004). "A rapid method to measure the solid-water distribution coefficient (Kd) for

pharmaceuticals and musk fragrances in sewage sludge." *Water Res* **38**(19): 4075-4084.

Ternes, T. A., M.-L. Janex-Habibi, K. Thomas, K. Norbert and S. Hansruedi (2004). Assessment of Technologies for the Removal of Pharmaceuticals and Personal Care Products in Sewage and Drinking Water Facilities to Improve the Indirect Potable Water Reuse: Detailed Report related to the overall project duration: January 1st, 2001 – June 30th, 2004, EU - Poseidon Project.

Ternes, T. A., J.-H. Marie-Laure, K. Thomas, K. Norbert and S. Hansruedi (2004). Assessment of Technologies for the Removal of Pharmaceuticals and Personal Care Products in Sewage and Drinking Water Facilities to Improve the Indirect Potable Water Reuse: Detailed Report related to the overall project duration: January 1st, 2001 – June 30th, 2004, EU - Poseidon Project.

Teske, A., E. Alm, J. M. Regan, S. Toze, B. E. Rittmann and D. A. Stahl (1994). "Evolutionary Relationships Among Ammonia Oxidizing and Nitrite Oxidizing Bacteria." *Journal of Bacteriology* **176**(21): 6623-6630.

Teske, A., E. Alm, J. M. Regan, S. Toze, B. E. Rittmann and D. A. Stahl (1994). "EVOLUTIONARY RELATIONSHIPS AMONG AMMONIA-OXIDIZING AND NITRITE-OXIDIZING BACTERIA." *Journal of Bacteriology* **176**(21): 6623-6630.

Tixier, C., H. P. Singer, S. Oellers and S. R. Muller (2003). "Occurrence and fate of carbamazepine, clofibric acid, diclofenac, ibuprofen, ketoprofen, and naproxen in surface waters." *Environmental Science & Technology* **37**(6): 1061-1068.

Topp, E., J. Hendel, D. Lapen and R. Chapman (2008). "Fate of the Nonsteroidal Anti-Inflammatory Drug Naproxen in Agricultural Soil Receiving Liquid Municipal Biosolids." *Environmental Toxicology and Chemistry* **27**(10): 2005-2010.

Topp, E., J. G. Hendel, D. R. Lapen and R. Chapman (2008). "Fate of the nonsteroidal anti-inflammatory drug naproxen in agricultural soil receiving liquid municipal biosolids." *Environmental Toxicology and Chemistry* **27**(10): 2005-2010.

Topp, E., S. C. Monteiro, A. Beck, B. B. Coelho, A. B. A. Boxall, P. W. Duenk, S. Kleywegt, D. R. Lapen, M. Payne, L. Sabourin, H. X. Li and C. D. Metcalfe (2008). "Runoff of pharmaceuticals and personal care products following application of biosolids to an agricultural field." *Science of the Total Environment* **396**(1): 52-59.

Tran, N. H., T. Urase and O. Kusakabe (2009). "The characteristics of enriched nitrifier culture in the degradation of selected pharmaceutically active compounds." *Journal of Hazardous Materials* **171**(1-3): 1051-1057.

United States Environmental Protection Agency (2010). Treating Contaminants of Emerging Concern: A Literature Review Database. Washington, DC.

Urase, T. and T. Kikuta (2005). "Separate estimation of adsorption and degradation of pharmaceutical substances and estrogens in the activated sludge process." *Water Research* **39**(7): 1289-1300.

USEPA (2009). Inventory of U.S. Greenhouse Gas Emissions and Sinks: 1990-2006. Washington, D.C.

Vadivelu, V. M., J. Keller and Z. G. Yuan (2006). "Stoichiometric and kinetic characterisation of Nitrosomonas sp in mixed culture by decoupling the growth and energy generation processes." *Journal of Biotechnology* **126**(3): 342-356.

Valentin-Vargas, A., G. Toro-Labrador and A. A. Massol-Deya (2012). "Bacterial Community Dynamics in Full-Scale Activated Sludge Bioreactors: Operational and Ecological Factors Driving Community Assembly and Performance." *Plos One* **7**(8).

van der Star, W. R. L., W. R. Abma, B. Kartal and M. C. M. van Loosdrecht (2011). *Application of the Anammox Process*. Washington, Amer Soc Microbiology.

van Loosdrecht, M. C. M. (2008). *Innovative Nitrogen Removal*. London, Iwa Publishing.

Vezzaro, L., E. Eriksson, A. Ledin and P. S. Mikkelsen (2012). "Quantification of uncertainty in modelled partitioning and removal of heavy metals (Cu, Zn) in a stormwater retention pond and a biofilter." *Water Research* **46**(20): 6891-6903.

Vezzaro, L. and P. S. Mikkelsen (2012). "Application of global sensitivity analysis and uncertainty quantification in dynamic modelling of micropollutants in stormwater runoff." *Environmental Modelling & Software* **27-28**: 40-51.

Viswanadhan, V. N., A. K. Ghose, G. R. Revankar and R. K. Robins (1989). "Atomic physicochemical parameters for three dimensional structure directed quantitative structure-activity relationships. 4. Additional parameters for hydrophobic and dispersive interactions and their application for an automated superposition of certain naturally occurring nucleoside antibiotics." *J Chem Inf Model* **29**(3): 163-172.

Waiser, M. J., D. Humphries, V. Tumber and J. Holm (2011). "Effluent dominated streams. Part 2: Presence and possible effects of pharmaceutical and personal care products in Wascana Creek, Saskachewan, Canada." *Environmental Toxicology and Chemistry* **30**(2): 508-519.

Wammer, K. H. and C. A. Peters (2005). "Polycyclic aromatic hydrocarbon biodegradation rates: A structure-based study." *Environmental Science & Technology* **39**(8): 2571-2578.

Wang, S. and C. K. Gunsch (2011). "Effects of selected pharmaceutically active compounds on treatment performance in sequencing batch reactors mimicking wastewater treatment plants operations." *Water Res* **45**(11): 3398-3406.

Wang, S., R. M. Holzem and C. K. Gunsch (2008). "Effects of pharmaceutically active compounds on a mixed microbial community originating from a municipal wastewater treatment plant." *Environmental Science & Technology* **42**(4): 1091-1095.

Wang, S. Y. and C. K. Gunsch (2011). "Effects of selected pharmaceutically active compounds on the ammonia oxidizing bacterium Nitrosomonas europaea." *Chemosphere* **82**(4): 565-572.

Wang, X., X. Wen, C. Criddle, G. Wells, J. Zhang and Y. Zhao (2010). "Community analysis of ammonia-oxidizing bacteria in activated sludge of eight wastewater treatment systems." *Journal of Environmental Sciences-China* **22**(4): 627-634.

WEF (2005). *Clarifier Design: WEF Manual of Practice No. FD-8*. New York, McGraw-Hill.

WEF (2007). Microconstituents Glossary. Alexandria, VA, Water Environment Federation.

Weidinger, K., B. Neuhauser, S. Gilch, U. Ludewig, O. Meyer and I. Schmidt (2007). "Functional and physiological evidence for a Rhesus-type ammonia transporter in Nitrosomonas europaea." *Fems Microbiology Letters* **273**(2): 260-267.

Westerhoff, P., Y. Yoon, S. Snyder and E. Wert (2005). "Fate of endocrine-disruptor, pharmaceutical, and personal care product chemicals during simulated drinking water treatment processes." *Environmental Science & Technology* **39**(17): 6649-6663.

Wick, A., G. Fink, A. Joss, H. Siegrist and T. A. Ternes (2009). "Fate of beta blockers and psycho-active drugs in conventional wastewater treatment." *Water Research* **43**(4): 1060-1074.

Wilderer, P. A. and W. G. Characklis (1989). Structure and Function of Biofilms. *Structure and Function of Biofilms*. W. G. Characklis and P. A. Wilderer. **46:** 5-17.

Winkler, M. K. H., J. P. Bassin, R. Kleerebezem, D. Y. Sorokin and M. C. M. van Loosdrecht (2012). "Unravelling the reasons for disproportion in the ratio of AOB and NOB in aerobic granular sludge." *Applied Microbiology and Biotechnology* **94**(6): 1657-1666.

Xue, W., C. Wu, K. Xiao, X. Huang, H. Zhou, H. Tsuno and H. Tanaka (2010). "Elimination and fate of selected micro-organic pollutants in a full-scale anaerobic/anoxic/aerobic process combined with membrane bioreactor for municipal wastewater reclamation." *Water Res* **44**(20): 5999-6010.

Yi, T. and W. F. Harper, Jr. (2007). "The effect of biomass characteristics on the partitioning and sorption hysteresis of 17alpha-ethinylestradiol." *Water Res* **41**(7): 1543-1553.

Zahn, J. A., D. M. Arciero, A. B. Hooper and A. A. DiSpirito (1996). "Evidence for an iron center in the ammonia monooxygenase from Nitrosomonas europaea." *FEBS Letters* **397**(1): 35-38.

Zimmerman, M. J. (2005). Occurrence of organic wastewater contaminants, pharmaceuticals, and personal care products in selected water supplies, Cape Cod, Massachusetts, June 2004, USGS.

Zorita, S., L. Martensson and L. Mathiasson (2009). "Occurrence and removal of pharmaceuticals in a municipal sewage treatment system in the south of Sweden." *Science of the Total Environment* **407**(8): 2760-2770.

Appendices

Appendix A: Studies evaluating the removal and biodegradation of PhACs in biological wastewater treatment processes

Table App.A-1. Studies included that evaluate removal of PhACs during biological treatment. Studies are summarized by process types (e.g., suspended growth, MBR, batch studies) and reported operating SRT of the process. SRT is reported as being in one of four categories: <5 d, 5 – 10 d, 10 – 20 d and >20 d, where SRT is not reported – study is classified under N/D (No/Data)

Process	SRT (d)				
	<5	5 - 10	10 - 20	>20	N/D
Suspended Growth		Majewsky et. al. (2011)		Majewsky et. al. (2011)	
		Sui et al. (2011)	Sui et al. (2011)	Suarez et al. (2010) (2)	Kimura et al. (2005a); Kimura et al. (2005b); Kimura et al. (2007)
		Jelic et al. (2011) (2)	Jelic et al. (2011)	(Reif et al., 2011)	
		Zorita et al. (2009)	Chiron et al. (2010)		
	Wick et al. (2009)		Wick et al. (2009)		
	Radjenovic et al. (2007); Perez and Barcelo (2008)	Smook et al. (2008)	Tran et al. (2009)		
	Stephenson and Oppenheimer (2007) (2)	Stephenson and Oppenheimer (2007) (2)	Stephenson and Oppenheimer (2007) (2)	Stephenson and Oppenheimer (2007) (2)	
		Maurer et al. (2007)	Maurer et al. (2007)		
			Gobel et al. (2007)	Gobel et al. (2007)	
		Kimura et al. (2005a); Kimura et al. (2005b); Kimura et al. (2007)		De Wever et al. (2007)	
		Batt et al. (2007)	Batt et al. (2007) (2)	Batt et al. (2007)	
		Yu et al. (2006)			
	Nakada et. al. (2006) (2)	Nakada et. al. (2006) (3)			
	(Lishman et al., 2006) (1)	Lishman et al.,(2006) (5)	(Lishman et al., 2006) (2)	(Lishman et al., 2006) (1)	
		Carucci et al. (2006) (2)	Carucci et al. (2006) (3)		
			Bernhard et al. (2006)		
		Batt et al. (2006)	Batt et al. (2006)		

Table App.A-1. Studies included that evaluate removal of PhACs during biological treatment. Studies are summarized by process types (e.g., suspended growth, MBR, batch studies) and reported operating SRT of the process. SRT is reported as being in one of four categories: <5 d, 5 – 10 d, 10 – 20 d and >20 d, where SRT is not reported – study is classified under N/D (No/Data)

Process	SRT (d)				
	<5	5 - 10	10 - 20	>20	N/D
				Suarez et al. (2005)	
			Joss et al. (2005)	Joss et al. (2005) (2)	
	Clara et al. (2004); Clara et al. (2005b)			Clara et al. (2004); Clara et al. (2005b) (4)	
	Clara et al. (2003); Kreuzinger et al. (2004); Strenn et al. (2004); Clara et al. (2005a) (3)	Clara et al. (2003); Kreuzinger et al. (2004); Strenn et al. (2004); Clara et al. (2005a) (3)	Clara et al. (2003); Kreuzinger et al. (2004); Strenn et al. (2004); Clara et al. (2005a) (3)	Clara et al. (2003); Kreuzinger et al. (2004); Strenn et al. (2004); Clara et al. (2005a) (3)	
					(Carballa et al., 2004; Carballa et al., 2005b)
MBR		Sarp et al. (2011)	Sui et al. (2011)	Tadkaew et al. (2010)	De Gusseme et al. (2009); De Gusseme et al. (2011)
		Yu et al. (2006)	Xue et al. (2010)	Delgado et al. (2009); Delgado et al. (2010a); Delgado et al. (2010b)	Smook et al. (2008)
			Smook et al. (2008)	Aubenneau et al. (2010)	
			Stephenson and Oppenheimer (2007)	Abegglen et al. (2009)	
			Kimura et al. (2005a); Kimura et al. (2005b); Kimura et al. (2007)	Kimura et al. (2005a); Kimura et al. (2005b); Kimura et al. (2007)	Kimura et al. (2005a); Kimura et al. (2005b); Kimura et al. (2007)
				Radjenovic et al. (2007); Perez and Barcelo (2008)	
				Reif et al. (2008)	

Table App.A-1. Studies included that evaluate removal of PhACs during biological treatment. Studies are summarized by process types (e.g., suspended growth, MBR, batch studies) and reported operating SRT of the process. SRT is reported as being in one of four categories: <5 d, 5 – 10 d, 10 – 20 d and >20 d, where SRT is not reported – study is classified under N/D (No/Data)

Process	SRT (d)				
	<5	5 - 10	10 - 20	>20	N/D
			Gobel et al. (2007)	Gobel et al. (2007)	
				De Wever et al. (2007)	
				Gonzalez et al. (2006)	
				Bernhard et al. (2006)	
			Joss et al. (2005)	Joss et al. (2005)	
				De Wever et al. (2004); Quintana and Reemtsma (2004); Quintana et al. (2005)	
			Clara et al. (2004); Clara et al. (2005b)	Clara et al. (2004); Clara et al. (2005b) (2)	
				Clara et al. (2003); Kreuzinger et al. (2004); Strenn et al. (2004); Clara et al. (2005a) (3)	

Table App.A-1. Studies included that evaluate removal of PhACs during biological treatment. Studies are summarized by process types (e.g., suspended growth, MBR, batch studies) and reported operating SRT of the process. SRT is reported as being in one of four categories: <5 d, 5 – 10 d, 10 – 20 d and >20 d, where SRT is not reported – study is classified under N/D (No/Data)

Process	SRT (d)				
	<5	5 - 10	10 - 20	>20	N/D
Batch			Xue et al. (2010)	Suarez et al. (2010) (2)	De Gusseme et al. (2009); De Gusseme et al. (2011)
			Chiron et al. (2010)	Kimura et al. (2005a); Kimura et al. (2005b); Kimura et al. (2007)	Abegglen et al. (2009)
			Wick et al. (2009)		Urase and Kikuta (2005)
			Tran et al. (2009)		
			Kosjek et al. (2007); Kraigher et al. (2008); Kosjek et al. (2009); Kraigher and Mandic-Mulec (2011)		
			Maurer et al. (2007)		
			Joss et al. (2006)	Joss et al. (2006)	
			Batt et al. (2006)		
				De Wever et al. (2004); Quintana and Reemtsma (2004); Quintana et al. (2005)	
Other Fixed Film Processes					Batt et al. (2007)
					Gonzalez et al. (2006)

Table App.A-2. Removal of PhACs during biological wastewater treatment summarized by study. The following data are provided for removals of each PhAC evaluated in each study: the number of data (N_{DATA}), average (Avg.), standard deviation (SD), minimum (Min.), 25th , median and 75th percentile (Q1, Median and Q3) and maximum (Max.).

PhAC	Study Reference	N_{DATA}	Avg.	SD	Min.	Q1	Median	Q3	Max.
ACM	Radjenovic et. al., 2007	1	0.98		0.98		0.98		0.98
ACM	Sarp et. al., 2011	1	0.99		0.99		0.99		0.99
ACM	Radjenovic et. al., 2009	3	1.00	0.00	1.00	1.00	1.00	1.00	1.00
ATN	Wick et. al., 2009	3	0.37	0.25	0.08	0.08	0.49	0.54	0.54
ATN	Sarp et. al., 2011	1	0.39		0.39		0.39		0.39
ATN	Jelic et. al., 2011	3	0.54	0.39	0.09	0.09	0.68	0.83	0.83
ATN	Radjenovic et. al., 2009	3	0.69	0.08	0.61	0.61	0.70	0.77	0.77
ATN	Maurer et. al., 2007	2	0.76	0.04	0.73		0.76		0.79
ATV	Jelic et. al., 2011	3	0.13	0.07	0.07	0.07	0.12	0.21	0.21
AZI	Gobel et. al., 2007	4	0.62	0.32	0.22	0.30	0.66	0.92	0.97
BIS	Wick et. al., 2009	3	0.17	0.12	0.04	0.04	0.21	0.27	0.27
BZF	Jelic et. al., 2011	3	0.44	0.32	0.12	0.12	0.44	0.76	0.76
BZF	Radjenovic et. al., 2007	1	0.48		0.48		0.48		0.48
BZF	Radjenovic et. al., 2009	3	0.86	0.05	0.81	0.81	0.88	0.90	0.90
CBZ	Xue et. al., 2010	1	0.08		0.08		0.08		0.08
CBZ	Jelic et. al., 2011	3	0.10	0.11	0.00	0.00	0.08	0.21	0.21
CBZ	Wick et. al., 2009	2	0.10	0.08	0.04		0.10		0.16
CBZ	Tran et. al., 2009	3	0.17	0.16	0.05	0.05	0.10	0.35	0.35
CBZ	Sarp et. al., 2011	1	0.44		0.44		0.44		0.44
CIM	Jelic et. al., 2011	3	0.65	0.27	0.42	0.42	0.60	0.94	0.94
CLA	Tran et. al., 2009	3	0.12	0.03	0.10	0.10	0.10	0.15	0.15
CLA	Jelic et. al., 2011	1	0.21		0.21		0.21		0.21
CLA	Radjenovic et. al., 2007	1	0.28		0.28		0.28		0.28
CLA	Kimura et. al., 2007	3	0.61	0.19	0.50	0.50	0.50	0.82	0.82
CLM	Gobel et. al., 2007	6	0.25	0.22	0.04	0.08	0.15	0.49	0.58
CPL	Wick et. al., 2009	2	0.09	0.05	0.05		0.09		0.12

Table App.A-2. Removal of PhACs during biological wastewater treatment summarized by study. The following data are provided for removals of each PhAC evaluated in each study: the number of data (N_{DATA}), average (Avg.), standard deviation (SD), minimum (Min.), 25th , median and 75th percentile (Q1, Median and Q3) and maximum (Max.).

PhAC	Study Reference	N_{DATA}	Avg.	SD	Min.	Q1	Median	Q3	Max.
DCF	Xue et. al., 2010	1	0.10		0.10		0.10		0.10
DCF	Jelic et. al., 2011	3	0.29	0.20	0.09	0.09	0.28	0.50	0.50
DCF	Tran et. al., 2009	3	0.35	0.36	0.05	0.05	0.25	0.75	0.75
DCF	Radjenovic et. al., 2009	3	0.50	0.25	0.22	0.22	0.63	0.66	0.66
DCF	Radjenovic et. al., 2007	1	0.50		0.50		0.50		0.50
DCF	Kosjek et al., 2007	2	0.54	0.07	0.49		0.54		0.59
DCF	Kimura et. al., 2007	3	0.58	0.21	0.42	0.42	0.51	0.82	0.82
DCF	Sarp et. al., 2011	1	0.84		0.84		0.84		0.84
DXP	Wick et. al., 2009	1	0.39		0.39		0.39		0.39
DZP	Jelic et. al., 2011	1	0.12		0.12		0.12		0.12
ENA	Jelic et. al., 2011	3	0.96	0.02	0.94	0.94	0.96	0.98	0.98
ERY	Radjenovic et. al., 2007	1	0.24		0.24		0.24		0.24
ERY	Radjenovic et. al., 2009	3	0.35	0.09	0.25	0.25	0.35	0.43	0.43
ERY	Gobel et. al., 2007	4	0.39	0.36	0.06	0.07	0.39	0.72	0.74
ERY	Xue et. al., 2010	1	0.93		0.93		0.93		0.93
FAM	Radjenovic et. al., 2009	3	0.57	0.09	0.47	0.47	0.60	0.65	0.65
FAM	Jelic et. al., 2011	3	0.59	0.47	0.06	0.06	0.79	0.93	0.93
FENA	Jelic et. al., 2011	2	0.60	0.48	0.26		0.60		0.94
FLX	Radjenovic et. al., 2009	3	0.76	0.37	0.33	0.33	0.98	0.98	0.98
FPN	Tran et. al., 2009	3	0.44	0.41	0.12	0.12	0.30	0.90	0.90
FUR	Jelic et. al., 2011	3	0.59	0.21	0.36	0.36	0.65	0.76	0.76
GLC	Radjenovic et. al., 2007	1	0.45		0.45		0.45		0.45
GLC	Radjenovic et. al., 2009	3	0.75	0.26	0.46	0.46	0.82	0.96	0.96
GMF	Radjenovic et. al., 2009	2	0.37	0.07	0.33		0.37		0.42
GMF	Radjenovic et. al., 2007	1	0.39		0.39		0.39		0.39
GMF	Tran et. al., 2009	3	0.42	0.35	0.10	0.10	0.35	0.80	0.80
GMF	Jelic et. al., 2011	1	0.89		0.89		0.89		0.89
HCT	Radjenovic et. al., 2007	1	0.76		0.76		0.76		0.76

Table App.A-2. Removal of PhACs during biological wastewater treatment summarized by study. The following data are provided for removals of each PhAC evaluated in each study: the number of data (N_{DATA}), average (Avg.), standard deviation (SD), minimum (Min.), 25th , median and 75th percentile (Q1, Median and Q3) and maximum (Max.).

PhAC	Study Reference	N_{DATA}	Avg.	SD	Min.	Q1	Median	Q3	Max.
IBP	Tran et. al., 2009	3	0.62	0.46	0.10	0.10	0.75	1.00	1.00
IBP	Radjenovic et. al., 2007	1	0.83		0.83		0.83		0.83
IBP	Kosjek et al., 2007	2	0.91	0.00	0.91		0.91		0.92
IBP	Kimura et. al., 2007	3	0.97	0.02	0.95	0.95	0.98	0.98	0.98
IBP	Radjenovic et. al., 2009	3	0.99	0.00	0.99	0.99	0.99	1.00	1.00
IDM	Radjenovic et. al., 2007	1	0.23		0.23		0.23		0.23
IDM	Jelic et. al., 2011	2	0.34	0.11	0.26		0.34		0.42
IDM	Tran et. al., 2009	3	0.35	0.44	0.05	0.05	0.15	0.85	0.85
IDM	Radjenovic et. al., 2009	2	0.41	0.01	0.40		0.41		0.41
IOP	Batt et. al., 2006	4	0.61	0.43	0.00	0.16	0.74	0.94	0.97
KET	Tran et. al., 2009	3	0.43	0.39	0.08	0.08	0.35	0.85	0.85
KET	Radjenovic et. al., 2009	3	0.48	0.06	0.44	0.44	0.44	0.55	0.55
KET	Radjenovic et. al., 2007	1	0.52		0.52		0.52		0.52
KET	Kimura et. al., 2007	2	0.69	0.20	0.55		0.69		0.83
KET	Jelic et. al., 2011	3	0.83	0.13	0.69	0.69	0.85	0.94	0.94
KET	Kosjek et al., 2007	2	0.90	0.01	0.90		0.90		0.91
LOR	Radjenovic et. al., 2009	2	0.24	0.13	0.15		0.24		0.34
LZP	Jelic et. al., 2011	2	0.29	0.01	0.29		0.29		0.30
MET	Wick et. al., 2009	3	0.10	0.10	0.03	0.03	0.05	0.21	0.21
MET	Maurer et. al., 2007	2	0.30	0.01	0.29		0.30		0.31
MET	Radjenovic et. al., 2009	3	0.33	0.10	0.25	0.25	0.30	0.44	0.44
MET	Jelic et. al., 2011	1	0.33		0.33		0.33		0.33
MET	Xue et. al., 2010	1	0.70		0.70		0.70		0.70
MEV	Jelic et. al., 2011	2	0.82	0.25	0.65		0.82		1.00
MFA	Radjenovic et. al., 2007	1	0.29		0.29		0.29		0.29
MFA	Radjenovic et. al., 2009	2	0.38	0.04	0.36		0.38		0.41
MFA	Jelic et. al., 2011	3	0.45	0.29	0.12	0.12	0.56	0.66	0.66
MFA	Kimura et. al., 2007	3	0.81	0.11	0.72	0.72	0.77	0.93	0.93

Table App.A-2. Removal of PhACs during biological wastewater treatment summarized by study. The following data are provided for removals of each PhAC evaluated in each study: the number of data (N_{DATA}), average (Avg.), standard deviation (SD), minimum (Min.), 25th , median and 75th percentile (Q1, Median and Q3) and maximum (Max.).

PhAC	Study Reference	N_{DATA}	Avg.	SD	Min.	Q1	Median	Q3	Max.
MNZ	Jelic et. al., 2011	1	0.17		0.17		0.17		0.17
NAD	Jelic et. al., 2011	3	0.54	0.15	0.37	0.37	0.59	0.67	0.67
NAP	Tran et. al., 2009	3	0.35	0.34	0.04	0.04	0.30	0.72	0.72
NAP	Kimura et. al., 2007	2	0.80	0.23	0.64		0.80		0.96
NAP	Jelic et. al., 2011	3	0.85	0.11	0.76	0.76	0.80	0.98	0.98
NAP	Radjenovic et. al., 2009	3	0.85	0.11	0.72	0.72	0.91	0.92	0.92
NAP	Radjenovic et. al., 2007	1	0.85		0.85		0.85		0.85
NAP	Kosjek et al., 2007	2	0.90	0.05	0.87		0.90		0.94
NAP	Sarp et. al., 2011	1	1.00		1.00		1.00		1.00
OFL	Radjenovic et. al., 2007	1	0.24		0.24		0.24		0.24
OFL	Radjenovic et. al., 2009	3	0.87	0.10	0.76	0.76	0.91	0.95	0.95
OZP	Wick et. al., 2009	1	0.10		0.10		0.10		0.10
PAR	Radjenovic et. al., 2007	1	0.91		0.91		0.91		0.91
PPZ	Tran et. al., 2009	3	0.17	0.20	0.03	0.03	0.08	0.40	0.40
PPZ	Radjenovic et. al., 2007	1	0.43		0.43		0.43		0.43
PPZ	Radjenovic et. al., 2009	3	0.54	0.15	0.38	0.38	0.61	0.65	0.65
PRA	Jelic et. al., 2011	3	0.57	0.10	0.45	0.45	0.62	0.64	0.64
PRA	Radjenovic et. al., 2007	1	0.62		0.62		0.62		0.62
PRA	Radjenovic et. al., 2009	3	0.76	0.15	0.59	0.59	0.83	0.86	0.86
PRI	Wick et. al., 2009	3	0.32	0.19	0.15	0.15	0.30	0.52	0.52
PRO	Wick et. al., 2009	2	0.11	0.05	0.08		0.11		0.14
PRO	Maurer et. al., 2007	2	0.32	0.05	0.28		0.32		0.35
PRO	Radjenovic et. al., 2009	3	0.67	0.10	0.59	0.59	0.66	0.78	0.78
RAN	Radjenovic et. al., 2009	3	0.33	0.10	0.25	0.25	0.30	0.44	0.44
RAN	Radjenovic et. al., 2007	1	0.42		0.42		0.42		0.42
RAN	Jelic et. al., 2011	3	0.44	0.27	0.18	0.18	0.42	0.73	0.73
RMY	Gobel et. al., 2007	7	0.34	0.18	0.05	0.18	0.38	0.42	0.61
SAL	Jelic et. al., 2011	3	0.49	0.08	0.43	0.43	0.45	0.58	0.58

Table App.A-2. Removal of PhACs during biological wastewater treatment summarized by study. The following data are provided for removals of each PhAC evaluated in each study: the number of data (N_{DATA}), average (Avg.), standard deviation (SD), minimum (Min.), 25th , median and 75th percentile (Q1, Median and Q3) and maximum (Max.).

PhAC	Study Reference	N_{DATA}	Avg.	SD	Min.	Q1	Median	Q3	Max.
SMX	Gobel et. al., 2007	5	0.51	0.24	0.09	0.35	0.62	0.63	0.64
SMX	Radjenovic et. al., 2007	1	0.56		0.56		0.56		0.56
SMX	Sarp et. al., 2011	1	0.63		0.63		0.63		0.63
SMX	Radjenovic et. al., 2009	3	0.78	0.04	0.74	0.74	0.78	0.81	0.81
SMZ	Jelic et. al., 2011	3	0.48	0.35	0.14	0.14	0.47	0.83	0.83
SOT	Wick et. al., 2009	3	0.23	0.15	0.05	0.05	0.30	0.33	0.33
SOT	Maurer et. al., 2007	2	0.27	0.01	0.26		0.27		0.27
SOT	Jelic et. al., 2011	2	0.29	0.27	0.10		0.29		0.48
SOT	Radjenovic et. al., 2009	3	0.35	0.16	0.21	0.21	0.30	0.53	0.53
TIM	Jelic et. al., 2011	3	0.42	0.04	0.37	0.37	0.43	0.45	0.45
TMP	Gobel et. al., 2007	6	0.31	0.30	0.03	0.10	0.17	0.69	0.72
TMP	Batt et. al., 2006	4	0.37	0.30	0.01	0.07	0.38	0.65	0.70
TMP	Jelic et. al., 2011	2	0.40	0.01	0.39		0.40		0.41
TMP	Radjenovic et. al., 2009	3	0.52	0.14	0.40	0.40	0.48	0.67	0.67

Table App.A-3. Reported pseudo first order biodegradation rates (k_{BIO}, L/g-SS.d) for PhACs during biological wastewater treatment summarized by study (see Table App.A-3 for study details). The following data are provided for k_{BIO} of each PhAC evaluated in each study: the number of data (N_{DATA}), average (Avg.), standard deviation (SD), minimum (Min.), 25th , median and 75th percentile (Q1, Median and Q3) and maximum (Max.).

PhAC	Study Reference	N_{DATA}	Average	Std. Dev.	Min.	Q1	Median	Q3	Max.
ACM	Joss et. al., 2006	2	121.00	73.54	69.00		121.00		173.00
ATN	Maurer et. al., 2007	1	0.98		0.98		0.98		0.98
ATN	Wick et. al., 2009	2	1.50	0.57	1.10		1.50		1.90
AZI	Abegglen et. al., 2009	1	0.17		0.17		0.17		0.17
BIS	Wick et. al., 2009	2	0.71	0.09	0.64		0.71		0.77
BTL	Wick et. al., 2009	2	6.00	0.00	6.00		6.00		6.00
BZF	Abegglen et. al., 2009	1	0.77		0.77		0.77		0.77
BZF	Joss et. al., 2006	2	3.25	0.99	2.55		3.25		3.95
BZF	Clara et. al., 2005	12	9.74	17.78	0.07	0.24	3.69	12.88	63.60
CBZ	Urase and Kikuta, 2005	2	0.21	0.08	0.15		0.21		0.27
CBZ	Clara et. al., 2005	4	0.10	0.07	0.07	0.07	0.07	0.18	0.21
CIT	Suarez et. al., 2010	2	1.75	1.77	0.50		1.75		3.00
CLA	Abegglen et. al., 2009	1	0.09		0.09		0.09		0.09
CLA	Joss et. al., 2006	2	0.36	0.27	0.17		0.36		0.55
CLA	Urase and Kikuta, 2005	3	0.68	0.81	0.15	0.15	0.27	1.61	1.61
CLM	Abegglen et. al., 2009	2	0.12	0.12	0.03		0.12		0.20
CPL	Wick et. al., 2009	2	0.21	0.04	0.18		0.21		0.24
DCF	Suarez et. al., 2010	1	1.20		1.20		1.20		1.20
DCF	Urase and Kikuta, 2005	3	3.24	3.29	0.57	0.57	2.25	6.92	6.92
DCF	Clara et. al., 2005	7	0.28	0.23	0.06	0.07	0.30	0.53	0.64
DXP	Wick et. al., 2009	2	0.49	0.28	0.29		0.49		0.68
ERY	Suarez et. al., 2010	2	3.08	4.14	0.15		3.08		6.00
ERY	Xue et. al., 2010	3	0.22	0.06	0.17	0.17	0.21	0.28	0.28
FLX	Suarez et. al., 2010	2	7.00	2.83	5.00		7.00		9.00
FNA	Joss et. al., 2006	2	5.03	5.62	1.05		5.03		9.00

Table App.A-3. Reported pseudo first order biodegradation rates (k_{BIO}, L/g-SS.d) for PhACs during biological wastewater treatment summarized by study (see Table App.A-3 for study details). The following data are provided for k_{BIO} of each PhAC evaluated in each study: the number of data (N_{DATA}), average (Avg.), standard deviation (SD), minimum (Min.), 25th , median and 75th percentile (Q1, Median and Q3) and maximum (Max.).

PhAC	Study Reference	N_{DATA}	Average	Std. Dev.	Min.	Q1	Median	Q3	Max.
FPN	Joss et. al., 2006	2	8.30	5.23	4.60		8.30		12.00
FPN	Urase and Kikuta, 2005	4	3.98	3.78	1.44	1.47	2.50	7.97	9.47
GMF	Joss et. al., 2006	2	4.58	4.84	1.15		4.58		8.00
GMF	Urase and Kikuta, 2005	4	2.26	1.35	0.47	0.93	2.40	3.44	3.75
IBP	Abegglen et. al., 2009	1	1.33		1.33		1.33		1.33
IBP	Joss et. al., 2006	2	21.75	8.84	15.50		21.75		28.00
IBP	Suarez et. al., 2010	2	10.75	13.08	1.50		10.75		20.00
IBP	Urase and Kikuta, 2005	4	3.04	1.59	1.61	1.66	2.84	4.63	4.88
IBP	Clara et. al., 2005	12	15.38	14.95	0.71	1.74	9.59	31.50	38.00
IDM	Urase and Kikuta, 2005	4	3.06	1.65	1.23	1.47	3.07	4.64	4.88
IOP	Abegglen et. al., 2009	2	0.10	0.03	0.08		0.10		0.12
IOP	Joss et. al., 2006	2	1.78	0.39	1.50		1.78		2.05
KET	Urase and Kikuta, 2005	4	1.75	2.48	0.31	0.37	0.61	4.26	5.46
KET	Xue et. al., 2010	4	0.08	0.05	0.03	0.04	0.08	0.14	0.15
MET	Maurer et. al., 2007	1	0.82		0.82		0.82		0.82
MET	Wick et. al., 2009	2	0.38	0.04	0.35		0.38		0.40
MET	Xue et. al., 2010	4	0.11	0.06	0.03	0.05	0.12	0.16	0.17
NAP	Abegglen et. al., 2009	1	0.08		0.08		0.08		0.08
NAP	Suarez et. al., 2010	1	9.00		9.00		9.00		9.00
NAP	Joss et. al., 2006	2	1.03	0.60	0.60		1.03		1.45
NAP	Urase and Kikuta, 2005	4	1.68	2.53	0.12	0.20	0.57	4.26	5.46
NZP	Wick et. al., 2009	1	0.13		0.13		0.13		0.13
PPZ	Urase and Kikuta, 2005	3	1.01	0.75	0.27	0.27	0.99	1.77	1.77
PRI	Abegglen et. al., 2009	1	0.02		0.02		0.02		0.02
PRO	Maurer et. al., 2007	1	0.55		0.55		0.55		0.55
PRO	Wick et. al., 2009	2	0.41	0.07	0.36		0.41		0.46
RMY	Abegglen et. al., 2009	2	0.02	0.00	0.02		0.02		0.02

Table App.A-3. Reported pseudo first order biodegradation rates (k_{BIO}, L/g-SS.d) for PhACs during biological wastewater treatment summarized by study (see Table App.A-3 for study details). The following data are provided for k_{BIO} of each PhAC evaluated in each study: the number of data (N_{DATA}), average (Avg.), standard deviation (SD), minimum (Min.), 25th , median and 75th percentile (Q1, Median and Q3) and maximum (Max.).

PhAC	Study Reference	N_{DATA}	Average	Std. Dev.	Min.	Q1	Median	Q3	Max.
RMY	Suarez et. al., 2010	2	4.60	6.22	0.20		4.60		9.00
SDM	Abegglen et. al., 2009	1	0.19		0.19		0.19		0.19
SDZ	Abegglen et. al., 2009	1	0.13		0.13		0.13		0.13
SMX	Suarez et. al., 2010	1	0.30		0.30		0.30		0.30
SMX	Abegglen et. al., 2009	2	0.20	0.01	0.19		0.20		0.20
SMX	Joss et. al., 2006	2	5.43	1.87	4.10		5.43		6.75
SMZ	Abegglen et. al., 2009	2	0.21	0.10	0.14		0.21		0.28
SOT	Maurer et. al., 2007	1	0.41		0.41		0.41		0.41
SOT	Wick et. al., 2009	2	0.42	0.02	0.40		0.42		0.43
SPY	Abegglen et. al., 2009	1	0.20		0.20		0.20		0.20
TMP	Abegglen et. al., 2009	1	0.22		0.22		0.22		0.22
TMP	Suarez et. al., 2010	1	0.15		0.15		0.15		0.15
TMP	Xue et. al., 2010	3	0.56	0.46	0.05	0.05	0.67	0.95	0.95
TOP	Abegglen et. al., 2009	1	0.01		0.01		0.01		0.01

Appendix B: Overview of the Sorption Studies Used to Obtain PhAC K_D Data used in this Research

Data for Sorption coefficients (K_D) for PhACs in biological treatment processes during wastewater treatment were compiled from the peer reviewed sources summarized in Table App.B-1. For each study, the following information is included:

Expt. Type	**Experiments are classified into Batch and Continuous**
Expt'l MLSS (mg L^{-1})	Where provided the mixed liquor concentration of the experiments is provided. In some cases, only the mixed liquor volatile suspended solids (MLVSS). Where no data is provided – this is indicated by n/d
Biomass Inactivation Method	Where applicable, the physical and/or chemical method used to inactivate biomass is specified
Expt. pH	When provided, the experimental pH is noted. Where data are not provided – this is indicated by n/d
Unit Operation	The type of unit operation where the mixed liquor is collected (e.g., suspended growth or MBR). Where data are not provided – this is indicated by n/d
SRT (d)	When provided, the SRT of the process/unit operation where the mixed liquor is collected is provided (in days). Where data are not provided – this is indicated by n/d
Process MLSS (mg L^{-1})	Where provided the mixed liquor concentration of the process/unit operation where the mixed liquor is collected is provided. In some cases, only the mixed liquor volatile suspended solids (MLVSS). Where no data is provided – this is indicated by n/d
PhACs included	A list of the PhACs included in each study is provided

Table App.B-1. Studies included that evaluate sorption of pharmaceuticals in biological treatment processes.

Reference	Expt. Type	Expt'l MLSS (mg L^{-1})	Biomass Inactivation Method	Expt. pH	Expt. Dur. (h)	Unit Operation	SRT (d)	Process MLSS (mg L^{-1})	PhACs included	Comments
Ternes et al. (2004)	Batch	4,000	none specifically	n/d	14	Suspended Growth	11-13		DCF IBP CBZ CLA DZP	• Oxygen in headspace replaced with Argon which should (a) limit aerobic biological activity and (b) limit incursion of air into reactor during sorption experiment.
Urase and Kikuta (2005)	Batch	2,500	none	6.7 7.0 5.6 4.4 7.2 7.0	96	n/d	n/d	n/d	DCF IBP KET NAP FPN IND CBZ CLA GMF	• Expts designed to evaluate sorption and biodegradation using one batch experiment

Table App.B-1. Studies included that evaluate sorption of pharmaceuticals in biological treatment processes.

Reference	Expt. Type	Expt'l MLSS (mg L^{-1})	Biomass Inactivation Method	Expt. pH	Expt. Dur. (h)	Unit Operation	SRT (d)	Process MLSS (mg L^{-1})	PhACs included	Comments
Maurer et al. (2007)	Batch	MLVSS: 2,460 3,380 4,500	$HgCl_2$	n/d		Suspended Growth	~20	4,360	ATN PRO MET SOT	• All β-blockers • Authors report biomass concentration in g_{COD} L^{-1}. Biomass COD:VSS ratio of 1.42 used to calculate MLVSS
Abegglen et al. (2009)	Continuous	3,800 6,200	none	7.7		UF MBR – greywater system	>150	3,800 6,200	IBP KET	• Expts in pilot scale MBR treating household waste from 3-person household

Table App.B-1. Studies included that evaluate sorption of pharmaceuticals in biological treatment processes.

Reference	Expt. Type	Expt'l MLSS (mg L^{-1})	Biomass Inactivation Method	Expt. pH	Expt. Dur. (h)	Unit Operation	SRT (d)	Process MLSS (mg L^{-1})	PhACs included	Comments
Radjenovic et al. (2009)	Continuous	*See process MLSS*	n/a	n/d	n/a	Suspended Growth	10	n/d	IBP KET DCF MEF ACM CBZ ERY SMX LOR TMP ATN PRO GLC GMF HCT	• Expts in continuously operating WWTP (11 mgd)
		See process MLSS	n/a	n/d	n/a	MF MBR	n/d	Varies 6,700 – 26,000		• Expts in continuously operated pilot scale MF-MBR
		See process MLSS	n/a	n/d	n/a	UF MBR	n/d	Varies 1,400 – 8,400		• Expts in continuously operated pilot scale UF-MBR
Wick et al. (2009)	Batch	9,000	NaN_3	n/d	14	Suspended Growth - MLE	0.5	9,000	MOR COD DHC OXY TRA MDN DIA NDP OZP	• MLE process is the 2nd stage of a 3-stage WWTP (Frankfurt-Niederrad) • 1st stage is a HRAS process & 3rd stage is upflow post-denit BAF (Biostyr®)

Table App.B-1. Studies included that evaluate sorption of pharmaceuticals in biological treatment processes.

Reference	Expt. Type	Expt'l MLSS (mg L^{-1})	Biomass Inactivation Method	Expt. pH	Expt. Dur. (h)	Unit Operation	SRT (d)	Process MLSS (mg L^{-1})	PhACs included	Comments
Xue et al. (2010)	Batch	1,000	none	n/d	24	A2/O with MBR	20	AN: 4,300 AX: 7,900 AE: 9,400 M: 11,500	DCF TRI KET SUL MET CBZ ERY CAF	• Expts designed to evauate sorption and biodegradation • Model of Urase and Kikuta (2005) used to calculate K_D • Redox conditions varied to simulate conditions in an MBR process [process/batch expt. DO (mg L^{-1})]: mem.tank/6; AE/4; AX/0.5;AN/0
Stevens-Garmon et al. (2011)	Batch	Varies ~500 - ~8,800	Freezing, lyophilization	7.0		Suspended Growth	Varies 5 - 6	Varies 1,500 2,600	DCF ATV IBP DZP NAP ATN ACM SMX CBZ TMP AMT CLZ GMF VRP RIS	• Also tested chemical inactivation methods (NaN_3 with $BaCl_2$ & $NiCl_2$)

Table App.B-1. Studies included that evaluate sorption of pharmaceuticals in biological treatment processes.

Reference	Expt. Type	Expt'l MLSS (mg L^{-1})	Biomass Inactivation Method	Expt. pH	Expt. Dur. (h)	Unit Operation	SRT (d)	Process MLSS (mg L^{-1})	PhACs included	Comments
Horsing et al. (2011)	Batch	1,000	freeze dried heated (103°C) – 3h	7.0	12	Suspended Growth	2-3	8,000	AFL AMT HAL ATN HYZ ATR IRB AZE KCZ BIP LOP BUP MAP CPT MEG CIT MIA CMP NEF CZP OZP CHD PAR DCV PIZ DLOR PGS DPZ REP DXT RIS ETO SER EZE SMX FEX TEL FLU TRA FLX TMP GLC VER GLM	
				6.0 7.0 8.0			10	4,000		

Table App.B-1. Studies included that evaluate sorption of pharmaceuticals in biological treatment processes.

Reference	Expt. Type	Expt'l MLSS (mg L^{-1})	Biomass Inactivation Method	Expt. pH	Expt. Dur. (h)	Unit Operation	SRT (d)	Process MLSS (mg L^{-1})	PhACs included	Comments
Hyland et al. (2012)	Batch	n/d	Lyophylization	n/d			3 7 17		AMT CBZ CIM KET DCF NAP DZP HTC FLX SMX GMF TMP IBP	

Appendix C: Summary of Measured Sorption Coefficients for 66 PhACs included in this Research

Table A-2. Measured sorption coefficients (K_D) for the 66 PhACs assessed in this review. For each measured K_D values are provided with reported experimental pH, charge of dominant PhAC species at experimental conditions (Dom.Sp.Expt.pH), fraction of dominant species (%Dom.Species) and fraction of uncharged PhAC species (α_0 Expt.pH). Note that where the pH employed for the experiments was not reported (n/r) by the authors the information about the dominant species was not determined (n/d).

Name & Acronym		pKa	Protonation	Expt pH	Dom.Sp. Expt.pH		%Dom. Species	α_0 Expt. pH	K_D (L g^{-1} SS)	log K_D	Reference
Acetaminophen	ACM	9.38	monoprotic	n/r	n/d	n/d	n/d	n/d	1.160	0.064	Radjenovic et. al., 2009
			monoprotic	n/r	n/d	n/d	n/d	n/d	0.238	-0.623	Radjenovic et. al., 2009
			monoprotic	n/r	n/d	n/d	n/d	n/d	0.126	-0.900	Radjenovic et. al., 2009
Alfuzosin	AFL		multiprotic	6	Positive	+1	0.74	0.05	0.120	-0.921	Horsing et. al., 2011
			multiprotic	7	Positive	+1	0.52	0.33	0.730	-0.137	Horsing et. al., 2011
			multiprotic	8	Uncharged	0	0.83	0.83	1.100	0.041	Horsing et. al., 2011
Alprazolam	ALP		multiprotic	7	Positive	+1	0.94	0.06	0.430	-0.367	Horsing et. al., 2011
Amitryptilyine	AMT	9.4	monoprotic	6	Positive	+1	1.00	0.00	2.800	0.447	Horsing et. al., 2011
			monoprotic	7	Positive	+1	1.00	0.00	1.800	0.255	Horsing et. al., 2011
			monoprotic	8	Positive	+1	0.96	0.04	4.000	0.602	Horsing et. al., 2011
			monoprotic	7	Positive	+1	1.00	0.00	2.800	0.447	Horsing et. al., 2011
			monoprotic	n/r	n/d	n/d	n/d	n/d	0.003	-2.595	Hyland et. al., 2012
			monoprotic	n/r	n/d	n/d	n/d	n/d	0.003	-2.514	Hyland et. al., 2012
			monoprotic	n/r	n/d	n/d	n/d	n/d	0.003	-2.502	Hyland et. al., 2012
			monoprotic	n/r	n/d	n/d	n/d	n/d	0.003	-2.573	Hyland et. al., 2012
			monoprotic	n/r	n/d	n/d	n/d	n/d	0.003	-2.544	Hyland et. al., 2012
			monoprotic	n/r	n/d	n/d	n/d	n/d	0.003	-2.548	Hyland et. al., 2012
			monoprotic	n/r	n/d	n/d	n/d	n/d	0.003	-2.523	Hyland et. al., 2012

Table A-2. Measured sorption coefficients (K_D) for the 66 PhACs assessed in this review. For each measured K_D values are provided with reported experimental pH, charge of dominant PhAC species at experimental conditions (Dom.Sp.Expt.pH), fraction of dominant species (%Dom.Species) and fraction of uncharged PhAC species (α_0 Expt.pH). Note that where the pH employed for the experiments was not reported (n/r) by the authors the information about the dominant species was not determined (n/d).

Name & Acronym		pKa	Protonation	Expt pH	Dom.Sp. Expt.pH		%Dom. Species	α_0 Expt. pH	K_D (L g^{-1} SS)	log K_D	Reference
Atenolol	ATN	9.6	monoprotic	6	Positive	+1	1.00	0.00	1.600	0.204	Horsing et. al., 2011
			monoprotic	7	Positive	+1	1.00	0.00	1.600	0.204	Horsing et. al., 2011
			monoprotic	8	Positive	+1	0.98	0.02	1.600	0.204	Horsing et. al., 2011
			monoprotic	7	Positive	+1	1.00	0.00	1.900	0.279	Horsing et. al., 2011
			monoprotic	n/r	n/d	n/d	n/d	n/d	0.024	-1.617	Maurer et. al., 2007
			monoprotic	n/r	n/d	n/d	n/d	n/d	0.044	-1.356	Maurer et. al., 2007
			monoprotic	n/r	n/d	n/d	n/d	n/d	0.037	-1.433	Maurer et. al., 2007
			monoprotic	n/r	n/d	n/d	n/d	n/d	0.027	-1.569	Maurer et. al., 2007
			monoprotic	n/r	n/d	n/d	n/d	n/d	0.138	-0.861	Maurer et. al., 2007
			monoprotic	n/r	n/d	n/d	n/d	n/d	0.064	-1.194	Radjenovic et. al., 2009
			monoprotic	n/r	n/d	n/d	n/d	n/d	0.040	-1.398	Radjenovic et. al., 2009
			monoprotic	n/r	n/d	n/d	n/d	n/d	0.006	-2.229	Radjenovic et. al., 2009
			monoprotic	7	Positive	+1	1.00	0.00	0.035	-1.456	Stevens-Garmon et. al., 2011
Atorvastatin	ATV		multiprotic	7	Negative	-1	1.00	0.00	0.198	-0.703	Stevens-Garmon et. al., 2011
			multiprotic	7	Negative	-1	1.00	0.00	0.106	-0.975	Stevens-Garmon et. al., 2011
			multiprotic	7	Negative	-1	1.00	0.00	0.093	-1.032	Stevens-Garmon et. al., 2011

Table A-2. Measured sorption coefficients (K_D) for the 66 PhACs assessed in this review. For each measured K_D values are provided with reported experimental pH, charge of dominant PhAC species at experimental conditions (Dom.Sp.Expt.pH), fraction of dominant species (%Dom.Species) and fraction of uncharged PhAC species (α_0 Expt.pH). Note that where the pH employed for the experiments was not reported (n/r) by the authors the information about the dominant species was not determined (n/d).

Name & Acronym		pKa	Protonation	Expt pH	Dom.Sp. Expt.pH		%Dom. Species	α_0 Expt. pH	K_D (L g^{-1} SS)	log K_D	Reference
Azelastine	AZL	9.16	monoprotic	6	Positive	+1	1.00	0.00	2.000	0.301	Horsing et. al., 2011
			monoprotic	7	Positive	+1	0.99	0.01	0.870	-0.060	Horsing et. al., 2011
			monoprotic	8	Positive	+1	0.94	0.06	2.300	0.362	Horsing et. al., 2011
			monoprotic	7	Positive	+1	0.99	0.01	1.400	0.146	Horsing et. al., 2011
Biperiden	BIP	8.8	monoprotic	6	Positive	+1	1.00	0.00	0.760	-0.119	Horsing et. al., 2011
			monoprotic	7	Positive	+1	0.98	0.02	0.600	-0.222	Horsing et. al., 2011
			monoprotic	8	Positive	+1	0.86	0.14	1.000	0.000	Horsing et. al., 2011
			monoprotic	7	Positive	+1	0.98	0.02	0.840	-0.076	Horsing et. al., 2011
Bisoprolol	BIS	9.5	monoprotic	6	Positive	+1	1.00	0.00	0.060	-1.222	Horsing et. al., 2011
			monoprotic	7	Positive	+1	1.00	0.00	0.210	-0.678	Horsing et. al., 2011
			monoprotic	8	Positive	+1	0.97	0.03	0.080	-1.097	Horsing et. al., 2011
			monoprotic	7	Positive	+1	1.00	0.00	0.094	-1.027	Horsing et. al., 2011
			monoprotic	n/r	n/d	n/d	n/d	n/d	0.040	-1.398	Wick et. al., 2009
Buproprion	BUP	7.16	monoprotic	6	Positive	+1	0.94	0.06	0.140	-0.854	Horsing et. al., 2011
			monoprotic	7	Positive	+1	0.59	0.41	0.140	-0.854	Horsing et. al., 2011
			monoprotic	8	Uncharged	0	0.87	0.87	0.150	-0.824	Horsing et. al., 2011
			monoprotic	7	Positive	+1	0.59	0.41	0.200	-0.699	Horsing et. al., 2011

Table A-2. Measured sorption coefficients (K_D) for the 66 PhACs assessed in this review. For each measured K_D values are provided with reported experimental pH, charge of dominant PhAC species at experimental conditions (Dom.Sp.Expt.pH), fraction of dominant species (%Dom.Species) and fraction of uncharged PhAC species (α_0 Expt.pH). Note that where the pH employed for the experiments was not reported (n/r) by the authors the information about the dominant species was not determined (n/d).

Name & Acronym		pKa	Protonation	Expt pH	Dom.Sp. Expt.pH		%Dom. Species	α_0 Expt. pH	K_D (L g^{-1} SS)	log K_D	Reference
Bezafibrate	BZF	3.6	monoprotic	7.7	Negative	-1	1.00	0.00	0.087	-1.060	Abegglen et. al., 2009
			monoprotic	7.7	Negative	-1	1.00	0.00	0.050	-1.301	Abegglen et. al., 2009

Table A-2. Measured sorption coefficients (K_D) for the 66 PhACs assessed in this review. For each measured K_D values are provided with reported experimental pH, charge of dominant PhAC species at experimental conditions (Dom.Sp.Expt.pH), fraction of dominant species (%Dom.Species) and fraction of uncharged PhAC species (α_0 Expt.pH). Note that where the pH employed for the experiments was not reported (n/r) by the authors the information about the dominant species was not determined (n/d).

Name & Acronym		pKa	Protonation	Expt pH	Dom.Sp. Expt.pH		%Dom. Species	α_0 Expt. pH	K_D (L g^{-1} SS)	log K_D	Reference
Carbamezapine	CBZ	13.9	monoprotic	7.7	Uncharged	0	1.00	1.00	0.008	-2.097	Abegglen et. al., 2009
			monoprotic	7.7	Uncharged	0	1.00	1.00	0.008	-2.125	Abegglen et. al., 2009
			monoprotic	n/r	n/d	n/d	n/d	n/d	0.135	-0.870	Radjenovic et. al., 2009
			monoprotic	n/r	n/d	n/d	n/d	n/d	0.164	-0.785	Radjenovic et. al., 2009
			monoprotic	n/r	n/d	n/d	n/d	n/d	0.194	-0.712	Radjenovic et. al., 2009
			monoprotic	7	Uncharged	0	1.00	1.00	0.050	-1.301	Stevens-Garmon et. al., 2011
			monoprotic	7	Uncharged	0	1.00	1.00	0.036	-1.444	Stevens-Garmon et. al., 2011
			monoprotic	n/r	n/d	n/d	n/d	n/d	0.001	-2.921	Ternes et. al., 2004
			monoprotic	6.7	Uncharged	0	1.00	1.00	0.066	-1.180	Urase & Kikuta, 2005
			monoprotic	5.6	Uncharged	0	1.00	1.00	0.028	-1.553	Urase & Kikuta, 2005
			monoprotic	4.4	Uncharged	0	1.00	1.00	0.035	-1.456	Urase & Kikuta, 2005
			monoprotic	7.2	Uncharged	0	1.00	1.00	0.034	-1.469	Urase & Kikuta, 2005
			monoprotic	n/r	n/d	n/d	n/d	n/d	0.017	-1.770	Wick et. al., 2009
			monoprotic	n/r	n/d	n/d	n/d	n/d	0.940	-0.027	Xue et. al., 2010
			monoprotic	n/r	n/d	n/d	n/d	n/d	3.870	0.588	Xue et. al., 2010
			monoprotic	n/r	n/d	n/d	n/d	n/d	6.550	0.816	Xue et. al., 2010
			monoprotic	n/r	n/d	n/d	n/d	n/d	0.810	-0.092	Xue et. al., 2010

Table A-2. Measured sorption coefficients (K_D) for the 66 PhACs assessed in this review. For each measured K_D values are provided with reported experimental pH, charge of dominant PhAC species at experimental conditions (Dom.Sp.Expt.pH), fraction of dominant species (%Dom.Species) and fraction of uncharged PhAC species (α_0 Expt.pH). Note that where the pH employed for the experiments was not reported (n/r) by the authors the information about the dominant species was not determined (n/d).

Name & Acronym		pKa	Protonation	Expt pH	Dom.Sp. Expt.pH		%Dom. Species	α_0 Expt. pH	K_D (L g^{-1} SS)	log K_D	Reference
			monoprotic	n/r	n/d	n/d	n/d	n/d	0.002	-2.622	Hyland et. al., 2012
			monoprotic	n/r	n/d	n/d	n/d	n/d	0.002	-2.804	Hyland et. al., 2012
			monoprotic	n/r	n/d	n/d	n/d	n/d	0.002	-2.777	Hyland et. al., 2012
			monoprotic	n/r	n/d	n/d	n/d	n/d	0.002	-2.747	Hyland et. al., 2012
Cyproheptadine	CHD	8.87	monoprotic	6	Positive	+1	1.00	0.00	3.600	0.556	Horsing et. al., 2011
			monoprotic	7	Positive	+1	0.99	0.01	2.100	0.322	Horsing et. al., 2011
			monoprotic	8	Positive	+1	0.88	0.12	4.400	0.643	Horsing et. al., 2011
			monoprotic	7	Positive	+1	0.99	0.01	5.300	0.724	Horsing et. al., 2011
Cimetidine	CIM	6.89	monoprotic	n/r	n/d	n/d	n/d	n/d	0.002	-2.629	Hyland et. al., 2012
			monoprotic	n/r	n/d	n/d	n/d	n/d	0.003	-2.564	Hyland et. al., 2012
			monoprotic	n/r	n/d	n/d	n/d	n/d	0.002	-2.680	Hyland et. al., 2012
			monoprotic	n/r	n/d	n/d	n/d	n/d	0.003	-2.554	Hyland et. al., 2012
			monoprotic	n/r	n/d	n/d	n/d	n/d	0.003	-2.602	Hyland et. al., 2012
			monoprotic	n/r	n/d	n/d	n/d	n/d	0.002	-2.609	Hyland et. al., 2012

Table A-2. Measured sorption coefficients (K_D) for the 66 PhACs assessed in this review. For each measured K_D values are provided with reported experimental pH, charge of dominant PhAC species at experimental conditions (Dom.Sp.Expt.pH), fraction of dominant species (%Dom.Species) and fraction of uncharged PhAC species (α_0 Expt.pH). Note that where the pH employed for the experiments was not reported (n/r) by the authors the information about the dominant species was not determined (n/d).

Name & Acronym		pKa	Protonation	Expt pH	Dom.Sp. Expt.pH		%Dom. Species	α_0 Expt. pH	K_D (L g^{-1} SS)	log K_D	Reference
Clofibric Acid	CLA	3.2	monoprotic	7.7	Negative	-1	1.00	0.00	0.007	-2.155	Abegglen et. al., 2009
			monoprotic	n/r	n/d	n/d	n/d	n/d	0.005	-2.319	Ternes et. al., 2004
			monoprotic	6.7	Negative	-1	1.00	0.00	0.029	-1.538	Urase & Kikuta, 2005
			monoprotic	5.6	Negative	-1	1.00	0.00	0.162	-0.790	Urase & Kikuta, 2005
			monoprotic	4.4	Negative	-1	0.94	0.06	0.554	-0.256	Urase & Kikuta, 2005
			monoprotic	7.2	Negative	-1	1.00	0.00	0.024	-1.620	Urase & Kikuta, 2005
Clomipramine	CMP	9.46	monoprotic	6	Positive	+1	1.00	0.00	6.700	0.826	Horsing et. al., 2011
			monoprotic	7	Positive	+1	1.00	0.00	3.900	0.591	Horsing et. al., 2011
			monoprotic	8	Positive	+1	0.97	0.03	9.300	0.968	Horsing et. al., 2011
			monoprotic	7	Positive	+1	1.00	0.00	7.300	0.863	Horsing et. al., 2011
Celiprolol	CPL		multiprotic	n/r	n/d	n/d	n/d	n/d	0.085	-1.071	Wick et. al., 2009
Chlorprothixene	CPT	8.4	monoprotic	6	Positive	+1	1.00	0.00	20.000	1.301	Horsing et. al., 2011
			monoprotic	7	Positive	+1	0.96	0.04	10.000	1.000	Horsing et. al., 2011
			monoprotic	8	Positive	+1	0.72	0.28	28.000	1.447	Horsing et. al., 2011
Clotrimazol	CTZ	6.12	monoprotic	6	Positive	+1	0.57	0.43	36.000	1.556	Horsing et. al., 2011
			monoprotic	7	Uncharged	0	0.88	0.88	33.000	1.519	Horsing et. al., 2011
			monoprotic	8	Uncharged	0	0.99	0.99	40.000	1.602	Horsing et. al., 2011

Table A-2. Measured sorption coefficients (K_D) for the 66 PhACs assessed in this review. For each measured K_D values are provided with reported experimental pH, charge of dominant PhAC species at experimental conditions (Dom.Sp.Expt.pH), fraction of dominant species (%Dom.Species) and fraction of uncharged PhAC species (α_0 Expt.pH). Note that where the pH employed for the experiments was not reported (n/r) by the authors the information about the dominant species was not determined (n/d).

Name & Acronym		pKa	Protonation	Expt pH	Dom.Sp. Expt.pH		%Dom. Species	α_0 Expt. pH	K_D (L g^{-1} SS)	log K_D	Reference
Diclofenac	DCF	4.2	monoprotic	6	Negative	-1	0.98	0.02	0.800	-0.097	Horsing et. al., 2011
				7	Negative	-1	1.00	0.00	47.900	1.680	Horsing et. al., 2011
				8	Negative	-1	1.00	0.00	1.200	0.079	Horsing et. al., 2011
				n/r	n/d	n/d	n/d	n/d	0.118	-0.928	Radjenovic et. al., 2009
				n/r	n/d	n/d	n/d	n/d	0.321	-0.493	Radjenovic et. al., 2009
				n/r	n/d	n/d	n/d	n/d	0.197	-0.706	Radjenovic et. al., 2009
				n/r	n/d	n/d	n/d	n/d	0.016	-1.796	Ternes et. al., 2004
				6.7	Negative	-1	1.00	0.00	0.032	-1.495	Urase & Kikuta, 2005
				5.6	Negative	-1	0.96	0.04	0.159	-0.799	Urase & Kikuta, 2005
				4.4	Negative	-1	0.61	0.39	0.701	-0.154	Urase & Kikuta, 2005
				7.2	Negative	-1	1.00	0.00	0.016	-1.796	Urase & Kikuta, 2005
				n/r	n/d	n/d	n/d	n/d	0.100	-1.000	Xue et. al., 2010
				n/r	n/d	n/d	n/d	n/d	0.310	-0.509	Xue et. al., 2010
				n/r	n/d	n/d	n/d	n/d	0.090	-1.046	Xue et. al., 2010
				n/r	n/d	n/d	n/d	n/d	0.200	-0.699	Xue et. al., 2010
				n/r	n/d	n/d	n/d	n/d	0.002	-2.622	Hyland et. al., 2012
				n/r	n/d	n/d	n/d	n/d	0.002	-2.604	Hyland et. al., 2012
				n/r	n/d	n/d	n/d	n/d	0.002	-2.678	Hyland et. al., 2012
				n/r	n/d	n/d	n/d	n/d	0.002	-2.697	Hyland et. al., 2012

Table A-2. Measured sorption coefficients (K_D) for the 66 PhACs assessed in this review. For each measured K_D values are provided with reported experimental pH, charge of dominant PhAC species at experimental conditions (Dom.Sp.Expt.pH), fraction of dominant species (%Dom.Species) and fraction of uncharged PhAC species (α_0 Expt.pH). Note that where the pH employed for the experiments was not reported (n/r) by the authors the information about the dominant species was not determined (n/d).

Name & Acronym		pKa	Protonation	Expt pH	Dom.Sp. Expt.pH		%Dom. Species	α_0 Expt. pH	K_D ($L\ g^{-1}$ SS)	log K_D	Reference
				n/r	n/d	n/d	n/d	n/d	0.002	-2.721	Hyland et. al., 2012
				n/r	n/d	n/d	n/d	n/d	0.002	-2.664	Hyland et. al., 2012
Dicycloverin	DCV	8.54	monoprotic	6	Positive	+1	1.00	0.00	1.700	0.230	Horsing et. al., 2011
				7	Positive	+1	0.97	0.03	1.200	0.079	Horsing et. al., 2011
				8	Positive	+1	0.78	0.22	2.400	0.380	Horsing et. al., 2011
				7	Positive	+1	0.97	0.03	1.700	0.230	Horsing et. al., 2011
Desloratadine	DLR	8.65	monoprotic	6	Positive	+1	1.00	0.00	2.900	0.462	Horsing et. al., 2011
				7	Positive	+1	0.98	0.02	2.300	0.362	Horsing et. al., 2011
				8	Positive	+1	0.82	0.18	3.400	0.531	Horsing et. al., 2011
				7	Positive	+1	0.98	0.02	3.200	0.505	Horsing et. al., 2011
Donepezil	DPZ	8.8	monoprotic	6	Positive	+1	1.00	0.00	0.960	-0.018	Horsing et. al., 2011
				7	Positive	+1	0.98	0.02	0.480	-0.319	Horsing et. al., 2011
				8	Positive	+1	0.86	0.14	1.000	0.000	Horsing et. al., 2011
Doxepine	DXP	8	monoprotic	n/r	n/d	n/d	n/d	n/d	0.139	-0.857	Wick et. al., 2009
Duloxetine	DXT	9.4	monoprotic	6	Positive	+1	1.00	0.00	2.900	0.462	Horsing et. al., 2011
				7	Positive	+1	1.00	0.00	1.800	0.255	Horsing et. al., 2011
				8	Positive	+1	0.96	0.04	4.400	0.643	Horsing et. al., 2011
				7	Positive	+1	1.00	0.00	3.200	0.505	Horsing et. al., 2011

Table A-2. Measured sorption coefficients (K_D) for the 66 PhACs assessed in this review. For each measured K_D values are provided with reported experimental pH, charge of dominant PhAC species at experimental conditions (Dom.Sp.Expt.pH), fraction of dominant species (%Dom.Species) and fraction of uncharged PhAC species (α_0 Expt.pH). Note that where the pH employed for the experiments was not reported (n/r) by the authors the information about the dominant species was not determined (n/d).

Name & Acronym		pKa	Protonation	Expt pH	Dom.Sp. Expt.pH		%Dom. Species	α_0 Expt. pH	K_D (L g^{-1} SS)	log K_D	Reference
Diazepam	DZP	3.3	monoprotic	7	Uncharged	0	1.00	1.00	0.241	-0.618	Stevens-Garmon et. al., 2011
				7	Uncharged	0	1.00	1.00	0.161	-0.793	Stevens-Garmon et. al., 2011
				7	Uncharged	0	1.00	1.00	0.197	-0.706	Stevens-Garmon et. al., 2011
				n/r	n/d	n/d	n/d	n/d	0.021	-1.678	Ternes et. al., 2004
				n/r	n/d	n/d	n/d	n/d	0.053	-1.276	Wick et. al., 2009
				n/r	n/d	n/d	n/d	n/d	0.002	-2.721	Hyland et. al., 2012
				n/r	n/d	n/d	n/d	n/d	0.002	-2.609	Hyland et. al., 2012
				n/r	n/d	n/d	n/d	n/d	0.002	-2.658	Hyland et. al., 2012
				n/r	n/d	n/d	n/d	n/d	0.002	-2.701	Hyland et. al., 2012
				n/r	n/d	n/d	n/d	n/d	0.002	-2.688	Hyland et. al., 2012
				n/r	n/d	n/d	n/d	n/d	0.002	-2.670	Hyland et. al., 2012
				n/r	n/d	n/d	n/d	n/d	0.002	-2.658	Hyland et. al., 2012
Eprosartan	EPR		multiprotic	6	Negative	-1	0.88	0.02	0.050	-1.301	Horsing et. al., 2011
				7	Negative	-2	0.54	0.00	0.060	-1.222	Horsing et. al., 2011
				8	Negative	-2	0.92	0.00	0.080	-1.097	Horsing et. al., 2011

Table A-2. Measured sorption coefficients (K_D) for the 66 PhACs assessed in this review. For each measured K_D values are provided with reported experimental pH, charge of dominant PhAC species at experimental conditions (Dom.Sp.Expt.pH), fraction of dominant species (%Dom.Species) and fraction of uncharged PhAC species (α_0 Expt.pH). Note that where the pH employed for the experiments was not reported (n/r) by the authors the information about the dominant species was not determined (n/d).

Name & Acronym		pKa	Protonation	Expt pH	Dom.Sp. Expt.pH		%Dom. Species	α_0 Expt. pH	K_D (L g^{-1} SS)	log K_D	Reference
Erythromycin	ERY	8.16	monoprotic	n/r	n/d	n/d	n/d	n/d	0.074	-1.131	Radjenovic et. al., 2009
				n/r	n/d	n/d	n/d	n/d	0.011	-1.943	Radjenovic et. al., 2009
				n/r	n/d	n/d	n/d	n/d	0.183	-0.738	Radjenovic et. al., 2009
Ezetimibe	EZE	9.72	monoprotic	6	Uncharged	0	1.00	1.00	3.200	0.505	Horsing et. al., 2011
				7	Uncharged	0	1.00	1.00	3.000	0.477	Horsing et. al., 2011
				8	Uncharged	0	0.98	0.98	3.900	0.591	Horsing et. al., 2011
				7	Uncharged	0	1.00	1.00	8.500	0.929	Horsing et. al., 2011
Fexofenadine	FEX		multiprotic	6	Uncharged	0	0.99	0.99	0.360	-0.444	Horsing et. al., 2011
			multiprotic	7	Uncharged	0	0.99	0.99	0.350	-0.456	Horsing et. al., 2011
			multiprotic	8	Uncharged	0	0.91	0.91	0.100	-1.000	Horsing et. al., 2011
			multiprotic	7	Uncharged	0	0.99	0.99	0.670	-0.174	Horsing et. al., 2011
Flutamide	FLU	13.9	monoprotic	6	Uncharged	0	1.00	1.00	0.800	-0.097	Horsing et. al., 2011
				7	Uncharged	0	1.00	1.00	0.800	-0.097	Horsing et. al., 2011
				8	Uncharged	0	1.00	1.00	0.600	-0.222	Horsing et. al., 2011
				7	Uncharged	0	1.00	1.00	1.200	0.079	Horsing et. al., 2011

Table A-2. Measured sorption coefficients (K_D) for the 66 PhACs assessed in this review. For each measured K_D values are provided with reported experimental pH, charge of dominant PhAC species at experimental conditions (Dom.Sp.Expt.pH), fraction of dominant species (%Dom.Species) and fraction of uncharged PhAC species (α_0 Expt.pH). Note that where the pH employed for the experiments was not reported (n/r) by the authors the information about the dominant species was not determined (n/d).

Name & Acronym		pKa	Protonation	Expt pH	Dom.Sp. Expt.pH		%Dom. Species	α_0 Expt. pH	K_D (L g^{-1} SS)	log K_D	Reference
Fluoxetine	FLX	10.1	monoprotic	6	Positive	+1	1.00	0.00	6.100	0.785	Horsing et. al., 2011
				7	Positive	+1	1.00	0.00	3.700	0.568	Horsing et. al., 2011
				8	Positive	+1	0.99	0.01	8.700	0.940	Horsing et. al., 2011
				7	Positive	+1	1.00	0.00	5.700	0.756	Horsing et. al., 2011
				n/r	n/d	n/d	n/d	n/d	0.003	-2.535	Hyland et. al., 2012
				n/r	n/d	n/d	n/d	n/d	0.003	-2.495	Hyland et. al., 2012
				n/r	n/d	n/d	n/d	n/d	0.003	-2.506	Hyland et. al., 2012
				n/r	n/d	n/d	n/d	n/d	0.003	-2.547	Hyland et. al., 2012
				n/r	n/d	n/d	n/d	n/d	0.003	-2.519	Hyland et. al., 2012
				n/r	n/d	n/d	n/d	n/d	0.003	-2.516	Hyland et. al., 2012
				n/r	n/d	n/d	n/d	n/d	0.003	-2.483	Hyland et. al., 2012
Fenoprofen	FPN	4.2	monoprotic	6.7	Negative	-1	1.00	0.00	0.057	-1.244	Urase & Kikuta, 2005
				5.6	Negative	-1	0.96	0.04	0.306	-0.514	Urase & Kikuta, 2005
				4.4	Negative	-1	0.61	0.39	0.515	-0.288	Urase & Kikuta, 2005
				7.2	Negative	-1	1.00	0.00	0.026	-1.585	Urase & Kikuta, 2005

Table A-2. Measured sorption coefficients (K_D) for the 66 PhACs assessed in this review. For each measured K_D values are provided with reported experimental pH, charge of dominant PhAC species at experimental conditions (Dom.Sp.Expt.pH), fraction of dominant species (%Dom.Species) and fraction of uncharged PhAC species (α_0 Expt.pH). Note that where the pH employed for the experiments was not reported (n/r) by the authors the information about the dominant species was not determined (n/d).

Name & Acronym		pKa	Protonation	Expt pH	Dom.Sp. Expt.pH		%Dom. Species	α_0 Expt. pH	K_D (L g^{-1} SS)	log K_D	Reference
Glibenclamide	GLC		multiprotic	6	Negative	-1	0.98	0.02	1.400	0.146	Horsing et. al., 2011
				7	Negative	-1	1.00	0.00	1.100	0.041	Horsing et. al., 2011
				8	Negative	-1	1.00	0.00	1.100	0.041	Horsing et. al., 2011
				7	Negative	-1	1.00	0.00	2.300	0.362	Horsing et. al., 2011
				n/r	n/d	n/d	n/d	n/d	0.239	-0.622	Radjenovic et. al., 2009
				n/r	n/d	n/d	n/d	n/d	0.142	-0.848	Radjenovic et. al., 2009
				n/r	n/d	n/d	n/d	n/d	0.315	-0.502	Radjenovic et. al., 2009
Glimepiride	GLM	4.99	monoprotic	6	Negative	-1	0.91	0.09	0.960	-0.018	Horsing et. al., 2011
				7	Negative	-1	0.99	0.01	0.900	-0.046	Horsing et. al., 2011
				8	Negative	-1	1.00	0.00	0.960	-0.018	Horsing et. al., 2011
				7	Negative	-1	0.99	0.01	2.600	0.415	Horsing et. al., 2011

Table A-2. Measured sorption coefficients (K_D) for the 66 PhACs assessed in this review. For each measured K_D values are provided with reported experimental pH, charge of dominant PhAC species at experimental conditions (Dom.Sp.Expt.pH), fraction of dominant species (%Dom.Species) and fraction of uncharged PhAC species (α_0 Expt.pH). Note that where the pH employed for the experiments was not reported (n/r) by the authors the information about the dominant species was not determined (n/d).

Name & Acronym		pKa	Protonation	Expt pH	Dom.Sp. Expt.pH		%Dom. Species	α_0 Expt. pH	K_D (L g^{-1} SS)	log K_D	Reference
Gemfibrozil	GMF	4.8	monoprotic	n/r	n/d	n/d	n/d	n/d	0.019	-1.714	Radjenovic et. al., 2009
				n/r	n/d	n/d	n/d	n/d	0.028	-1.556	Radjenovic et. al., 2009
				n/r	n/d	n/d	n/d	n/d	0.019	-1.728	Radjenovic et. al., 2009
				7	Negative	-1	0.99	0.01	0.045	-1.347	Stevens-Garmon et. al., 2011
				7	Negative	-1	0.99	0.01	0.030	-1.523	Stevens-Garmon et. al., 2011
				6.7	Negative	-1	0.99	0.01	0.448	-0.349	Urase & Kikuta, 2005
				5.6	Negative	-1	0.86	0.14	0.401	-0.397	Urase & Kikuta, 2005
				4.4	Uncharged	0	0.72	0.72	0.403	-0.395	Urase & Kikuta, 2005
				7.2	Negative	-1	1.00	0.00	0.434	-0.363	Urase & Kikuta, 2005
				n/r	n/d	n/d	n/d	n/d	0.002	-2.686	Hyland et. al., 2012
				n/r	n/d	n/d	n/d	n/d	0.002	-2.648	Hyland et. al., 2012
				n/r	n/d	n/d	n/d	n/d	0.002	-2.676	Hyland et. al., 2012
				n/r	n/d	n/d	n/d	n/d	0.002	-2.614	Hyland et. al., 2012
				n/r	n/d	n/d	n/d	n/d	0.002	-2.775	Hyland et. al., 2012
				n/r	n/d	n/d	n/d	n/d	0.002	-2.695	Hyland et. al., 2012

Table A-2. Measured sorption coefficients (K_D) for the 66 PhACs assessed in this review. For each measured K_D values are provided with reported experimental pH, charge of dominant PhAC species at experimental conditions (Dom.Sp.Expt.pH), fraction of dominant species (%Dom.Species) and fraction of uncharged PhAC species (α_0 Expt.pH). Note that where the pH employed for the experiments was not reported (n/r) by the authors the information about the dominant species was not determined (n/d).

Name & Acronym		pKa	Protonation	Expt pH	Dom.Sp. Expt.pH		%Dom. Species	α_0 Expt. pH	K_D (L g^{-1} SS)	log K_D	Reference
Haloperidol	HAL	8.3	monoprotic	6	Positive	+1	1.00	0.00	2.900	0.462	Horsing et. al., 2011
				7	Positive	+1	0.95	0.05	1.200	0.079	Horsing et. al., 2011
				8	Positive	+1	0.67	0.33	2.800	0.447	Horsing et. al., 2011
				7	Positive	+1	0.95	0.05	1.700	0.230	Horsing et. al., 2011
Hydrochlorothiazide	HCT		multiprotic	n/r	n/d	n/d	n/d	n/d	0.020	-1.695	Radjenovic et. al., 2009
			multiprotic	n/r	n/d	n/d	n/d	n/d	0.022	-1.652	Radjenovic et. al., 2009
			multiprotic	n/r	n/d	n/d	n/d	n/d	0.024	-1.629	Radjenovic et. al., 2009
Hydrocodone	HYC	8.61	monoprotic	n/r	n/d	n/d	n/d	n/d	0.002	-2.654	Hyland et. al., 2012
				n/r	n/d	n/d	n/d	n/d	0.002	-2.654	Hyland et. al., 2012
				n/r	n/d	n/d	n/d	n/d	0.002	-2.780	Hyland et. al., 2012
				n/r	n/d	n/d	n/d	n/d	0.002	-2.717	Hyland et. al., 2012
				n/r	n/d	n/d	n/d	n/d	0.002	-2.688	Hyland et. al., 2012
Hydroxyzine	HYZ		multiprotic	6	Positive	+1	0.76	0.02	0.710	-0.149	Horsing et. al., 2011
				7	Positive	+1	0.67	0.13	0.530	-0.276	Horsing et. al., 2011
				8	Uncharged	0	0.60	0.60	0.300	-0.523	Horsing et. al., 2011
				7	Positive	+1	0.67	0.13	0.600	-0.222	Horsing et. al., 2011

Table A-2. Measured sorption coefficients (K_D) for the 66 PhACs assessed in this review. For each measured K_D values are provided with reported experimental pH, charge of dominant PhAC species at experimental conditions (Dom.Sp.Expt.pH), fraction of dominant species (%Dom.Species) and fraction of uncharged PhAC species (α_0 Expt.pH). Note that where the pH employed for the experiments was not reported (n/r) by the authors the information about the dominant species was not determined (n/d).

Name & Acronym		pKa	Protonation	Expt pH	Dom.Sp. Expt.pH		%Dom. Species	α_0 Expt. pH	K_D (L g^{-1} SS)	log K_D	Reference
Ibuprofen	IBP	4.5	monoprotic	7.7	Negative	-1	1.00	0.00	0.050	-1.301	Abegglen et. al., 2009
				7.7	Negative	-1	1.00	0.00	0.006	-2.222	Abegglen et. al., 2009
				7	Negative	-1	1.00	0.00	0.200	-0.699	Horsing et. al., 2011
				n/r	n/d	n/d	n/d	n/d	0.007	-2.155	Ternes et. al., 2004
				6.7	Negative	-1	0.99	0.01	0.080	-1.097	Urase & Kikuta, 2005
				5.6	Negative	-1	0.93	0.07	1.265	0.102	Urase & Kikuta, 2005
				4.4	Uncharged	0	0.56	0.56	0.470	-0.328	Urase & Kikuta, 2005
				7.2	Negative	-1	1.00	0.00	0.072	-1.143	Urase & Kikuta, 2005
				n/r	n/d	n/d	n/d	n/d	0.002	-2.674	Hyland et. al., 2012
				n/r	n/d	n/d	n/d	n/d	0.002	-2.625	Hyland et. al., 2012
				n/r	n/d	n/d	n/d	n/d	0.003	-2.577	Hyland et. al., 2012
				n/r	n/d	n/d	n/d	n/d	0.002	-2.688	Hyland et. al., 2012
				n/r	n/d	n/d	n/d	n/d	0.002	-2.660	Hyland et. al., 2012
				n/r	n/d	n/d	n/d	n/d	0.002	-2.674	Hyland et. al., 2012
				n/r	n/d	n/d	n/d	n/d	0.002	-2.662	Hyland et. al., 2012

Table A-2. Measured sorption coefficients (K_D) for the 66 PhACs assessed in this review. For each measured K_D values are provided with reported experimental pH, charge of dominant PhAC species at experimental conditions (Dom.Sp.Expt.pH), fraction of dominant species (%Dom.Species) and fraction of uncharged PhAC species (α_0 Expt.pH). Note that where the pH employed for the experiments was not reported (n/r) by the authors the information about the dominant species was not determined (n/d).

Name & Acronym		pKa	Protonation	Expt pH	Dom.Sp. Expt.pH		%Dom. Species	α_0 Expt. pH	K_D (L g^{-1} SS)	log K_D	Reference
Indomethacin	IDM	4.5	monoprotic	6.7	Negative	-1	0.99	0.01	0.039	-1.409	Urase & Kikuta, 2005
				5.6	Negative	-1	0.93	0.07	1.158	0.064	Urase & Kikuta, 2005
				4.4	Uncharged	0	0.56	0.56	2.851	0.455	Urase & Kikuta, 2005
				7.2	Negative	-1	1.00	0.00	0.028	-1.553	Urase & Kikuta, 2005
Ketoprofen	KET	4.45	monoprotic	n/r	n/d	n/d	n/d	n/d	0.016	-1.796	Radjenovic et. al., 2009
			monoprotic	n/r	n/d	n/d	n/d	n/d	0.165	-0.783	Radjenovic et. al., 2009
			monoprotic	n/r	n/d	n/d	n/d	n/d	0.072	-1.143	Radjenovic et. al., 2009
			monoprotic	6.7	Negative	-1	0.99	0.01	0.029	-1.538	Urase & Kikuta, 2005
			monoprotic	5.6	Negative	-1	0.93	0.07	0.072	-1.143	Urase & Kikuta, 2005
			monoprotic	4.4	Uncharged	0	0.53	0.53	0.429	-0.368	Urase & Kikuta, 2005
			monoprotic	7.2	Negative	-1	1.00	0.00	0.016	-1.796	Urase & Kikuta, 2005
			monoprotic	n/r	n/d	n/d	n/d	n/d	0.002	-2.714	Hyland et. al., 2012
			monoprotic	n/r	n/d	n/d	n/d	n/d	0.002	-2.646	Hyland et. al., 2012
			monoprotic	n/r	n/d	n/d	n/d	n/d	0.003	-2.590	Hyland et. al., 2012
			monoprotic	n/r	n/d	n/d	n/d	n/d	0.002	-2.710	Hyland et. al., 2012
			monoprotic	n/r	n/d	n/d	n/d	n/d	0.002	-2.611	Hyland et. al., 2012
			monoprotic	n/r	n/d	n/d	n/d	n/d	0.003	-2.583	Hyland et. al., 2012
			monoprotic	n/r	n/d	n/d	n/d	n/d	0.002	-2.721	Hyland et. al., 2012

Table A-2. Measured sorption coefficients (K_D) for the 66 PhACs assessed in this review. For each measured K_D values are provided with reported experimental pH, charge of dominant PhAC species at experimental conditions (Dom.Sp.Expt.pH), fraction of dominant species (%Dom.Species) and fraction of uncharged PhAC species (α_0 Expt.pH). Note that where the pH employed for the experiments was not reported (n/r) by the authors the information about the dominant species was not determined (n/d).

Name & Acronym		pKa	Protonation	Expt pH	Dom.Sp. Expt.pH		%Dom. Species	α_0 Expt. pH	K_D (L g^{-1} SS)	log K_D	Reference
			monoprotic	n/r	n/d	n/d	n/d	n/d	0.002	-2.690	Hyland et. al., 2012
Loperamide	LOP	8.86	monoprotic	6	Positive	+1	1.00	0.00	5.700	0.756	Horsing et. al., 2011
			monoprotic	7	Positive	+1	0.99	0.01	3.000	0.477	Horsing et. al., 2011
			monoprotic	8	Positive	+1	0.88	0.12	7.300	0.863	Horsing et. al., 2011
			monoprotic	7	Positive	+1	0.99	0.01	11.000	1.041	Horsing et. al., 2011
Loratidine	LOR	4.9	monoprotic	n/r	n/d	n/d	n/d	n/d	3.321	0.521	Radjenovic et. al., 2009
			monoprotic	n/r	n/d	n/d	n/d	n/d	2.214	0.345	Radjenovic et. al., 2009
			monoprotic	n/r	n/d	n/d	n/d	n/d	3.058	0.485	Radjenovic et. al., 2009
Maprotiline	MAP	10.31	monoprotic	6	Positive	+1	1.00	0.00	4.600	0.663	Horsing et. al., 2011
			monoprotic	7	Positive	+1	1.00	0.00	2.700	0.431	Horsing et. al., 2011
			monoprotic	8	Positive	+1	1.00	0.00	6.200	0.792	Horsing et. al., 2011
			monoprotic	7	Positive	+1	1.00	0.00	3.900	0.591	Horsing et. al., 2011

Table A-2. Measured sorption coefficients (K_D) for the 66 PhACs assessed in this review. For each measured K_D values are provided with reported experimental pH, charge of dominant PhAC species at experimental conditions (Dom.Sp.Expt.pH), fraction of dominant species (%Dom.Species) and fraction of uncharged PhAC species (α_0 Expt.pH). Note that where the pH employed for the experiments was not reported (n/r) by the authors the information about the dominant species was not determined (n/d).

Name & Acronym		pKa	Protonation	Expt pH	Dom.Sp. Expt.pH		%Dom. Species	α_0 Expt. pH	K_D (L g^{-1} SS)	log K_D	Reference
Metoprolol	MET	9.7	monoprotic	n/r	n/d	n/d	n/d	n/d	0.024	-1.617	Maurer et. al., 2007
			monoprotic	n/r	n/d	n/d	n/d	n/d	0.027	-1.569	Maurer et. al., 2007
			monoprotic	n/r	n/d	n/d	n/d	n/d	0.010	-2.003	Maurer et. al., 2007
			monoprotic	n/r	n/d	n/d	n/d	n/d	0.065	-1.187	Wick et. al., 2009
			monoprotic	n/r	n/d	n/d	n/d	n/d	0.010	-2.000	Xue et. al., 2010
			monoprotic	n/r	n/d	n/d	n/d	n/d	0.020	-1.699	Xue et. al., 2010
			monoprotic	n/r	n/d	n/d	n/d	n/d	0.010	-2.000	Xue et. al., 2010
			monoprotic	n/r	n/d	n/d	n/d	n/d	0.010	-2.000	Xue et. al., 2010
Mefenamic Acid	MFA	4.2	monoprotic	n/r	n/d	n/d	n/d	n/d	0.434	-0.363	Radjenovic et. al., 2009
			monoprotic	n/r	n/d	n/d	n/d	n/d	0.537	-0.270	Radjenovic et. al., 2009
			monoprotic	n/r	n/d	n/d	n/d	n/d	0.495	-0.305	Radjenovic et. al., 2009
Mianserin	MIA		multiprotic	6	Positive	+1	0.89	0.11	0.910	-0.041	Horsing et. al., 2011
			multiprotic	7	Uncharged	0	0.55	0.55	40.400	1.606	Horsing et. al., 2011
			multiprotic	8	Uncharged	0	0.92	0.92	0.620	-0.208	Horsing et. al., 2011
			multiprotic	7	Uncharged	0	0.55	0.55	0.520	-0.284	Horsing et. al., 2011

Table A-2. Measured sorption coefficients (K_D) for the 66 PhACs assessed in this review. For each measured K_D values are provided with reported experimental pH, charge of dominant PhAC species at experimental conditions (Dom.Sp.Expt.pH), fraction of dominant species (%Dom.Species) and fraction of uncharged PhAC species (α_0 Expt.pH). Note that where the pH employed for the experiments was not reported (n/r) by the authors the information about the dominant species was not determined (n/d).

Name & Acronym		pKa	Protonation	Expt pH	Dom.Sp. Expt.pH		%Dom. Species	α_0 Expt. pH	K_D (L g^{-1} SS)	log K_D	Reference
Naproxen	NAP	4.15	monoprotic	7.7	Negative	-1	1.00	0.00	0.010	-2.000	Abegglen et. al., 2009
			monoprotic	6.7	Negative	-1	1.00	0.00	0.024	-1.620	Urase & Kikuta, 2005
			monoprotic	5.6	Negative	-1	0.97	0.03	0.092	-1.036	Urase & Kikuta, 2005
			monoprotic	4.4	Negative	-1	0.64	0.36	0.444	-0.353	Urase & Kikuta, 2005
			monoprotic	7.2	Negative	-1	1.00	0.00	0.013	-1.886	Urase & Kikuta, 2005
			monoprotic	n/r	n/d	n/d	n/d	n/d	0.002	-2.678	Hyland et. al., 2012
			monoprotic	n/r	n/d	n/d	n/d	n/d	0.002	-2.650	Hyland et. al., 2012
			monoprotic	n/r	n/d	n/d	n/d	n/d	0.002	-2.631	Hyland et. al., 2012
			monoprotic	n/r	n/d	n/d	n/d	n/d	0.002	-2.703	Hyland et. al., 2012
			monoprotic	n/r	n/d	n/d	n/d	n/d	0.002	-2.627	Hyland et. al., 2012
			monoprotic	n/r	n/d	n/d	n/d	n/d	0.002	-2.717	Hyland et. al., 2012
			monoprotic	n/r	n/d	n/d	n/d	n/d	0.002	-2.719	Hyland et. al., 2012
Nefazodone	NEF		multiprotic	6	Positive	+1	0.92	0.08	8.800	0.944	Horsing et. al., 2011
			multiprotic	7	Positive	+1	0.55	0.45	6.300	0.799	Horsing et. al., 2011
			multiprotic	8	Uncharged	0	0.89	0.89	4.200	0.623	Horsing et. al., 2011
			multiprotic	7	Positive	+1	0.55	0.45	8.900	0.949	Horsing et. al., 2011

Table A-2. Measured sorption coefficients (K_D) for the 66 PhACs assessed in this review. For each measured K_D values are provided with reported experimental pH, charge of dominant PhAC species at experimental conditions (Dom.Sp.Expt.pH), fraction of dominant species (%Dom.Species) and fraction of uncharged PhAC species (α_0 Expt.pH). Note that where the pH employed for the experiments was not reported (n/r) by the authors the information about the dominant species was not determined (n/d).

Name & Acronym		pKa	Protonation	Expt pH	Dom.Sp. Expt.pH		%Dom. Species	α_0 Expt. pH	K_D (L g^{-1} SS)	log K_D	Reference
Orphenadrine	ORP	8.4	monoprotic	6	Positive	+1	1.00	0.00	0.650	-0.187	Horsing et. al., 2011
			monoprotic	7	Positive	+1	0.96	0.04	0.500	-0.301	Horsing et. al., 2011
			monoprotic	8	Positive	+1	0.72	0.28	0.820	-0.086	Horsing et. al., 2011
			monoprotic	7	Positive	+1	0.96	0.04	0.540	-0.268	Horsing et. al., 2011
Oxazepam	OZP		multiprotic	6	Uncharged	0	1.00	1.00	1.100	0.041	Horsing et. al., 2011
			multiprotic	7	Uncharged	0	1.00	1.00	1.900	0.279	Horsing et. al., 2011
			multiprotic	8	Uncharged	0	1.00	1.00	1.600	0.204	Horsing et. al., 2011
			multiprotic	7	Uncharged	0	1.00	1.00	1.600	0.204	Horsing et. al., 2011
			multiprotic	n/r	n/d	n/d	n/d	n/d	0.013	-1.886	Wick et. al., 2009
Paroxetine	PAR	9.72	monoprotic	6	Positive	+1	1.00	0.00	8.500	0.929	Horsing et. al., 2011
			monoprotic	7	Positive	+1	1.00	0.00	4.900	0.690	Horsing et. al., 2011
			monoprotic	8	Positive	+1	0.98	0.02	11.000	1.041	Horsing et. al., 2011
			monoprotic	7	Positive	+1	1.00	0.00	8.600	0.934	Horsing et. al., 2011
Pizotifen	PIZ	6.95	monoprotic	6	Positive	+1	0.90	0.10	3.100	0.491	Horsing et. al., 2011
			monoprotic	7	Uncharged	0	0.53	0.53	2.000	0.301	Horsing et. al., 2011
			monoprotic	8	Uncharged	0	0.92	0.92	4.300	0.633	Horsing et. al., 2011
			monoprotic	7	Uncharged	0	0.53	0.53	3.100	0.491	Horsing et. al., 2011

Table A-2. Measured sorption coefficients (K_D) for the 66 PhACs assessed in this review. For each measured K_D values are provided with reported experimental pH, charge of dominant PhAC species at experimental conditions (Dom.Sp.Expt.pH), fraction of dominant species (%Dom.Species) and fraction of uncharged PhAC species (α_0 Expt.pH). Note that where the pH employed for the experiments was not reported (n/r) by the authors the information about the dominant species was not determined (n/d).

Name & Acronym		pKa	Protonation	Expt pH	Dom.Sp. Expt.pH		%Dom. Species	α_0 Expt. pH	K_D (L g^{-1} SS)	log K_D	Reference
Propranolol	PRO	9.42	monoprotic	n/r	n/d	n/d	n/d	n/d	0.365	-0.438	Maurer et. al., 2007
			monoprotic	n/r	n/d	n/d	n/d	n/d	0.398	-0.401	Maurer et. al., 2007
			monoprotic	n/r	n/d	n/d	n/d	n/d	0.497	-0.304	Maurer et. al., 2007
			monoprotic	n/r	n/d	n/d	n/d	n/d	0.569	-0.245	Maurer et. al., 2007
			monoprotic	n/r	n/d	n/d	n/d	n/d	0.420	-0.376	Maurer et. al., 2007
			monoprotic	n/r	n/d	n/d	n/d	n/d	0.366	-0.437	Radjenovic et. al., 2009
			monoprotic	n/r	n/d	n/d	n/d	n/d	0.375	-0.426	Radjenovic et. al., 2009
			monoprotic	n/r	n/d	n/d	n/d	n/d	0.298	-0.526	Radjenovic et. al., 2009
			monoprotic	n/r	n/d	n/d	n/d	n/d	0.343	-0.465	Wick et. al., 2009
Repaglinide	REP		multiprotic	6	Negative	-1	0.94	0.06	0.100	-1.000	Horsing et. al., 2011
			multiprotic	7	Negative	-1	0.99	0.01	0.200	-0.699	Horsing et. al., 2011
			multiprotic	8	Negative	-1	1.00	0.00	0.070	-1.155	Horsing et. al., 2011
			multiprotic	7	Negative	-1	0.99	0.01	0.510	-0.292	Horsing et. al., 2011
Risperidone	RIS		multiprotic	6	Positive	+1	1.00	0.00	0.650	-0.187	Horsing et. al., 2011
			multiprotic	7	Positive	+1	0.98	0.02	0.420	-0.377	Horsing et. al., 2011
			multiprotic	8	Positive	+1	0.85	0.15	0.620	-0.208	Horsing et. al., 2011
			multiprotic	7	Positive	+1	0.98	0.02	0.330	-0.481	Horsing et. al., 2011

Table A-2. Measured sorption coefficients (K_D) for the 66 PhACs assessed in this review. For each measured K_D values are provided with reported experimental pH, charge of dominant PhAC species at experimental conditions (Dom.Sp.Expt.pH), fraction of dominant species (%Dom.Species) and fraction of uncharged PhAC species (α_0 Expt.pH). Note that where the pH employed for the experiments was not reported (n/r) by the authors the information about the dominant species was not determined (n/d).

Name & Acronym		pKa	Protonation	Expt pH	Dom.Sp. Expt.pH		%Dom. Species	α_0 Expt. pH	K_D (L g^{-1} SS)	log K_D	Reference
Sertraline	SER	9.47	monoprotic	6	Positive	+1	1.00	0.00	18.000	1.255	Horsing et. al., 2011
			monoprotic	7	Positive	+1	1.00	0.00	9.800	0.991	Horsing et. al., 2011
			monoprotic	8	Positive	+1	0.97	0.03	26.000	1.415	Horsing et. al., 2011
Sulfamethoxazole	SMX	5.7	monoprotic	7.7	Negative	-1	0.99	0.01	0.040	-1.398	Abegglen et. al., 2009
			monoprotic	7.7	Negative	-1	0.99	0.01	0.050	-1.301	Abegglen et. al., 2009
			monoprotic	6	Negative	-1	0.67	0.33	0.300	-0.523	Horsing et. al., 2011
			monoprotic	7	Negative	-1	0.95	0.05	0.300	-0.523	Horsing et. al., 2011
			monoprotic	8	Negative	-1	1.00	0.00	0.270	-0.569	Horsing et. al., 2011
			monoprotic	7	Negative	-1	0.95	0.05	0.280	-0.553	Horsing et. al., 2011
			monoprotic	n/r	n/d	n/d	n/d	n/d	0.077	-1.114	Radjenovic et. al., 2009
			monoprotic	n/r	n/d	n/d	n/d	n/d	0.063	-1.201	Radjenovic et. al., 2009
			monoprotic	n/r	n/d	n/d	n/d	n/d	0.060	-1.222	Radjenovic et. al., 2009
			monoprotic	n/r	n/d	n/d	n/d	n/d	0.003	-2.551	Hyland et. al., 2012
			monoprotic	n/r	n/d	n/d	n/d	n/d	0.002	-2.633	Hyland et. al., 2012
			monoprotic	n/r	n/d	n/d	n/d	n/d	0.002	-2.726	Hyland et. al., 2012
			monoprotic	n/r	n/d	n/d	n/d	n/d	0.002	-2.693	Hyland et. al., 2012
			monoprotic	n/r	n/d	n/d	n/d	n/d	0.002	-2.623	Hyland et. al., 2012
			monoprotic	n/r	n/d	n/d	n/d	n/d	0.003	-2.547	Hyland et. al., 2012

Table A-2. Measured sorption coefficients (K_D) for the 66 PhACs assessed in this review. For each measured K_D values are provided with reported experimental pH, charge of dominant PhAC species at experimental conditions (Dom.Sp.Expt.pH), fraction of dominant species (%Dom.Species) and fraction of uncharged PhAC species (α_0 Expt.pH). Note that where the pH employed for the experiments was not reported (n/r) by the authors the information about the dominant species was not determined (n/d).

Name & Acronym		pKa	Protonation	Expt pH	Dom.Sp. Expt.pH		%Dom. Species	α_0 Expt. pH	K_D (L g^{-1} SS)	log K_D	Reference
Sotalol	SOT		multiprotic	6	Positive	+1	1.00	0.00	0.400	-0.398	Horsing et. al., 2011
			multiprotic	7	Positive	+1	1.00	0.00	0.240	-0.620	Horsing et. al., 2011
			multiprotic	8	Positive	+1	0.96	0.04	0.300	-0.523	Horsing et. al., 2011
			multiprotic	7	Positive	+1	1.00	0.00	0.740	-0.131	Horsing et. al., 2011
			multiprotic	n/r	n/d	n/d	n/d	n/d	0.021	-1.672	Maurer et. al., 2007
			multiprotic	n/r	n/d	n/d	n/d	n/d	0.061	-1.214	Maurer et. al., 2007
			multiprotic	n/r	n/d	n/d	n/d	n/d	0.048	-1.316	Maurer et. al., 2007
			multiprotic	n/r	n/d	n/d	n/d	n/d	0.131	-0.884	Maurer et. al., 2007
			multiprotic	n/r	n/d	n/d	n/d	n/d	0.018	-1.745	Wick et. al., 2009
Telmisartan	TEL		multiprotic	6	Uncharged	0	0.51	0.55	1.000	0.000	Horsing et. al., 2011
			multiprotic	7	Negative	-1	0.88	0.12	0.900	-0.046	Horsing et. al., 2011
			multiprotic	8	Negative	-1	0.99	0.01	0.400	-0.398	Horsing et. al., 2011

Table A-2. Measured sorption coefficients (K_D) for the 66 PhACs assessed in this review. For each measured K_D values are provided with reported experimental pH, charge of dominant PhAC species at experimental conditions (Dom.Sp.Expt.pH), fraction of dominant species (%Dom.Species) and fraction of uncharged PhAC species (α_0 Expt.pH). Note that where the pH employed for the experiments was not reported (n/r) by the authors the information about the dominant species was not determined (n/d).

Name & Acronym		pKa	Protonation	Expt pH	Dom.Sp. Expt.pH		%Dom. Species	α_0 Expt. pH	K_D (L g^{-1} SS)	log K_D	Reference
Trimethoprim	TMP		multiprotic	6	Positive	+1	0.93	0.07	0.430	-0.367	Horsing et. al., 2011
			multiprotic	7	Positive	+1	0.59	0.41	0.348	-0.458	Horsing et. al., 2011
			multiprotic	8	Uncharged	0	0.87	0.87	0.280	-0.553	Horsing et. al., 2011
			multiprotic	7	Positive	+1	0.59	0.41	0.280	-0.553	Horsing et. al., 2011
			multiprotic	n/r	n/d	n/d	n/d	n/d	0.253	-0.597	Radjenovic et. al., 2009
			multiprotic	n/r	n/d	n/d	n/d	n/d	0.320	-0.495	Radjenovic et. al., 2009
			multiprotic	n/r	n/d	n/d	n/d	n/d	0.225	-0.648	Radjenovic et. al., 2009
			multiprotic	7	Positive	+1	0.59	0.41	0.119	-0.924	Stevens-Garmon et. al., 2011
			multiprotic	7	Positive	+1	0.59	0.41	0.135	-0.870	Stevens-Garmon et. al., 2011
			multiprotic	7	Positive	+1	0.59	0.41	0.193	-0.714	Stevens-Garmon et. al., 2011
			multiprotic	n/r	n/d	n/d	n/d	n/d	0.002	-2.633	Hyland et. al., 2012
			multiprotic	n/r	n/d	n/d	n/d	n/d	0.003	-2.565	Hyland et. al., 2012
			multiprotic	n/r	n/d	n/d	n/d	n/d	0.002	-2.690	Hyland et. al., 2012
			multiprotic	n/r	n/d	n/d	n/d	n/d	0.002	-2.642	Hyland et. al., 2012
			multiprotic	n/r	n/d	n/d	n/d	n/d	0.002	-2.642	Hyland et. al., 2012
			multiprotic	n/r	n/d	n/d	n/d	n/d	0.002	-2.658	Hyland et. al., 2012
Tramadol	TRA		multiprotic	n/r	n/d	n/d	n/d	n/d	0.047	-1.328	Wick et. al., 2009

Table A-2. Measured sorption coefficients (K_D) for the 66 PhACs assessed in this review. For each measured K_D values are provided with reported experimental pH, charge of dominant PhAC species at experimental conditions (Dom.Sp.Expt.pH), fraction of dominant species (%Dom.Species) and fraction of uncharged PhAC species (α_0 Expt.pH). Note that where the pH employed for the experiments was not reported (n/r) by the authors the information about the dominant species was not determined (n/d).

Name & Acronym		pKa	Protonation	Expt pH	Dom.Sp. Expt.pH		%Dom. Species	α_0 Expt. pH	K_D (L g^{-1} SS)	log K_D	Reference
Venlafaxine	VEN	9.26	monoprotic	6	Positive	+1	1.00	0.00	0.100	-1.000	Horsing et. al., 2011
			monoprotic	8	Positive	+1	0.95	0.05	0.060	-1.222	Horsing et. al., 2011
Verapamil	VRP	8.92	monoprotic	6	Positive	+1	1.00	0.00	0.380	-0.420	Horsing et. al., 2011
			monoprotic	7	Positive	+1	0.99	0.01	0.360	-0.444	Horsing et. al., 2011
			monoprotic	8	Positive	+1	0.89	0.11	0.400	-0.398	Horsing et. al., 2011
			monoprotic	7	Positive	+1	0.99	0.01	0.630	-0.201	Horsing et. al., 2011

Vita

Sandeep Sathyamoorthy's professional experience extends over a decade and across four continents in water and wastewater treatment in capacities ranging plant design, operations and management. Sandeep's personal interest in engineering and the chemistry of engineering processes, however, spans more than three decades. A native of Nairobi Kenya, Sandeep knew by age 6 he wanted to study chemical engineering in university. As a young boy, he toured a plastics manufacturing plant with his dad and even back then, he sought to understand the chemistry of plastics. Sandeep was hooked. In 1998, Sandeep graduated with honors from Cornell University with a Bachelor of Science degree in chemical engineering. Upon graduation, Sandeep worked as a pilot plant engineer, some days quite literally knee-deep in wastewater and sludge. This was a tremendous learning experience and foundation for his future career. Thereafter, Sandeep designed, built, operated and managed water and wastewater treatment plants ranging from a one-town waste management system to a project that spanned three countries. His experience in industry included a wide array of biological processes and technologies, advanced water reuse processes as well as management of people and complex projects. For Sandeep, industry and academics always sustained a symbiotic relationship.

After working for over a decade, he pursued a PhD in the Department of Civil and Environmental Engineering at Tufts University, where his research focused on the biodegradation of pharmaceuticals during nitrification. At Tufts, Sandeep had an opportunity to explore teaching – something he enjoyed tremendously. He developed and taught modules and served as a guest lecturer in core undergraduate courses. He

also had the privilege of training and mentoring undergraduate and graduate students for whom he designed and implemented a training program that combined fundamental knowledge and application oriented skills such as lab techniques. Sandeep values the role and responsibility of working with and training future engineers.

Sandeep is a member of the Water Environment Federation (WEF), the International Water Association (IWA), the American Chemical Society (ACS), the American Geophysical Union (AGU), the American Society of Engineering Education (ASEE) and the New England Water Environment Association (NEWEA). Sandeep currently serves as vice chairman of the NEWEA Microconstituents Committee and on the Young Professionals Committee for WEF. Sandeep was the recipient of the 2012 Tufts University, Department of Civil & Environmental Engineering Jonathan Curtis Fellowship. He was also awarded the Teagle Foundation Innovation in Teaching Grant in 2011 and the Tufts University Graduate Student Research Award in 2010. Sandeep is fluent in French, Swahili, Hindi and is proficient in Spanish, Tamil and Gujarati. His youngest student is his 17-month-old son, Aydyn Nikola Sathyamoorthy.